Geological Survey of Finland, Bulletin 313

THE PETROGRAPHY, MINERALOGY AND PETROCHEMISTRY OF THE SOKLI CARBONATITE MASSIF, NORTHERN FINLAND

BY

HEIKKI VARTIAINEN

with 106 figures and 30 tables in the text

GEOLOGINEN TUTKIMUSLAITOS
ESPOO 1980

Vartiainen, Heikki 1980. The petrography, mineralogy and petrochemistry of the Sokli carbonatite massif, northern Finland. *Geological Survey of Finland, Bulletin 313.* 126 pages, 106 figures and 30 tables.

The Sokli carbonatite complex is the westernmost deposit in the Kola alkaline rock province. The complex comprises a fenite aureole and a carbonatite massif with three parts: a transition zone of metasomatites, a metacarbonatite area and a magmatic core. The evolution of the complex started with an ultramafic instrusion that led to the crystallization of magnetite olivinite and pyroxenite. Afterwards the ultramafites were slightly altered during a peaceful episode. This was succeeded by an intense and intricate stage of alkali metasomatism. As a result highly complicated rock types that, however, exhibit a certain mineralogical and chemical regularity developed. Carbonatization has produced metasomatic carbonatites. The multi-stage carbonatite intrusion completed the evolution of the complex. The magmatic carbonatites crystallized during two main phases separated by a pneumatolytic-hydrothermal phase. The rocks formed in five stages. The magmatic carbonatites differ from the metasomatic carbonatites in petrography and in their higher average contents of Nb (and U, Ta, Th) and Sr.

Mineralogical studies show that the olivine in carbonatites usually has lower Ni (< 0.05 %) and higher MnO (0.5 to 1.25 %) than the MgO-rich olivines in the other magmatic rocks. The primary pyroxene was diopside that may have altered into aegirine through Na metasomatism. Abundant richterite characterizes the Sokli massif.

The bulk chemical composition of the magmatic carbonatites is rather close to the »typical» composition of carbonatites. The crystallization order of the magmatic carbonatites falls on a curve in the silicate + opagues — calcite — dolomite triangular diagram constructed on the basis of petrochemistry. In the U + Ta—Th—Nb/5 triangular diagram the crystallization curve of the magmatic carbonatites runs from the U + Ta corner towards the Nb/5 corner. During the metasomatic alterations in the ultramafites the rocks received Na, K, CO_2 and P from an external source and became depleted in Si, Mg, Fe, Ti and Mn.

Heikki Vartiainen, Rautaruukki Oy,
SF-96100 Rovaniemi 10, Finland

ISBN 951-690-134-4
ISSN 0367-522X

Vammala 1980, Vammalan Kirjapaino Oy

CONTENTS

INTRODUCTION

For several years after the discovery in 1967 of the Sokli complex (Fig. 1) by the steel company Rautaruukki Oy, the main objects of prospecting were the apatite—francolite regolith and the weathered crust of the carbonatite. In 1976 it was decided to step up geological investigation at Sokli and to start pilot plant tests of the apatite—francolite regolith. A comprehensive inventory of the ore regolith was carried out in 1976—1979, and the exploration diamond drilling of a pyrochlore mineralization in hard rock was intensified (Fig. 4, p. 8). Supplementary and detailed geophysics were also conducted. Thus

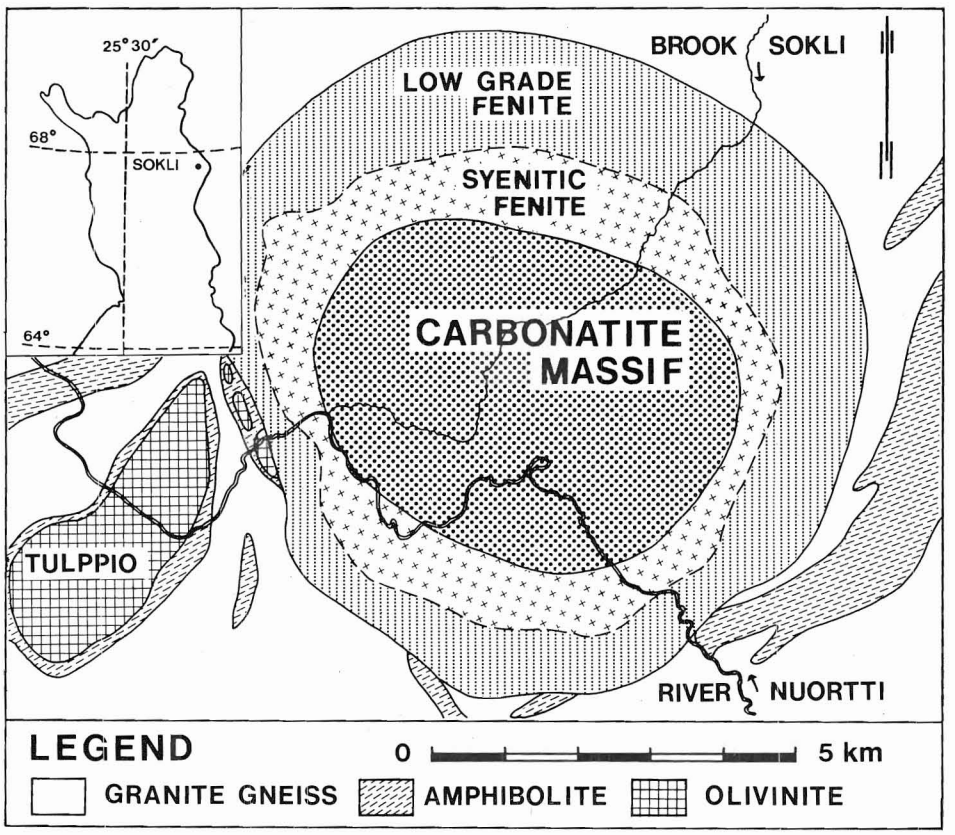

Fig. 1. Location of the Sokli carbonatite massif in Northern Finland and general geological map of the Sokli area.

a wealth of material was gathered for a detailed study of the Sokli massif.

The Sokli complex consists of a carbonatite massif and a fenite aureole (Fig. 1). The fenite aureole has earlier been described in detail and the surrounding country rocks briefly (Vartiainen and Woolley, 1976). The present paper contains some references to the olivinite of Tulppio (Fig. 1), a massif that is composed mainly of metaolivinite (90 %) and subordinately of olivinite (6 %) and other rocks. The olivinite is a dark green, granular and medium grained rock that is chiefly composed of olivine (85—95 vol-%).

The location of the Sokli complex in the alkaline rock province of the Kola Peninsula has been discussed by Vartiainen and Woolley (1974). It has been suggested that the emplacement of the complex was controlled by the long and active Kandalaksha deep fracture. The structure of the complex has been discussed on the basis of the geological and geophysical data (Vartiainen and Paarma, 1979). Dates for the carbonatite range from 334 to 378 Ma (Kononova *et al.*, 1973; Vartiainen and Woolley, 1974).

Earlier papers on the Sokli complex include a brief general account by Paarma

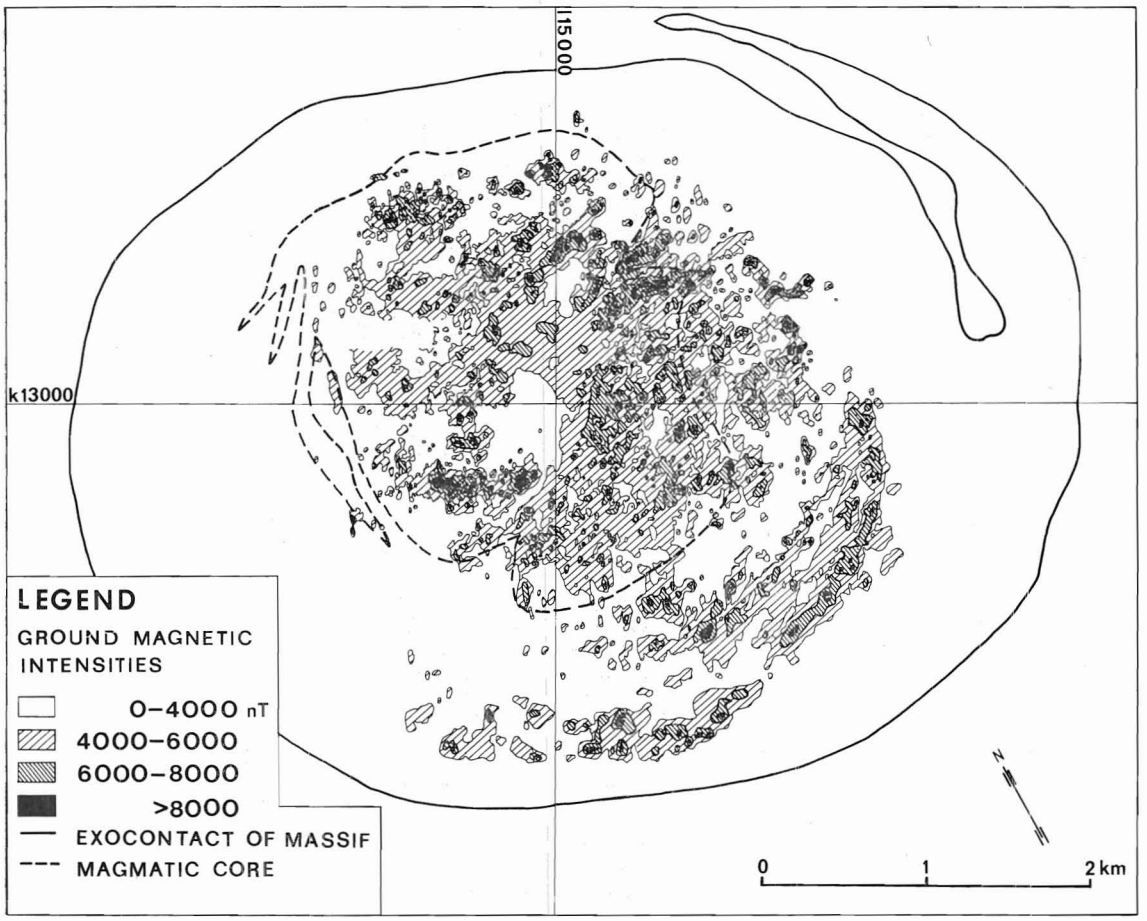

Fig. 2. Ground magnetic map of the Sokli carbonatite massif.

(1970) and by Vartiainen and Vuotovesi (1980); an interpretation of air photographs (Paarma *et al.*, 1968, 1977); an account of geochemical surveys on the Sokli complex (Nuutilainen, 1973); a brief description of the apatite–francolite regolith and its drilling (Vartiainen, 1975); an account of heavy mineral prospecting in stream beds (Vartiainen, 1976); a description of sulphur isotopes of magmatic carbonatites (Mäkelä and Vartiainen, 1978); an apatite fluid inclusion study (Haapala, 1978, 1980); a description of the alkaline lamprophyres (Vartiainen *et al.*, 1978); a pyrochlore study (Lindqvist and Rehtijärvi, 1979); and an account of remote sensing and geobotanical prospecting (Talvitie, 1979).

Wyllie (1966 a, p. 351) has stated: »Reconstruction of the history of each carbonatite complex is the responsibility of the geologists studying them in the field, and the function of the experimental petrologists is to provide a foundation of reasonable possibilities for sound reconstruction, and to test where possible, the hypotheses which are made.» The purpose of this paper is to satisfy the former requirement in respect of the carbonatite massif of Sokli and to give a petrograhical, mineralogical and petrochemical description of its rocks.

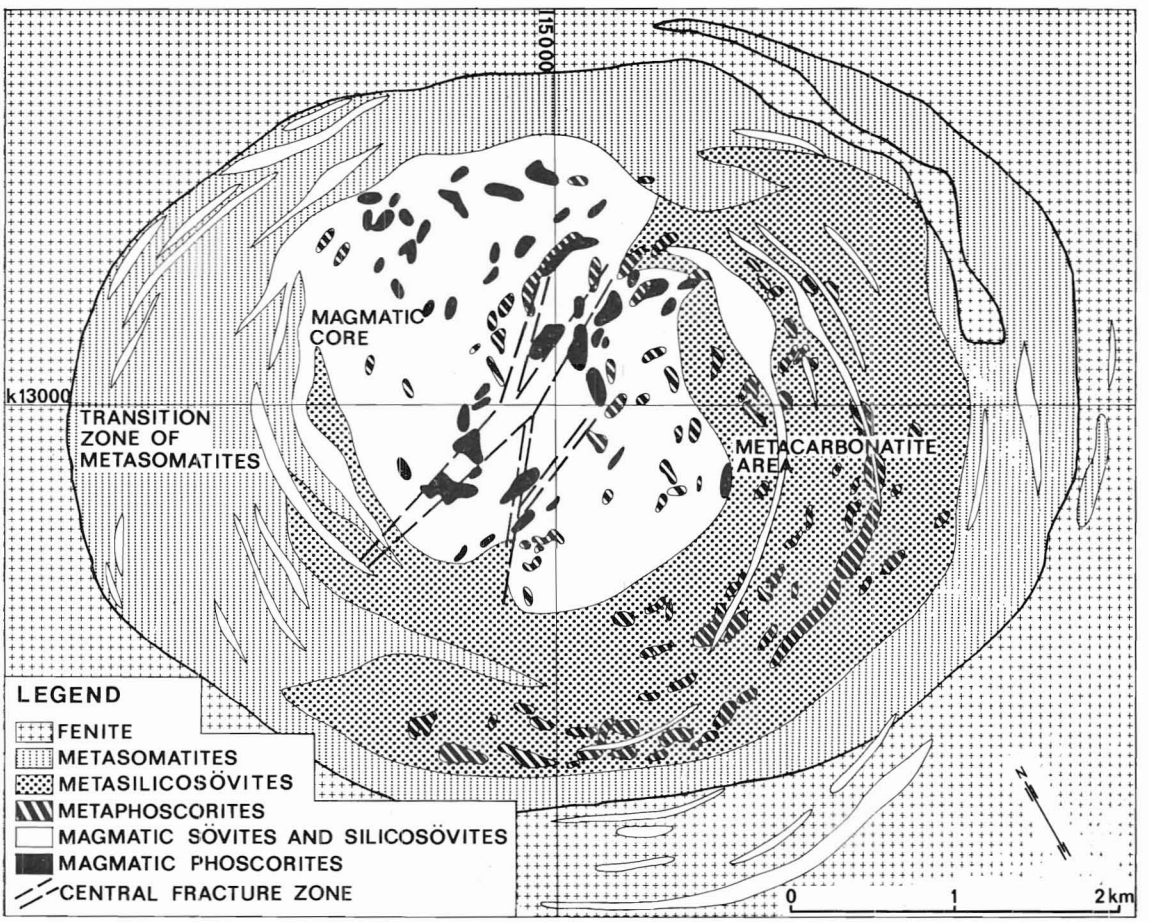

Fig. 3. Geological map of the Sokli carbonatite massif.

PETROGRAPHY

Methods

The Sokli carbonatite massif is totally covered by glacial drift and its top is almost wholly weathered. Hence, the geophysical data especially magnetic mapping (Fig. 2) has been important in compiling the geological map in Fig. 3. Observation for compiling on and description of petrographical features and relations on the rocks had to be made from drill hole cores (about 200 drill holes, average length 200 m). The locations of the drill holes are shown in Fig. 4. The drill holes whose analytical data are given in the various tables and which are referred to in the petrographical description are numbered in Fig. 4. All the chemical and mineralogical determinations were conducted on unweathered drill hole material. Some photographs were taken from the pits the location of which are shown in Fig. 4.

A »type sample suite» was collected for the descriptions of the main rock varieties. At least 500 points were counted per thin

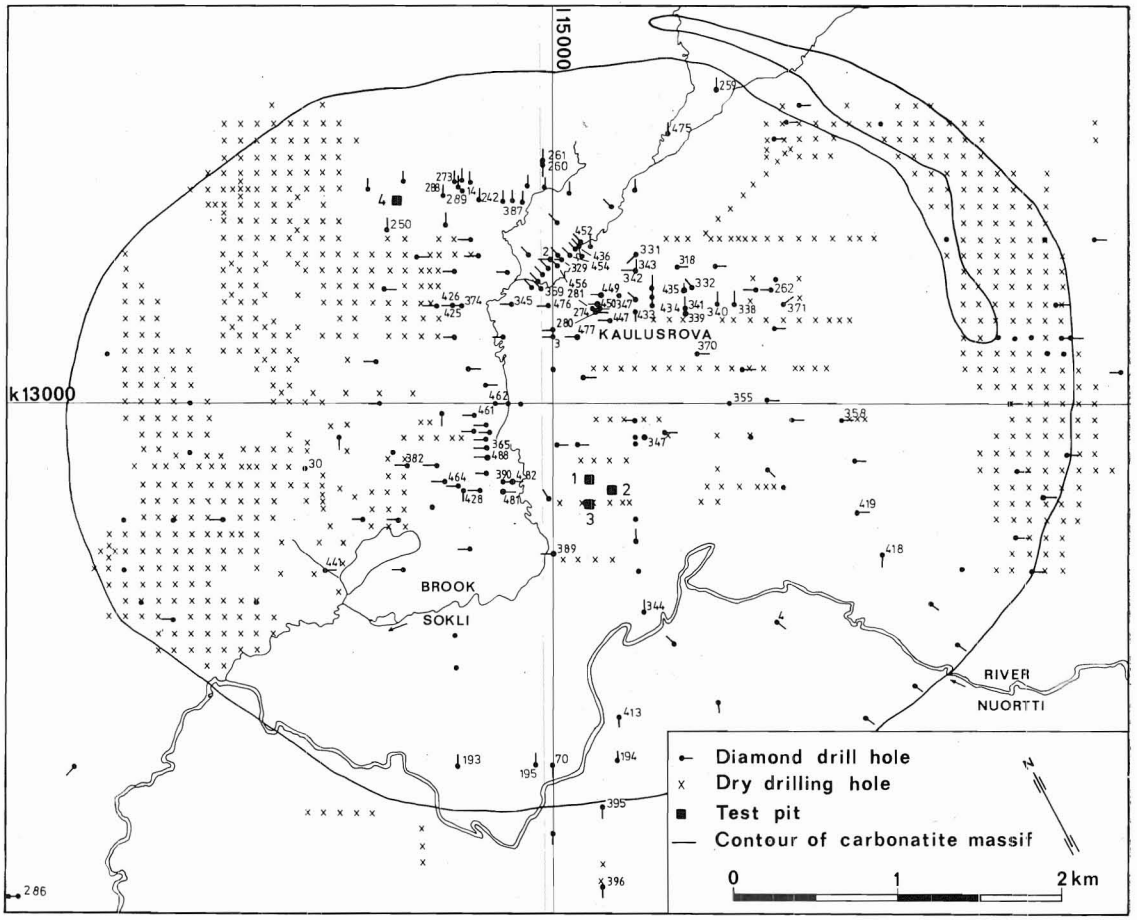

Fig. 4. The positions of the diamond drill holes, dry drilling holes and test pits used in compiling the geological map of the massif. The numbers of the diamond drill holes and the pits referred to in the text are indicated.

section; the corresponding samples were assayed by XRF, and the apatite, magnetite, carbonate and sulphide contents were calculated from the analytical data. The variations in mineral compositions were, however, larger than suggested by the mineral compositions given in the appropriate tables. Rock alterations were studied with the aid of sample series collected from the alteration zones, which are seldom more than some tens of centimetres or a few metres wide.

The term ferriphlogopite is used in this context to describe the orange, inversely pleochroic phlogopite that is generally called tetraferriphlogopite. The term carbonatite magma will be used instead of the correct term »liquidus with composition approaching possible carbonatite magma» suggested by Wyllie (1966 a, p. 350). For the sake of brevity the term pneumatolytic-hydrothermal is commonly replaced by hydrothermal.

Rock nomenclature

Ultramafites

The rocks formed from ultrabasic magma that intruded before the actual carbonatite intrusion are called ultramafites (ultramafic rocks) as defined by Wyllie (1967, p. 2). They comprise magnetite olivinites, olivine rock, orbicular olivine rock and pyroxenites.

Carbonatites and metacarbonatites

Heinrich (1966, p. 13) defines carbonatites as carbonate-rich rocks of apparent magmatic derivations or descent. According to the statement by Pecora (1956, p. 1538) that »The carbonatic fluid, whatever its temperature, concentration, or physical state, is an active invading agent capable of precipitating minerals», all the carbonate rocks within the fenite aureole of the Sokli complex could be regarded as carbonatites; however as suggested by Verwoerd, the term metacarbonatite has been adopted for the rocks that are the products of »a replacement process by which preexiting rocks of diverse compositions are wholly or partially transformed to carbonate or carbonate–silicate rocks» (Verwoerd, 1967, p. 13).

The lithological nomenclature of carbonatites lacks precision, and different terms are used by Western and Soviet geologists. The nomenclature introduced by Brögger (1921) and later modified by von Eckermann (1948) is widely employed in the West to define carbonatites rich in calcite (sövites) and dolomite (rauhaugites). In the USSR the corresponding variants are called calcite or dolomite carbonatites (Kukharenko *et al.* 1965, Ternovoy *et al.* 1969, Pozaritskaya and Samoilova 1972; Egorov, 1970). Von Eckermann's terms are used in this paper but owing to rapid mineralogical variations in the magmatic core and the streaky and uneven distribution of silicates, magnetite, sulphides and apatite, the mineral-qualifying names for the sövite and rauhaugite varieties that he proposed in 1948 are rejected. Accordingly, the rocks rich in carbonates are classified into the following groups:

Magmatic carbonatites	Meta-carbonatites	Carbonates	Dominative carbonate
Sövite	Metasövite	> 80 %	Calcite
Silicosövite	Metasilicosövite	50—80 %	Calcite
Beforsite	Metabeforsite	> 80 %	Dolomite

When the collective names of silicosövite and metasilicosövite are specified according to the prevailing silicates or opaques, the prefix silico is dropped as unnecessary and terms such as magnetite sövite or phlogopite metasövite are used instead.

Verwoerd (1967) has proposed that the term rauhaugite is to be abolished and replaced by beforsite. This is supported by Kresten (1980). Le Bas and Sörensen (1978) also recommend the term beforsite in connection with dolomite–carbonatite.

Carbonate-poor, medium- to coarse-grained rocks consisting chiefly of an intergrowth of magnetite, apatite, olivine (mostly altered), and micas are rather common at Sokli. These varieties are absent from the nomenclature of von Eckermann. Soviet authors call similar rocks camaforites, calcite–apatite–magnetite–forsterite rocks, (Borodin *et al.* 1973) or, by simply listing the chief minerals, calcite–magnetite–forsterite rocks, apatite–magnetite–phlogopite rocks etc. (Kukharenko *et al.*, 1965, Ternovoy *et al.*, 1969). In Palabora a similar rock has been called phoscorite (Russel *et al.*, 1954). An alternative spelling is foskorite (Palabora Mining etc, 1976). Egorov (1975) does not accept the term camaforite. The term phoscorite is adopted here for the carbonatites that contain less than 50 % carbonates and in which the chief minerals are those mentioned above. If the phoscoritic mineral composition is due to magmatic and hydrothermal processes the rock is called phoscorite; if due to metasomatic processes the name metaphoscorite is preferred.

Metasomatites

A wide range of metasomatic rocks of the second metasomatic generation occur in the Sokli massif. These rocks (pyroxene rocks, mica–amphibole rocks and mica rocks) are collectively called metasomatites.

Ultramafites

An ultramafic intrusion preceeding the carbonatite intrusion has produced ultramafites that initially occupied a greater volume than is suggested by the present state of the massif. This interpretation is based on findings from ultramafite fragments with original or sub-original mineralogical composition scattered thoughout the massif. An overwhelming proportion of the ultramafites are transformed into metaphoscorites. Ultramafite remnants occur most frequently in the metaphoscorite zone in the southeastern quarter of the massif (Fig. 3). The diameter of the fragments ranges from some centimetres to a few metres. The intrusive ultramafites are magnetite olivinites and pyroxenites. A peculiar rock variant, orbicular olivine rock, and isolated olivine rock body are described separately.

Magnetite olivinite

Magnetite olivinite is a dark green rock with coarse to pegmatoidal grain size. It is encountered as fairly fresh relics troughout the massif, e.g. in drill holes 419, 331 and 482 (Fig. 4). The mineral composition of the magnetite olivinite is simple, and its variation is as follows:

Olivine	50—80	volume-%
Magnetite	20—40	»
Apatite	1—10	»

Baddeleyite occurs as an accidental accessory mineral.

The olivine occurs primarily as idiomorphic crystals ranging from one to five centimetres in diameter. Even the olivine crystals

that are totally pseudomorphosed by a mixture of serpentine, carbonate and iddingsite show primary crystal forms with narrow rims of oxide. Magnetite, on the contrary, seldom displays idiomorphic habit although it looks otherwise fresh. The largest magnetite crystals have been over 10 centimetres across, but they are now broken up (Fig. 21, p. 23). The magnetite is titaniferous and is characterized by an abundance of ilmenite exsolutions as lamellae, rods and grains.

Apatite occurs as separate grains or aggregates with a grain length up to three millimetres. These are the biggest apatite grains found in the Sokli massif.

Olivinites may occupy a considerable proportion of the other carbonatite complexes in the Kola province, as in the Kovdor massif (Kukharenko *et al.*, 1965) where the olivinites have lower magnetite contents (5—8 %) than at Sokli. Extreme examples of a carbonatite complex rich in olivinite are in the Siberian Maimecha—Kotui region where olivinites make up about two thirds of the Gulinskaya complex (Egorov, 1970). The most common mode of occurence of olivinite in carbonatite complexes are stock-like bodies (Nemakit intrusion, Egorov, 1970), block xenoliths (Essej complex, Landa *et al.*, 1971) and small relics (Shawa complex, Heinrich, 1966). The mode of occurence of the magnetite olivinite in the Sokli complex is analogous to that in the Essej and Shawa complexes.

Pyroxenite

Wholly fresh intrusive pyroxenite has not been encountered in the drill holes. The best remaining sections occur in the metaphoscorite zone in DH 194 and DH 358 (Fig. 4), although here too, the original structure has been disturbed by later carbonate introduction (Fig. 5). The pyroxenite in the magmatic core is intensely scattered and altered. Its earlier occurence is indicated by isolated

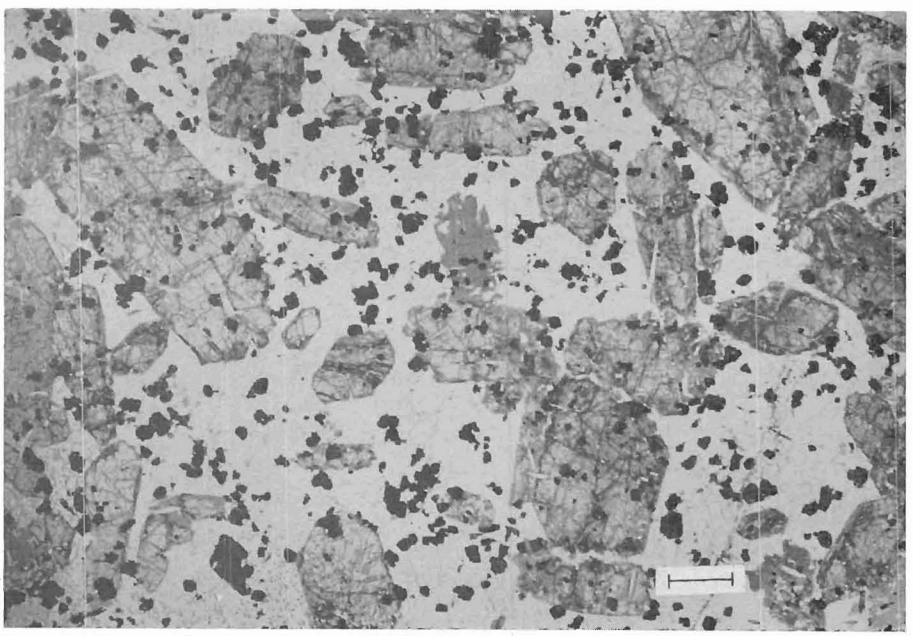

Fig. 5. Carbonatized and recrystallized pyroxenite. Diopside (grey) occurs as almost euhedral crystals, and magnetite (black) as fine-grained crystalline dissemination. Calcite is white. One nicol. Drill hole 193 at 133.5 metres. Scale bar, 1.2 mm.

pyroxene grains. The pyroxenite is medium to darkish green in colour and massive in texture. The average grain size is 1—10 mm, but some of the pyroxene crystals may attain a length of 3—4 cm. The mineral composition of the pyroxenites is:

Pyroxene	70—90 %
Magnetite	5—25 %
Apatite	1—5 %

Baddeleyite, which is often altered into zircon, is an accessory mineral.

The pyroxene is diopsidic in composition. Only recrystallized grains are well defined and idiomorphic in habit (Fig. 5). The diopside commonly contains apatite and magnetite inclusions.

The magnetite exhibits two generations: The first one occurs as big xenomorphic grains interstitial to the pyroxene; the second is present as small, idiomorphic and recrystallized crystals (Fig. 5). The former magnetite replaces the pyroxene. In composition and exsolutions the magnetite in the pyroxenite is comparable to that in magnetite olivinite. The occurrence of apatite also resembles that in magnetite olivinite.

The pyroxenite at Sokli is similar to the pyroxenite at Kovdor (Kukharenko *et al.*, 1965) but differs from that at Vuorijärvi, which is characterized by the presence of perovskite (Kapustin, 1976, b). Pyroxenites are more common in carbonatite complexes than are olivinites (Heinrich, 1966). Pyroxenitic rocks are often the principal components of the complexes, as at Vuorijärvi (Kapustin, 1976 b), Palabora (Hanekom *et al*,. 1965) and Gargill, Canada (Sandvik and Erdosh, 1977). The pyroxenites in carbonatite complexes are characterized by more or less intense alteration. In the Sebljavr massif in the Kola Peninsula, as at Sokli, primary unaltered pyroxenite is rarely found although pyroxenite is a predominant rock in the complex (Lapin, 1976).

Orbicular olivine rock

A peculiar, orbicular olivine rock (Fig. 6) occurs in one drill hole (DH 434, Fig. 4) as an intersection four metres long. The rock has fairly sharp contacts against the surrounding magnetite-bearing olivine sövite of magmatic Stage II. The diameter of the orbicules ranges from two to 15 millimetres, the average being 7—10 mm (Fig. 6). The orbicules are spherical or ellipsoidal in form but some extreme case may be scretched out into a few centimetres long discus. The ellipsoidal orbicules do not show any preferred orientation. Late dolomite veinlets cut both orbicules and groundmass. The orbicules display a rhyth-

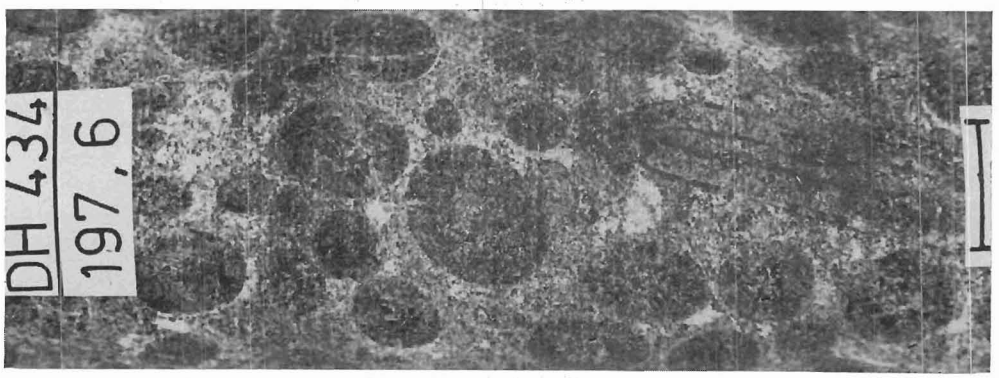

Fig. 6. Orbicular olivine rock. Scale bar, 1.0 cm.

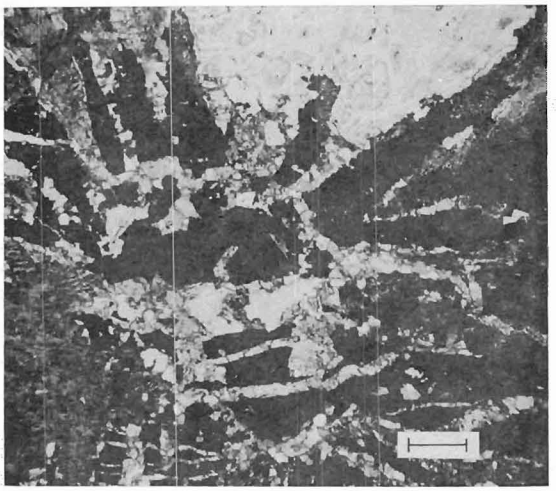

Fig. 7. Spherulitic magnetite growths from the centre of an orbicule. Orbicular olivine rock. One nicol. Drill hole 434 at 197.6 metres. Scale bar, 0.5 mm.

mic, concentrically zoned texture. The central part is composed primarily of olivine and magnetite. The latter often shows a spherulitic growth (Fig. 7). The olivine is commonly altered into serpentine, and the magnetite is corroded by and riddled with carbonate and fine-flaked mica. The outer contour of the central part may be marked by fine-grained magnetite. Next follows a monomineralic olivine zone that may be intruded by wedge-shaped magnetite from the core. In two neighbouring orbicules the olivine zone may be almost fresh in one and completely serpentinized in the other (Fig. 8). The outer shell, which invariable contains a serpentine—iddingsite matrix, is generally 0.5 mm thick. It has a knife-sharp contact against the interorbicular groundmass, but when the shell is covered by fine magnetite grains the contours are serrated. The groundmass is equigranular and fine-grained, and is composed of carbonate, phlogopite, serpentinized olivine and magnetite.

A very similar orbicular rock has been described from the Vuorijärvi massif where

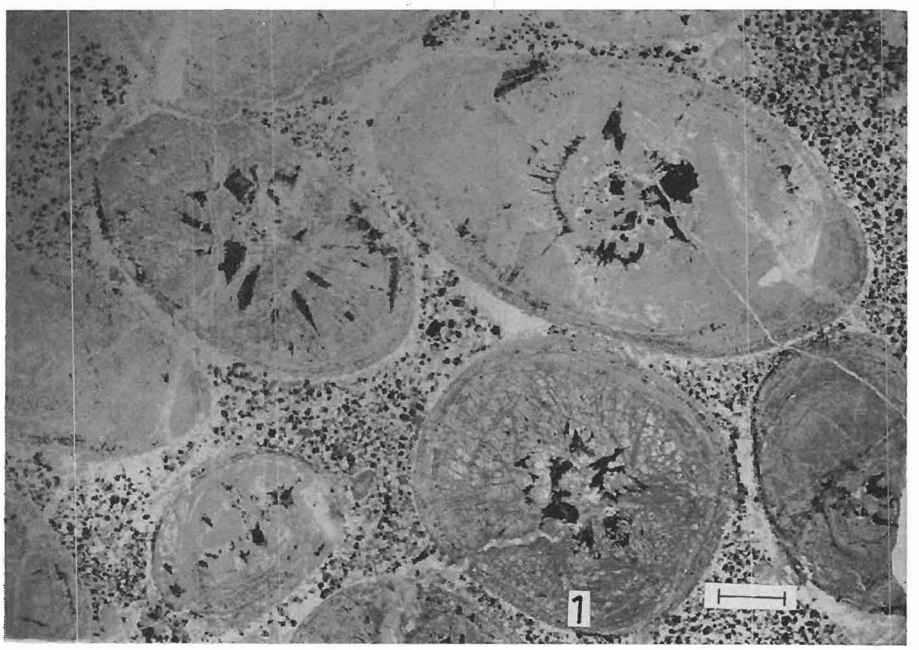

Fig. 8. Orbicules in orbicular olivine rock. In one orbicule (number 1) olivine (white) is moderately serpentinized (grey). In the other orbicules olivine is completely altered into serpentine. Magnetite is black. Note the knife-sharp contours of the orbicules against the interorbicular groundmass. One nicol. Drill hole 434 at 194.2 metres. Scale bar, 2.0 mm.

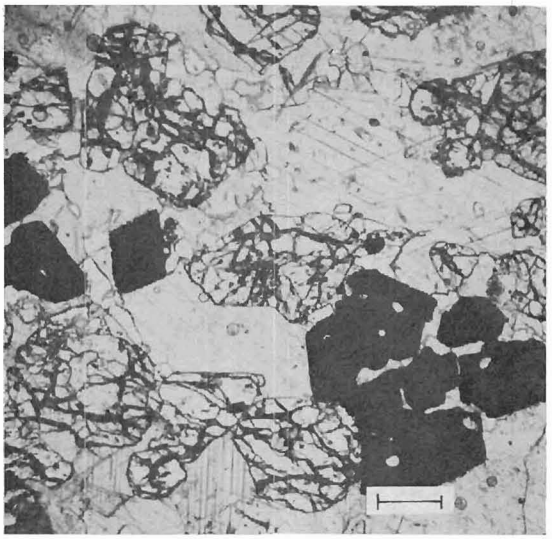

Fig. 9. Olivine rock showing recrystallized olivine (white, high relief) and magnetite (black). One nicol. Drill hole 433 at 172.3 metres. Scale bar, 0.5 mm.

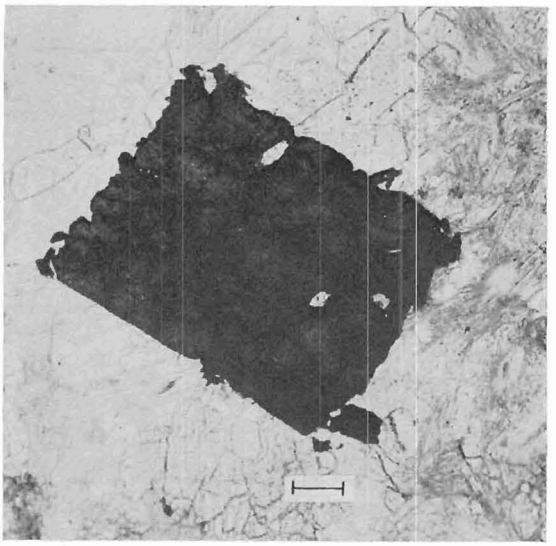

Fig. 10. Cubic perovskite crystal in olivine rock. Thin richterite needles to the right. One nicol. Drill hole 433 at 166.4 metres. Scale bar, 0.3 mm.

it occurs with a spherulite textured rock (Lapin, 1976). These textures are regarded as fairly convincing proof of the limited miscibility between ore—silicate and carbonate liquids. It is suggested that liquation was involved in the process of formation and separation of the rocks of carbonatite (sövite) and camaforite (phoscorite) series. Verwoerd (1967) has described pisolitic metacarbonatite from the Goudini complex, South Africa. The rock is highly altered but, presumably, it represents an igneous rock of ultrabasic composition.

Olivine rock

In Kaulusrova area, an isolated olivine rock body has been intersected by drill hole 433 (Fig. 4). The body was indicated by a high velocity zone detected by vertical seismic sounding. The olivine rock has a moderate magnetite content, in places up to 30 per cent. It is dark grey, massive and idiomorphic textured and from fine- to medium-grained (grain size averaging 1—3 mm). It is notably different from the coarser-grained magnetite olivinite, magmatic phoscorite and metaphoscorite. The rock is typified by idiomorphic olivine and magnetite crystals which are embedded in equigranular calcite (Fig. 9). The texture indicates recrystallization. The accessory minerals are phlogopite, apatite, zircon and perovskite. The presence of perovskite as cubic crystals (Fig. 10) is exceptional and has been noted in no other rocks at Sokli. Towards the margins of the olivine rock the amount of calcite increases and corrodes both olivine and magnetite, which adopt skeletal form. The olivine rock is gradually transformed into the sövite of magmatic Stage II. Mineralogically this is revealed by the increase in sugary calcite and the appearance of baddeleyite and pyrochlore.

Similar apatite—forsterite—magnetite rocks, which have been interpreted as metasomatites after olivinites, pyroxenites and ijolite—melteigites by multiphase processes of alka-

line and CO_2 emanations and fluids, occur in the Kovdor massif (Kukharenko *et al.*, 1965). The olivine rock at Sokli shows clear recrystallization features, and it is suggested that the rock was transformed at elevated temperature from ultramafites (olivinites) before the carbonatite magma intrusion. Magmatic carbonate injections later replaced the rock, and in the margins it grades into magmatic sövites.

Alteration of ultramafites

Ultramafites, which originally probably constituted stocks and other type of intrusive bodies and were distributed throughout of the present carbonatite massif, have undergone complicated alterations. As a result of these irregular and chemically varying processes rocks with variable mineral assemblages were formed. The ultramafites are characterized by the widespread development of a system of local fracturing, crushing and shearing and complicated multi-stage veining. All these furthered the alteration of the ultramafites into metaphoscorites, phlogopite and amphibole rocks, and metasilicosövites. The

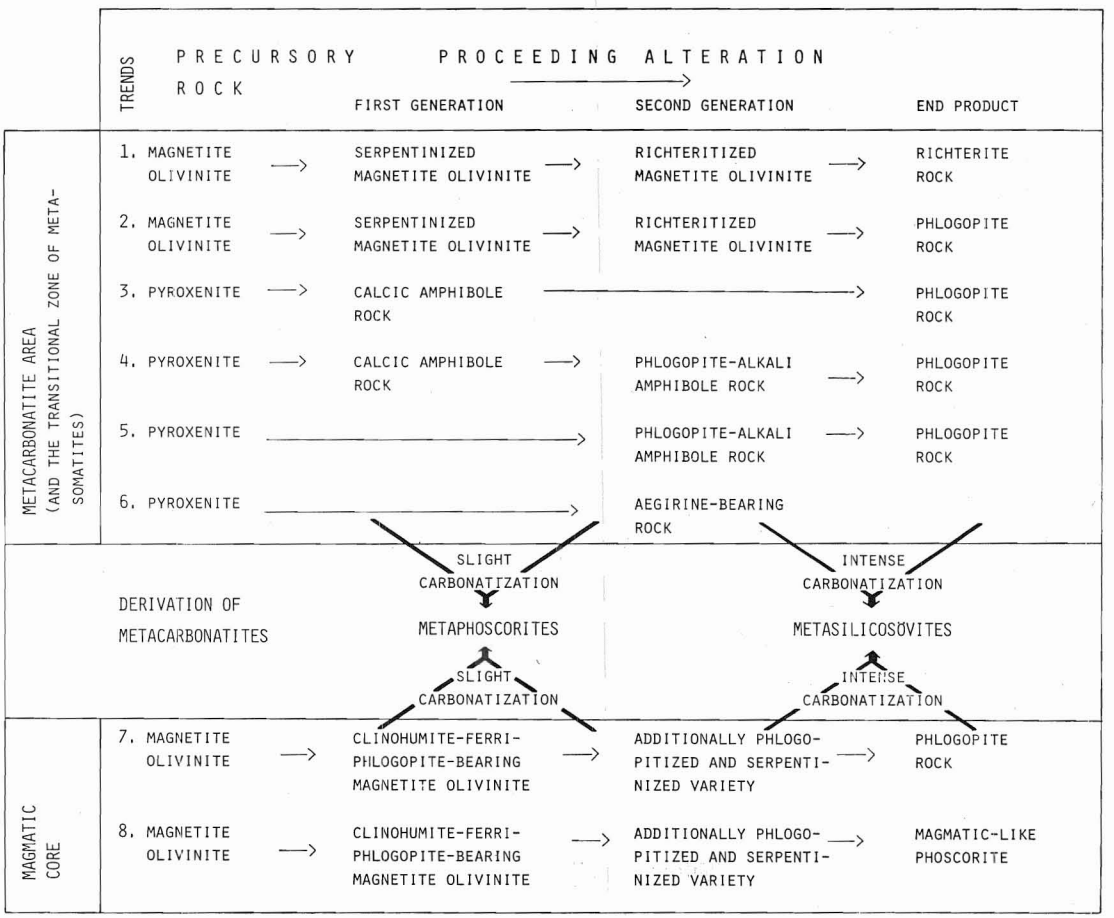

Fig. 11. Alteration trends in the ultramafites and the correlation of the metacarbonatites to them.

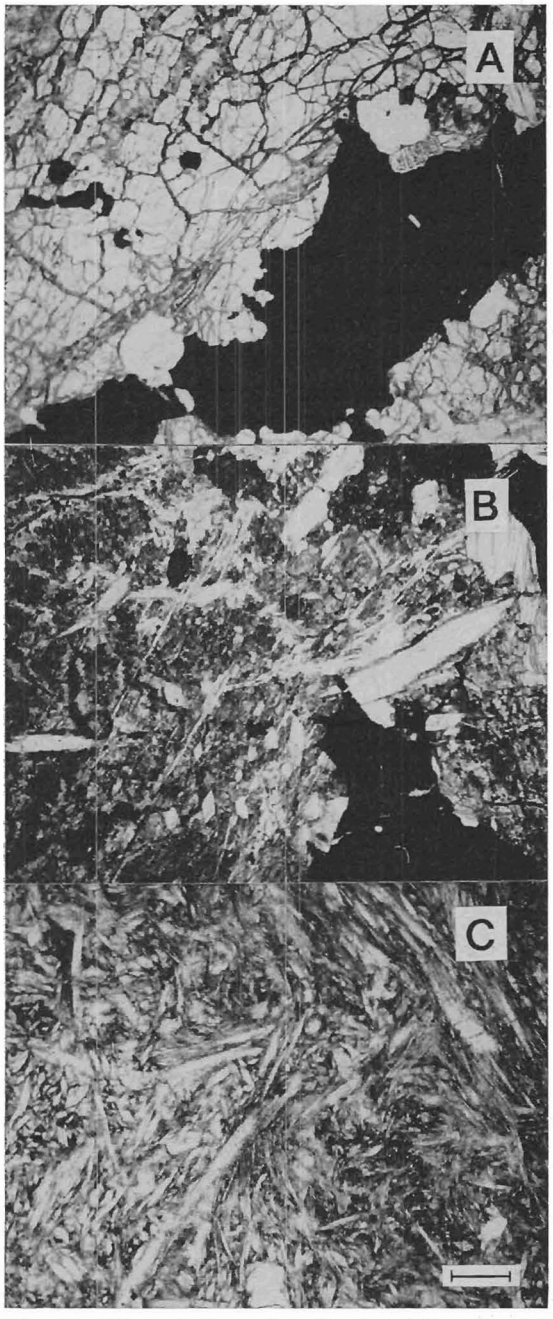

Fig. 12. Microphotographs showing alteration of magnetite olivinite into richterite-rich rock. One nicol. Scale bar, 0.5 mm.
A. Almost unaltered magnetite olivinite. Drill hole 331 at 169.0 metres.
B. Olivine is altered into serpentine—iddingsite matrix (dark grey) and mica and richterite (white to pale grey). Richterite is distinguished as thin needles. Magnetite (black) is strongly corroded. Drill hole 358 at 118.5 metres.
C. Almost monomineralic richterite rock developed from magnetite olivinite. Drill hole 194 at 358.7 metres.

alteration products are locally recognisable within a few metres or tens of centimetres around the remnants of the ultramafites. It is also possible to follow some alteration trends by collecting selected samples from separate units at different stages of the alteration sequence. There are marked differences in the transformation, depending on whether it took place in the meta carbonatite area or in the magmatic core. The main alteration trends observed in these areas are illustrated in Fig. 11 and will be described separately.

Alteration in metacarbonatite area

Alteration of magnetite olivinite into richterite-rich rock (Fig. 11, trend 1)

The sample suite for the description of this alteration trend was collected from separate rock units. A starting sample was taken from drill hole 331 (Fig. 4), which, for a distance of several metres, intersected a fairly fresh magnetite olivinite. The altered samples were collected from the metaphoscorite zone in the southeastern part of the massif (DH 194, 358 and 413, Fig. 4). The mineralogical changes towards richterite-rich rock are illustrated by the photomicrograph in Fig. 12. The alteration begins with autometasomatic serpentinization of olivine (Fig. 12 A). This is followed by carbonatization and accompanied by replacement of magnetite by the above minerals. Needles of richterite, which grow in size and abundance appear in a comparatively homogeneous matrix of olivine (Fig. 12 B). Simultaneously, phlogopite flakes appear and zircon crystallizes, partly at the expense of baddeleyite.

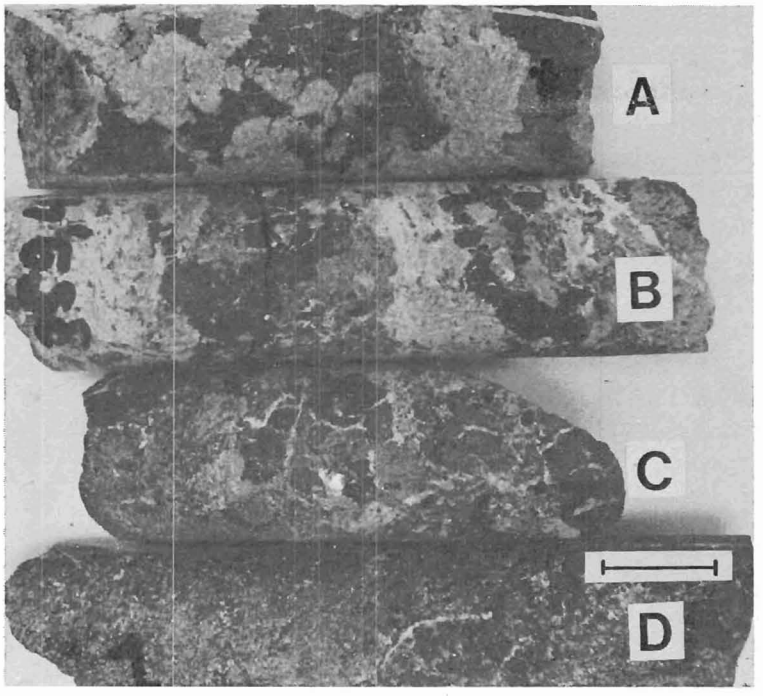

Fig. 13. Specimens showing the development of a phlogopite rock from richteritized magnetite olivinite. Drill hole 194. Scale bar, 1.0 cm.

A. At 358.7 metres. Richteritized magnetite olivinite.

B. At 359.7 metres. Phlogopite (dark grey) begins to develop between ragged magnetite grains (black) and richterite matrix (pale grey).

C. At 360.4 metres. Phlogopite has become predominant mineral.

D. At 360.8 metres. Phlogopite rock with some magnetite relics. White dots and threads are calcite and apatite.

The end product of this process is a rock composed mainly of richterite (Fig. 12 C) with subordinate corroded magnetite, primary apatite, irregularly shaped carbonate and accessory zircon. The rock is typically massive but in shear zones it exhibits a schistose texture at the same time as richterite becomes increasingly dominant.

Development of phlogopite rock from richteritized magnetite olivinite (Fig. 11, trend 2)

After the richteritization of the magnetite olivinite the alteration may continue with the development of phlogopite rock. The process can even be traced megascopically, as is seen in Fig. 13. In a speckled specimen (Fig. 13 A), the light part of the rock consists of richterite with subordinate carbonate and phlogopite. The black portion is corroded magnetite. In the next specimens phlogopite appears at the expense of magnetite and richterite. The phlogopite is discernible as dark grey grains (Fig. 13 B and C). Ultimately, phlogopitization results in an almost monomineralic phlogopite rock (Fig. 13 D). All that has survived of the original magnetite olivinite are apatite grains commonly coated by fine-grained iron oxide. Zircon, one of the alteration generation minerals may attain a size of up to 10 mm. Phlogopite occurs as randomly oriented big flakes (length, 0.4—0.8 mm) displaying a subparallel arrangement. Reversed pleochroism of phlogopite indicates that it is ferriphlogopite in composition. We may conclude that the magnetite and apatite in magnetite olivinite best resist alteration and that olivine is the first mineral to decompose. Fine-grained ragged relics of magnetite occur in intensely altered rocks. Apatite, which is encountered as angular-grained aggregates in otherwise completely phlogopitized rocks, has survived still better. Serpentine, iddingsite, carbonates, richterite,

phlogopite (ferriphlogopite) and zircon are the minerals of the alteration generation.

The forsterite–magnetite rocks at Kovdor, Vuorijärvi and Arbarastah resemble the magnetite olivinite at Sokli although their alterations show different trends (Borodin *et al.*, 1973). Apatitization has played an important role in the Russian complexes and given rise to apatite–forsterite–magnetite rocks. Forsterite may have been recrystallized, but the richteritization so essential in the metacarbonatite area of Sokli has not been reported. Carbonatitization has introduced ferriphologopite, clinohumite, pyrochlore, baddeleyite and zirkelite in these rocks. Mineralization corresponding to the magnetite olivinite at Sokli has been found only in the magmatic carbonatite core as a result of hydrothermal activity.

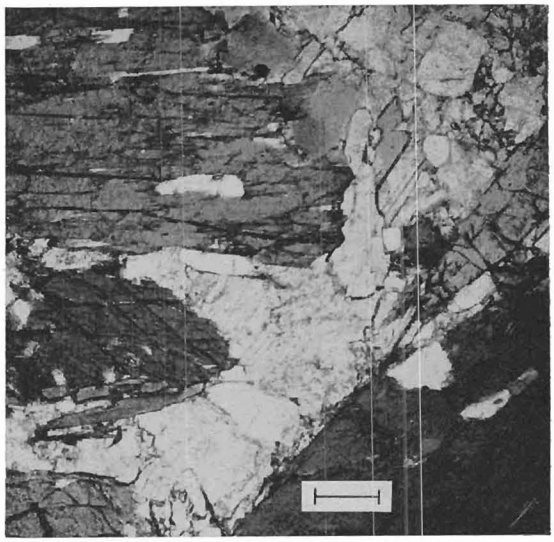

Fig. 15. Calcic amphibole rock developed from pyroxenite. Carbonate (white) has not affected the crystals of calcic amphibole (sodian edenite, grey to dark grey). One nicol. Drill hole 195 at 144.9 metres. Scale bar, 0.5 mm.

Alteration of pyroxenite

The alteration of pyroxenite in the metacarbonatite area has yielded more complicated products than that of magnetite olivinite. It follows four main trends that, not uncommonly, overlap each other (Fig. 11):

1. Alteration into calcic amphibole rock
2. Alteration into phlogopite–alkali amphibole rock
3. Alteration into aegirine-bearing rock
4. Alteration into phlogopite rock.

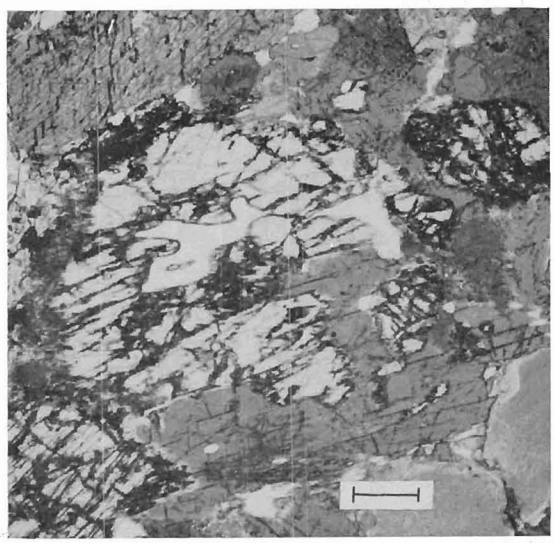

Fig. 14. Poikiloblastic development of calcic amphibole (grey) around pyroxene crystals (white) in pyroxenite that is altering towards calcic amphibole rock. One nicol. Drill hole 419 at 84.7 metres. Scale bar, 0.5 mm.

No regularity in the areal distribution of the alteration types has been found in the area of metacarbonatite and metasomatites. The petrographical changes in the alteration sequences are described.

Alteration into calcic amphibole rock is the first transformation of pyroxenite and seems to have preceeded the phase of alkaline metasomatism. Diopside prisms are altered into amphibole as in uralitization. The amphibole also grows poikiloblastically around diopside (Fig. 14). Simultaneously some mica may appear. In places the amphibole occupies 80 to 90 per cent of the volume of the rock, the other minerals being apatite, carbonate

and baddeleyite or zircon. Such a rock is dark green, medium-grained and massive in texture. It is encountered as a fragmental rock mostly in the areas of metacarbonatite and in the metasomatic transition zone but also within the magmatic carbonatite core. There is evidence of a carbonatization generation that had slight or no effect on the amphibole (Fig. 15) in the amphibole rock. The amphibole prisms show fresh or extremely thin blue rims against an interstitial carbonate that contains rounded primary apatite grains. The amphibole in the amphibole rocks is one of the calcic amphiboles, sodian edenite with subcalcic varieties in composition (see p. 75).

Alteration into phlogopite–alkali amphibole rock. The alteration of diopside into alkali amphibole is much more widespread than the calcic amphibolization of diopside. The development of alkali amphibole may begin directly from diopside prisms or come after the formation of calcic amphibole (Fig. 85, p. 71). It is not unusual for the one part of the diopside crystal to be altered into calcic amphibole and the other into alkali amphibole (Fig. 84, p. 71). The alkali amphibolization is associated with phlogopitization and moderate carbonatization. At the same time magnetite is replaced by carbonate, and its grain size is reduced. This paragenetic sequence of alteration has led to the development of rocks called, for brevity, mica–amphibole rocks. They are widely distributed in the area of metacarbonatites and in the transition zone of metasomatites.

The mica–amphibole rock is fine to medium-grained, massive, sometimes weakly foliated in texture. The mutual abundances of alkali amphibole and phlogopite vary as do those of magnetite, apatite and carbonate. Baddeleyite has altered into zircon. Characteristic of the alkali amphibole are small-bladed crystals although bigger laths also occur. The pale bluish green hue and abnormal bluish interference colour suggest a composition of the arvfedsonite–eckermannite series. This is verified by one mineral analysis of a mica–amphibole rock and another of an alkali amphibole-bearing phlogopite rock; both show eckermannitic composition (p. 74). Phlogopite has replaced amphiboles. The size of the phlogopite flakes ranges from 0.5 mm to 2.0 mm. In addition, there is a coarser-flaked generation up to some centimetres in diameter. The phlogo-

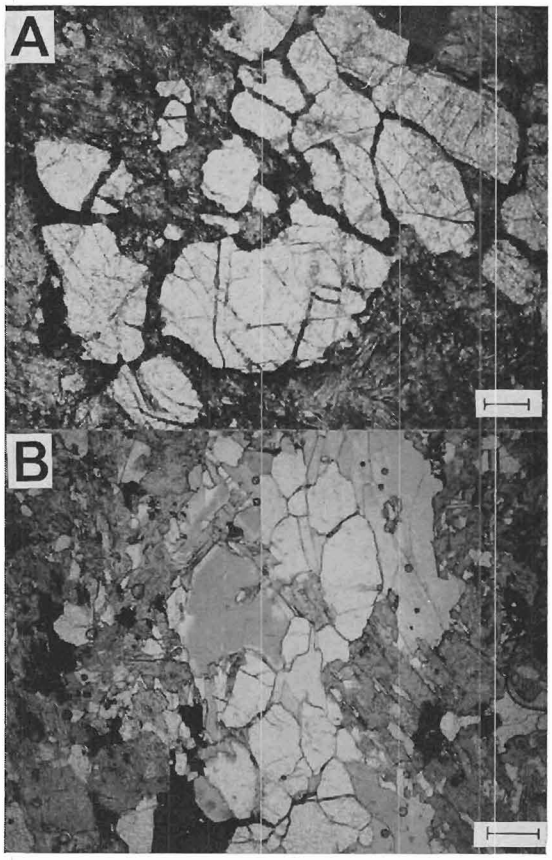

Fig. 16. Different apatite generations in mica–alkali amphibole rock derived from pyroxenite. One nicol.

A. Primary apatite characteristically fractured and coated by iron pigment. Drill hole 193 at 212.6 metres. Scale bar, 0.3 mm.

B. Metasomatically introduced apatite (white, clean grains) concentrated in a vague phlogopite (grey) band. Alkali amphibole grains are dark grey. Drill hole 358 at 267.7 metres. Scale bar, 0.5 mm.

pite in this alteration sequence displays strikingly constant pleochroism: Z = pale green, X = pale orange yellow. The apatite abundance may locally exceed 20 volume per cent. Primary apatite (Fig. 16, A) and, in larger quantities, metasomatically introduced apatite (Fig. 16, B) are both present.

The apatite inclusions common in magnetite and diopside witness the presence of primary apatite. Metasomatic apatite accompanies phlogopitization. This is demonstrated by the concentration of loosely packed apatite aggregates in phlogopite-rich bands, giving rise to a vague banded texture in the mica—amphibole rock (Fig. 16, B). In connection with the most intense apatitization some sulphides (pyrrhotite) has been introduced. Carbonate occurs as small xenomorphic grains interstitial to other minerals.

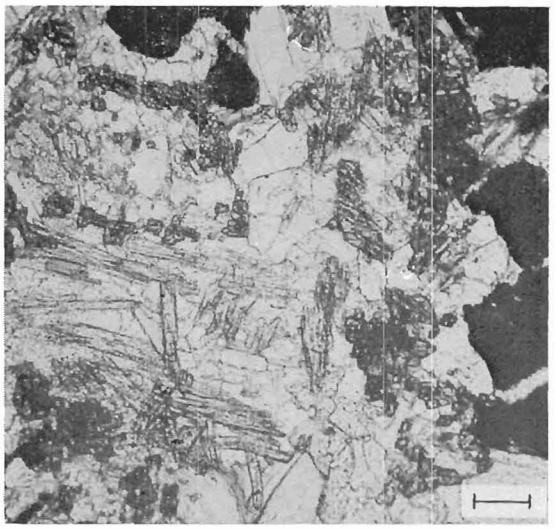

Fig. 17. Small aegirine needles (pale grey longitudinal sections, dark grey cross sections) in fine-grained aegirine rock developed from pyroxenite. White matrix is mainly carbonate. One nicol. Drill hole 193 at 125.0 metres. Scale bar, 0.3 mm.

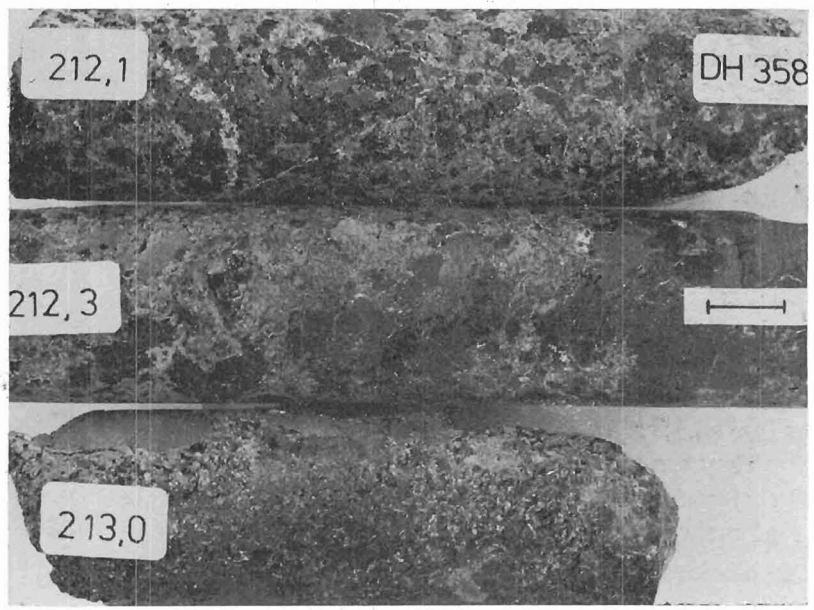

Fig. 18. Specimens showing development of porphyroblastic phlogopite rock from medium-grained, slightly altered pyroxenite. Drill hole 358. Scale bar, 1.0 cm.

At 212.1 metres. Medium-grained slightly altered pyroxenite. Ragged magnetite (black). Diopside, phlogopite, alkaline amphibole (medium to dark grey).

At 212.3 metres. Transitional stage of phlogopitization. Developing phlogopite (dark grey) is best dicernable adjacent to magnetite (black).

At 213.0 metres. Porphyroblastic phlogopite rock. Phlogopite porphyroblasts in upper part of specimen. White dots in fine-flaked phlogopite matrix are carbonate and subordinate apatite.

Alteration into aegirine-bearing rock has been encountered only in drill holes close to the fenite aureole (Fig. 4, DH 70, 193, 194, 195). Isolated aegirine grains have, however, been found in some thin sections from the area of the magmatic core. The aegirinization of pyroxenite is not a separate process but is associated with the development of alkali amphibole and phlogopite and also with carbonatization obviously stronger than in the alteration sequences described above. Diopside prisms are replaced by aegirine in the margins and along cleavage planes until the aegirine pseudomorphs have completely replaced the diopside crystals (Fig. 81, p. 70). The initial apatite and magnetite inclusions have survived in the aegirine prisms, but the magnetite is so extensively replaced by carbonate that only ilmenite lamellae show the original crystal boundaries (Fig. 82, p. 70). Alkali amphibole, together with some green phlogopite, has developed in like fashion. Baddeleyite is unaltered. At this stage, when diopside still exists, the rock shows the original, medium grain size. Further alteration reduces the grain size of all the minerals (Fig. 17). In the final stage diopside has disappeared, baddeleyite has altered into zircon, phlogopite has lost its colour and aegirine occurs as clusters of small needles. No apatite was introduced during aegirinization.

Alteration into phlogopite rock follows two trends begining with similar medium-grained pyroxenites (Figs. 11, 18 and 19). In the first stage, before marked development of alkali amphibole, large-flaked dark green phlogopite crystallized at the expense of calcic amphibole (Fig. 18). This phlogopitization occasionally led to the formation of an almost monomineralic phlogopite rock that consists

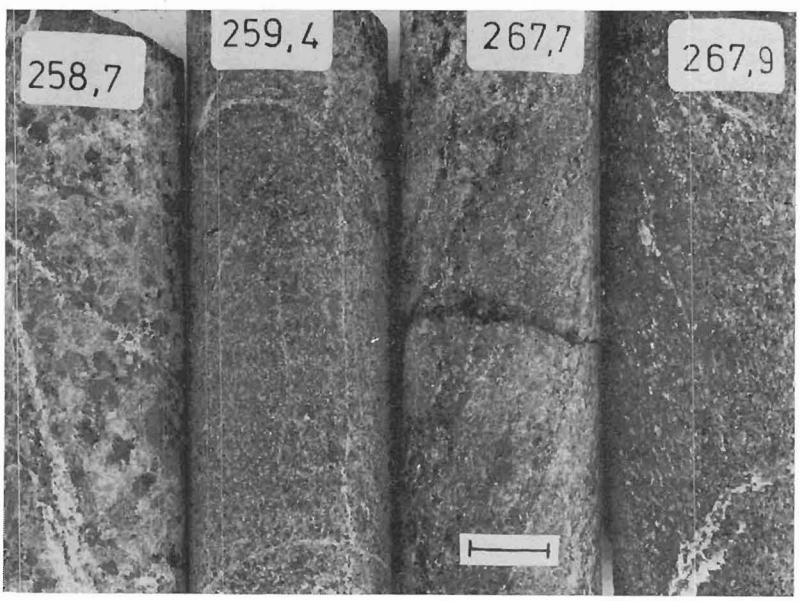

Fig. 19. Specimens showing development of fine-flaked phlogopite rock from medium-grained moderately altered pyroxenite. Drill hole 358. Scale bar, 1.0 cm.
At 258.7 metres. Moderately altered pyroxenite.
At 259.4 metres. Fine-grained alkaline amphibole rock developed from pyroxenite.
At 267.7 metres. Phlogopitized (dark grey) alkaline amphibole rock in vague bands.
At 267.9 metres. Fine-flaked phlogopite rock. White dots are apatite and subordinate carbonate.

of porphyroblastic dark green phlogopite up to 5 cm in diameter in the finer-flaked (0.5—3.0 mm) and slightly paler green phlogopite matrix. The primary silicates and magnetite are wholly replaced by phlogopite, and all that remains are some apatite grains and zircon pseudomorphs after baddeleyite. The matrix contains secondary carbonate. The other phlogopitization trend is connected with the development of alkali amphibole. In this alteration sequence the primary grain size of pyroxenite is gradually reduced (Fig. 19). The transformation proceeds as in the mica—amphibole rock except that the phlogopitization extends further. Sometimes, as illustrated in Fig. 19, the pyroxenite alters first into an alkali amphibole-rich rock that is then phlogopitized. In the transitional stage the phlogopitization may manifest itself as vague banding. Note that simultaneous apatitization is associated with phlogopitization. The final fine-grained phlogopite rock is green, massive or weakly foliated and contains abundant apatite (10—20 volume per cent), some magnetite and alkaline amphibole and subordinate carbonate. Zircon is an accessory mineral.

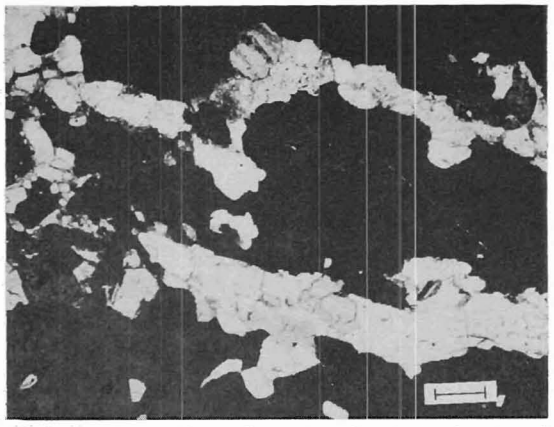

Fig. 20. Magmatic carbonatite shoots in fractured magnetite (black) of coarse-grained magnetite olivinite. White shoots are fine-grained calcite and apatite containing also pyrochlore crystals (dark grey). One nicol. Drill hole 390 at 169.0 metres. Scale bar, 0.5 mm.

Alteration in the magmatic core

Alteration of magnetite olivinite

Magnetite olivinite has been encountered in the magmatic core as nearly unaltered fragments. Its alteration, due to magmatic carbonatite activity, follows a path somewhat different from the alteration in the metacarbonatite area. The first signs of alteration appear in the fissures that intersect the rock, and along which carbonatite shoots, sometimes with pyrochlore have intruded (Fig. 20). Olivine begins to alter into clinohumite on the grain boundaries, and ferriphlogopite begins to crystallize. Then follows rapid development of large phlogopite flakes alongside serpentinization and carbonatization of the olivine. From this stage two main trends can be distinguished: magmatic phoscoritization, and the development of phlogopite rock.

The development of phlogopite rock (Fig. 11, trend 7) from magnetite olivinite is a more simple process than that of phoscoritization described next. Intense carbonatization and carbonatite veining is typically associated with phlogopitization. The rock is cut by carbonate veinlets of different generation from some millimetres to 1—3 cm thick. Even megascopically it is seen how the pegmatoidal magnetite is gradually replaced by phlogopite and how in the final stage the rock is transformed into nearly monomineralic phlogopite rock (Fig. 21). Phlogopitization has been so effective that all the primary minerals have been altered and no other silicate mineral has been produced. Other minerals present in the phlogopite rock are calcite, baddeleyite and pyrochlore. The porphyroblastic phlogopite (Fig. 21, C) derived from the first stage of alteration at the same time as richterite was formed. The phlogo-

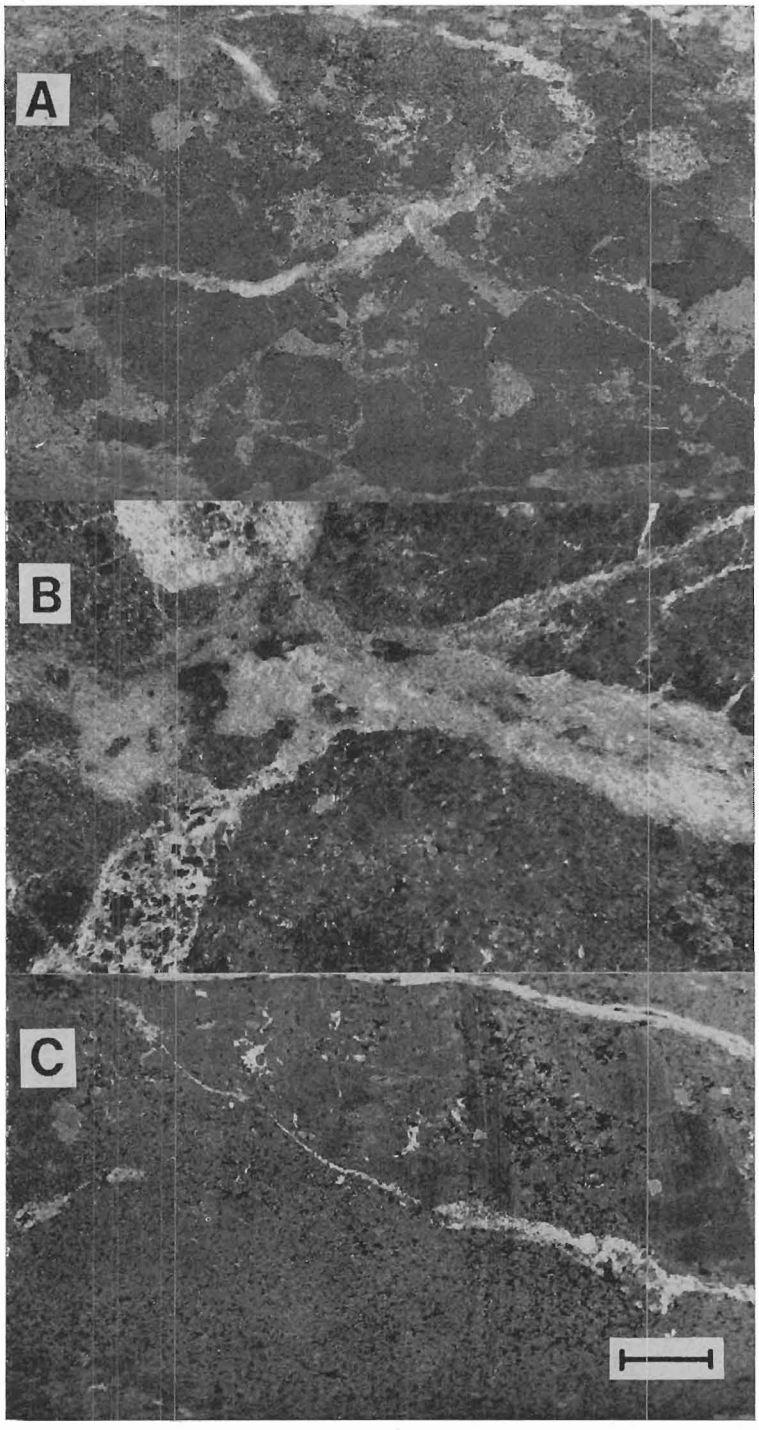

Fig. 21. Specimens of drill core showing development of phlogopite rock from pegmatoidal magnetite olivinite. Drill hole 436. Scale bar, 1.0 cm.

A. Moderately phlogopitized magnetite (black). At 24.5 metres.

B. Veinlets of carbonate and carbonatite cutting intensely phlogopitized rock. Magnetite (black) occurs as small relics. At 34.6 metres.

C. A phlogopite rock. Porphyroblastic phlogopite is hardly discernible in fine-flaked phlogopite mass. At 34.8 metres.

pite of the intense phlogopitization is fine-flaked ranging in size from 0.1 mm to 1.0 mm. The phlogopite displays weak or moderate pleochroism Z = colourless, X = light orange. The inverse pleochroism refers to ferriphlogopitic composition. Carbonate forms irregular interstitial nests in the phlogopite mass. Baddeleyite and pyrochlore occur in these nests as accessory minerals. The baddeleyite exists as idiomorphic prisms or xenomorphic grains (Fig. 22). In several thin sections pyrochlore invariably shows deep orange colour without any marked zonation.

The high uranium content in the whole rock analyses indicates that pyrochlore is uranium-bearing. Baddeleyite and uranopyrochlore are early minerals that seem to have crystallized during phlogopitization. This suggests that the phlogopitization, or potassium metasomatism, preceded the phoscoritization of the magnetite olivinite.

Magmatic phoscoritization (Fig. 11, trend 8) causes slightly altered, coarse-grained magnetite olivinite to pass into a medium-grained rock. This is indicated by the granulation and replacement of magnetite and phlogopite by a fine-grained ferriphlogopite—carbonate matrix. An essential mineralogical change at this stage is the formation of a new, fine-grained ferriphlogopite generation (Fig. 23). The large, older phlogopite flakes break down and the fragments are rimmed by a dark orange ferriphlogopite. The first richterite needles crystalize in the serpentine—iddingsite—carbonate matrix that was formed from olivine. Pyrochlore dissemination and zircon crystals appear. The further process brings about increasing amount of richterite, carbonate, zircon, pyrochlore and, in the final stage, ilmenite. The ilmenite contains ferriphlogopite and richterite inclusions indicating the late crystallization of the ilmenite. Ultimately the rock achieves a mineralogical composition close to that of the magmatic phoscorite of Stage III, which was transformed from the phoscorite of Stage I by a similar hydrothermal process. The al-

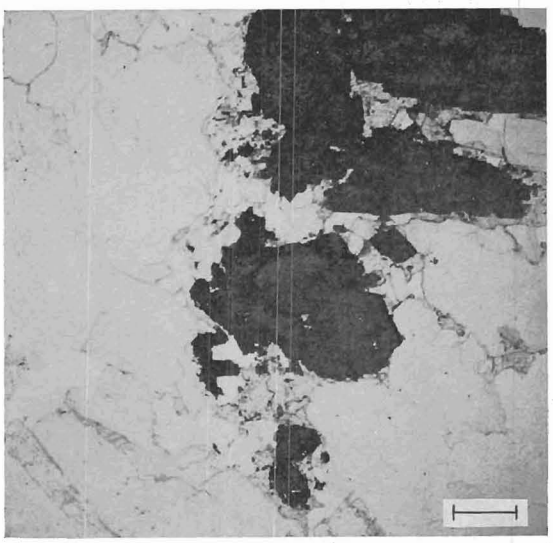

Fig. 22. Phlogopite rock derived from magnetite olivinite. All primary minerals except baddeleyite (dark grains) are replaced by phlogopite (pale grey). One nicol. Drill hole 436 at 38.6 metres. Scale bar, 0.5 mm.

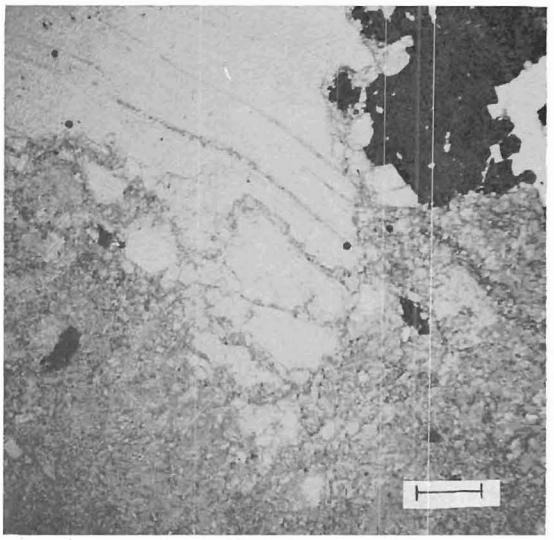

Fig. 23. Micatized magnetite olivinite with close affinity to the ferriphlogopite rich phoscorite of the magmatic stage III. Note large — and fine-flaked ferriphlogopite generations. Magnetite is black. One nicol. Drill hole 456 at 122.9 metres. Scale bar, 0.5 mm.

teration of magnetite olivinite into a rock resembling magmatic phoscorite may take place within a range of one metre.

Alteration of pyroxenite

No continuous rock suites of pyroxenite have been found so far in drill holes intersecting the magmatic core. Hence, it has not been possible to study the alteration of pyroxenite in the magmatic core. All that has been encountered are some scarce and almost completely decomposed remnants of pyroxenite and isolated diopside grains (Fig. 24). This can be interpreted in two ways: the pyroxenite was more susceptible to alteration than the magnetite olivinite and was therefore nearly completely digested by carbonatite, or the ultramafites contained subordinate amount of pyroxenite in place of the present carbonatite core. The rare findings show that the diopside presumably altered into light green alkali amphibole before the intrusion of carbonatite (Fig. 24). Magnetite was intensely carbonatized.

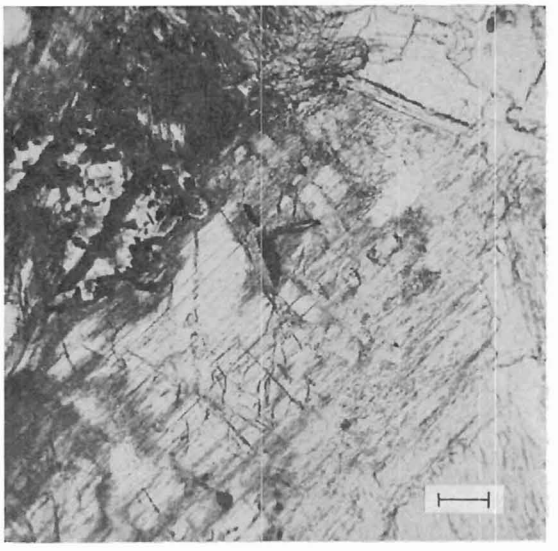

Fig. 24. Pyroxenite relic in magmatic sövite of stage II. Diopside (white) is altered partly or totally into alkali amphibole (pale grey) and magnetite is replaced by carbonate. Outlines of magnetite are marked by ilmenite lamellae (black). One nicol. Drill hole 3 at 66.2 metres. Scale bar, 0.3 mm.

Metacarbonatites

Metacarbonatites occupy a considerable portion (about one third) of the Sokli massif. They form a well-defined metacarbonatite area in the eastern and southern part of the massif (Fig. 3). They also occur in marked amount in the transition zone of metasomatites and as isolated fragments in the magmatic core. In the metacarbonatite area metaphoscorites and metasilicosövites alternate in an intricate replacement pattern that is further complicated by magmatic carbonatite injections. Structurally the metacarbonatite area is a continuation of the transition zone of metasomatites towards the magmatic carbonatite core. Metasilicosövites which are the predominant rocks in the metacarbonatite area, form like a matrix in which fragments of metaphoscorites occur. The occurrence of metaphoscorites has been drawn on the geological map (Fig. 3) mainly on the basis of data from detailed magnetic mapping (Fig. 2).

Metaphoscorites

Metaphoscorites are regarded as slightly carbonatized alteration varieties of ultramafites (Fig. 11). During polyphased metasomatic alteration processes the ultramafites were reconstituted by the addition of aegirine, amphiboles, micas, apatite, carbonates,

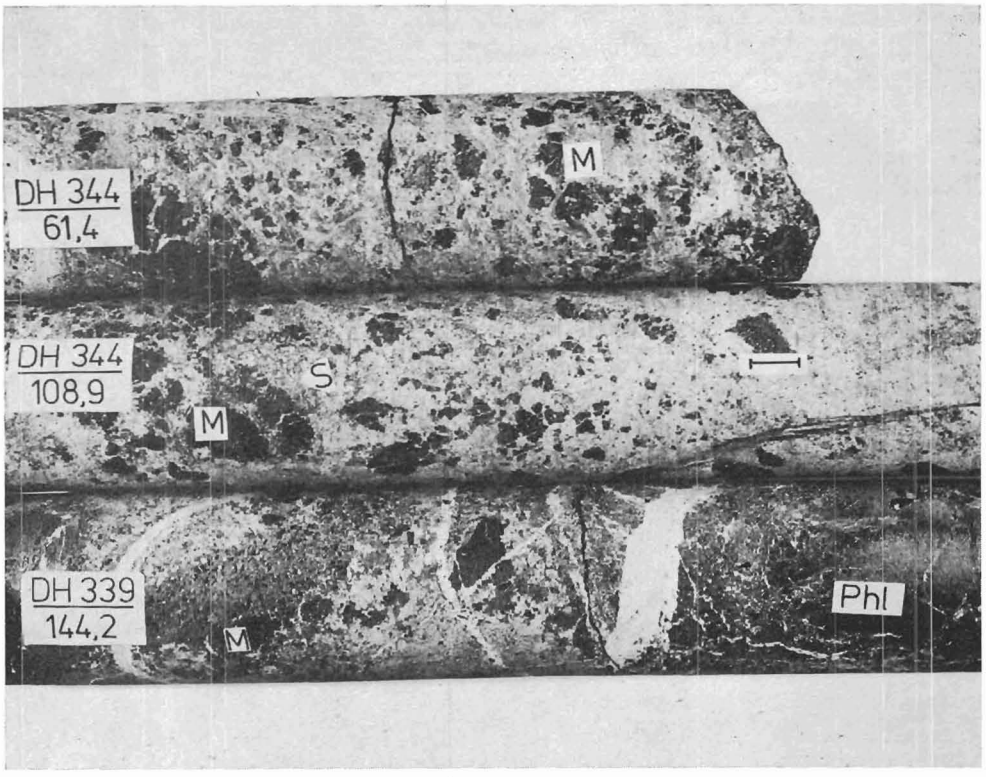

Fig. 25. Typical specimens of metaphoscorites from the metacarbonatite area. M = magnetite, S = sulphides, Phl = phlogopite. The grey to pale grey matrix consists of serpentine, iddingsite, carbonate, fine-flaked phlogopite and ferriphlogopite, richterite and apatite. Scale bar, 1.0 cm.

sulphides and zircon. Within the magmatic core, where metaphoscorites were trapped during the intrusion of the core-plug, the variable effects of magmatic carbonatites complicated still further the development of metaphoscorites. Characteristic phenomena wherever metaphoscorites occur are the fading of ultramafites into metaphoscorites together with every possible transitional rock variety. A description of the alteration of ultramafites is, in fact, a description of the development of metaphoscorites, and this has already been given. The following descriptions refer to metaphoscorites only:

1. Metaphoscorites occur as fragments ranging in size from some centimetres to several metres. The fragments are mainly embedded in metasilicosövites and cut by carbonate veins and dykes.
2. Metaphoscorite is a dark or polycoloured and massive textured rock with coarse grain size. The largest grains are always magnetite and porphyroblastic phlogopite (Fig. 25).
3. Metaphoscorites display highly variable modal compositions as shown in Table 1.
4. The precursors of metaphoscorites are recognizable only in rocks representing the early stages of alteration of ultramafites. These rocks contain primary minerals (olivine, pyroxene, magnetite) or their pseudomorphs.

The metaphoscorites are distinguishable from magmatic phoscorites by their more

Table 1

Mineralogical composition of metaphoscorites of Sokli (percentage by volume)

Minerals	Derived from magnetite olivinite			Derived from pyroxenite			Unknown primary rock		
	Drill hole and depth								
	344 108.9	358 118.5	4 153.5	262 142.3	193 122.0	343 137.0	339 152.2	341 163.2	195 135.5
Clinohumite	20	—	—	—	—	—	—	—	—
Serpentine, iddingsite	10	48	25	—	—	—	6	—	—
Carbonate	4	2	15	40	30	20.0	6	35	2
Richterite	4	8	15	—	—	—	20	19	—
Diopside	—	—	—	9	—	—	—	—	—
Aegirine	—	—	—	—	20	—	—	—	—
Alkali amphibole	—	—	—	30	—	25	—	—	—
Phlogopite	—	—	—	—	25	20	—	—	—
Ferriphlogopite	4	10	10	—	—	—	30	10	36
Apatite	30	—	4	16	15.5	9	18	18	15
Zircon	—	—	1	1	1.5	1	—	—	—
Magnetite	28	32	30	4	8	25	20	18	47

heterogeneous character, coarser grain size, more advanced replacement, corrosion and recrystallization textures, absence of pyrochlore and scarcity of clinohumite. Pyroxene is not encountered in magmatic phoscorites.

Metasilicosövites

Extensive carbonatization was the main process in the conversion of altered derivatives of ultramafites into metasilicosövites (Fig. 11). This is demonstrated mineralogically by the gradual decrease in silicates and magnetite and increase in carbonate during the transformation of metaphoscorites, amphibole rocks, mica—amphibole rocks and mica rocks into metasilicosövites. The metasilicosövites contain thin shreds, relict streaks and decomposed blocks of all the rocks from

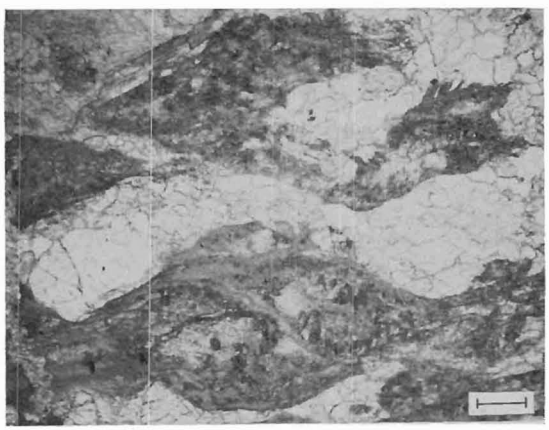

Fig. 26. Relics of alkali amphibole rock (grey) in metasilicosövite. Primary apatite grain (white, to the left) is highly fractured. One nicol. Drill hole 194 at 331.6 metres. Scale bar, 0.5 mm.

Table 2

Mineralogical composition of metasilicosövites of Sokli (percentage by volume)

Minerals	Phlogopite–richterite metasövite			Phlogopite metasövite		
	Drill hole and depth					
	339 285.9	289 39.2	4 53.4	195 139.5	30 26.5	242 145.4
Carbonate	66	70	70	50	62	70
Phlogopite	—	10	—	24	23	19
Ferri-phlogopite	10	—	9	—	—	—
Alkali amphibole	—	—	—	15	4	—
Richterite	5	5	5	—	—	—
Apatite	15	9	11	8.5	9	7
Magnetite	4	6	5	1.7	2	3
Sulphides	—	—	—	0.5	—	1
Zircon	+	+	+	0.3	+	+

+ = detected

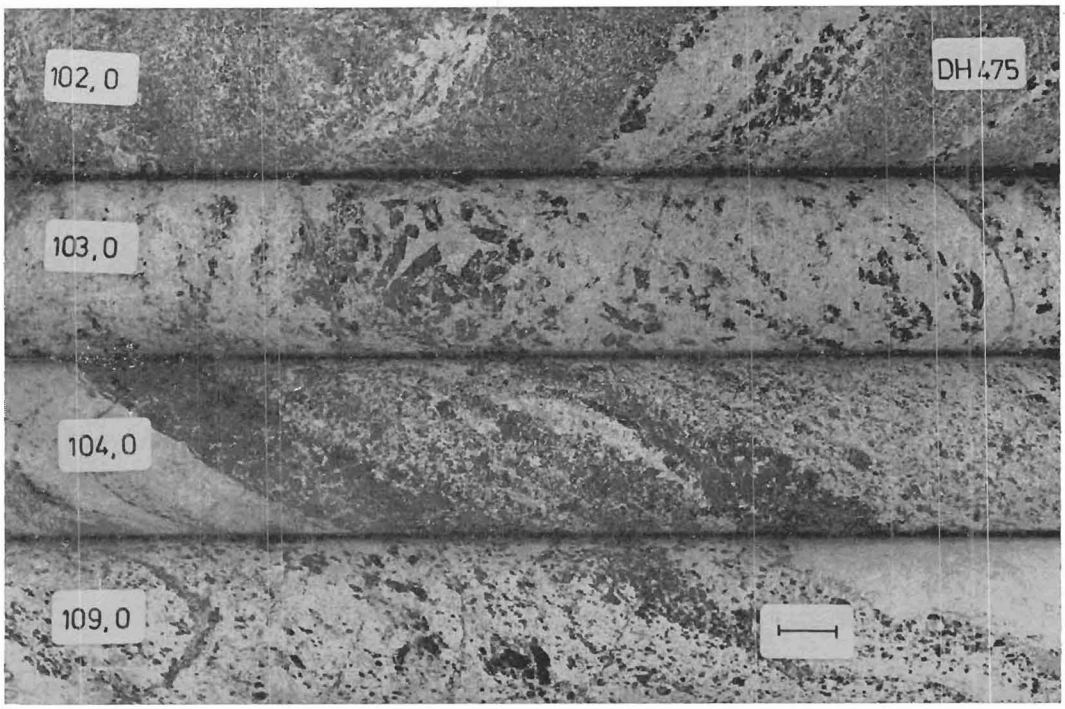

Fig. 27. Specimens of core from drill hole 475 showing typical variants of metasilicosövites in the transitional zone of metasomatites. Scale bar, 1.0 cm.
At 102.0 metres. A pyroxene bearing amphibole rock passes into banded metasilicosövite.
At 103.0 metres. Slightly oriented metasilicosövite. Alkali amphibole laths (dark) after pyroxene occur as loosely packed accumulations or isolated grains.
At 104.0 metres. An intensely banded metasilicosövite. Dark bands consist of calcic amphibole or alkali amphibole and phlogopite. The rock is cut by a magmatic sövite (to the left) conformable with banding.
At 109.0 metres. The most typical phlogopitic metasilicosövite. The phlogopite (dark) occurs as vague bands, schlierens and impregnation. Thin richterite needles are not visible megascopically. Sövitic dyke (to the right) cuts the rock.

which they were formed (Figs. 26 and 30, B, C). Carbonatization and other metasomatic processes and variable dynamic elements have produced locally a high variety of metasilicosövites (Figs. 27, 28, 30, B, C). Two main petrographical types of more or less regular areal distribution can be distinguished. Table 2 gives some modal compositions of each type.

Phlogopite–richterite metasövite is the prevailing type in the metacarbonatite area. The rock varies between white and green and is dotted with black magnetite grains. It is medium-grained and most characteristically consists of more or less persistent schlieren-like bands with various degrees of contortion and waving. The bands show variable textures and mineralogical compositions; they have sharp contacts or they gradually fade into each other with much interfingering (Fig. 28). Individual bands are some centimetres or tens of centimetres thick. In the metacarbonatite area fairly homogenous and more massive types occur locally as shown by drill hole intersections tens of metres long. The green bands are composed of phlogopite, richterite and magnetite with interstitial carbonate. Variously coloured phlogopite is either evenly disseminated or occurs in clots.

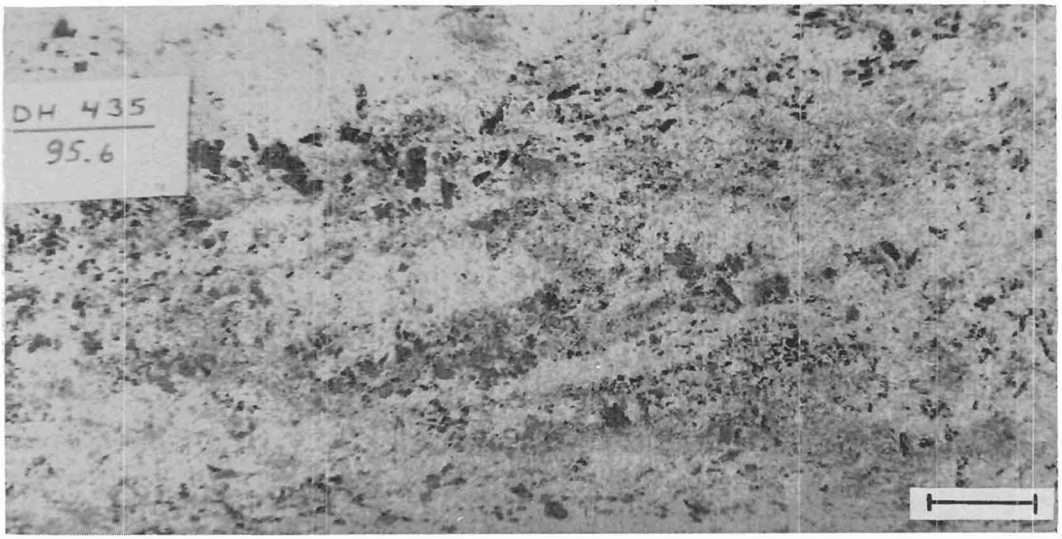

Fig. 28. Phlogopite-richterite metasövite showing vague, schlieren-like bands of accumulations of phlogopite and richterite. Scale bar, 1.0 cm.

A prevailing phlogopite variety is ferriphlogopite with inverse pleochroism: Z = colourless, X = pale orange. The flake boundaries may be thinly rimmed by intensely orange ferriphlogopite. Remnants of large phlogopite flakes from precursory rocks have preserved their green colour but show pale speckles, especially at the edges. The flakes have been decomposed and replaced by an apatite-bearing carbonate phase (Fig. 29).

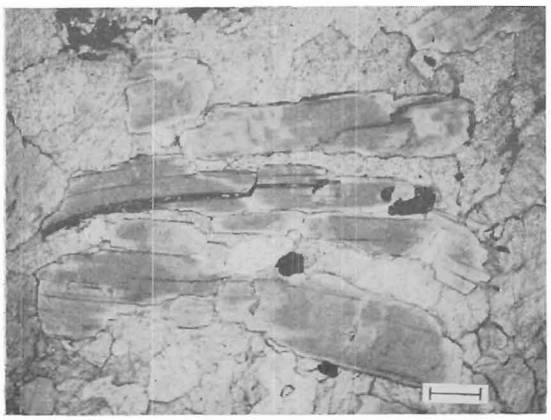

Fig. 29. Speckled phlogopite flakes (grey) are scattered and replaced by carbonate (pale grey). Phlogopite-richterite metasövite. One nicol. Drill hole 242 at 133.6 metres. Scale bar, 0.5 mm.

Richterite, colourless in thin section, occurs as thin needles and fibrous sheaves arranged parallel to the general lineation. As a rule the prismatic richterite is replaced by carbonate, but it is often preserved as pseudomorphs and relics. Alkali amphibole occurs only in massive types as isolated prisms or loosely packed prism aggregates. Primary magnetite grains are scattered and replaced by carbonate so that they form a mealy, fine-grained mass around which the original grain boundaries are sometimes detectable. Apatite at the carbonatization stage is fairly evenly disseminated as small rounded grains in a carbonate mosaic. They differ markedly from primary coarse-grained apatite that is fractured and split into smaller grains. Zircon and sulphides occur as accessory minerals.

Phlogopite metasövite, the dominant metasilicosövite in the transition zone of metasomatites, is encountered wherever carbonatization is extensive. It has often developed as a result of carbonatization and foliation in mica—amphibole and mica rocks. Mica rocks pass into schlierens of dark green phlogopite that eventually die out. The phlogopite is ar-

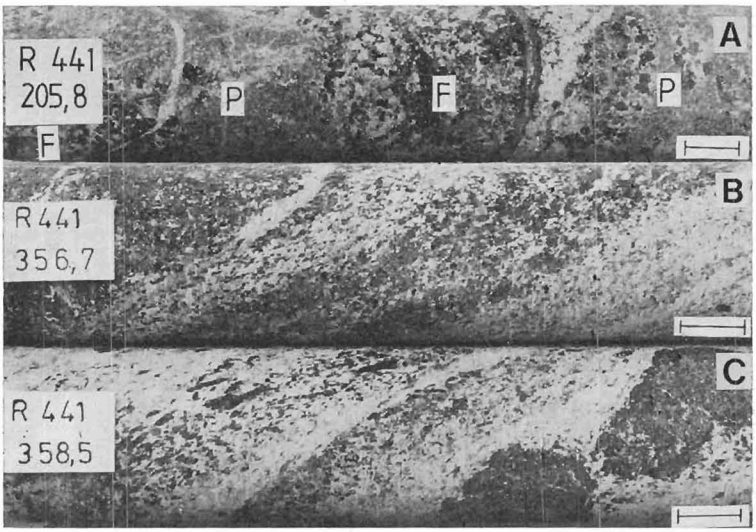

Fig. 30. Specimens from drill hole 441. Scale bars, 1.0 cm.
A. A fenite (F) transformed into a pyroxene rock (P). Note the sharp boundaries between the rocks.
B. A mica–amphibole rock (to the left) gradually grading into phlogopitic metasövite.
C. Fragments of mica–amphibole rock (to the right) derived from fenite in metasilicosövite.

ranged into moderately regular and parallel bands with white apatite-bearing carbonate bands. The rock is foliated and banded. The colour varies between dark and white (Fig. 30, B, C). The width of the dark bands rich in phlogopite range from some millimetres to tens of centimetres. Drill core data suggest that they continue rather linearly but bend around the edges of mica rock and other rock remnants (Fig. 30). Under the microscope fine-grained minerals are seen to swirl around larger phlogopite relics and magnetite grains, and mica and carbonate-rich bands to grade more or less into each other. All the minerals tend to be arranged parallel to the general foliation. Carbonate is equigranular and xenomorphic. Phlogopite flakes show ragged ends. Pleochroism is from light green to pale yellow. Weak zoning is revealed by pale rims. Ferriphlogopite with reversed pleochroism (Z = colourless, X = pale orange) is present in places.

The apatite of the carbonatization generation occurs as well rounded, egg-shaped grains. It is slightly concentrated in the phlogopite-rich bands. Prisms of alkali amphibole and calcic amphibole are present in the phlogopite metasövite that developed as a result of the carbonatization of amphibole and mica–amphibole rocks. The magnetite preserved from the precursory rocks displays xenomorphic habit; recrystallized magnetite occurs as idiomorphic crystals. Because phlogopite metasövite is a fairly equigranular rock, the average grain sizes of its main minerals are given: carbonate 0.5 mm, lenght of mica flakes 1.0 mm, xenomorphic magnetite grains 1.0 mm, magnetite crystals 0.1 mm, apatite 0.2 mm. Sulphides and zircon occur as accessory minerals.

Tectonized metasilicosövite. In addition to the metasilicosövites described above, a highly tectonized metasilicosövite has been encountered in drill holes 193, 194 and 195 in

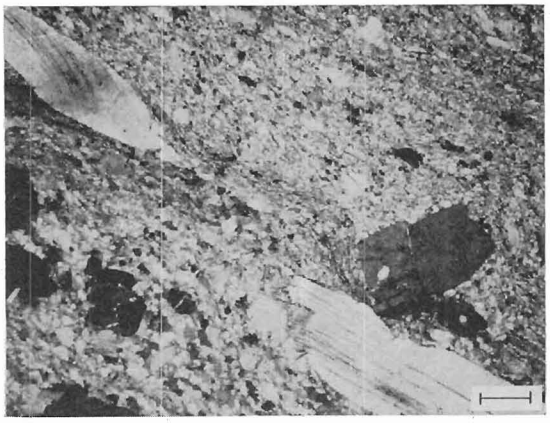

Fig. 31. Tectonized metasilicosövite. Fine-grained, lineated matrix consisting mainly of carbonate and subordinately of richterite and phlogopite. Phlogopite flakes (pale grey) are contorted and resorbed at the edges. Apatite grains (dark grey) are fractured and broken. Crossed nicols. Drill hole 193 at 85.5 metres. Scale bar, 0.5 mm.

the southern part of the massif (Fig. 4), between the metaphoscorite blocks and the metasilicosövites into which it rapidly grades.

The tectonized metasövite is pale in colour and is compressed into a vertically dipping schistose structure with mylonitic features. Remnants of neighbouring rocks are so broken and scattered that only isolated rolled grains of phlogopite, magnetite and apatite are left (Fig. 31). Cataclasis is also revealed by twisted phlogopite flakes and continuously repeated thin shear planes. Fibrous richterite has crystallized on the shear planes (Fig. 32). Carbonate grains have been sheared throughout the rock into a fine-grained mass with distinct orientation.

The intense foliation and lineation, the vertical orientation, the scattering of the rock fragments into small grains and other cataclastic features all indicate upward movements of metasilicosövite, partly in a solid plastic state. These structures and textures occur in the vicinity of the fenite aureole, showing that the movements in the carbonatite massif were accentuated towards the fenite aureole.

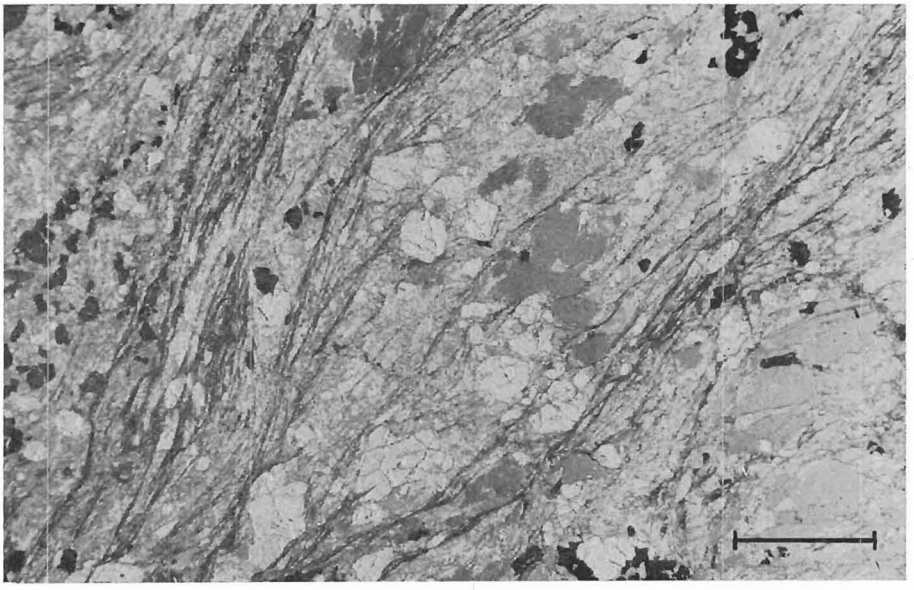

Fig. 32. Fibrous richterite on the shear planes of tectonized metasilicosövite. One nicol. Drill hole 194 at 223.6 metres. Scale bar, 3.0 mm.

Rocks of the transition zone of metasomatites

The transition zone of the metasomatites forms a girdle between the fenite aureole and the metacarbonatite area (Fig. 3). The metasomatite zone is composed of fragments of fenites, pyroxene rocks, amphibole rocks, mica–amphibole rocks and mica rocks embedded in metasilicosövites. The geological data on the zone derive from a few shallow drill holes only (Fig. 4). It is difficult to estimate reliably the distribution and relative proportions of the various rocks in the metasomatite zone and to check the presence of ultramafites as indicated locally by geophysical data. Nevertheless the ultramafites are believed originally to have been distributed throughout the extensive transition zone of metasomatites and to have been metasomatically transformed largely into amphibole, mica–amphibole and mica rocks in the manner already described (p. 15—22). Carbonatization then converted these rocks into metasilicosövites (Fig. 30) as described on page 27.

The fenite fragments and their transformations occupy a considerable portion of the metasomatite zone. The two main alteration trends of fenite are:

Fenite → Pyroxene rock → Calcic amphibole–alkali amphibole rock → Mica–alkali amphibole rock → Mica rock

Fenite → Alkali amphibole rock → Mica–alkali amphibole rock → Mica rock

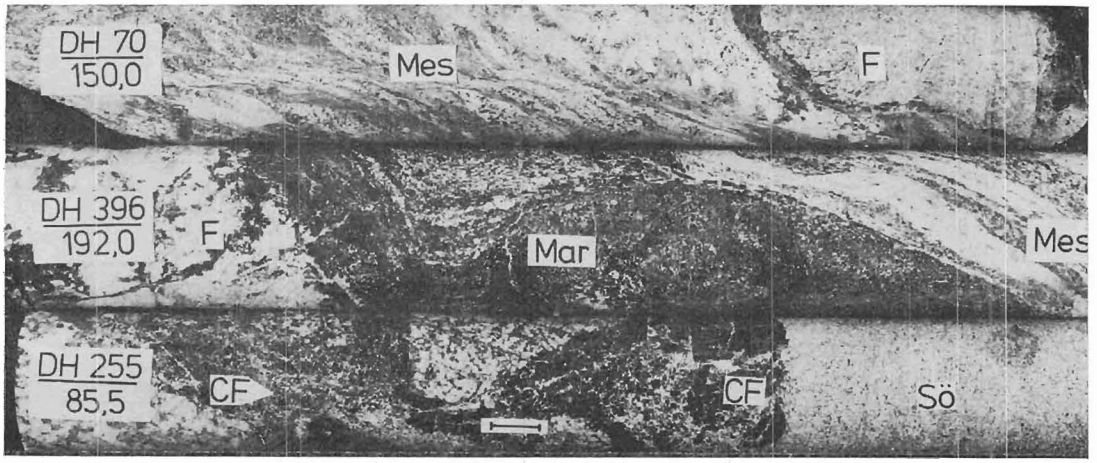

Fig. 33. Drill core specimens showing sharp boundaries between fenite and rocks derived from them. Scale bar, 1.0 cm.

DH 70 at 150.0 metres. A fragment of fenite (F) enveloped by a narrow phlogopite-rich reaction zone (dark) against metasilicosövite (Mes).

DH 396 at 192.0 metres. Dark green, fine-grained mica-amphibole rock (Mar) between a fenite fragment (F) and metasilicosövite (Mes).

DH 255 at 85.5 metres. A carbonate-rich mica rock (CF) in a crushed fenite zone. Mica rock cut sharply by magmatic sövite (Sö).

DH 259, 387 and 441 show good intersections of the alteration sequences of fenites in a metasilicosövite environment (Fig. 4). The description of the alterations of fenite is based mainly on the observations and analyses made on these drill holes. Intense brecciation of the fenitic zones has led the development of alterations into various rock types. The boundary between the fenite fragments and the altered rocks is often sharp (Figs. 30, A and 33). This suggests that breccia fractures played an important role in the modification of fenites into rocks of various kinds. The altered rocks display textural heterogeneity and irregularity in composition. The main rock types of the alteration trends are described in the next section.

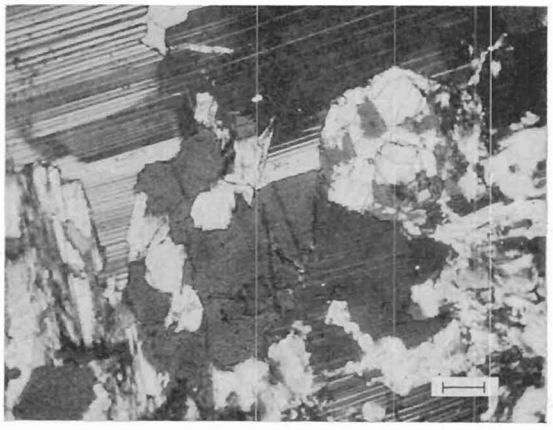

Fig. 35. Recrystallized albite enclosing poikiloblastically pyroxene (white grain) and pyroxene grains altered into calcic amphibole (dark grey, in the middle). Crossed nicols. Drill hole 441 at 337.0 metres. Scale bar, 0.3 mm.

Pyroxene rock

At its purest, pyroxene rock is an almost monomineralic rock with subordinate interstitial carbonate (Fig. 34). The rock is light green and massive and it occurs as irregular fragments ranging in size from some centimetres to a few metres. It is encountered in drill holes along the western and northern boundaries between the metacarbonatites and the zone of metasomatites. Pyroxene displays prismatic forms and is almost free from inclusions. The mineral appears to have been introduced metasomatically during recrystallization. The pyroxene crystals are generally 0.5 mm wide and 1.5 mm long. Pleochroism colours range from bright green to light yellow. One microprobe analysis indicates acmitic diopside composition (Table 11, No. 8). Large poikilitic plates of clear albite enclose the pyroxene prisms (Fig. 35) near the unaltered fenite. Farther from the fenite contact the pyroxene prisms become enclosed poikiloblastically in plates of calcic amphibole. Metasomatism has altered the pyroxene into alkali amphibole to a varying extent. In some places thin carbonate veinlets have transformed the pyroxene into colourless richterite.

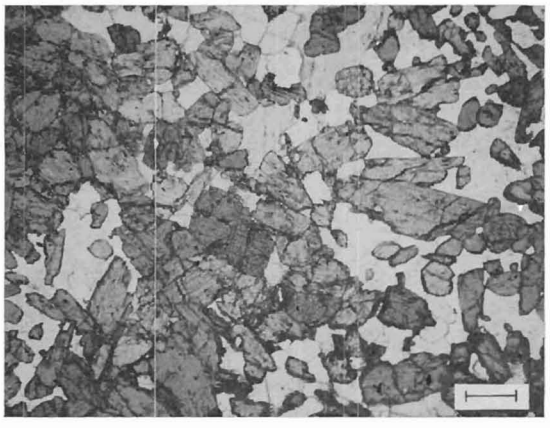

Fig. 34. Fine-grained metasomatic pyroxene rock transformed from fenite. One nicol. Drill hole 441 at 285.8 metres. Scale bar, 0.5 mm.

Amphibole rocks

There are three varieties of amphibole rocks in the area of the metasomatite zone:

1. Calcic amphibole rock derived from the magmatic pyroxenite.

2. Calcic amphibole — alkali amphibole rock transformed from the metasomatic pyroxene rock.
3. Alkali amphibole rock formed from fenite.

The calcic amphibole rock and its development from pyroxenites were described on p. 18. The calcic amphibole — alkali amphibole rock is a product of progressive metasomatism from pyroxene rock that itself is a metasomatic transformation from fenite. Increasing alkali amphibolization towards the outer margins of the pyroxene rock fragments produces a calcic amphibole-bearing alkali amphibole rock. Intersections of this rock in drill holes may measure several metres, but smaller fragments some tenths of centimetres long are more common. It is a fine- to coarse-grained rock (Fig. 36), medium or dark green, and massive in texture. Calcic amphibole occurs as large hypidiomorphic grains that are usually devoid of inclusions but that show recrystallization features. The

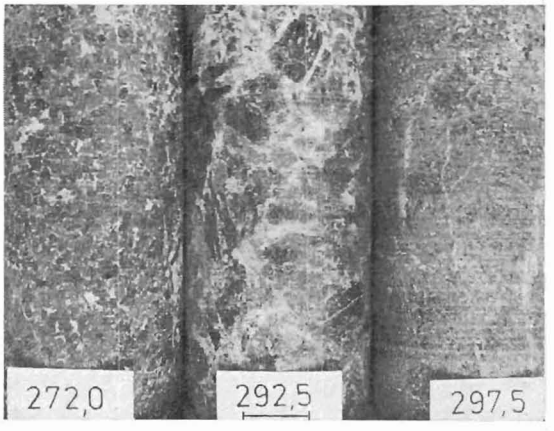

Fig. 36. Specimens of drill core showing variation in grain size in the calcic amphibole-alkali amphibole rock. Drill hole 441. Scale bar, 1.0 cm.
At 272.0 metres. The predominant medium-grained type.
At 292.5 metres. Coarse-grained type. White colour is apatite-bearing carbonate matrix showing intense carbonatization that succeeded amphibolization.
At 297.5 metres. Fine-grained type. The rock contains appreciable phlogopite. In mineral composition close to a mica-amphibole rock.

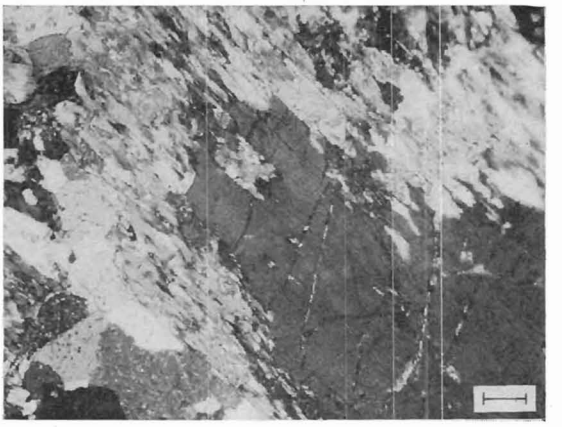

Fig. 37. Alkali amphibole (pale grey) replaces calcic amphibole (dark grey) in calcic amphibole–alkali amphibole rock. Crossed nicols. Drill hole 441 at 287.7 metres. Scale bar, 0.3 mm.

colour is characteristically deep green with moderate pleochroism towards yellowish tints. The interference colours are normal. The alkali amphibole represents the metasomatic generation after pyroxene and calcic amphibole (Fig. 37). Its blue-green colour and anomalous bluish interference colour distinguish it from the calcic amphibole. The mineral occurs around the pyroxene and the calcic amphibole as alteration rims (Fig. 37) or as large pseudomorphic grains after the former minerals or as a fine-grained generation. The development of alkali amphibole is usually accompanied by the intergrowth of some phlogopite. Carbonate with rounded apatite grains is met with interstitially to the amphibole grains.

The alkali amphibole rock that formed from fenite is represented in the fenite aureole as thin cross-cutting veins composed almost exclusively of alkali amphibole. In the transitional zone of metasomatites intense crushing of fenite has encouraged the development of alkali amphibole rock into units tens of centimetres or even some metres thick. The alkali amphibole rock is always fine-grained and is also distinguished from the other amphibole rocks by its characteristic

dark green colour. Its texture is massive or slightly oriented. The alkali amphibole rock is not monomineralic but always contains variable amounts of phlogopite, carbonate and subordinate apatite. Relict albite grains are present in places.

Mica—amphibole rocks

Mica—amphibole rocks are transitional varieties in the alteration trends of pyroxene rock and amphibole rocks towards mica rocks. In the ideal cases the mica—amphibole rocks occur as vague portions between pyroxene and amphibole rocks and mica rocks in isolated fragments embedded in the metasilicosövites. Not uncommonly these fragments have wholly achieved the mineral composition of mica—amphibole rock. The fragments which are rounded and broken up, have been contorted into smooth folds and schlieren by upward movements of remobilized metasilicosövite (Fig. 30, C).

The mica—amphibole rock has characteristically developed from the precursory rock by the phlogopitization of pyroxene and amphiboles. The phlogopitization is usually accompanied by the introduction of carbonate and apatite. All the same time the rock may have acquired oriented texture or it may have preserved its original massive texture. Mica—amphibole rock is typically an equigranular fine to medium-grained, and medium or dark green rock. The mica is green phlogopite and the amphibole is alkali amphibole. Calcic amphibole is also encountered. Subordinate minerals are carbonate and apatite.

Mica rock

Mica rock represents an end product, of the alteration that started in the fenite fragments

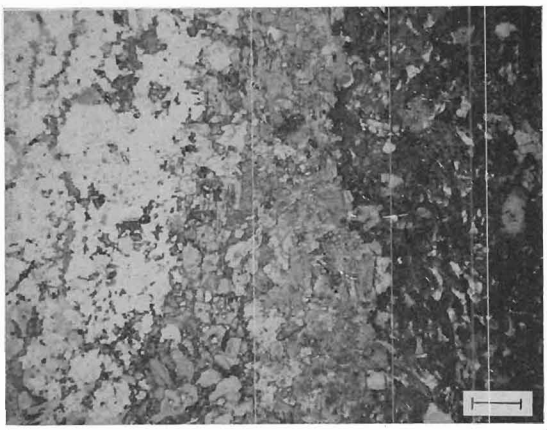

Fig. 38. Gradation of fenite (to the left) via thin phlogopite rim (in the middle) into fine-grained mica-amphibole rock (to the right). One nicol. Drill hole 259 at 85.7 metres. Scale bar, 0.5 mm.

in the transitional zone of metasomatites. Mica rock may, however, develop directly from fenite owing to the effect of carbonate veins and metasilicosövite cutting the fenite fragments. The mica rock thus developed may be restricted to a narrow zone along the contacts with the veins and rocks (Fig. 33) or form pods and lenses sometimes up to 0.5—1.0 metres thick inside and around the fenite fragments. In thin section the mica rock appears to be almost pure phlogopite rock with subordinate carbonate and relict alkali amphibole prisms preserved from the fenite. The contact between the mica rock and the fenite is sometimes suprisingly sharp (Fig. 38).

Most of the mica rocks in the transition zone are believed to have developed from mica—amphibole rocks by increasing potassium metasomatism. The progress of phlogopitization is shown as a network extending around the amphibole prisms, which are gradually replaced inwards (Fig. 39). This alteration trend seldom produces a monomineralic mica rock; instead the rock contains ragged amphibole grains that have resisted replacement by phlogopite. Some carbonate and apatite are usually present as well. In-

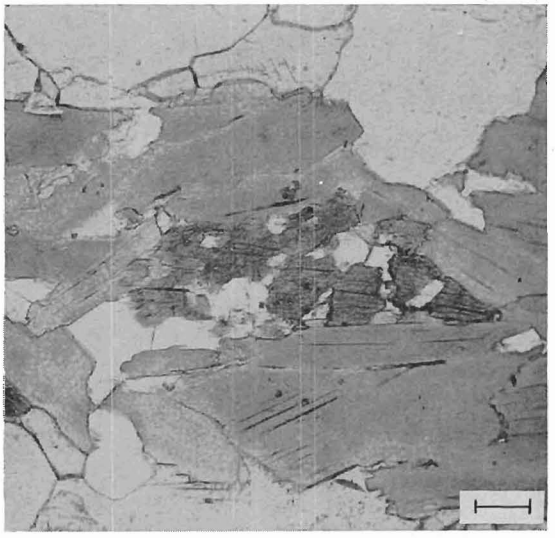

Fig. 39. Calcic amphibole relics (grey) in mica rock developed from calcic amphibole rock. Apatite and calcite are white. One nicol. Drill hole 387 at 196.0 metres. Scale bar, 0.3 mm.

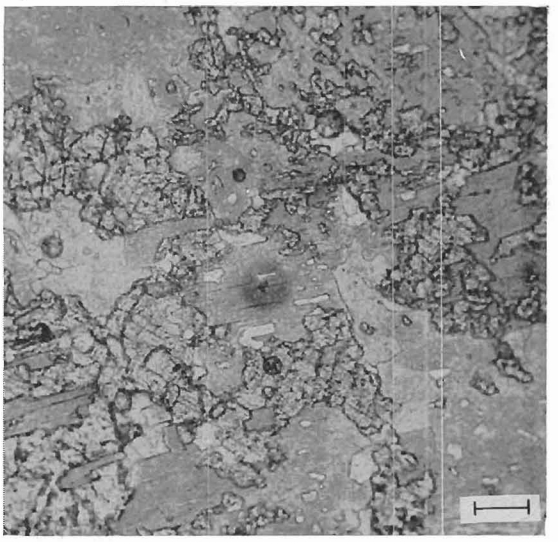

Fig. 40. Metasomatic pyroxene rock is altering into mica rock. Pyroxene is distinguished from phlogopite by higher relief. One nicol. Drill hole 387 at 175.3 metres. Scale bar, 0.3 mm.

tense potassium metasomatism has sometimes affected the pyroxene rock, resulting in the direct development of mica rock as a result of the phlogopitization of pyroxene (Fig. 40).

The mica rocks that developed in one way or another from fenite fragments are characterized by their fine to medium grain size and dark green colour. Intersections of the rock in drill holes barely exceed one or two metres. The texture of the mica rock is generally massive, but preferable orientation of the phlogopite flakes also occurs. The mica is green phlogopite with normal pleochroism. These mica rocks are distinguished from those derived from ultramafites by their even grain size and more homogenous habit. The latter are commonly more coarse-grained and porphyroblastic in texture.

Magmatic carbonatites

Magmatic carbonatites form a plug-like central core in the Sokli massif. The structure of the massif and the core have been described earlier and visualized by a generalized block diagram based on diamond drilling and geophysical data (Vartiainen and Paarma, 1979). The magmatic core contains xenoliths of ultramafites, fenites, metasomatites and metacarbonatites and small-scale segregations, banding, veining, alterations and replacements in unmappable units, all of which add to the highly complicated and composite nature of the core (Fig. 41). The magmatic carbonatites also form cone-sheets and irregular intrusions protruding from the central core and extending across the metacarbonatite area and the transitional zone of metasomatites into the fenite aureole (Fig. 3). The magmatic carbonatites are believed to have been formed pulsatively and successively in three phases, which are divided into five stages:

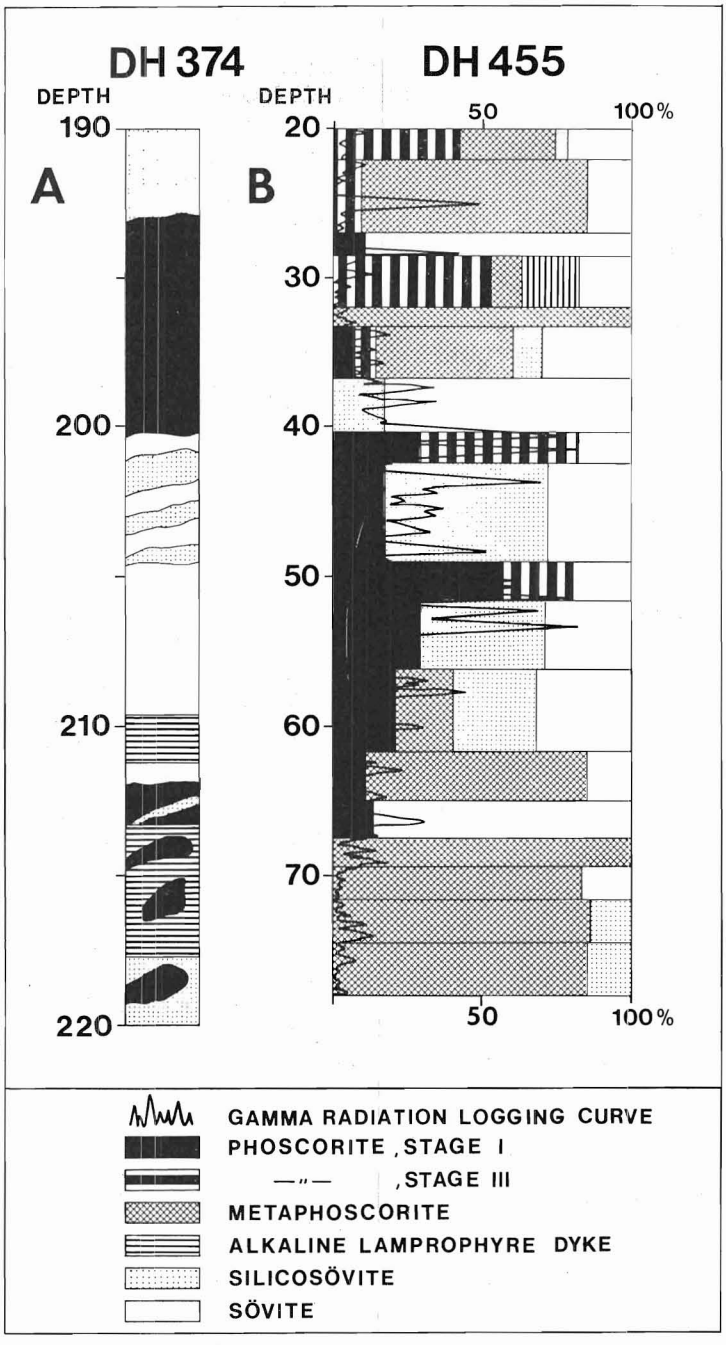

Fig. 41. A drawing and a diagram showing rapid lithological variation in the magmatic carbonatite core.

A. A lithology of a drill core for a length of 30 metres in drill hole 374. The rocks belong to Stages I and II and are intersected by alkaline lamprophyre dykes.

B. Diagram showing lithological variation in volume percentage in drill hole 455 for a length of 60 metres. Rock variation observed with an accuracy of 5 centimetres.

Phases	Stages
First intrusive magmatic phase	I Segregation of phoscorite from carbonatite magma.
	II Crystallization of massive sövitic rocks from carbonatite magma.
Pneumatolytic or hydrothermal phase	III Intense pneumatolytical-hydrothermal activity.
Second intrusive magmatic phase	IV Crystallization of banded (and massive) sövites and beforsites from fluidal carbonatite magma.
	V Crystallization of late veins from the residual melt of carbonatite magma.

The occurrence and petrography of the rocks of each magmatic stage will be described separately in the following chapters.

Stage I, phoscorite

The segregations of the composite mineral assemblages called phoscorites are regarded as the first manifestations of magmatic carbonatites. Phoscorites are met with only in the magmatic core, as irregularly distributed, fragmental rock bodies forming loosely packed and elongated fragmental rock zones some tens of metres wide and hundreds of metres long. The zones seem to have a vertical downward extension. Individual phoscorite fragments range from some centimetres to several metres in size; the spaces between them are of the same size. The fragments

Table 3

Mineralogical composition of Stage I Sokli phoscorite (percentage by volume)

Minerals	Drill hole and depth							
	435 66.5	435 71.0	332 41.4	330 135.1	260 77.0	288 67.0	289 112.1	Palabora *
Carbonate	21	38	7	10	—	6	6	18
Olivine	33	—	17	20	10	—	—	—
Clinohumite	1.5	—	10	3	5	1	—	—
Serpentine	—	2	—	—	1	—	10	22**
Richterite	1.0	2	—	—	—	0.5	5	—
Phlogopite	9	6	—	—	—	10	1	+
Ferri-phlogopite	—	11	3	0.5	0.5	—	10	—
Apatite	3	17	13	45	40	35	30	25
Magnetite	28	16	43	25	33	38	30	35
Sulphides	3	6	3	1	3	10	7	—
Pyrochlore	0.5	2.0	1.0	—	0.5	0.5	0.2	—
Baddeleyite	—	+	—	0.5	0.1	—	0.5	+
Zirkelite	—	—	—	—	—	+	—	—

* Hanekom *et al.* (1965), average mineral composition of serpentinized phoscorite
** includes vermiculite and others
+ = detected

display angular forms and are commonly cut by thin carbonate veinlets. Sparse and small phoscorite fragments are dispersed throughout the Stage II sövite bodies.

Owing to its considerable magnetite content, phoscorite produces magnetic highs (Fig. 2). Drilling of the anomalies has revealed that the rocks are either magmatic phoscorites or metaphoscorites transformed from ultramafites (Fig. 41, B). The former rocks show characteristic petrographic features and, as a result of thorium- and/or uranium-bearing pyrochlore in the magmatic phoscorites, they can be recognized by scintillometric measurements in drill holes (Fig. 41, B). The geological map (Fig. 3) shows the magmatic phoscorite zones that have been checked by drilling. The unaltered or slightly altered Stage I phoscorites are associated with the Stage II sövitic rocks (Fig. 41, A). In the more complicated environments, where the primary phoscorites were first affected by hydrothermal activity and later by carbonatite intrusions, only small amounts of primary phoscorites are present (Fig. 41, B).

The phoscorites are dark coloured, medium- to coarse-grained rocks with massive structure. The rock-forming minerals in the primary, unaltered phoscorite are magnetite, olivine, phlogopites, apatite and calcite. Variation in the relative abundances of these minerals give rise to a diversity of types (Table 3). Sulphides, pyrochlore and baddeleyite are the most important accessory minerals. For comparison, the average mineralogical composition of phoscorite from the type locality, Palabora, is also given in Table 3. The abundances of the essential minerals, magnetite, apatite, olivine and its alteration products, are about the same. The Palabora phoscorite is distinguished by the absence of sulphides and pyrochlore.

Owing to later magmatic introduction of calcite into the phoscorite, recrystallized magnetite occurs in places (Fig. 42). Similar

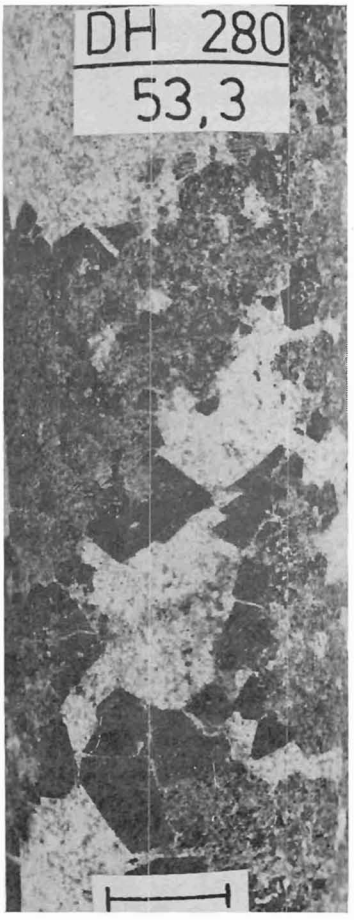

Fig. 42. Recrystallized magnetite (black) between Stage I magmatic phoscorite (dark) and Stage II sövite (light). Scale bar, 1.0 cm.

textures are widely developed in the apatite—forsterite—magnetite ores (= phoscorites) at Kovdor (Borodin *et al.*, 1973). At Sokli, however, the phoscorites usually grade into crystallized sövites (Fig. 70, p. 58) or they are brecciated by the sövites (Figs. 68, p. 57 and 69, p. 57).

On the basis of mineral inclusions and mineral boundaries the crystallization order of the minerals in the phoscorite is:

olivine, pyrochlore, baddeleyite
magnetite
apatite, phlogopite
calcite.

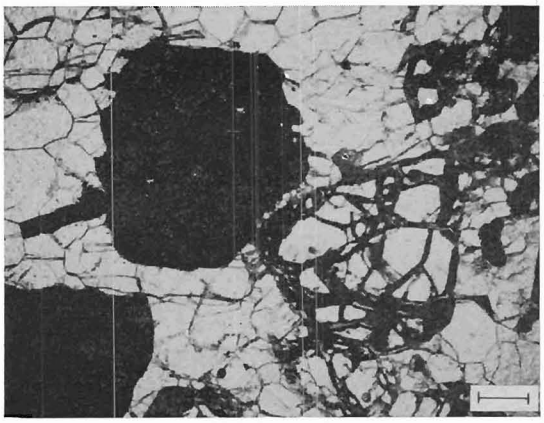

Fig. 43. Idiomorphic and hypidiomorphic minerals in Stage I magmatic phoscorite. Iron oxide pigment covers and fills the fractures of an olivine crystal (in the middle). Apatite occurs as acicular grains (white), and magnetite (black) displays crystal forms. Baddeleyite is present as a black prism (to the left). One nicol. Drill hole 250 at 139.0 metres. Scale bar, 0.5 mm.

When primary mineral assemblages are present, the minerals all display more or less idiomorphic habits (Fig. 43). Deuteric processes and later calcite generations have often affected the mineral shapes and caused alterations in the minerals. Olivine may have altered into serpentine, iddingsite and bowlingite. In places these alterations appear suddenly and sharply, one side of a sample being fresh and the other totally altered (Fig. 44). Iddingsitization is less common. The first signs of clinohumitization of the olivine appear in the deuteric stage even though clinohumitization at large was one of the alteration processes of the hydrothermal phase.

Occasionally magnetite and phlogopite are corroded and apatite prisms rounded by carbonate. Apatite, too, disfigures the crystal habits of magnetite and pyrochlore.

Primary calcite differs from later calcite by its intense twinning, larger grain size and more clear-cut grain boundaries. Phlogopite has faint pleochroism: Z = very pale green, X = colourless. Pyrochlore is dark orange or red brown in colour.

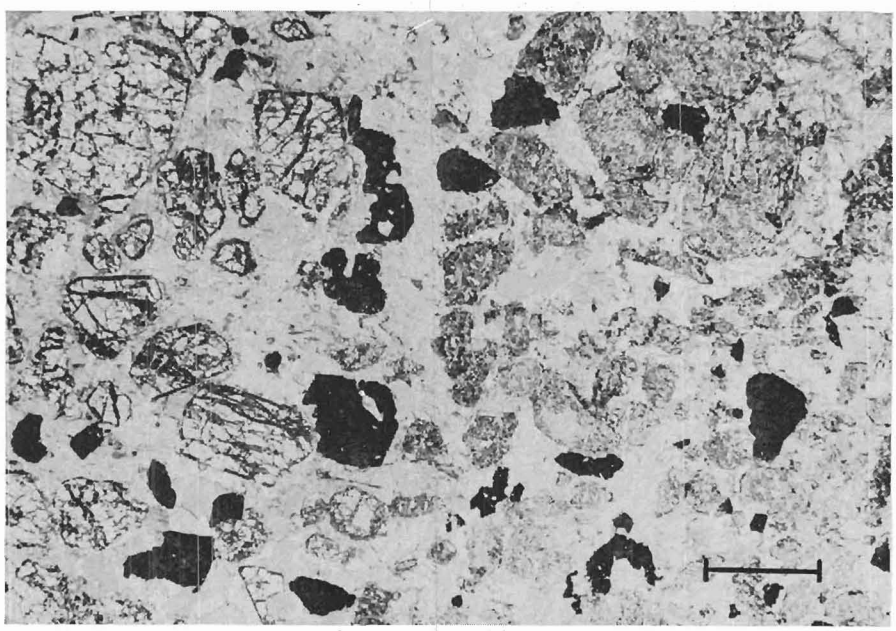

Fig. 44. Stage I magmatic phoscorite showing rapid variation in the alteration of olivine. To the left olivine crystals are almost fresh, to the right they are completely serpentinized. One nicol. Drill hole 281 at 62.3 metres. Scale bar, 2.0 mm.

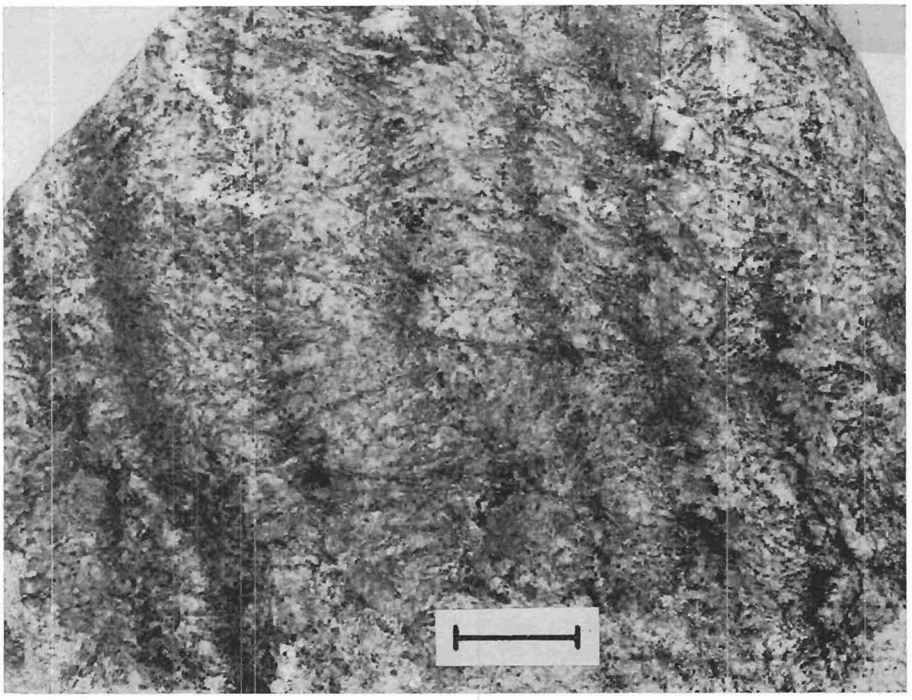

Fig. 45. Rhythmic layering in a Stage II magnetite—olivine sövite. Boulder from test pit 4. Scale bar, 0.5 m.

The minerals can be grouped into coarse grained varieties: magnetite 1—15 mm, olivine 1—10 mm, phlogopite 1—15 mm, calcite 1—15 mm; and fine-grained varieties: apatite, pyrochlore, baddeleyite and zirkelite 0.1—0.4 mm each.

Stage II, sövites and silicosövites

Stage II comprises crystallization products of the first calcite-rich carbonatite magma, and thus the rocks are sövites and silicosövites. These occupy large and fairly homogeneous rock units in the core, which can be recognized as magnetic lows and as blocks of homogeneous velocity on seismic profiles.

The longest drilling intersections (150, 120 and 98 metres) of sövites and silicosövites are encountered in drill holes 246, 386 and 350 respectively (Fig. 4). These bodies are cut by numerous alkaline lamprophyre dykes and they include some small phoscorite fragments. The sövites and silicosövites grade into each other. Smaller sövite—silicosövite bodies, such as lenses and fragments occur as inclusions in the later sövites and silicosövites, in which case the first stage sövitic rocks are altered, replaced and assimilated to a varying extent.

Arcuate, cone sheet-like intrusions of Stage II silicosövites occur in the metacarbonatite area and in the transition zone of metasomatites. Features shared by all the variants are their greyish colour, fine to medium grain size and massive texture.

The massive, medium-grained sövite passes locally into a rock showing special structure and texture. A rock from pit 4 (Fig. 4) has a banded structure resembling rhythmic or zebra layering (Fig. 45). The dark bands, which are rich in magnetite and olivine, are

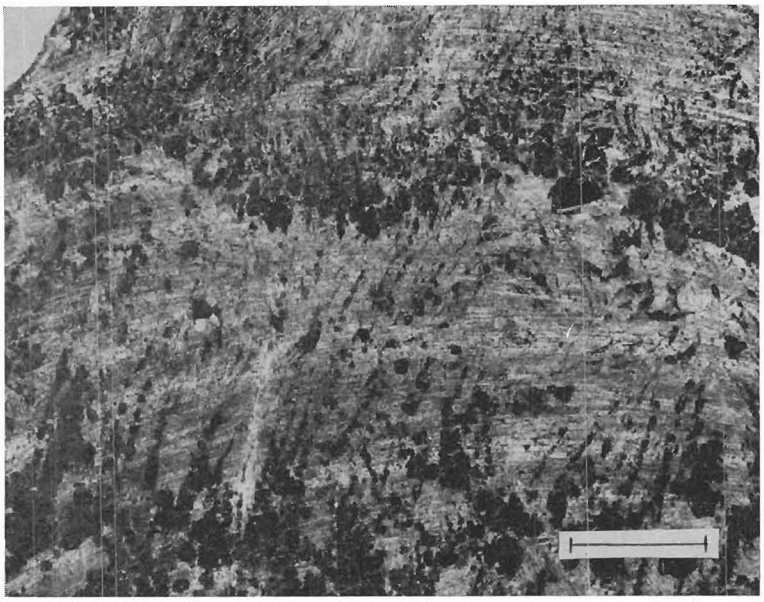

Fig. 46. Detail from layered structure of Stage II magnetite–olivine sövite. Large magnetite crystals have settled at the »bottom» of the layers from which finer-grained magnetite with olivine has crystallized »upwards» to form grass-like texture. Boulder from test pit 4. Scale bar, 2.0 cm.

a few centimetres thick and separated by thick calcite rich bands about 10 centimetres thick. The texture of the dark bands shows some regularity. Large, idiomorphic magnetite crystals have been segregated down to the »bottom» of the smoothly curving bands (Fig. 46). Fine-grained magnetite with olivine has crystallized »upwards» along tabular calcite forming a grass-like texture in the bands (Fig. 46). The orientation of the primary banding is unknown, since the only large scale observation derives from a loose block of the weathered crust. The structure has not been noted in the drill cores. The dark bands have a mineralogical affinity for phoscoritic composition. These segregations are similar to the massive crystallization of first-stage phoscorite except that the former developed later and on a smaller scale. Hanekom and his co-workers (1965) have described primary banding in the older carbonatite at Palabora, where it generally conforms with the attitude of the contacts between the carbonatite and the phoscorite.

A peculiar tabular texture associated with the banding structure described above is not uncommon in the Stage II magnetite—olivine sövites. Calcite tabulae from a half to several centimetres long and from one to ten millimetres wide (Fig. 47) may occur as individuals with random orientation or in almost parallel groups of several tabulae. They consist of one or more calcite grains with long sharp edges. All the other minerals, olivine, magnetite, apatite, phlogopite, fine-grained calcite generation, pyrochlore and baddeleyite, occur in the interstices between the tabulae as aggregates or grain-chains. Exceptionally, magnetite forms thick shells around thin calcite tabulae (Fig. 48). The tabular calcite, which is without mineral inclusions, does not replace the other minerals. These features indicate that the tabular calcite was the first mineral to crystallize in

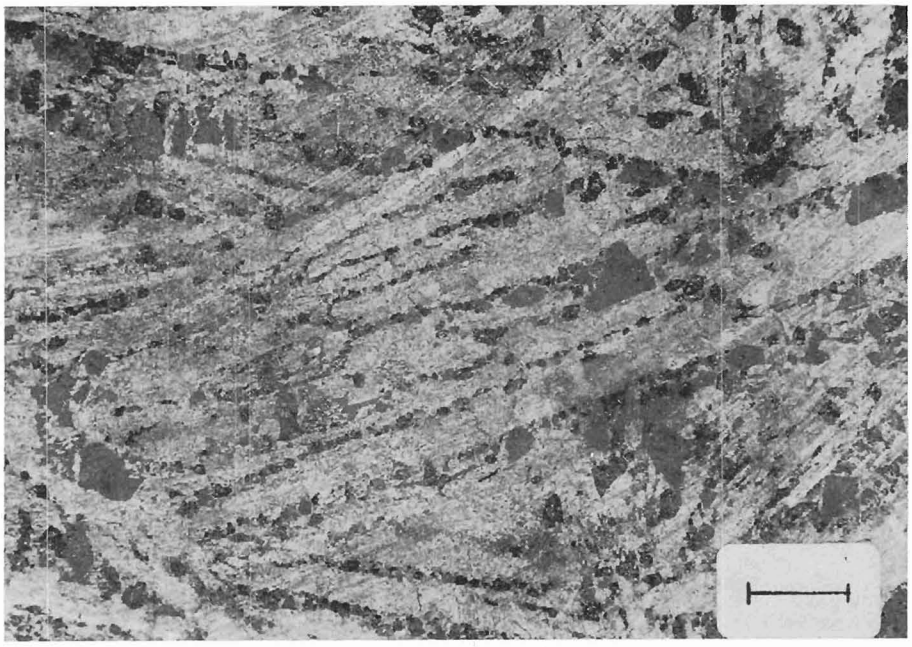

Fig. 47. Tabular texture in Stage II magnetite–olivine sövite. Calcite tabulae (white) consist of one or more calcite grains. Boulder from test pit 4. Scale bar, 1.0 cm.

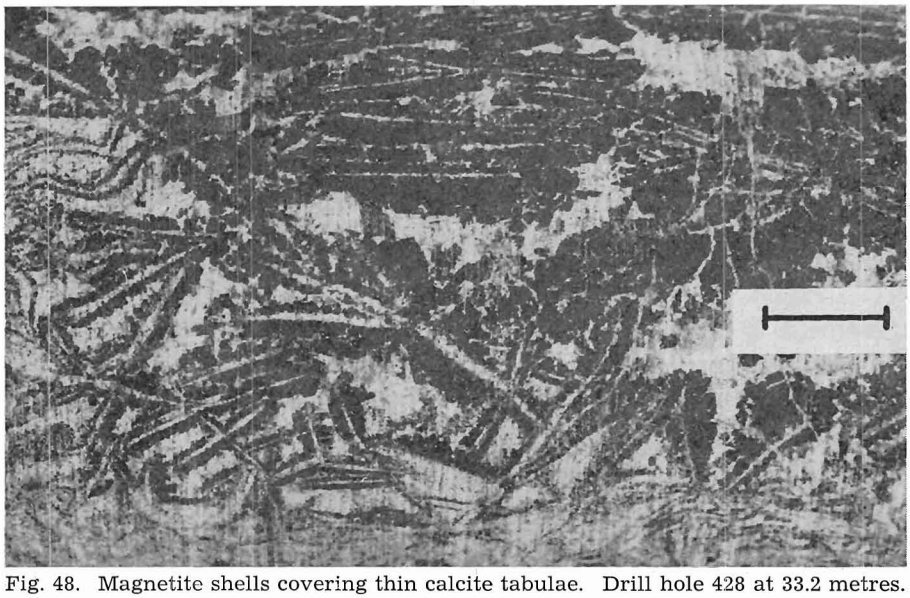

Fig. 48. Magnetite shells covering thin calcite tabulae. Drill hole 428 at 33.2 metres. Scale bar, 1.0 cm.

this rock. Pozaritzkaya and Samoilova (1972), who have described similar tabular textures from some Siberian carbonatite complexes and the Kovdor complex, interpret them as metasomatic textures due to replacement and recrystallization.

Table 4

Mineralogical composition of Stage II Sokli silicosövites and sövites (percentage by volume)

Minerals	Silicosövites			Sövites		
	Drill hole and depth					
	374 *	425 116.8	250 128.8	274 122.5	281 179.1	338 108.3
Calcite	58	76	75	85	92	97
Olivine	9	—	4.5	—	—	—
Serpentine	2	1	—	—	—	—
Phlogopite	1	3	0.2	4.5	1	1.0
Apatite	12	9	12	8	5	1.0
Magnetite	16		8	2.5	1	0.5
Sulphides	1	10	—	—	1	0.5
Pyrochlore group	1	1	—	—	—	+
Baddeleyite	+	+	0.3	+	—	—
Zirkelite	—	—	+	+	—	—

* composite sample
+ = detected

The mineralogical compositions of sövites and silicosövites presented in Table 4 differ only slightly from each others, showing that the division into subgroups is rather artificial. The uniform mineralogical compositions, massive and other textures refer to slow and stable crystallization conditions.

As a rule the first minerals to crystallize were olivine and magnetite. They occur as idiomorphic or hypidiomorphic grains but, with calcite, they may also form skeletal and dentritic textures that can be interpreted as products of simultaneous crystallization of these minerals. Similar textures at Kola (Kukharenko *et al.*, 1965) and Siberian (Pozaritzkaya and Samoilova, 1972) carbonatite massifs have been attributed to the replacement of carbonate. The olivine is usually fresh even when it shows skeletal and dentritic texture, which is odd if the textures originated by metasomatic replacement processes. These textures are not encountered in the ultramafites with extensively developed metasomatic and replacive alterations, although they are present in the recrystallized magnetite olivine rock in which magnetite, olivine and calcite grew contemporaneously.

In places the olivine is wholly serpentinized. Calcite occurs as equigranular grains in irregular forms with clear-cut boundaries. Twinning is common. Mineral inclusions are often absent from calcite. Apatite grains display short prismatic habits and are usually arranged as aggregates or net-like chains in the interstices between the calcite grains.

Phlogopite flakes are generally rounded at their margins but locally they display idiomorphic forms. The pleochroism is: Z = pale green, X = colourless. Pyrochlore is a well crystallized, dark orange mineral. Baddeleyite occurs as scattered crystals or as clusters of crystals. The average grain sizes of the minerals in millimetres are: calcite 1—3, apatite 0.1—0.3, olivine 0.5—2, magnetite 2—4, phlogopite 1—2, pyrochlore 0.2—4, baddeleyite 0.1—0.2.

Stage III, hydrothermal phoscorite and apatite—ferriphlogopite rock

The rocks of the hydrothermal phase (Stage III) are regarded as the alteration varieties of the earlier magmatic Stages I and II. The first carbonatite intrusion phase was accompanied by hydrothermal or pneumatolytic solutions. These solutions appear to have impregnated both phoscorite (I) and sövite (II) causing mineral alterations and depositing apatite—ferriphlogopite rocks before the second magmatic phase. Thus the hydrothermal phase is an interlude between two magmatic phases. All gradations occur from unaltered to mineralogically wholly altered rocks. Accordingly, the mineralogical and chemical compositions of the Stage III rocks are highly variable. Except for apatite-ferriphlogopite rock, it is difficult to show typical rock variants; hence, mineralogical alterations rather than rocks are described.

Hydrothermal processes were most active in the vicinity of fault zones but signs of slight alterations are seen throughout the magmatic core. The magmatic carbonatites outside the core also contain hydrothermal variants. Alteration processes have affected the metacarbonatites and given rise to true hybridic rocks. The Stage I phoscorites were more susceptible to alterations than were Stage II sövites and silicosövites. The Stage III phoscorites have preserved their massive texture or exhibit slight foliation. Their grain size is comparable to that of the primary rocks, being medium to coarse, but the colours have a reddish tint. Likewise the sövites and silicosövites are macroscopically comparable to their unaltered counterparts even though they commonly display oriented textures.

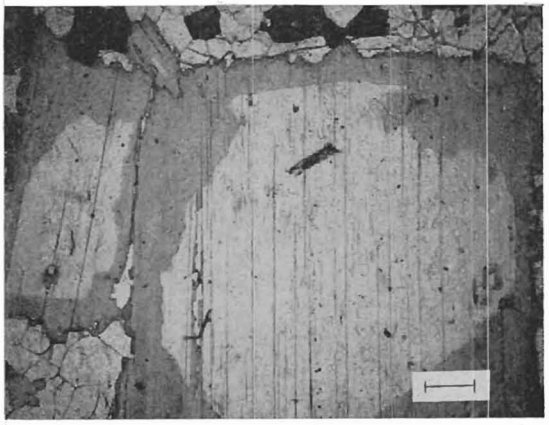

Fig. 49. Sharply zoned phlogopite in Stage III hydrothermal phoscorite. The outer rim is dark orange ferriphlogopite and the core pale green phlogopite. One nicol. Drill hole 332 at 84.2 metres. Scale bar, 0.5 mm.

The mineralogical alteration phenomena are best traced under the microscope using hydrothermally altered phoscorites. Hence, the mineralogical observations were conducted on these rocks. The development of the mineralogical composition in Stage III can be summarized as follows:

1. Green phlogopite alters into red brown phlogopite (ferriphlogopite) and the total amount of mica increases. All gradations from narrow ferriphlogopitized rims of primary green phlogopite to pure ferriphlogopite are to be seen within some tenths of centimetres. Sharp zoning illustrates rhytmic alteration processes (Fig. 49). In places the ferriphlogopite displays idiomorphic hexagonal flakes suggesting complete recrystallization. The ferriphlogopite invariably shows reversal pleo-

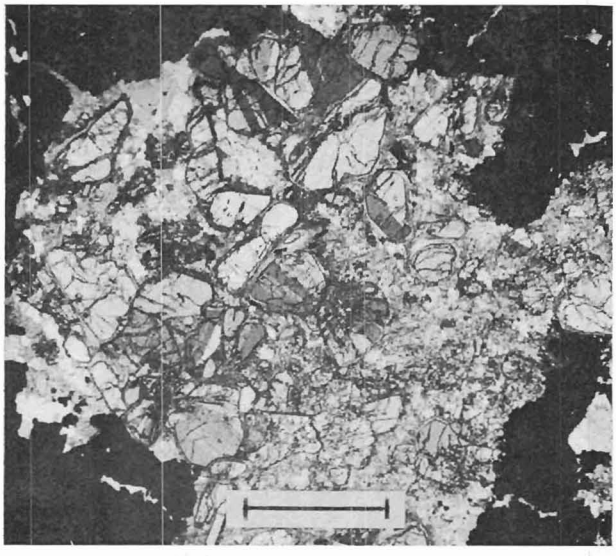

Fig. 50. Accumulation of twinned clinohumite crystals in Stage III hydrothermal phoscorite. Crossed nicols. Drill hole 251 at 77.4 metres. Scale bar, 2.0 mm.

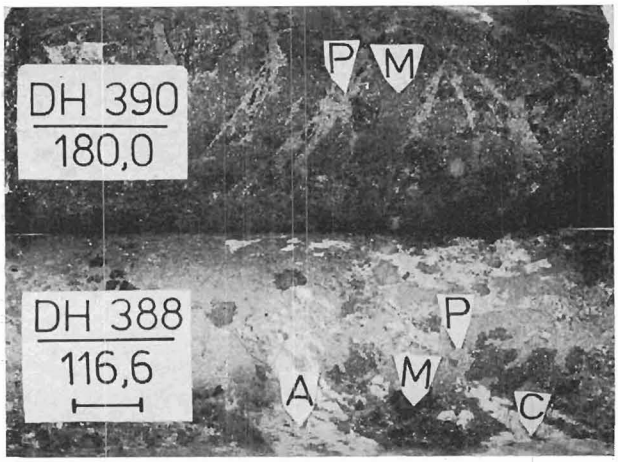

Fig. 51. Sulphidization in Stage III hydrothermal phoscorite. Pyrrhotite (P) fills the cracks and replaces magnetite (M) (lower figure) A = apatite aggregate. C = carbonate schlieren. Scale bar, 1.0 cm.

chroic colour: X = orange or reddish brown, Z = pale yellow. The biggest ferriphlogopite flakes are up to 5 cm in diameter.

2. Olivine alters into clinohumite and the minerals of the serpentine group. Clinohumitization begins at the edges or in the cracks of the olivine grains and proceeds to cover the whole grains. Local twinned clinohumite crystals (Fig. 50) indicate the recrystallization of these grains. Similar clinohumite crystals are encountered at Kovdor (Borodin *et al.*, 1973).
3. Richterite develops from olivine. It occurs as thin needles shooting off from the olivine grains (Fig. 87, p. 75). In extreme cases it forms tight fascicles that can occupy 30—50 % of the volume of the rock.
4. Dolomite is formed.
5. Sulphidization has produced mainly pyr-

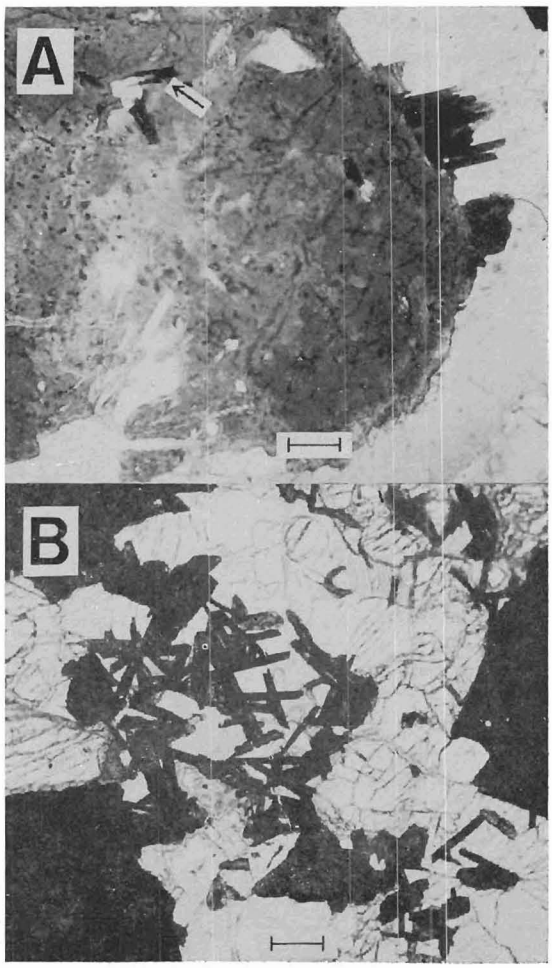

Fig. 52. Zirkelite in Stage III phoscorites.

A. Zirkelite prisms grown on a pyrochlore crystal. Arrow point to zirkelite within pyrochlore. One nicol. Drill hole 332 at 84.2 metres. Scale bar, 0.3 mm.

B. Separate zirkelite prisms (in the middle). Magnetite is black, apatite and carbonate white. One nicol. Drill hole 378 at 269.6 metres. Scale bar, 0.3 mm.

Table 5

Mineralogical composition of Stage III hydrothermal phoscorites and apatite-ferriphlogopite rocks at Sokli (percentage by volume)

Minerals	Phoscorites					Apatite-ferriphlogopite rocks		
	Drill hole and depth							
	332 84.2	329 183.0	274 78.0	436 42.7	435 83.0	330 110.8	425 111.7	425 104.4
Carbonates	4	10	11	30	34	10	—	7
Olivine	5	10	4	—	—	—	—	—
Clinohumite	8	15	5	0.5	6	—	—	—
Serpentine	—	—	5	9	7	—	—	—
Richterite	5	—	0.5	13.5	1	—	—	—
Ferri-phlogopite	20	13	44	9	11	27	26	30
Apatite	20	35	12	16	22	38	49	35
Magnetite	30	15	} 16	} 18	} 19	} 17	} 23	} 21
Sulphides	5	1.5		4		17		
Pyrochlore	1	—	2	+	+	0.5	2	6
Baddeleyite	—	0.5	0.5	+	—	—	—	1
Zirkelite	+	+	+	—	—	+	+	+
Zircon	+	—	—	+	+	—	—	—

+ = detected

rhotite and minor chalcopyrite. The pyrrhotite occurs as dissemination, schlierens, veinlets, rod-like aggregates and fine-grained masses several centimetres in diameter. The mineral fills the small cracks and envelops earlier minerals such as magnetite (Fig. 51). The chalcopyrite is encountered as fine-grained dissemination.

6. Thorium-rich pyrochlore is a hydrothermal mineral. This pyrochlore differs microscopically from the pyrochlore of Stages I and II by its finer grain size (0.05—0.3 mm) and markedly lighter colour (pale yellow). Larger, distinctly zoned pyrochlore crystals also occur. Primary red brown pyrochlore is replaced by carbonate and the crystals have occasionally altered into resorbed sieve-like grains. The red brown pyrochlore is rimmed by a pale variety. In places the alteration in colour is so advanced that only a small spot of the primary pyrochlore is preserved in the centre of the crystal.
7. Zirkelite has formed at the expense of pyrochlore and occurs around and as inclusions in pyrochlore (Fig. 52, A). Separate zirkelite prisms are also encountered (Fig. 52, B).

Table 5 shows examples of the mineralogical compositions of the Stage III phoscorites derived from the Stage I varieties. The considerable variation in the abundance of all the minerals is striking. The mineral compositions of the apatite—ferriphlogopite rock, which are also given in the Table 5, indicate material transport during hydrothermal activity. These rocks are fracture fillings that owe their origin to some process directly related to hydrothermal fluids. The occurrence of apatite—ferriphlogopite rock exhibits dyke-like habit (Fig. 74, p. 60) and the width of the dykes varies from 1 to 200 cm. The apatite-ferriphlogopite rocks prefer the vicinity of the central fault zone from where they branch off in all directions. They are also encountred in the fenite aureole as fragments within the cone sheets composed of Stage IV

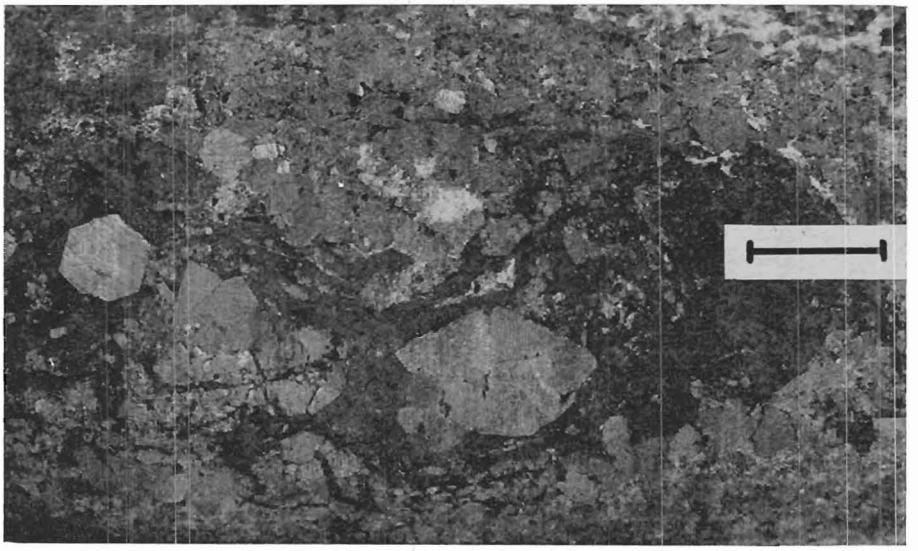

Fig. 53. Hexagonal ferriphlogopite (grey) in Stage III apatite-ferriphlogopite rock. Pyrrhotite (dark grey) forms a fairly compact aggregate enclosing ferriphlogopite. Drill hole 428 at 111.7 metres. Scale bar, 1.0 cm.

silicosövite. The latter contains apatite as small (0.1—0.3 mm) prismatic crystals that form fairly composite accumulations with other minerals. The ferriphlogopite is distinctly zoned and occurs locally as idiomorphic hexagonal flakes (Fig. 53). Pyrrhotite is disseminated or it occurs as schlierens of irregular shape. The pyrochlore content is higher than in any other rock in the Sokli massif; in some samples it may exceed five

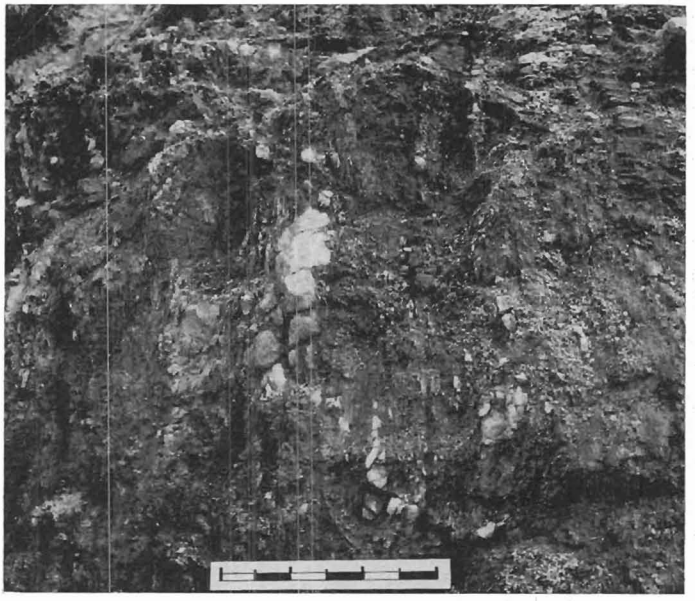

Fig. 54. Vertical banding in Stage IV magmatic sövite-silicosövite. Test pit 3. Scale bar, 0.3 m.

percent (Table 5). Magnetite, which is present in some dykes, was presumably captured from the surrounding rocks. Pyrochlore, baddeleyite, zircon and zirkelite are the general accessory minerals in the Stage III rocks.

Stage IV, silicosövite, sövite and beforsite

The two phase magmatic carbonatite cycle manifests itself in the second phase as silicosövites, sövites and beforsites. They occupy the largest volume of the magmatic core but also occur as cone-sheets and irregular intrusions protruding from the central core and extending across the metacarbonatite area and the transition zone of metasomatites into the fenite aureole.

The Stage IV rocks display three mode of occurrence: 1) Rocks with banded structure (Fig. 54), which predominate in the boundary zone of the magmatic core and have a width of a few hundred metres; 2) A more massive yet somewhat oriented type, which prevails in the central part of the core; 3) Dyke-like units of fine-grained, sugary textured sövites and beforsites, which are scattered throughout the massive. The bright white colour and the existence of ferriphlogopite in these rocks distinguishes them clearly from the greyish and massive Stage II sövites and silicosövites. The petrographic differences are most marked in the metacarbonatite area and in the transition zone of metasomatites, where the Stage IV rocks and metasilicosövites occur side by side. Foliation, schistosity and cataclastic features are more advanced in the metasilicosövites than in the magmatic varieties, which are more coarse-grained and contain pyrochlore (Fig. 55, B), a mineral that is totally absent from the metasilicosövites. Richterite may be present in both rock types but alkaline amphiboles only in the metasomatic ones.

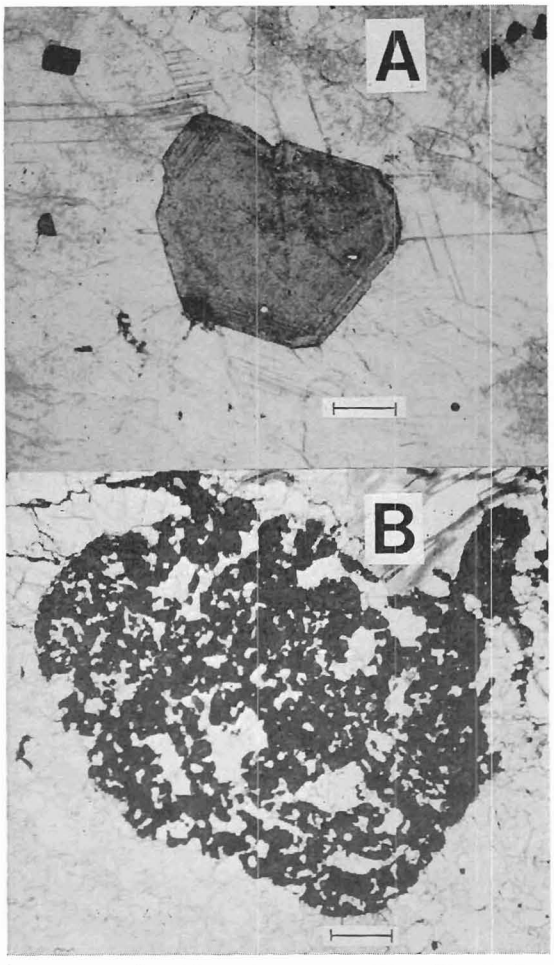

Fig. 55. Pyrochlore in Stage IV silicosövites.
A. Pale, idiomorphic and zonal pyrochlore. One nicol. Drill hole 342 at 110.2 metres. Scale bar, 0.5 mm.
B. Resorbed pyrochlore (dark grey) in cone sheet of Stage IV magmatic sövite. Plane polarized light. Drill hole 194 at 10.45 metres. Scale bar, 0.5 mm.

The subvertical banding (Fig. 54) is due to the parallel arrangement of stringes, streaks and bands rich in, ferriphlogopite, magnetite and apatite. The banding in silicosövite results from flow structure as is evidenced by its behaviour around rock fragments of earlier stages (Figs. 69 and 75). Microscopic examinations show that all the minerals have a linear arrangement parallel

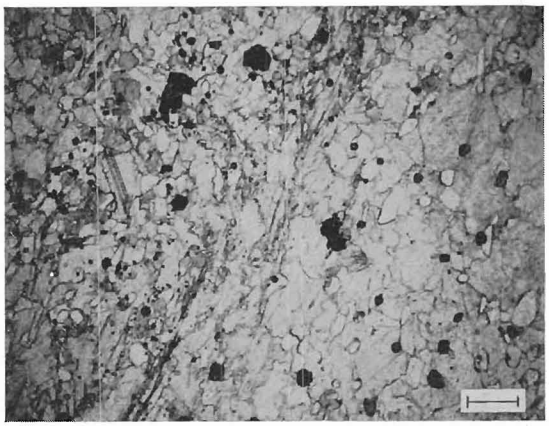

Fig. 56. Boundary between a richterite–ferriphlogopite-rich band (to the left) and a carbonate-rich band in Stage IV magmatic sövite. The major axes of all the minerals tend to be parallel to banding. Small black crystals in carbonate-rich band (to the right) are pyrochlore. One nicol. Drill hole 318 at 56.3 metres. Scale bar, 0.5 mm.

to the general banding (Fig. 56). Garson (1955) has described similar structures from the carbonatites of southern Malawi and regards them as distinctive flow features comparable to those in magmatic rocks. In the banded silicosövites apatite exhibits acicular forms that are more typical of the apatite of earlier stages. The rocks also contain clinohumitized olivine and ragged magnetite. These minerals may derive from earlier carbonatites, suggesting that the banded structure developed at the begining of Stage IV. Pyrochlore is fairly evenly disseminated throughout the rocks, and magnetite occurs as small idiomorphic crystals.

Under the microscope massive, medium-grained sövite and silicosövite in the inner part of the core show some degree of orientation due to the subparallel arrangement of apatite grains, apatite aggregates and separate ferriphlogopite flakes. Weakly elongated calcite grains are also oriented in the same direction. In these rocks apatite occurs typically as rounded or subrounded grains (Fig. 58, A). Ferriphlogopite is commonly zonal with dark orange rims. Magnetite is mostly idiomorphic. Pyrrhotite may form disproportionally large schlierens in an otherwise equigranular sövite (Fig. 57). Two types of pyrochlore are encountered: orange yellow with corroded grains and pale yellow with idiomorphic crystals (Fig. 55, A).

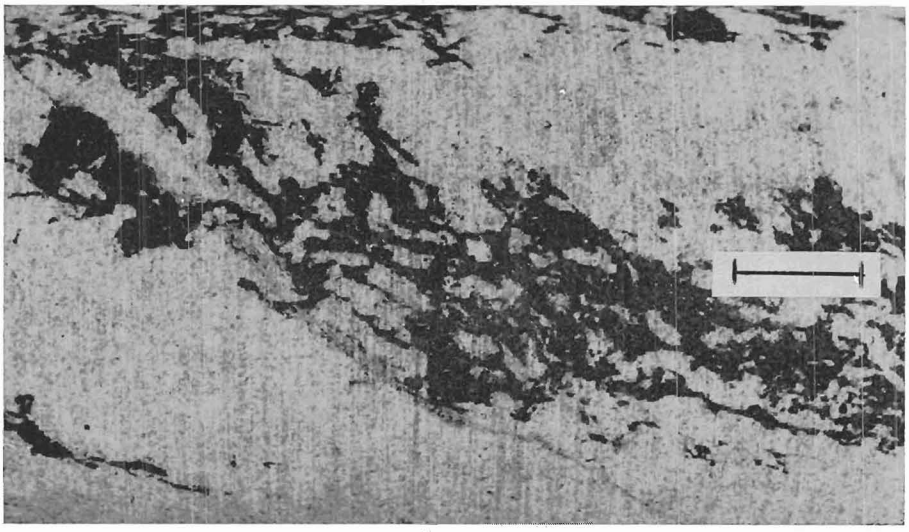

Fig. 57. Irregular pyrrhotite schlieren (dark grey) in massive Stage IV sövite. Drill hole 426 at 80.0 metres. Scale bar, 1.0 cm.

Table 6

Mineralogical compositions of Stage IV magmatic carbonatite rocks at Sokli (percentage by volume)

Minerals	Silico-sövite	Sövite		Beforsite		
	Drill hole and depth					
	365 *	342 110.2	343 198.5	333 34.2	274 119.0	344 176.8
Carbonates	78	80	88	99	92	100
Clinohumite	2	—	—	—	—	—
Ferri-phlogopite	5	3.5	3.5	0.5	0.8	—
Apatite	7	10	7	—	—	—
Magnetite	6	5	1	0.5	—	—
Sulphides	1.5	0.5	—	—	0.5	—
Pyrochlore	0.5	1.0	0.5	—	0.2	—

* composite sample

Table 6 gives typical mineral compositions of the Stage IV rocks. The average grain sizes of the minerals in the banded and more massive silicosövites and sövites are: calcite 0.5—1.5 mm, apatite 0.1—0.3 mm, magnetite 0.5—2.0 mm, ferriphlogopite 0.5—1.0 mm, pyrochlore 0.05—0.3 mm.

The latest rocks of Stage IV are dyke-like units of fine-grained, sugary sövite and beforsite. They may occur as monomineralic rocks (Table 6), yet in places their apatite content reaches ten per cent. Apatite occurs as elongated aggregates of small acicular crystals (Fig. 58, B).

Orbicular structure in sövite. An orbicular structure in magmatic sövite has been found in one drill hole (DH 355/depth 81, Fig. 4) at Sokli. The structure occurs as a 20 cm long section in the sövite of magmatic Stage IV. The orbicules are rounded but conform plastically with the contours of the neighbouring orbicules when in contact with them (Fig. 59). The cores are filled mainly with granular calcite and idiomorphic magnetite. Richterite and ferriphlogopite occur in smaller amount. The rhythmic texture of the orbicules is due to the variation in magnetite habit and concentration of magnetite grains in the shell around the core. The innermost part of the orbicules consists of idiomorphic magnetite crystals (0.1—0.3 mm across) accumulated in the core. This is followed by the thickest part of the shell composed of very fine-grained magnetite, calcite and ferriphlogopite. The third layer consists of a calcite-rich rim with subordinate

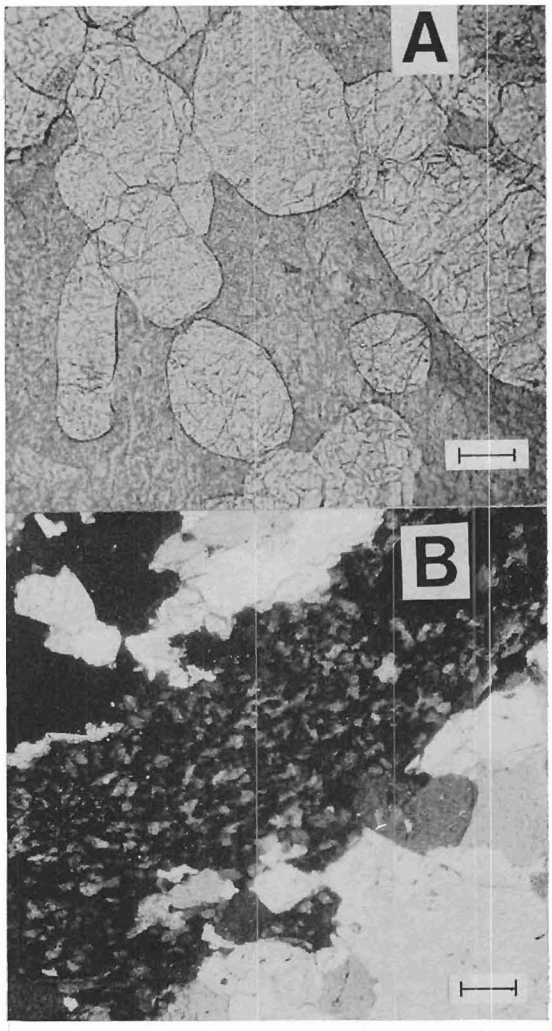

Fig. 58. Shapes of apatite in Stage IV rocks.
A. Rounded and subrounded apatite grains (white) in Stage IV magmatic sövite. One nicol. Drill hole 273 at 86.1 metres. Scale bar, 0.3 mm.
B. A fine-grained apatite aggregate in Stage IV beforsite. Crossed nicols. Drill hole 274 at 66.8 metres. Scale bar, 0.3 mm.

ferriphlogopite and richterite. The outer surface of the orbicules is covered by idiomorphic magnetite crystals. Calcite is the main mineral in the groundmass around the orbicules. Calcite occurs as equigranular xenomorphic grains. The other minerals are idiomorphic magnetite, small-flaked ferriphlogopite, fibrous richterite and scarce pyrochlore. The texture of the orbicular sövite resembles that of the orbicular olivine rock.

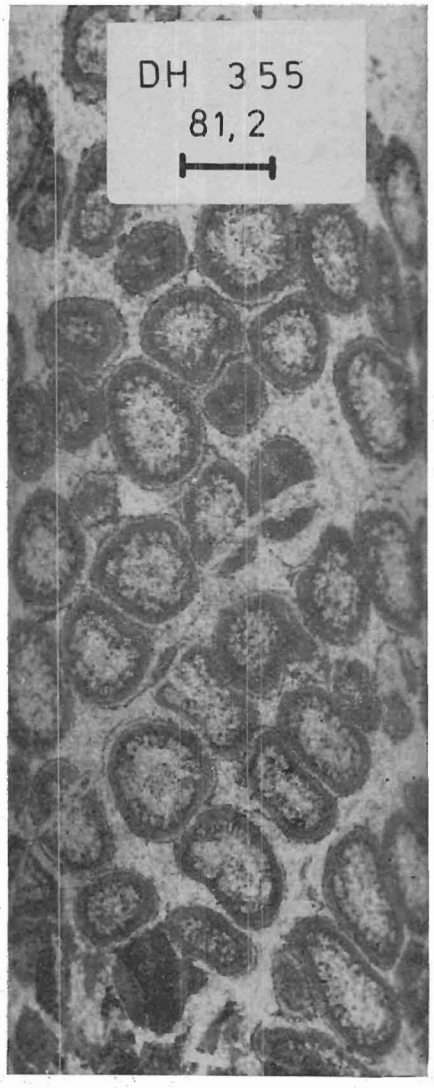

Fig. 59. Orbicular structure in Stage IV magmatic sövite. Scale bar, 1.0 cm.

Stage V, late-stage veins

The final stage in the evolution of the magmatic carbonatites is represented by late carbonatite veins. These are closely associated with the central and other internal fault zones in the core. The fracture zones provide loci for the emplacement of late-stage veins, from which they spread randomly outwards into the surrounding rocks. The veins intersect all the other rocks, indicating that they are the youngest rocks in the Sokli massif. In spite of the large number of late-stage veins, they represent a quantitatively subordinate phase of carbonatite intrusion.

The veins are from 0.1—15 m thick and possibly hundreds of metres long. The longest drilling intersection of about 50 metres (DH 462) is probably along a vein. The veins are polycoloured, varying between white, green, brown, and red, and medium- to coarse-grained. They display cavernous and drusy structures and contain numerous cavities filled with minerals crystallized from the latest solutions (Fig. 60).

The minerals in the veins include trapped relics from the enclosing carbonatites and minerals actually crystallized in the late stage. The amounts of these minerals and the compositions of the veins vary considerably. The trapped minerals are: magnetite with corroded grains 1—10 mm in diameters, pyrrhotite clusters up to 5 cm long, (pyrrhotite is partly altered into pyrite), ferriphlogopite flakes, small subrounded grains of apatite, and chlorite clusters that obviously represent pseudomorphs after olivine. Dolomite is the predominant vein mineral. It occurs in three generations: large (1—5 mm) clean grains with clear-cut boundaries; fine-

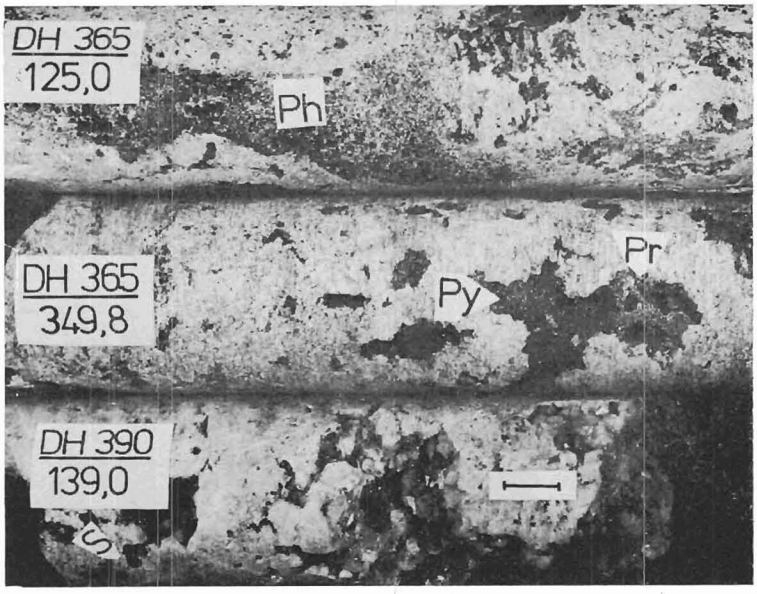

Fig. 60. Specimens of Stage V late carbonatite veins.
Drill hole 365 at 125.0 metres: (Ph) a strongly assimilated fragment of Stage III phoscorite in a late-stage vein.
Drill hole 365 at 349.8 metres: A pyrrhotite aggregate (Py) captured from wall rock and pyrite (Pr) of vein generation crystallized in the cavity.
Drill hole 390 at 139.0 metres: dolomite crystallized in a cavity and an aggregate of black sphalerite (S). Scale bar, 1.0 cm.

grained (0.1—0.5 mm) ragged grains; and crystals in the cavities. Baryte occurs with the fine-grained dolomite generation as very ragged grains of variable size (0.5—3.0 mm). The following accessory minerals have been identified: pyrite, sphalerite, galena, hematite, ancylite and witherite. Mineral species of REE-carbonates have not yet been studied.

Contact relations

According to Pecora (1956, p. 1550) contact relations are crucial, perhaps more so than mineral composition, in defining the succession of rocks. In the Sokli massif the interpretation of the contact relations is based primarily on observations on drill cores and secondarily on test pits. The contact relations of alkaline lamprophyres have been described earlier (Vartiainen *et al.*, 1978).

The evidence from drill holes reveals that the oldest rocks in the Sokli massif are the ultramafites and fenites. They and their altered derivatives which occur as xenoliths in the magmatic carbonatites, are cut by remobilized metacarbonatites (Figs. 61 and 62). Metaphoscorite and the fine-grained mica—amphibole rock derived from fenite display sharp contacts, the metaphoscorite apparently cutting the mica—amphibole rock (Fig. 62). This indicates that the former is either younger or was remobilized with respect to the mica—amphibole rock.

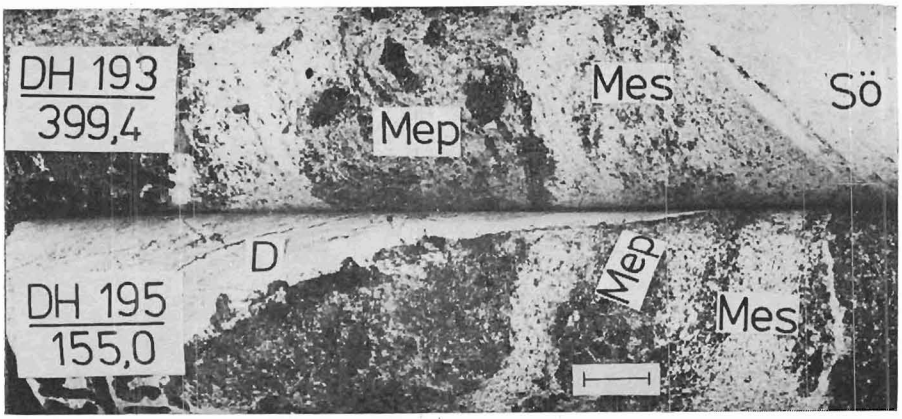

Fig. 61. Specimens showing contact relations between metaphoscorite, metasilicosövite and magmatic carbonatites. Metaphoscorite (Mep) is brecciated and assimilated by metasilicosövite (Mes). Both are cut by magmatic carbonatites (Sö = sövite, D = beforsite). Scale bar, 1.0 cm.

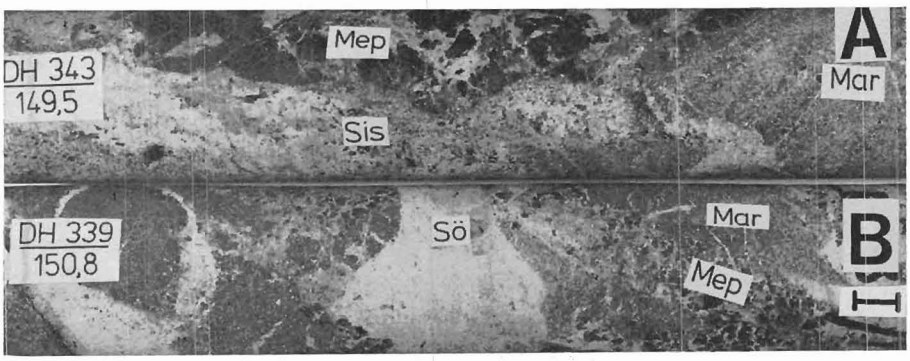

Fig. 62. Specimens showing contact relations between metaphoscorite and mica–amphibole rock. Scale bar, 1.0 cm.
A. Sharp contact between coarse-grained metaphoscorite (Mep) and fine-grained mica–amphibole rock (Mar) that possibly derived from fenite. Both are cut by Stage IV magmatic silicosövite (Sis).
B. To the right, medium-grained metaphoscorite (Mep) intersects mica–amphibole rock (Mar). To the left an obscure contact between these rocks. Magmatic sövite (Sö) cuts both rocks.

Reliable observations on the internal age sequence in the ultramafites — magnetite olivinite and pyroxenite — have not been recorded owing to the intense alteration and fragmental mode of occurrence of the rocks. Gradational contacts have not been observed and the boundaries between the altered varieties are sharp (Fig. 63), indicating that magnetite olivinite and pyroxenite intruded separately.

The metasomatites (pyroxene rock, amphibole rock, mica–amphibole rock and mica rock) and metaphoscorites are invariable cut, brecciated and assimilated by metasilicosövites (Figs. 27, 30 and 33). This indicates that intense carbonatization was the final metasomatic process before the intrusion of magmatic carbonatites. The contacts of the ultramafites, metacarbonatites and metasomatites with the magmatic carbonatites are visible

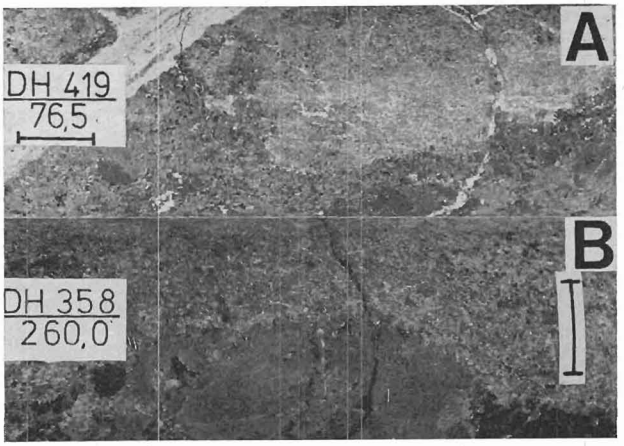

Fig. 63. Specimens showing sharp contact between altered pyroxenite and altered magnetite olivinite. Scale bar, 1.0 cm.

A. Upper part intensely alkali amphibolized pyroxenite, lower part intensely phlogopitized magnetite olivinite (metaphoscorite). Both are offset by a sövite veinlet.

B. Upper part slightly altered pyroxenite, lower part pegmatoidal, phlogopitized magnetite olivinite (metaphoscorite).

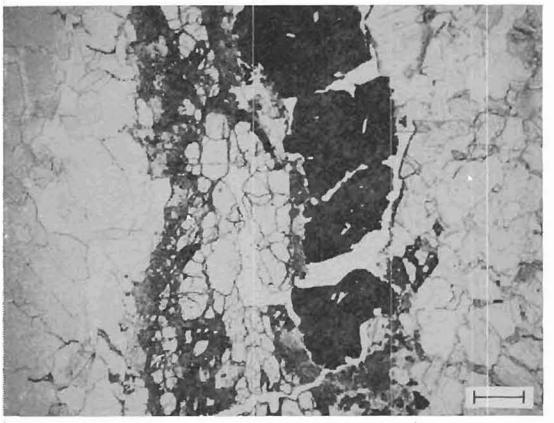

Fig. 64. Veinlet of Stage II magmatic sövite (in the middle) cutting phlogopite rock originated from magnetite olivinite. One nicol. Drill hole 436 at 36.5 metres. Scale bar, 0.5 mm.

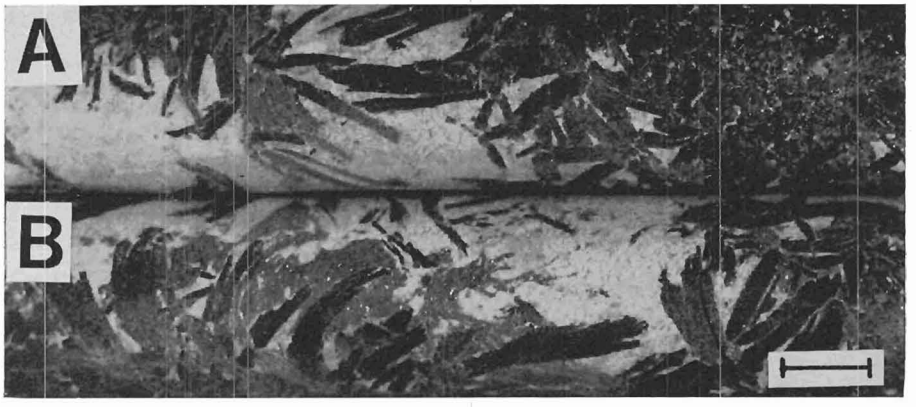

Fig. 65. Grass-like phlogopite growths in the contact zone between magmatic sövite (Stage IV) and a mica rock fragment (to the right). Pyrrhotite (grey) accumulated around phlogopite flakes (dark grey to black). Drill hole 485. Scale bar, 1.0 cm.

A. At 164.0 metres.
B. At 165.0 metres.

Fig. 66. Irregular injections of Stage IV magmatic sövite (white) into phlogopite–richterite metasövite. Scale bar, 1.0 cm.

Fig. 67. Sharp contact between coarse-grained metaphoscorite (to the left) and medium-grained Stage I magmatic phoscorite that has been moderately altered by Stage III hydrothermal activity. Scale bar, 1.0 cm.

in a number of drill core. They show the cutting and intrusive character of the magmatic carbonatites in relation to the older rocks (Figs. 22, 33, 61, and 64). Marked signs of reaction between these rocks are seldom encountered. An exceptional case is in drill hole 485 where grass-like phlogopite has developed in the contact between sövite (Stage IV) and a mica rock fragment (Fig. 65). The development of the metasomatites was encountered by reactionary carbonatization around the fenite fragments. This took place largely before the intrusion of the magmatic carbonatites because the later rocks intersect these alteration zones and the metasomatites (Figs. 33, 61 and 62). The metasilicosövites and the magmatic sövites display ill-defined contacts, the magmatic sövites protruding as irregular, schlieren-like injections into the metasilicosövites (Fig. 66). The contact between magmatic phoscorite and metaphoscorite is gradational in places; more

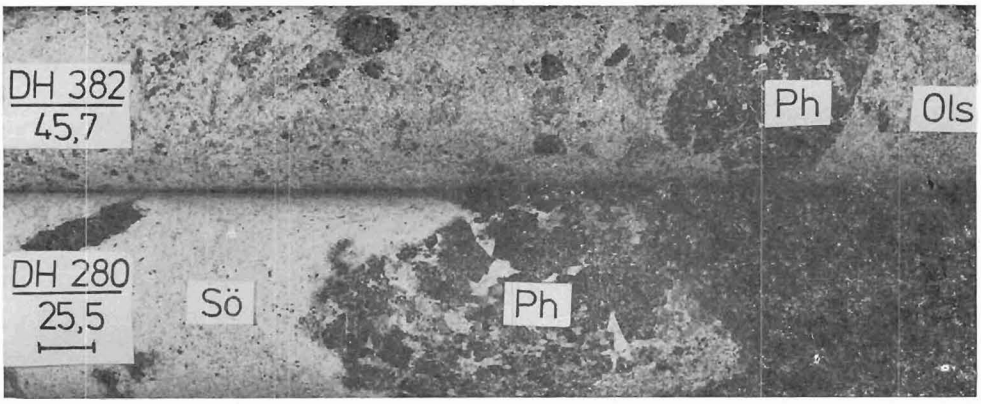

Fig. 68. Specimens showing Stage I phoscorite (Ph) as sharp-contoured fragments in Stage II sövite (Sö) and olivine sövite (Ols). Scale bar, 1.0 cm.

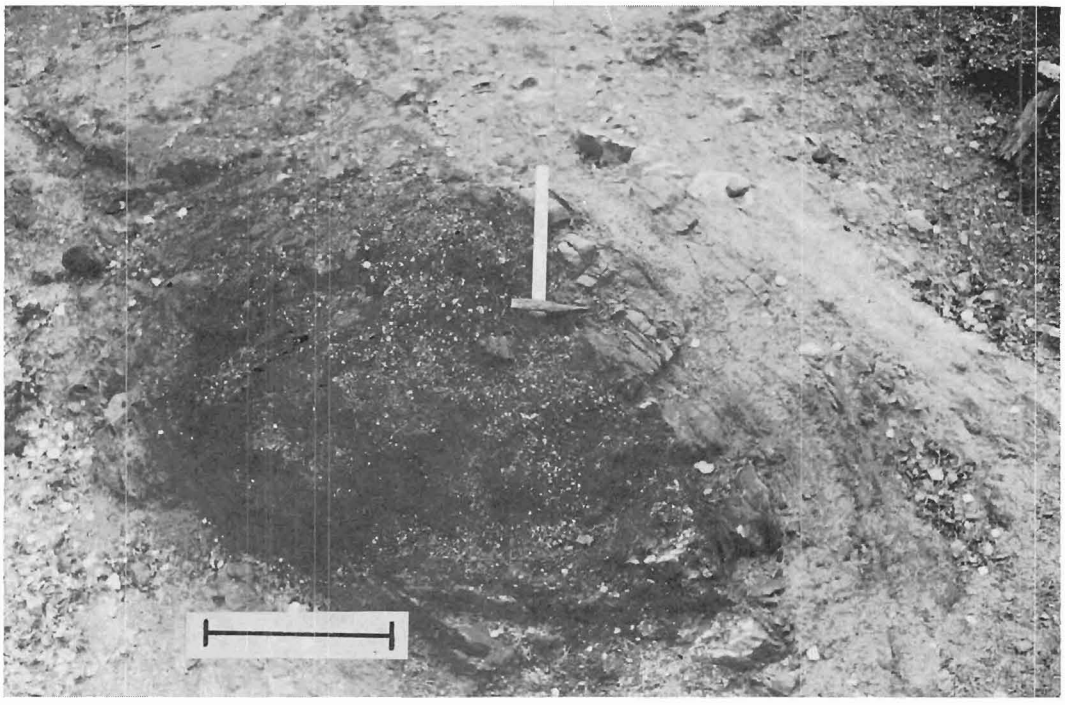

Fig. 69. A Stage I phoscorite fragment (black) in foliated Stage IV sövite (to the right). Note the fragments of sövite II (white) between the phoscorite fragment and the Stage IV sövite. Scale bar, 0.5 m.

often, however, it is sharp and transgressive, implying the intrusive origin (Fig. 67) of magmatic phoscorite.

The succession of magmatic carbonatites can be established from the internal contacts between these rocks. Stage I phoscorite or its altered varieties occur as sharp-contoured fragments in all the intrusive magmatic carbonatites, i.e., in the sövites of Stages II and IV (Figs. 68 and 69) and in late veins of Stage

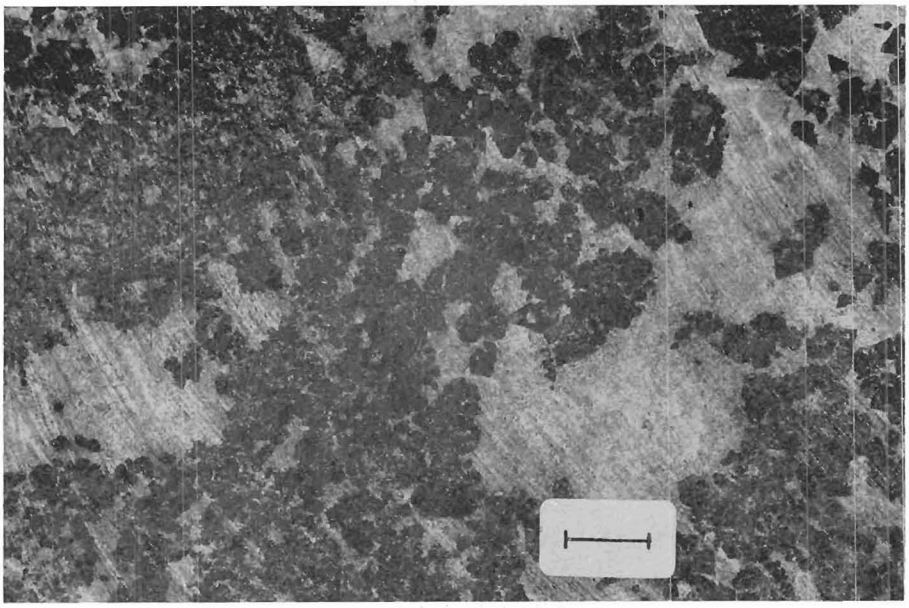

Fig. 70. Gradation between Stage I phoscorite (black) and Stage II sövite (white). Hand specimen, test pit 4. Scale bar, 1.0 cm.

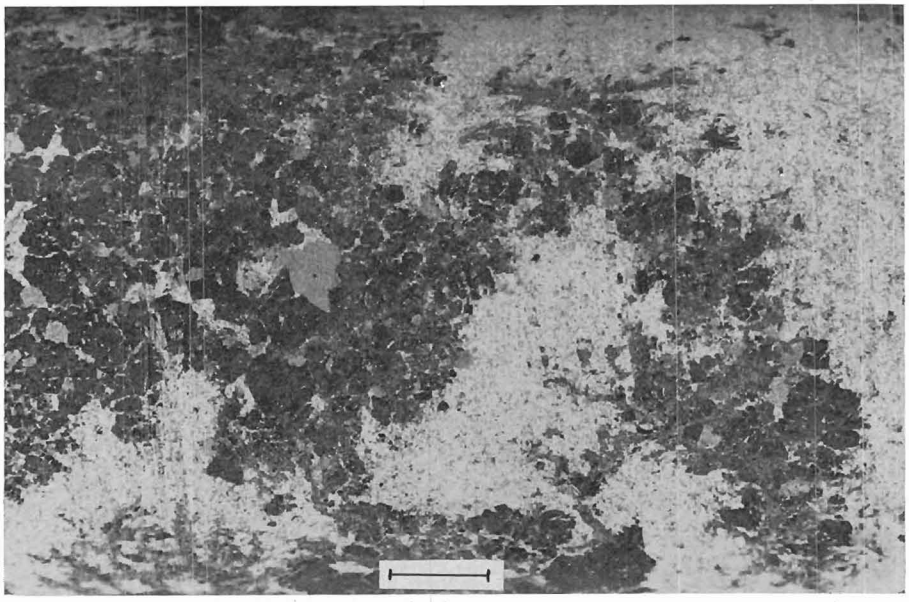

Fig. 71. An interdigitating contact between Stage I phoscorite (black) and Stage II sövite (white). Drill hole 428 at 57.1 metres. Scale bar, 1.0 cm.

V, showing that phoscorite is the oldest rock. On the other hand, the contacts between phoscorite and sövite II are gradational and interdigitating (Figs. 70 and 71). This may imply contemporaneous or nearly contemporaneous crystallization for phoscorite I and sövite II and the segregative character of the phoscorite.

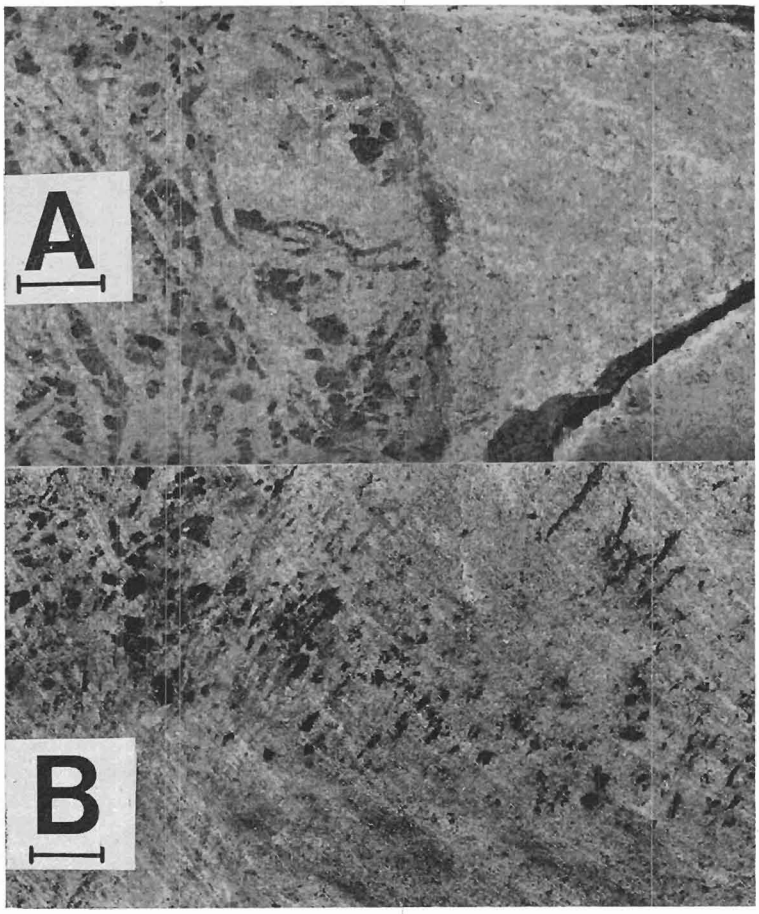

Fig. 72. Specimens showing internal rock relations of Stage II. Scale bar, 1.0 cm.
A. A sharp contact between tabular textured olivine–magnetite sövite (to the left) and massive sövite. Drill hole 428 at 127.5 metres.
B. Olivine–magnetite sövite that is fading out or is assimilated by finer-grained sövite. Drill hole 428 at 41.8 metres.

Although always massive in texture, Stage II sövites often show distinct internal boundaries between different sövite varieties as shown in Fig. 72. This indicates the heterogeneity of Stage II crystallization. Rocks of this stage occur as fragments in the rocks of Stage IV (Fig. 73) or are assimilated by them (Fig. 76).

The rocks of Stage III are predominantly alteration products of earlier carbonatites and thus the transitions between them are due to mineralogical gradations. The only manifestation of stage III — the apatite–ferriphlogopite rock — occurs as sharply cutting fracture fillings in earlier rocks (Figs. 74 and 75).

The foliated and banded Stage IV silicosövites cut and brecciate earlier rocks commonly with sharp contacts (Figs. 69, 73 and 76) but also with gradational and vague contacts. The massive sövite and beforsite of Stage IV which occur as lenses and dyke-like units, are the youngest units in that stage. They pass sharply or with rapid

Fig. 73. White, massive textured fragments of sövite II embedded in foliated, weathered Stage IV silicosövite. Test pit 1. Scale bar, 0.3 m.

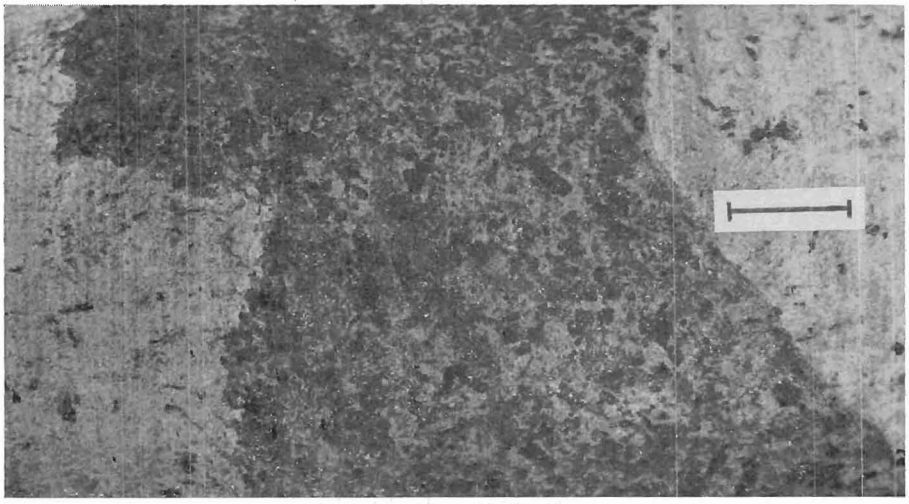

Fig. 74. Stage III apatite–ferriphlogopite rock (dark) cutting Stage II sövite as a fracture filling. Drill hole 428 at 37.1 metres. Scale bar, 1.0 cm.

gradation into the foliated and banded varieties. These massive rocks sometimes contain assimilated remnants of older rocks.

The veins of Stage V cut all the other rocks and include fragments from all the former stages; thus they are products of the latest crystallization of the magmatic carbonatites (Fig. 60).

Contact relations in the Sokli massif indicate the succession of rocks from oldest to youngest:

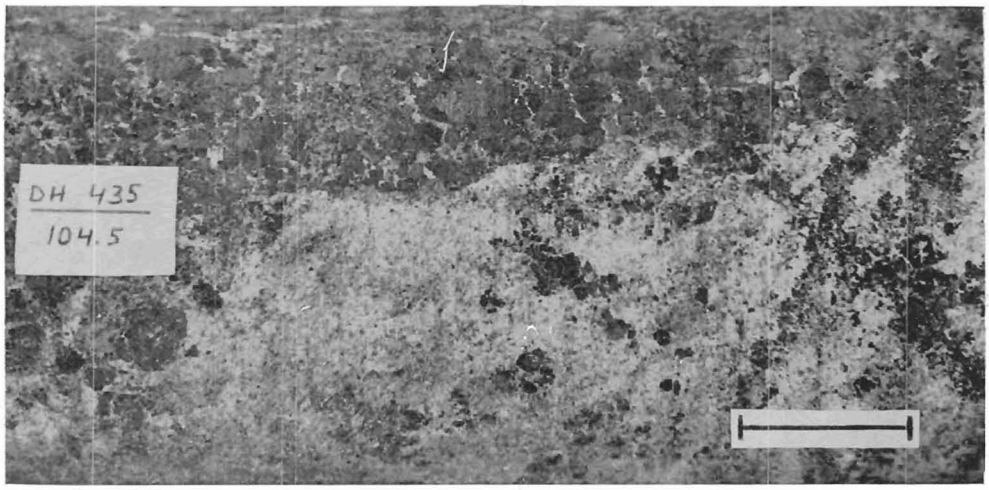

Fig. 75. Sharp contact between Stage III apatite–ferriphlogopite rock (dark) and metasilicosövite (light). Scale bar, 2.0 cm.

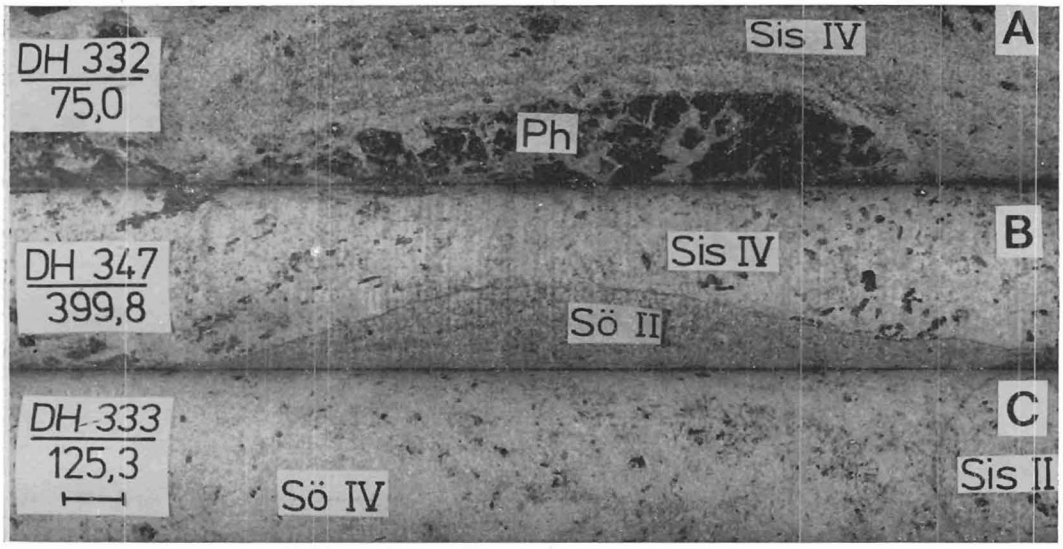

Fig. 76. Specimens showing contact relations between Stage IV and earlier rocks. Scale bar, 1.0 cm.
A. A fragment of Stage I phoscorite (Ph) in foliated Stage IV silicosövite (Sis).
B. Sharp contact between sövite II and Stage IV silicosövite.
C. Assimilated remnants of sövite II (pale grey) in sövite IV (white).

Ultramafites
↓
Fenites and alteration varieties of ultramafites
↓
Metasilicosövites
↓
Magmatic carbonatites

MINERALOGY

The minerals so far identified from the Sokli carbonatite massif, and which are listed in Table 7, include minerals of phosphorus ore, weathered crust and fresh rock. The number of mineral species is:

Sulphides	6
Oxides and hydroxides	16
Silicates	18
Carbonates	8
Phosphates	5
Others	3

The crystallization succession of primary minerals in the ultramafites and at each stage of the magmatic carbonatites and the formation of the minerals due to metasomatic or hydrothermal alteration in the metasomatites, metacarbonatites and in the rocks of magmatic Stage III are shown schematically in Fig. 77.

The feldspars, amphiboles, pyroxenes, and phlogopite of the fenite aureole have been described earlier (Vartiainen and Woolley, 1976), but there are no mineralogical accounts of the carbonatite massif itself. Descriptions of the micas, sulphides, apatite, magnetite and pyrochlore are being prepared. In the following, olivines, pyroxenes, amphiboles, and calcite–dolomite relations will be described.

Olivines, pyroxenes and amphiboles were analysed with a JEOL JXA-3SM electron microprobe at the Institute of Electron Optics, University of Oulu. The selected points were analysed under the following conditions: Si, Ti, Al, Fe, Mg, Ca, Na and K at an accelerating voltage of 15 kV and a specimen current of about 0.05 μA (measured on metallic Cu), and the other elements at an accelerating voltage of 15 kV and a specimen current of about 0.3 μA. The following stan-

Table 7

Minerals identified from the Sokli carbonatite massif

Sulphides	Oxides and hydroxides	Silicates	Carbonates	Phosphates
Galena	Hematite	Forsterite	Calcite	Apatite
Sphalerite	Ilmenite	Clinohumite	Dolomite	Francolite
Chalcopyrite	Magnetite	Aegirine	Siderite	Rhabdophane
Pyrrhotite	Götite	Diopside	Strontianite	Crandallite
Pyrite	Lepidocrocite	Edenite	Ankerite	Cheralite
Marcasite	Psilomelane	Richterite	Barytocalcite	*Others*
	Rutile	Eckermannite	Ancylite	Fluorite
	Anatase	Ferri-eckermannite	Witherite	Barite
	Baddeleyite	Biotite		Whewellite
	Perovskite	Phlogopite		
	Dysanalyte	Ferriphlogopite		
	Zirkelite	Vermiculite		
	Calzirtite	Iddingsite		
	Pyrochlore	Serpentine		
	Uranpyrochlore	Pennite		
	Hatchettolite	Stilpnomelane		
		Albite		
		Zircon		

dards were used: quartz for Si, TiO for Ti, synthetic sapphire for Al, hematite for Fe, periclase for Mg, wollastonite for Ca, albite for Na, potassium feldspar for K, metallic Mn for Mn, and metallic Cr for Cr. The ZAF corrections were processed on a UNIVAC 1108 computer using the MK1 program (Mason *et al.*, 1969).

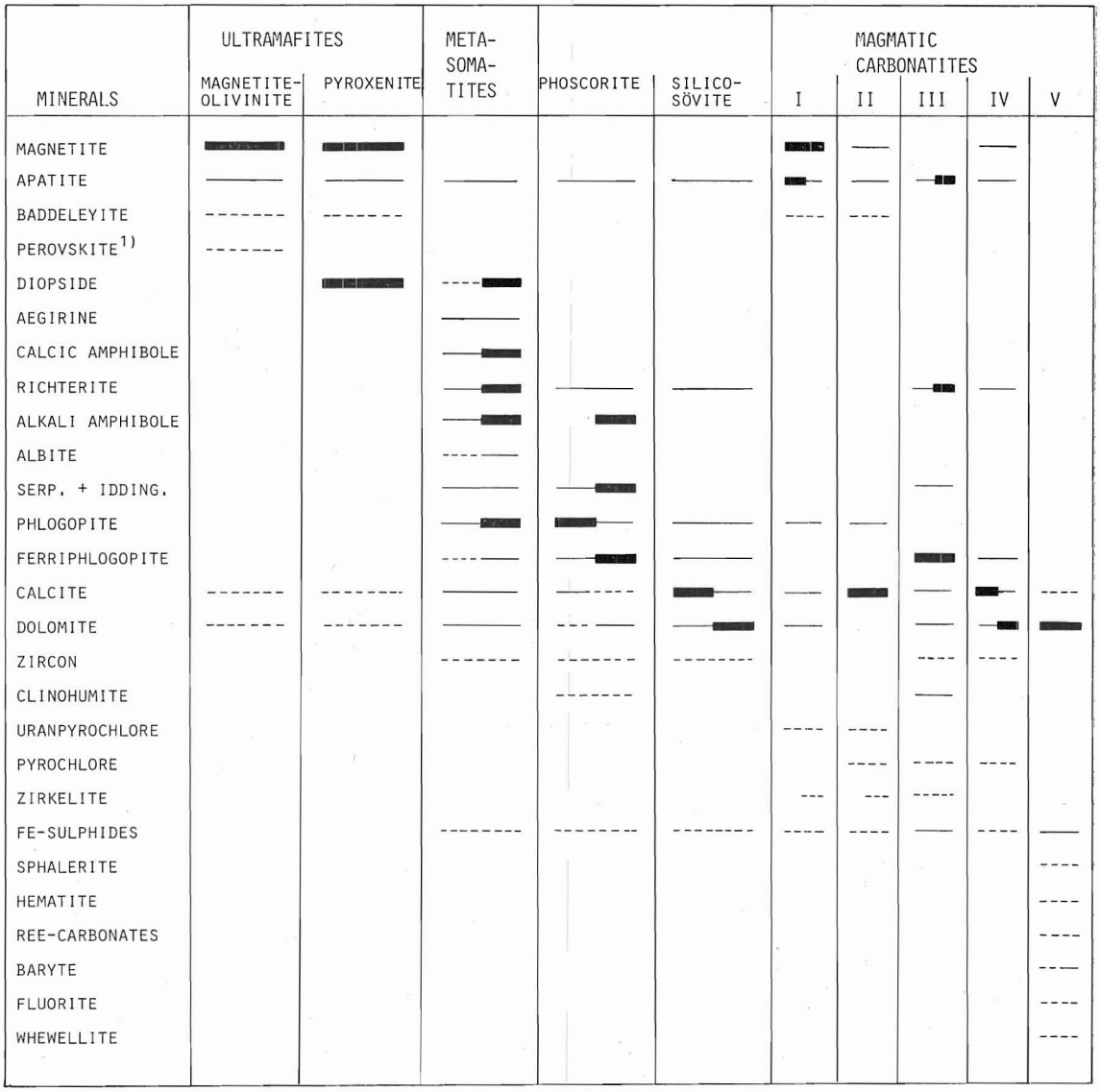

1) In olivine rock

Fig. 77. Schematic sequence of crystallization of primary minerals (in ultramafites and magmatic carbonatites) and formation of metasomatic and hydrothermal minerals (in metasomatites, metacarbonatites and in hydrothermal Stage III of magmatic carbonatites). Broad line, main mineral; thin line, minor mineral; dashed line, accessory mineral.

Olivine

Olivine is encountered in the Sokli area in the Tulppio olivinite massif near the carbonatite complex (Fig. 1), in the ultramafites within the carbonatite complex, in the magmatic carbonatites and in alkaline lamprophyres. The mode of occurrence and composition of olivine in each rock will be described. Table 8 gives the essential characteristics and secondary alteration products of olivine in the rocks at Sokli.

Occurrence

In the Tulppio olivinite massif olivine forms almost monomineralic bodies that are some hundreds of metres in diameter and grades into metaolivinites. The olivinite is a massive, granular rock in which olivine occurs as fresh, hypidiomorphic grains. Weak serpentinization appears along the cleavages but grows stronger towards the metaolivinites where it is often complete.

The ultramafites within the carbonatite massif contain magnetite olivinites that are metasomatically altered into metaphoscorites and other rocks. In the present relict rocks the abundance of olivine is generally 5—30 %. The grains are anhedral and intensely altered into various products (Table 8), predominantly bowlingite and carbonate.

In the magmatic carbonatites olivine is met with only in the rocks of the first three stages. Its mode of occurrence displays a certain regularity. In the rocks of the first stage, phoscorites, the olivine is a rock-forming mineral that occurs as moderately altered euhedral or subhedral grains. A special alteration feature of this olivine is iron oxide that appears along cleavages (Fig. 42) and which may spread from these to occupy half of the grain. There are also rapid changes in the intensity of serpentinization. In extreme cases one half of a thin section contains fresh olivine and the other half completely serpentinized olivine (Fig. 44). The sövites

Table 8

Abundance, grain size, shape and alteration products of the olivines from the rocks in the Sokli area

Host rocks	Quantity vol-%	General grain size, mm	Shape	Alterations	
				Major	Minor
Olivinite, Tulppio	85—95	0.3—3.0	Subhedral	—	Serpentine
Ultramafites, carbonatite massif	0—30	0.5—15.0	Anhedral	Bowlingite Carbonate	Serpentine Iron oxides Clinohumite
Carbonatites					
Stage I	0—40	0.3—10.0	Euhedral-subhedral	Serpentine Iron oxides	Bowlingite Clinohumite
Stage II	0—5	0.3—2.0	Subhedral	Serpentine	Clinohumite
Stage III	0—30	0.1—5.0	Anhedral	Clinohumite	Serpentine Bowlingite Iddingsite Richterite
Alkaline lamprophyre	20—40	0.5—4.0	Euhedral	Serpentine Bowlingite Carbonate	Iddingsite Phlogopite Iron oxides Clinohumite

of the second stage usually contain small amounts of olivine as separate, subhedral grains that usually have narrow reaction rims against calcite and are moderately altered. The olivine in the phoscorites of the third (hydrothermal) stage is intensely altered and thus differs from those of the earlier stages. Only a minor proportion of those shown in Table 8 are fresh olivine. Most typically olivine is altered into clinohumite. The alteration begins in the grain boundaries and spreads inwards with it affects the whole grain, especially when the olivine grains are granulated. The clinohumite has a strong pleochroism with X = deep yellow, Z = colourless. At Stage III the alteration has produced iddingsite and richterite as well.

In alkaline lamprophyres olivine occurs as a phenocrystal phase. Fresh olivine is encountered only in porphyritic and xenolithic dykes; in other types of dykes the alteration into a variety of minerals has reached completion. The alkaline lamprophyres have been described earlier in greater detail (Vartiainen *et al.*, 1978).

A notable feature of the Sokli olivines is their alteration into clinohumite (Fig. 50). Some clinohumitization of olivine is encountered in all the rocks of the Sokli complex, but it is intensely developed only in the Stage III phoscorites, where it is a dominant alteration product (Fig. 50). Hydrothermal processes are most pronounced in these rocks. Green phlogopite has altered into reddish ferriphlogopite, and richterite, sulphides and apatite have developed simultaneously with clinohumitization. Study of the liquid inclusions in the Sokli apatite (Haapala, 1978) has

Table 9

Microprobe analyses of olivine from Tulppio and Sokli

	Olivinite	Ultramafites			Carbonatites					Alkaline lamprophyres	
					Stage I	Stage II		Stage III			
	1	2	3	4	5	6	7	8	9	10	11
SiO_2	42.1	41.2	39.1	41.4	41.5	43.0	42.9	40.5	43.4	40.9	41.5
FeO	8.0	16.5	9.2	13.6	5.4	4.5	6.4	12.5	6.1	8.5	10.1
MnO	0.11	1.25	1.00	0.71	0.85	0.67	0.72	0.83	0.59	0.10	0.14
NiO	0.46	< 0.05	< 0.05	< 0.05	< 0.05	< 0.05	< 0.05	< 0.05	< 0.05	0.38	0.25
MgO	48.3	41.3	48.6	45.7	53.2	54.5	49.2	46.8	51.6	49.3	46.7
CaO	0.13	0.16	< 0.05	0.07	0.13	0.15	0.35	0.05	0.05	0.19	0.08
Total	99.2	100.4	97.9	101.5	101.1	102.8	99.6	100.7	101.7	99.4	98.6
Number of ions on the basis of 4 oxygen atoms											
Si	1.032	1.037	0.982	1.016	0.990	1.002	1.037	1.000	1.025	1.006	1.030
Fe	0.164	0.347	0.194	0.279	0.108	0.088	0.130	0.258	0.120	0.175	0.210
Mg	1.765	1.549	1.820	1.672	1.892	1.892	1.772	1.723	1.817	1.807	1.728
Mn	0.002	0.027	0.021	0.015	0.017	0 013	0.015	0.017	0.012	0.002	0.000
Ca	0.003	0.004	0.000	0.002	0.003	0 004	0.009	0.001	0.000	0.005	0.002
Atomic ratios											
Mg	91.5	81.7	90.4	85.7	94.6	95.6	93.2	87.0	93.8	91.2	89.2
Fe^{+2}	8.5	18.3	9.6	14.3	5.4	4.4	6.8	13.0	6.2	8.8	10.8

1. Trench 3, Tulppio.
2. Drill hole 395 at 148.0 metres.
3. Drill hole 331 at 168.0 metres.
4. Drill hole 413 at 41.0 metres.
5. Drill hole 260 at 77.0 metres.
7. Drill hole 14 at 29.4 metres.
8. Drill hole 332 at 84.2 metres.
9. Drill hole 340 at 135.5 metres.
10. Drill hole 347 at 403.0 metres.
11. Drill hole 2 at 50.0 metres.

shown that hydrothermal activity permeated the entire magmatic core of the carbonatite massif. Hydrothermal activity presumably provided favourable conditions for the development of clinohumite.

There are few descriptions of clinohumite from other carbonatites. Clinohumite has been recorded from some complexes at Kola (Borodin *et al.*, 1973) and from Siberia (Egorov, 1970). Melcher (1966, p. 177) mentions red clinohumite associated with olivine in the Jacupiranga carbonatite. Chondrodite, a closely related mineral, occurs in similar fashion in the Palabora (S. Africa) and Bukusu (Uganda) complexes (Deans, pers. comm.).

Composition

Microprobe analyses of the olivines were conducted by directing the beam to the centre

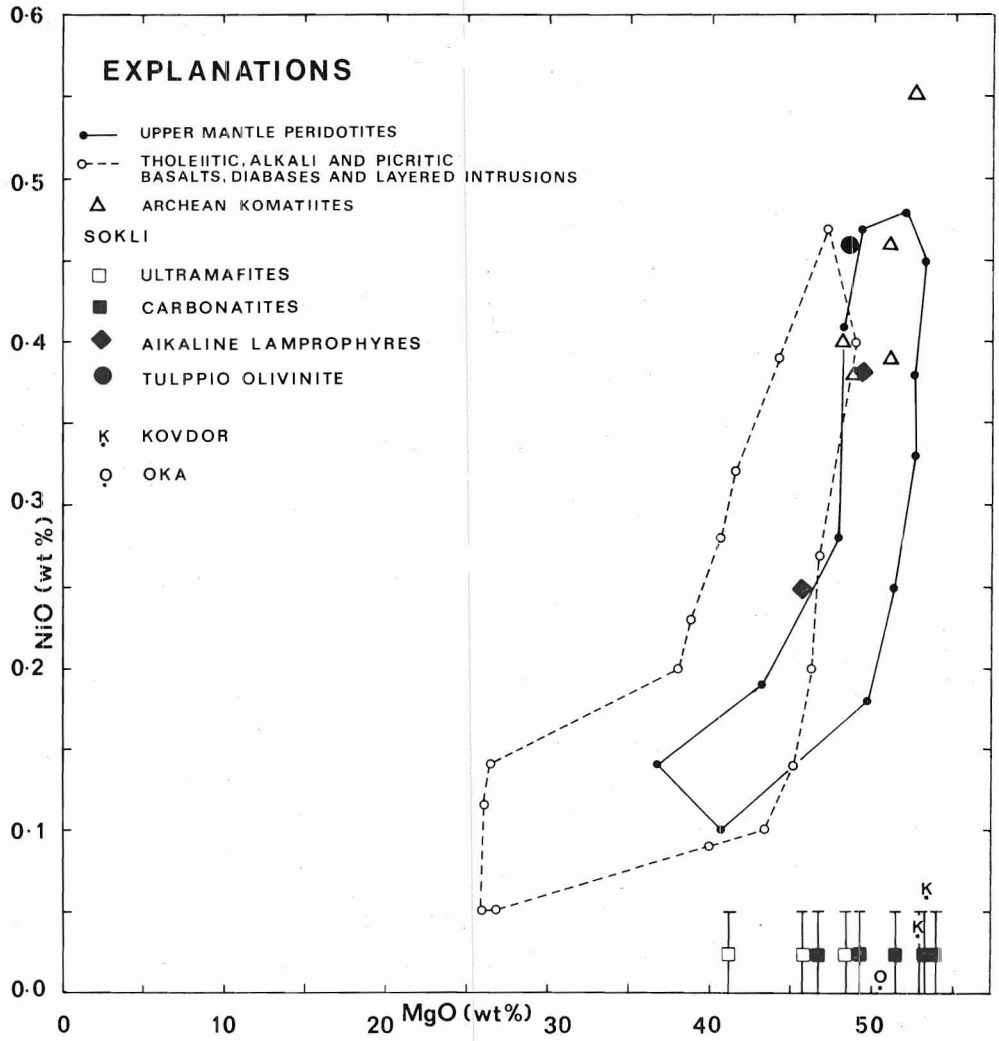

Fig. 78. NiO—MgO correlation diagram of olivine compiled according to Fleet *et al.* (1977). Host rocks are shown by symbols.

of the grains. The results of the analyses are given in Table 9. The olivines are all forsteritic in composition. The slight variation in Mg contents does not correlate with the host rock. The distribution of Ni and Mn divides the olivines into two groups:

1. High NiO (0.25—0.46 %) and low MnO (0.10—0.14 %); olivinite in the Tulppio and alkaline lamprophyres
2. Low NiO (< 0.05 %) and high MnO (0.59—1.25 %); ultramafites and carbonatites.

The Ni content. In Fig. 78 the Sokli analyses and the data from the carbonatites of Kovdor (Kukharenko *et al.*, 1965) and Oka (Simkin and Smith, 1970) are plotted in a NiO versus MgO diagram. The figure reveals that the olivines of the Sokli carbonatites and ultramafites and those of Oka and Kovdor form a distinct group characterized by higher MgO (46—55 %) and lower NiO (< 0.10 %) than in the olivines of magmatic rocks from other environments.

The Mn content of the Sokli olivines has a similar distribution trend to that of Ni: the olivines of the Tulppio olivinite and the alkaline lamprophyres fall within the general field of plutonic and extrusive rocks in the manganese—magnesium correlation diagram,

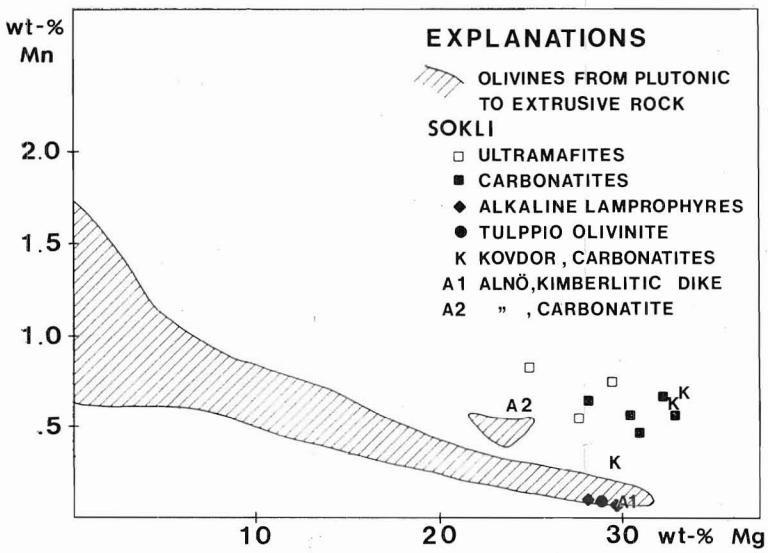

Fig. 79. Manganese — magnesium correlation diagram of olivine according to Simkin and Smith (1970). Host rocks are shown by symbols.

Table 10

Average bulk composition of olivine-bearing rocks from Sokli (XRF-analysis, wt-%, analysed by Rautaruukki Oy)

Rocks	SiO_2	FeO *	MgO	CaO	CO_2 **	Olivine NiO	Olivine MnO
Olivinite, Tulppio	40	9	48	0.12	0.50	0.46	0.11
Ultramafites	25	32	24	8	3.50	< 0.05	1
Carbonatites							
Stage I, phoscorites	12	30	19	20	8	< 0.05	0.85
» II, sövite	1.5	4	3	49	38	< 0.05	0.54
» III, phoscorite	15	26	18	20	3	< 0.05	0.71
Alkaline lamprophyres	25	20	18	13	13	0.32	0.12

* Total iron
** Calculated from the total carbon content determined on a Leco IR 12.

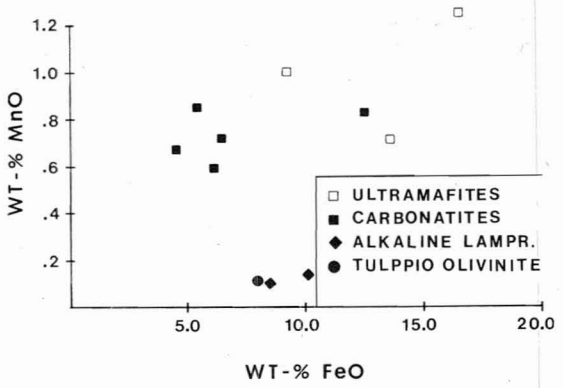

Fig. 80. MnO—FeO correlation diagram of olivine. Host rocks are shown by symbols.

whereas the olivines of the carbonatites and ultramafites form a separate group in the Mg-rich part of the diagram (Fig. 79). The olivines from the Kovdor (Kukharenko *et al.*, 1965) and Alnö (von Eckermann, 1974) carbonatite follow the latter trend. Simkin and Smith (1970, p. 316) have found that: »Manganese is strongly tied to the Fe content in olivines and the data suggest that variations from the main trend are more likely to result from the bulk chemistry of the host rock than from its crystallization environment.» Table 10 shows the bulk chemistry of the olivine-bearing rocks of Sokli and Fig. 80 the manganese oxide-iron oxide correlation diagram of olivine. In spite of the differences in the bulk chemistry of the host rocks the olivines of the sövites, phoscorites and the ultramafites have a similar trend in MnO—FeO correlation. The difference in the bulk chemistry of the host rock may explain the deviation of the Tulppio olivine from this trend but not that of the alkaline lamprophyres, which is near to the phoscorites but far from the olivinite in chemistry (Table 10).

The CaO content in the Sokli olivines varies in the range < 0.05—0.35 % (Table 8). The average CaO contents in the Sokli olivines are near each other as shown by the following data arranged according to the sequence of emplacement of the host rocks:

	CaO %
Tulppio olivinite	0.13
Ultramafites	0.09
Carbonatites	0.14
Alkaline lamprophyres	0.14

The olivine from the Oka carbonatite contains 0.11—0.14 % CaO (Simkin and Smith, 1970, analyses 97 and 98). The typical CaO value of olivines in plutonic carbonatites is presumably between 0.05 and 0.15 per cent.

Simkin and Smith (1970) have reported a positive correlation between MgO and NiO in olivines and state that »no obvious correlation exists between Ni content and crystallization environment, but the bulk composition of the rock seems to correlate well with the Ni content» (p. 318). On the other hand, Fleet *et al.* (1977, p. 192) state that a distinctly separate NiO distribution exists for olivine from the upper mantle and crustal rock associations (see Fig. 78).

Hart and Davis (1977) have shown that the partitioning of Ni between olivine and silicate melt is strongly dependent on the composition of the melt. Ni analyses of olivines from other carbonatite complexes (Kovdor, Oka) show a low Ni content as well (Fig. 78). This may be due to NiO deficiency in carbonatite magmas in general. According to Gold (1966 b), the average Ni content in carbonatites is only 32.4 ppm, the average for magmatic rocks being 100 ppm. Bulakh *et al.* (1975) report from the Turyi massif that Ni is almost completely absent from carbonatites (phoscorites).

With the exception of the low MnO content (0.08 per cent) in olivine from a beforsite dyke at Alnö (von Eckermann, 1974, p. 156), olivines from other carbonatites (Fig. 79) have a high MnO content (> 0.4 per cent). It may be concluded that the olivines in carbonatites

are generally characterized by lower NiO (< 0.10 per cent) and higher MnO (> 0.4 per cent) than in the high MgO olivines from other magmatic rocks (Figs. 78 and 79).

The low CaO content in olivine (< 0.1 per cent) indicates a plutonic crystallization environment for the host rock whereas olivines from extrusive and hypabyssal rocks contain 0.1 per cent or more CaO (Simkin and Smith, 1970, p. 318). Ferguson (1978) has elaborated on this in respect of extrusive rocks by showing that the Ca enrichment in olivines occurs only in lavas devoid of plagioclase. The rocks in the Sokli carbonatite complex have crystallized in the same plutonic environment but there is a variation in the CaO content even within given host rock types: < 0.05—0.16 per cent in the ultramafites and < 0.05—0.35 per cent in the magmatic carbonatites. This may be because a small intrusion has a more heterogeneous crystallization environment than plutons in general.

Pyroxene

Pyroxene is a subordinate mineral in the Sokli carbonatite complex but it plays a significant role as an index mineral in the evolution of the complex. The mode of occurrence and alteration of pyroxene is described, and six electron microprobe analyses are given.

Occurrence

Pyroxene is encountered in four groups of rocks in the Sokli area: in metaolivinites of the Tulppio ultramafic massif (Fig. 1); in ultramafites; in xenoliths in magmatic carbonatites and in the fenite aureole. The mode of occurrence and alteration of pyroxene is described from all of these except the fenite aureole, from which pyroxene has been described earlier (Vartiainen and Woolley, 1976).

In the metaolivinite the pyroxene is enstatite that has developed into large (10—20 mm) anhedral grains occupying, in places, as much as 50—60 per cent of the volume. It replaces olivine. The enstatite is colourless, and slightly corroded by calcite and replaced to a small extent by colourless amphibole and chlorite (kotschubeite, x-ray identification).

The ultramafites have two pyroxenes: diopside and aegirine. The disopside predominates. Together with a small amount of magnetite it presumably formed nearly two-mineralic magnetite-bearing pyroxenites that later altered into metaphoscorites and other rock varieties. The best preserved diopside grains may be up to 2—3 cm long. The common grain size is 0.5—1.0 cm. Fig. 5 shows recrystallized diopside. The diopside often contains inclusions of apatite and opaque minerals (Figs. 81 and 82).

Alteration is common and intense, but irregular with regard to the developing minerals. Grass green amphibole, the first alteration product in diopside, probably developed during the ultramafic magmatic stage. Ultimately, pyroxenite may have altered into amphibole rock in which only small relict diopside grains, if any, remain.

Alkaline alteration has converted diopside into aegirinic pyroxene. The extent of aegirinization varies so rapidly that, of two neighbouring grains, one may be only slightly rimmed by aegirine while the other is totally altered into aegirine (Fig. 81). Simultaneously with aegirinization the parting in the grains changes from moderate to intense, bringing about a fibrous habit. The pseudo-

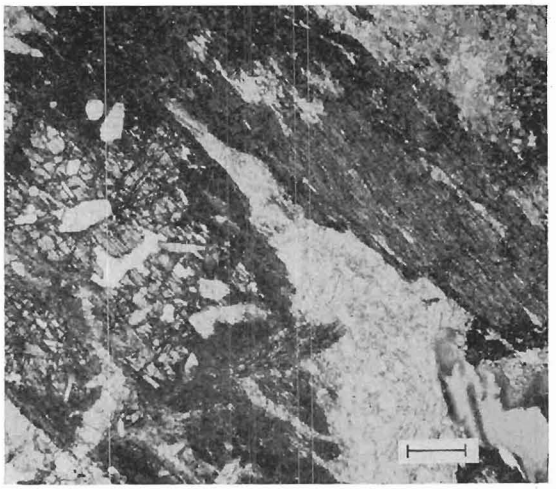

Fig. 81. Ragged diopside prism narrowly rimmed by aegirine (to the left) contains apatite inclusions. The diopside (to the right) is almost totally altered into aegirine. One nicol. Drill hole 193 at 130.5 metres. Scale bar, 0.5 mm.

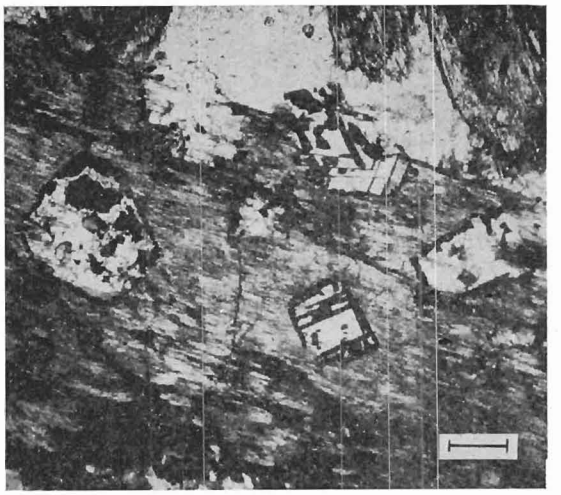

Fig. 82. Aegirine prism containing totally carbonatized magnetite. Only unaltered ilmenite lamellae (black) remain. One nicol. Drill hole 193 at 130.5 metres. Scale bar, 0.5 mm.

morphs have, however, often preserved the forms of the original diopsidic pyroxene and the grains still contain apatite and magnetite inclusions as relics of the diopsidic stage. The magnetite inclusions are totally carbonatized, only the ilmenite lamellae are still unaltered (Fig. 82). The aegirine usually alters into alkali amphibole as narrow rims. Wherever carbonate has extensively replaced aegirine, the grains are decomposed and eventually fade into ghost grains (Fig. 83).

The grain size in the aegirine of the ultramafites is larger than that in the aegirine of the fenite aureole. In the fenites aegirine

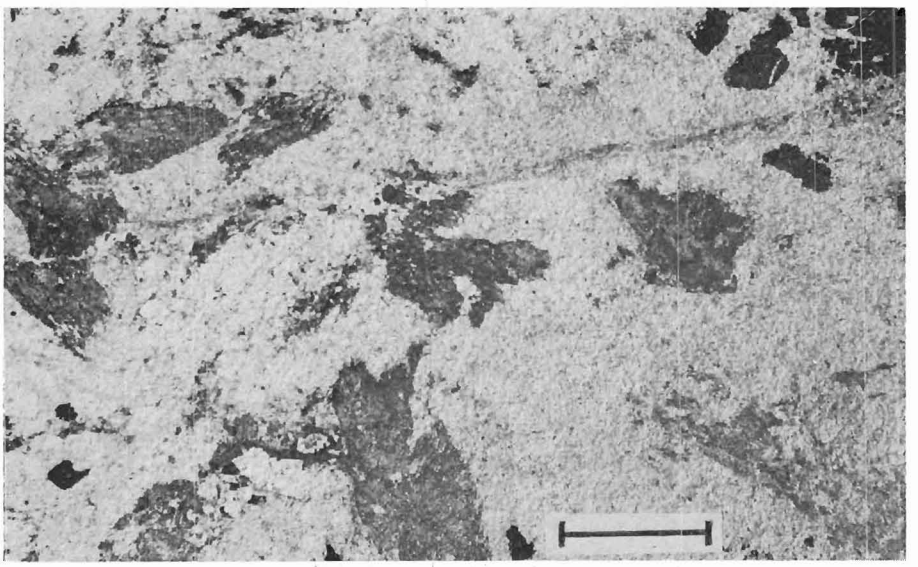

Fig. 83. Moderately to strongly carbonatized aegirine grains in metaphoscorite. One nicol. Drill hole 193 at 122.0 metres. Scale bar, 3.0 mm.

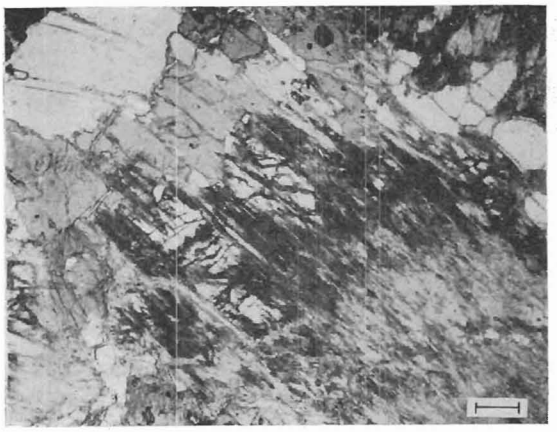

Fig. 84. Diopside prism altered into alkali amphibole (bottom right) and at the other end into calcic amphibole (top left). One nicol. Drill hole 358 at 220.0 metres. Scale bar, 0.3 mm.

characteristically occurs as small crystals that form clusters of radiating needles and a vague reticulate pattern of veins. Larger stout prisms close to the carbonatite contact (Vartiainen and Woolley, 1976, p. 27) may actually be relics of the fenitized ultramafite fragments, as is also suggested by the structure of these fenitic rocks in which the usual fenite veinlet network is poorly developed.

Alkaline alteration has also transformed diopside into alkali amphibole. Bluish green amphibole may have grown directly from diopside grains (Fig. 84) but not uncommonly the alteration pattern show successive rims of aegirine or calcic amphibole and alkali amphibole (Fig. 85). The alteration processes described above give some indication of the evolution of the pyroxene-bearing rocks. The bulk of the pyroxene was probably destroyed by the invasion of carbonate and mica during the later stages of development of the carbonatite complex.

Pyroxene-bearing xenoliths in the magmatic carbonatites consist of intensely altered fragments of pyroxenites and fenites. The xenoliths range from some centimetres to several metres in diameter. They are encountered even at the centre of the magmatic core but more frequently in the metacarbonatite area and in the transitional zone against the fenite aureole. The pyroxenes in these xenoliths are dissimilar. The primary pyroxene in the pyroxenitic xenoliths is similar to that in the pyroxenite in the metaphoscorite zone; but is, however, reduced in grain size and more altered, so that even semi-preserved grains are scarce. In close association with the fenite fragments a metasomatic pyroxene occurs that is quite distinct from the primary pyroxene. It forms small stout prisms averaging 0.2 mm × 0.5 mm and shows strong pleochroism from bright green to greenish yellow. The prisms are almost free from inclusions.

Composition

The compositions of seven pyroxenes are given in Table 11. Analyses 2 and 3 are from the same sample, the former being a wet chemical analysis made at the laboratory of the British Museum, and the latter a microprobe analysis. The results generally coincide fairly well. The pyroxene analyses are

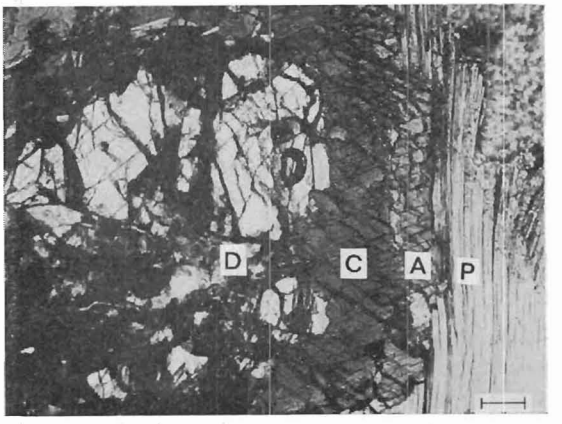

Fig. 85. Successive alteration rims in diopside, D = diopside, C = calcic amphibole, A = alkali amphibole, P = phlogopite. One nicol. Drill hole 358 at 207.3 metres. Scale bar, 0.3 mm.

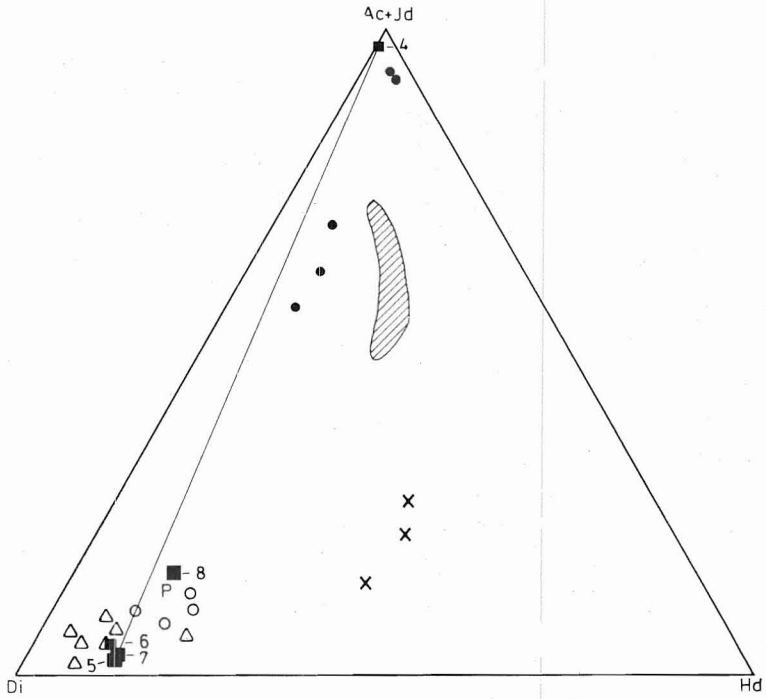

Fig. 86. Plot of pyroxenes in terms of acmite + jadeite—diopside—hedenbergite. Numbers refer to analyses in Table 11; filled circles, aegirines and aegirine—augites from the Sokli fenites (Vartiainen and Woolley, 1976); open circles, aegirine—augites from sövites of Alnö and X, aegirine—augites from sövite—pegmatites of Alnö (von Eckermann, 1974); triangles, diopsides from pyroxenites and metasomatic calcite—amphibole—diopside rocks of Kovdor and Afrikanda (Kukharenko *et al.*, 1965); shaded area, pyroxenes from carbonatites and P, pyroxene from pyroxenite of East Africa (Tyler and King, 1967). Analyses 4 and 5 from the same sample is joined by tie line.

plotted on an acmite + jadeite—diopside—hedenbergite diagram (Fig. 86) as proposed by Yoder and Tilley (1962).

The use of total iron has had little effect on the calculation of pyroxene relations. Owing to low Al the Tschermak molecule is low, and it is neglected as an »error of closure» triangle in the plotting. The comparatively small amounts of the other constituents have justified the recalculation of the proportions acmite + jadeite, hedenbergite and diopside to 100 %. The pyroxene of the Sokli complex is marked by its diopside-rich composition. Thus it differs conspicuously from the pyroxenes in the carbonatites of Uganda, where the pyroxene probably crystallized from carbonatite magma (Tyler and King, 1967), and from the aegirine augites in the sövite pegmatites of Alnö (Fig. 86). Diopsides from the pyroxenites and the metasomatic calcite—amphibole—diopside rocks of Kovdor and Africanda, aegirine augites from the Alnö sövites, pyroxene from the Uganda pyroxenites and the Sokli diopsides form a distinct group in the diopsidic corner of acmite + jadeite—diopside—hedenbergite diagram (Fig. 86).

At Sokli the diopsides in both the pyroxenite and pyroxenitic xenoliths in the magmatic carbonatite are similar in composition but differ from the more acmitic pyroxene in the metasomatic pyroxene rock transformed from fenite (Fig. 86). There are also differences in minor components of pyroxenes as follows (Table 11):

	Pyroxenites	Metasomatic pyroxene rock
ZrO_2	0.05—0.16 %	0.00 %
MnO	0.08—0.23 %	0.49 %
Na_2O	0.26—0.59 %	1.83 %

Diopside and aegirine were analysed from the same sample (numbers 4 and 5 in drill hole 193 at 130.5 metres, Table 11). The data

Table 11

Microprobe analyses of Sokli pyroxenes

	Enstatite	Aegirines			Diopsides			Acmitic diopside
	1	2	3	4	5	6	7	8
SiO_2	57.8	52.4	53.3	52.9	53.6	56.0	52.7	53.2
TiO_2	< 0.05	1.25	2.40	2.0	0.55	0.28	0.26	0.35
ZrO_2	n.d.	0.108	0.20	0.24	0.16	0.05	0.05	n.d.
Al_2O_3	0.19	1.34	0.28	1.5	1.7	0.67	0.43	0.61
Fe_2O_3	—	29.7	29.8	29.3	—	—	—	—
FeO	6.5	—	—	—	5.0	5.0	4.0	8.6
MnO	0.38	0.07	< 0.05	< 0.05	0.08	0.15	0.23	0.49
NiO	0.10	n.d.	< 0.05	< 0.05	< 0.05	< 0.05	< 0.05	< 0.05
MgO	33.3	0.67	1.0	0.7	17.0	18.1	15.8	11.6
CaO	0.07	0.41	0.10	0.20	24.0	23.9	25.7	22.0
Na_2O	0.05	12.82	12.8	13.5	0.26	0.59	0.33	1.83
Total	98.44	99.67	99.98	100.44	102.40	104.79	99.55	99.73
Number of ions on the basis of 6 oxygen atoms								
Si	2.023	2.014	2.174	2.146	1.931	1.964	1.958	2.017
Al	0.008	0.061	0.013	0.072	0.069	0.028	0.019	0.027
Ti	0.000	0.036	0.074	0.061	0.015	0.007	0.007	0.010
Fe^{+3}	—	0.816	0.914	0.896	—	—	—	—
Fe^{+2}	0.191	0.044	—	—	0.151	0.147	0.124	0.274
Mg	1.731	0.038	0.061	0.042	0.913	0.946	0.875	0.655
Mn	0.011	0.002	0.000	0.000	0.002	0.004	0.007	0.016
Ca	0.003	0.017	0.004	0.009	0.926	0.898	1.023	0.894
Na	0.000	0.955	1.012	1.062	0.018	0.040	0.024	0.135
Mg	89.5	4.2	6.2	4.5	45.8	47.4	43.1	35.7
Fe	10.4	94.0	93.3	94.6	7.7	7.6	6.5	15.7
Ca	0.1	1.8	0.4	0.9	46.5	45.0	50.4	48.6
100 Mg: (Mg + Fe Mn)	89.5	4.4	6.2	4.5	85.6	86.2	86.9	69.4
Colour	Colour-less	Green	Green	Green	Pale yellow	Colour-less	Pale yellow	Light green

n.d. = not detected
1. Metaolivinite of Tulppio. Drill hole 286 at 59.3 metres.
2. Syenitic fenite. Drill hole 210 at 95.0 metres (chemical analyses by British Museum).
3. Syenitic fenite. Drill hole 210 at 95.0 metres.
4. Slightly altered pyroxenite. Drill hole 193 at 130.5 metres.
5. Slightly altered pyroxenite. Drill hole 193 at 130.5 metres.
6. Slightly altered pyroxenite. Drill hole 358 at 207.3 metres.
7. Pyroxene relic in metasilicosövite fragment from magmatic core. Drill hole 262 at 141.2 metres.
8. Metasomatic pyroxene rock derived from fenite. Drill hole 387 at 175.5 metres.

indicate that the change in composition is due to sodium metasomatism and increasing oxidation, as suggested by Tyler and King (1967) for the pyroxenes of East African carbonatites.

The enstatite of the Tulppio olivinite massif differs in minor components from the pyroxenes of the carbonatite complex, having lower TiO_2 and higher NiO. Thus these components show a similar trend in distribution as in the olivines of these rocks. Within the carbonatite complex, the aegirine is more enriched in TiO_2 and ZrO_2 and more depleted in MnO than the diopside.

The mode of occurrence, alteration and composition the pyroxenes in the Sokli area permit the following conclusions:

1. The pyroxene — enstatite — of the Tulppio olivinite massif differs in origin from the pyroxenes of the carbonatite complex.
2. Diopside, the primary pyroxene in the carbonatite massif, crystallized in magmatic pyroxenite.
3. The aegirine in the carbonatite massif developed by alteration of the diopside due to sodium metasomatism.
4. The pyroxenes in the magmatic carbonatites are relics of the fragments of pyroxenites and metasomatic pyroxene rocks transformed from the fenites.
5. The aegirine--augites in the fenites close to the carbonatite contacts may, partly, be relics of altered fragments of pyroxenite.

Table 12

Electron microprobe analyses of Sokli amphiboles

	Calcic amphiboles		Richterites				Alkali amphiboles		
	1	2	3	4	5	6	7	8	9
SiO_2	45.2	46.7	56.5	57.3	57.0	53.3	59.2	57.0	51.0
TiO_2	1.42	0.29	0.08	0.26	0.11	0.63	0.43	0.20	0.27
Al_2O_3	8.06	8.6	0.05	0.62	0.05	1.65	4.0	0.50	2.5
FeO	9.78	11.0	2.21	3.17	2.5	2.6	13.7	6.7	10.3
MnO	0.24	0.47	0.14	0.17	0.06	0.11	0.24	0.15	0.21
MgO	15.0	15.9	21.8	21.6	22.8	22.4	14.9	21.8	18.2
CaO	11.5	9.4	5.78	6.11	6.5	8.4	2.5	3.0	2.5
Na_2O	4.41	5.8	7.09	7.07	6.1	5.5	11.0	9.2	10.1
K_2O	0.50	0.70	1.00	0.14	1.5	0.8	0.10	0.7	0.70
Total	96.7	98.9	94.7	96.4	96.6	95.4	99.8	99.3	95.8
Number of ions on the basis of 23 oxygen atoms									
Si	6.768	6.778	8.053	8.008	7.984	7.616	7.567	7.898	7.536
Ti	0.158	0.032	0.009	0.027	0.012	0.068	0.046	0.021	0.030
Al	1.232	1.222	0.008	0.102	0.003	0.278	0.433	0.082	0.435
Fe^{2+}	1.209	1.335	0.263	0.371	0.293	0.311	1.639	0.776	1.273
Mn	0.030	0.058	0.017	0.020	0.007	0.013	0.029	0.018	0.026
Mg	3.304	3.440	4.631	4.500	4.760	4.771	3.177	4.502	4.008
Ca	1.821	1.462	0.883	0.915	0.975	1.286	0.383	0.445	0.396
Na	1.264	1.632	1.959	1.916	1.657	1.524	3.051	2.475	2.893
K	0.094	0.130	0.182	0.025	0.268	0.146	0.018	0.124	0.132
100 Mg: (Mg + Fe + Mn)	72.7	71.2	94.3	92.0	94.1	93.6	65.6	85.0	75.5

1. Metaphoscorite probably transformative from pyroxenite. Drill hole 419 at 82.5 metres.
2. Amphibole rock derived from pyroxenite. Drill hole 30 at 15.2 metres.
3. Metaphoscorite. Drill hole 389 at 210.6 metres.
4. Altered magnetite olivinite. Drill hole 418 at 60.5 metres.
5. Phoscorite of stage III. Drill hole 332 at 84.2 metres.
6. Alkaline lamprophyre. Drill hole 347 at 403.0 metres.
7. Amphibole rock derived from pyroxenite. Drill hole 30 at 15.2 metres.
8. Metasilicosövite. Drill hole 289 at 39.2 metres.
9. Amphibole bearing mica rock. Drill hole 70 at 201.3 metres.

Amphiboles

The classification of amphiboles is in accordance with the amphibole nomenclature recommended by the Subcommittee on amphiboles, I.M.A. (Leake, 1978). The amphiboles in this study were analysed by microprobe (as spot analyses), and thus only total iron has been determined. This makes it impracticable to use the ratio $Mg/Fe^{2+} + Mg$) to subdivide the amphiboles because there is no recommended procedure for adjusting the total cations, excluding (Ca + Na + K), to 13, by varying the ratio Fe^{2+}/Fe^{3+} (Leake, 1978).

The totals of all the analyses of the amphiboles are less than 100 % (Table 12), mainly because the water and fluorine contents were not determined. Earlier analyses of water and fluorine from alkali amphiboles in Sokli fenites give averages of 1.22 per cent and 1.48 per cent, respectively (Vartiainen and Woolley, 1976, p. 40).

Calcic amphibole

Grass green amphibole is due to the alteration of diopsidic pyroxene in the ultramafites (Fig. 14). Complete amphibolization ultimately yields amphibole rocks in which only small or no pyroxene relics are preserved. The replacing amphibole grows as prismatic grains that may be up to 10 mm in diameter, but which most commonly are 1—3 mm. The uralitic type of amphibolization is seldom encountered. Typically the amphibole shows intense pleochroism: Z = grass green > X = pale yellow, but bluish tints are not uncommon and the mineral may contain apatite and opaque inclusions. The calcic amphibole alters into green mica and bluish alkali amphibole (Fig. 37). The calcic amphibole in the xenoliths in the magmatic carbonatite core is often replaced by carbonate.

Two analyses of the calcic amphibole in the carbonatite massif (Table 12) show that they differ is composition from the calcic amphibole in the basement amphibolite (Vartiainen and Woolley, 1976, p. 41, Table 4, anal., 27), which is ferrotschermakitic hornblende. The former is edenitic in composition $(Na + K)_A \geq 0.50$; $Ti < 0.50$, $Si = 6.75$—7.50 and $Mg/(Fe^{2+} + Mg)$ over 0.50 owing to high Mg (Leake, 1978). Both amphiboles analyzed have Na contents exceeding 1.0 % (1.264 and 1.632) and are therefore sodian. The sodian edenite from the amphibole rock (no. 2, Table 12), which represents a more advanced transformation from pyroxenite, has less than 1.50 Ca (1.462), and may be called subcalcic sodian edenite.

Richterite

Richterite is the most widely distributed amphibole in the Sokli carbonatite massif.

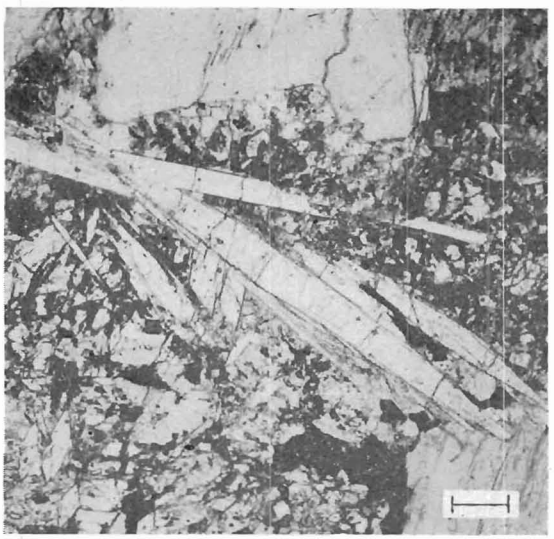

Fig. 87. Richterite prisms developed as alteration products of olivine in the Stage III hydrothermal phoscorite. One nicol. Drill hole 332 at 84.2 metres. Scale bar, 0.3 mm.

It occurs as the alteration product of olivine in the ultramafites, magmatic carbonatites and alkaline lamprophyres. Hydrothermal processes (magmatic Stage III) activated the development of richterite in the magmatic phoscorites (Fig. 87). The phoscorites have locally altered into a richterite rich rock in which it is a predominant mineral. In the silicosövites of magmatic Stage IV richterite occurs as a regular accessory mineral. Richterite together with micas is a predominant silicate in the metacarbonatites. Thin prisms have developed within serpentine matrix derived from olivine (Fig. 12). The shear planes so common in the metacarbonatites and in the rocks of the transitional zone are covered by fibrous richterite (Fig. 32). Larger, isolated prisms also occur.

Richterite is colourless. It displays bright (from yellow to blue) interference colours quite different from the abnormal bluish interference colours of the alkali amphiboles. The lathy prisms are locally intensely replaced by carbonate. There is no alteration into micas.

All four richterites analysed from Sokli are comparable to the richterite composition defined by Leake (1978):

	Analyses from Table 12			
Leake, 1978	no. 3	no. 4	no. 5	no. 6
$(Ca + Na)_B \geq 1.34$	2.00	2.00	1.95	1.96
Na_B 0.67—1.34	1.12	1.08	0.97	0.67
$(Na + K)_A \geq 0.50$	1.02	0.87	0.96	1.00
Si 7.50—8.00	8.05	8.01	7.98	7.62

Further, the $Mg/(Fe^{2+} + Mg)$ ratio must exceed 0.50 owing to the high Mg compared with Fe in all the richterites analyzed (Table 12).

Alkali amphiboles

In the carbonatite massif the alkali amphiboles have developed as alteration products at the expense of pyroxenes and calcic amphibole. The alkali amphiboles are present, albeit as narrow rims, in all the pyroxene and calcic amphibole bearing rock varieties in the massif. The largest concentrations of alkali amphiboles occur in the transitional zone between the carbonatite massif and the fenite aureole. The alkali amphiboles exhibit three modes of occurrence:

1. Alteration rims around pyroxene and calcic amphibole grains (Figs. 24 and 37).
2. Radiating bunches of thin prisms, fibrous nodules or vague fibrous aggregates mainly as replacement of pyroxenes (Fig. 88).
3. Isolated large pseudomorphous prisms after pyroxenes (Fig. 89).

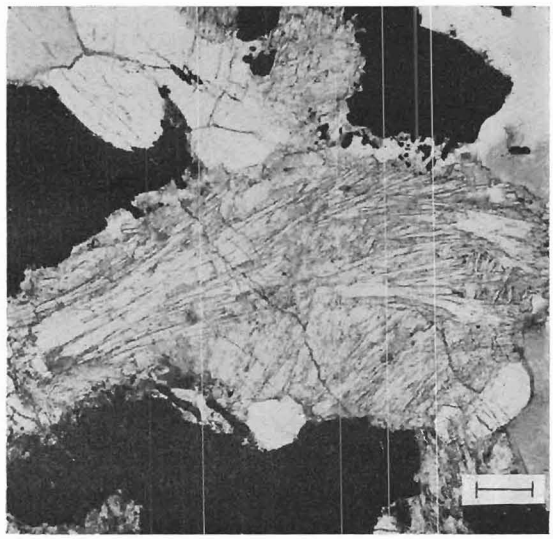

Fig. 88. A bunch of alkali amphibole prisms and needles in mica–alkali amphibole rock derived from pyroxenite. One nicol. Drill hole 358 at 270.6 metres. Scale bar, 0.2 mm.

Pleochroism is less distinct in the alkali amphiboles than in calcic amphibole: Z = bluish green — weak bluish green > X pale green — colourless. Abnormal bluish interference colour are typical. Occasionally

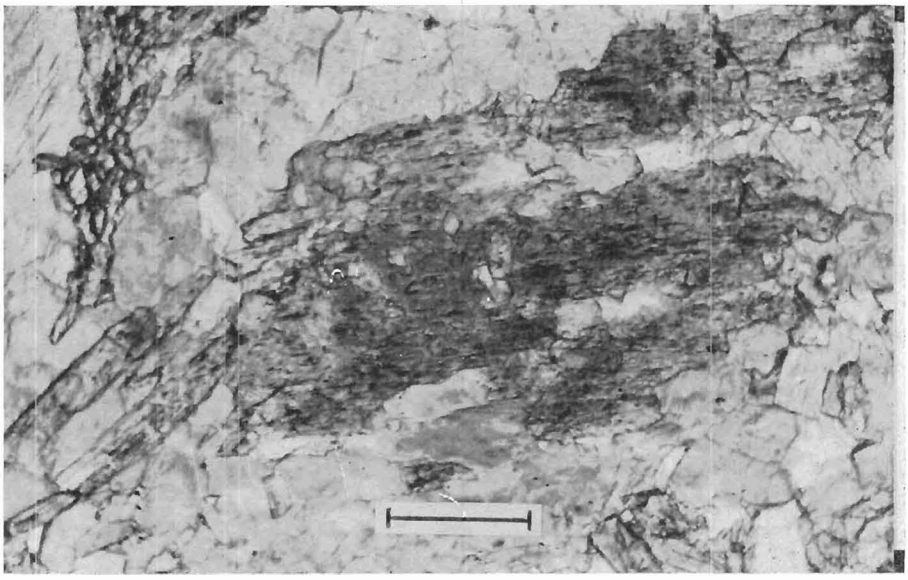

Fig. 89. Ragged alkali amphibole prisms (medium grey) developed from pyroxene. Mica–alkali amphibole rock. One nicol. Drill hole 255 at 90.0 metres. Scale bar, 0.5 mm.

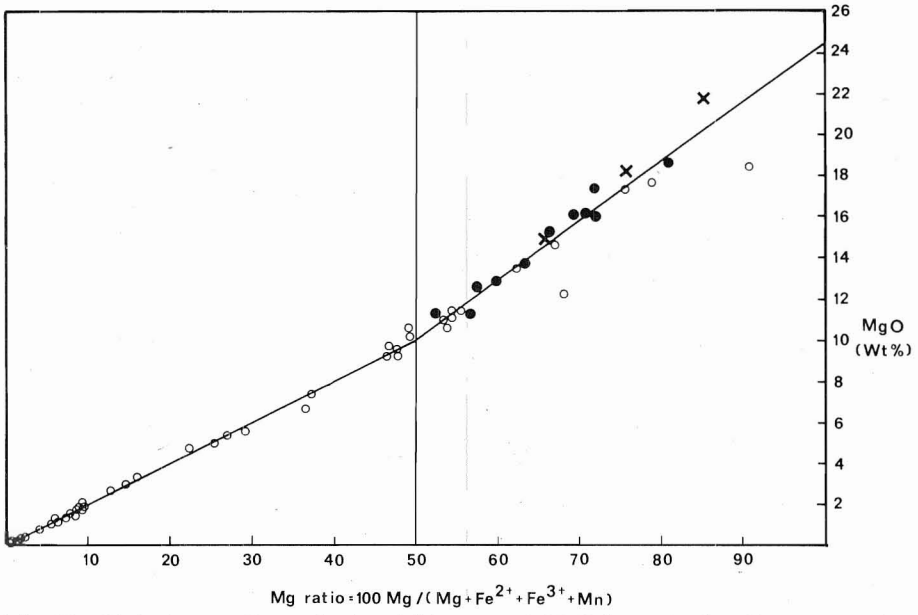

Fig. 90. Plot of mg ratio against weight per cent MgO for arfvedsonites, magnesio-arfvedsonites and eckermannites according to Vartiainen and Woolley (1976). Filled circles, data from the fenite aureole of Sokli; open circles, data taken from the literature (as specified for Fig. 32 in Vartiainen and Woolley, 1976); x, new Sokli data.

the alkali amphiboles have been altered into green mica; they may also have been intensely replaced by calcite (Fig. 89).

The total alkalis of the alkali amphiboles exceed 2.5 atoms. The Y group is dominated by iron and magnesium. Calcium is about

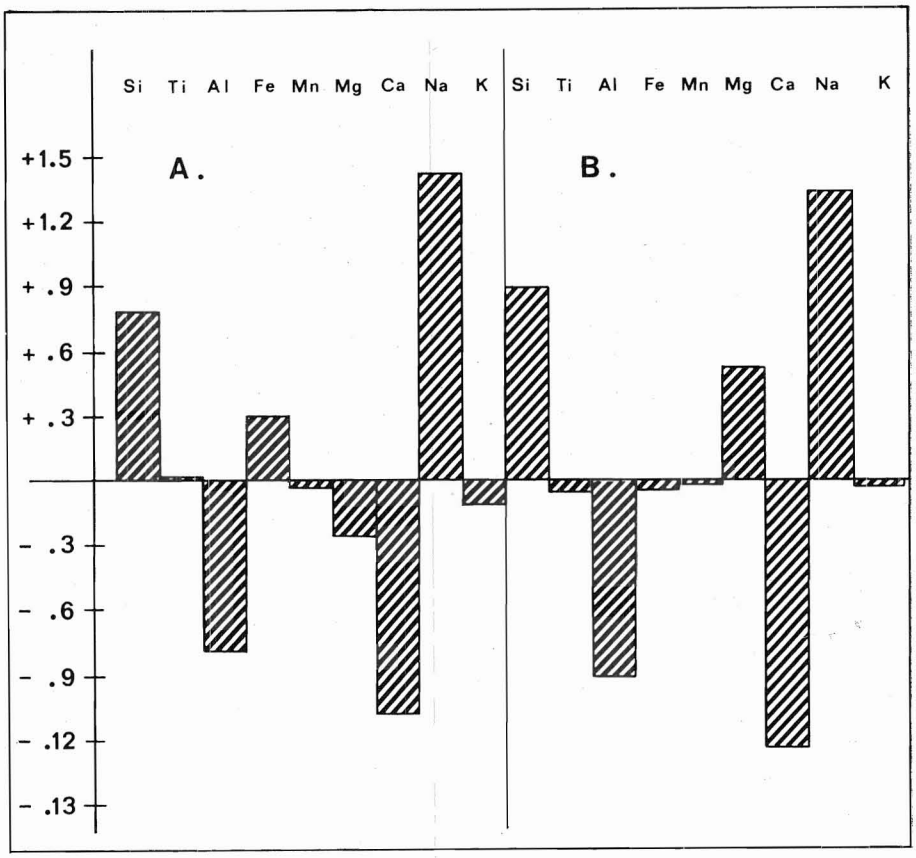

Fig. 91. Addition/subtraction diagram for major elements in the alteration of calcic amphibole into alkali amphibole.
A. Alteration within a single sample (2 and 7, Table 12).
B. Averages of two calcic amphibole and three alkali amphiboles (Table 12).

to 0.5 atom. Thus the amphiboles belong to the arfvedsonite—eckermannite series, the same series to which the alkali amphiboles of the fenite aureole also belong. The three new analyses are plotted on the diagram (Fig. 90) of the alkali amphiboles from the Sokli fenites (Vartiainen and Woolley, 1976, p. 43). They coincide fairly well with the line of the mg ratio against MgO weight percentage, although the ratio in the MgO-rich part of the diagram seems to show a tendency to rise more steeply. According to the earlier subdivision (op. cit. p. 44), one of the new analyses of alkaline amphiboles refers to ferri-eckermannite (mg ratio between 50—75) and two of them to eckermannites (mg ratio > 75).

The three amphiboles analyzed meet the requirements defined by Leake (1978) for alkali amphiboles ($Na_B \geq 1.34$), and belong to arfvedsonite—eckermannite series $(Na + K)_A \geq 0.50$; further subdivision is not possible for lack of distinction between Fe^{2+} and Fe^{3+}.

According to Heinrich (1966) amphiboles are much less common in carbonatites than are pyroxenes or micas. In the Sokli carbonatite massif, however, amphiboles are more abundant than pyroxenes but not so abundant as micas. The richterite in the Stage IV magmatic silicosövites may have crystallized

from carbonatite magma, whereas all the other amphiboles are products of alteration or metasomatism. The calcic amphibole originated from pyroxene, presumably before the carbonatite intrusion.

The alkali amphiboles developed by alkali metasomatism from calcic amphiboles and pyroxenes. This is illustrated by the addition/subtraction diagram, which show the changes involved in passing from the calcic amphibole to alkali amphibole in the same sample (Fig. 91, A). The diagram shows the significant losses of Al, Mg, and Ca, and the major additions of Si, Fe, and Na. In general, also Mg is added (Fig. 91, B). The metasomatic alteration of a country rock which altered calcic amphibole into an alkali amphibole has been discussed earlier (Vartiainen and Woolley, 1976). The trends in element changes are similar except that for Mg, which is declining. Consequently the development of the alkali amphiboles from calcic amphiboles within the carbonatite massif was due to alkali metasomatism comparable to the fenitization of hornblende schist/amphibolite into sodic fenite in the fenite aureole (op. cit. p. 75). Note that this process liberated calcium within the carbonatite massif as well.

Table 13

Calcite-dolomite proportions and CO_2 weight % in metacarbonatites of Sokli

Sample	I 104 *		Dol-% + Cal-% = 100		CO_2	Rocks
	Dol	Cal	Dol-%	Cal-%		
946—0013	174	6	97	3	5.5	METAPHOSCORITES
—0064	81	20	72	28	27.9	Derived from magnetite olivinite
—0065	57	16	78	22	1.0	
—0066	**	113	**	> 70	7.8	Derived from pyroxenites
—0067	13	121	10	90	11.1	
—0068	**	139	—	> 70	18.8	
—0069	—	53	—	100	3.3	Unknown primary rock
—0070	21	161	12	88	6.8	
—0071	29	11	73	27	1.5	
—0072	29	8	78	22	0.9	
—0073	29	156	16	84	17.0	
—0074	24	18	37	43	4.0	
—0075	122	9	93	7	0.5	
—0077	110	11	91	9	1.1	
—0078	88	6	94	6	1.0	
—0079	206	35	85	15	2.8	
—0080	98	25	80	20	1.0	
—0081	14	72	16	84		
—0055	2	160	1	99	24.9	METASILICOSÖVITES
—0056	—	248	—	100	33.8	
—0057	76	124	38	62	27.7	
—0058	70	175	29	71	24.2	
—0059	101	94	52	48	12.8	
—0060	2	185	1	99	33.5	
—0061	25	220	10	90	28.8	
—0062	152	118	56	44	26.2	
—0088	71	184	28	72		

* Intensity of 104 peak
** Aegirine overlaps

Calcite–dolomite proportions

Quantitative calcite–dolomite proportions of the carbonatites were determined using the X-ray diffraction techniques proposed by Royse *et al.* (1971). X-ray runs were performed at the Research Laboratory of Rautaruukki Oy. The dolomite standards were NBS 88 a (98 %) and BCS 368 (98.4 %). Table 13 shows the results for the metacarbonatites and Table 14 for the magmatic carbonatites. The CO_2 analysed from the same samples is also given in the tables. The purpose here is to estimate the variation in the proportions

Table 14

Calcite-dolomite proportions and CO_2 weight % in magmatic carbonatites of Sokli

Sample	I 104 *		Dol-% + Cal-% = 100		CO_2	Rocks
	Dol	Cal	Dol-%	Cal-%		
946—0017	102	22	82	18	1.5	STAGE I
—0018	94	17	85	15	2.9	Phoscorites
—0019	157	243	39	61	21.4	
—0020	14	—	100	—	4.2	
—0021	17	68	20	80	4.3	
—0022	15	4	79	21	2.0	
—0023	123	9	93	7	16.4	
—0027	—	258	—	100	33.3	STAGE II
—0028	—	184	—	100	40.3	Sövites and silico-
—0029	21	181	10	90	33.2	sövites
—0030	2	248	1	99	40.3	
—0031	2	240	1	99	39.9	
—0032	14	205	6	94	35.4	
—0033	31	173	16	84	35.7	
—0034	—	257	—	100	42.7	
—0035	30	50	38	62	4.0	STAGE III
—0036	17	53	24	76	5.3	Phoscorites
—0037	86	62	58	42	5.5	
—0038	89	9	91	9	1.6	
—0039	46	7	87	13	1.2	
—0040	24	9	73	27	2.9	Apatite-ferriphlogopite
—0041	9	106	8	92	3.3	rocks
—0042	197	185	52	48	22.2	STAGE IV
—0043	17	163	9	91	33.3	Silicosövites and
—0044	9	202	4	96	38.3	sövites
—0045	15	180	8	92	37.5	
—0046	180	232	44	56	27.7	
—0047	23	154	13	87	41.4	
—0048	23	183	11	89	41.0	
—0052	222	267	45	55	39.9	
—0049	141	2	99	1	41.7	Beforsites
—0050	153	3	98	2	40.1	
—0051	156	12	93	7	46.2	
—0084	242	—	100	—	30.0 **	STAGE V
—0085	145	—	100	—		Late veins
—0086	120	6	95	5		

* Intensity of 104 peak
** Estimated from other similar analyses.

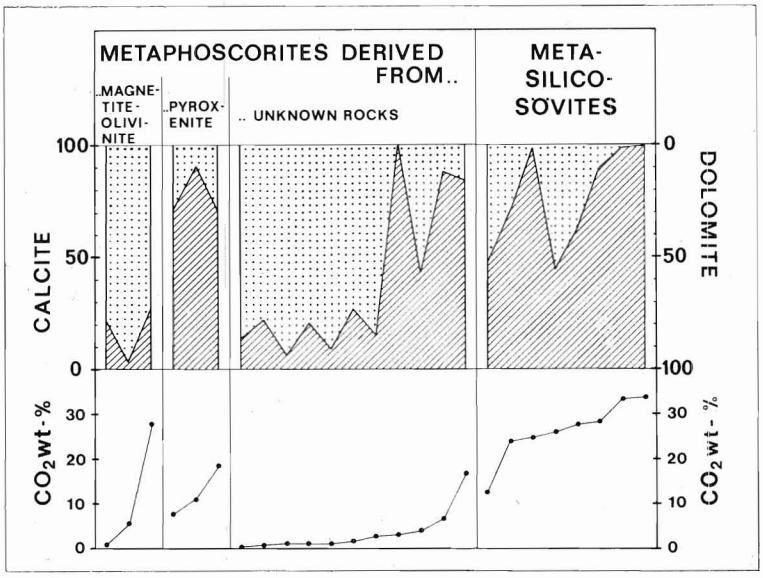

Fig. 92. Calcite-dolomite proportions of the metacarbonatites plotted against increasing CO_2 within some rock groups.

of calcite—dolomite in the metacarbonatites and magmatic carbonatites. Textural and exsolution relationships between calcite and dolomite were not investigated.

Metacarbonatites

The variation in the calcite—dolomite proportions is given diagrammatically in Fig 92 by plotting against the increasing CO_2. The CO_2 shows the approximate bulk of carbonates. By multiplying CO_2 by 2.3 one obtains the average amount of pure calcite; by 2.1 that of pure dolomite. The CO_2 determinations indicate that the metaphoscorites that derived from magnetite olivinite and pyroxenite show similar variations in total carbonate contents but that the calcite—dolomite proportions differ conspicuously. Aegirine inteferes with the determination of the calcite—dolomite proportion in the pyroxenitic metaphoscorite and thus two calcite proportions appear as minimums at 70 % (Fig. 92).

Conversely, the dolomite proportion is over 70 % in the metaphoscorites derived from the magnetite olivinite. Note that the CO_2 metasomatism produced mainly dolomite in magnetite olivinite and calcite in pyroxenites. This is consistent with the MgO and CaO content in the host rocks (from Table 16):

	MgO %	CaO %
Magnetite olivinite	24.1	5.3
Pyroxenite	9.6	18.5

Dolomite predominates in the metaphoscorites of unknown primary rocks when the carbonate content is low (1—5 %) but, with increasing CO_2, calcite becomes predominant (Fig. 91). An alternative interpretation is that the metaphoscorites of low CO_2 were primarily magnetite olivinites and those of high calcite proportions pyroxenitic in origin. The calcite—dolomite proportions in the metasilicosövites show an irregular variation within the range of about 25—60 per cent carbonates (CO_2 12.8—33.8 %); in the rocks with a higher CO_2 content, however, calcite is distinctly the predominant mineral.

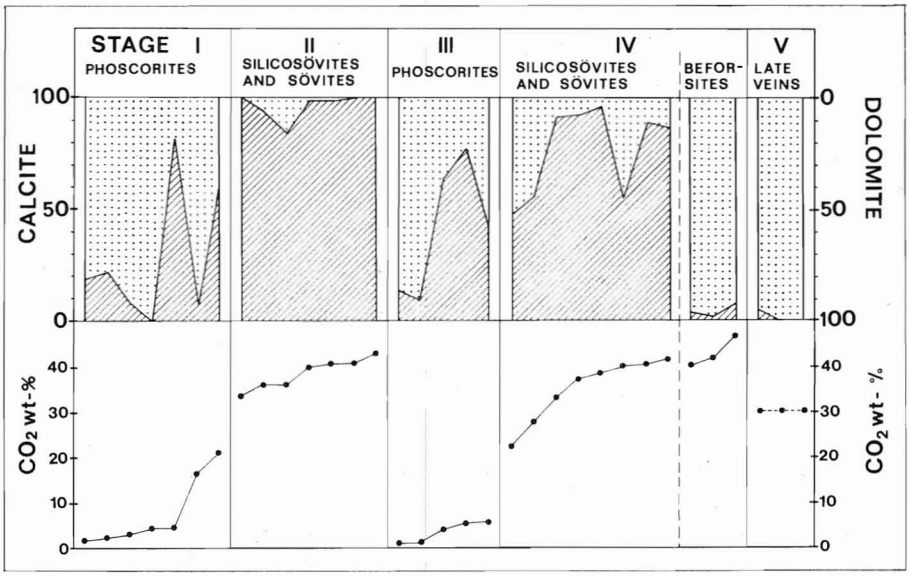

Fig. 93. Calcite-dolomite proportions of the magmatic carbonatites plotted against increasing CO_2 within successive stages.

Magmatic carbonatites

The calcite—dolomite proportions in successive magmatic carbonatite stages are plotted against increasing CO_2 in Fig. 93. The calcite—dolomite proportions of Stage I phoscorites are randomly distributed independent of the CO_2 contents, for example two samples containing roughly the same amounts of CO_2 (4.1 % and 4.2 %) show 100 % dolomite and 80 % calcite, respectively (Table 14). This suggests, at least partly, that external introduction of CO_2 produced dolomite in the MgO-rich (15 %) rocks. The Stage II silicosövites and sövites are indisputably the rocks richest in calcite in the Sokli carbonatite massif. The small amounts of dolomite (1—16 %) presumably occur as exsolutions in calcite. The calcite—dolomite proportions of Stage III phoscorites, which are altered varieties of Stage I phoscorites, are similar to those in the former phoscorites.

The next stage represents the second phase of magmatic carbonate introduction. The calcite—dolomite proportions show that the Stage IV silicosövites and sövites are mainly calcitic (Fig. 93). In some samples, however, the dolomite proportion may exceed 50 %. The calcite—dolomite proportions vary randomly with increasing CO_2 content. The beforsites, dyke-like and latest Stage IV rocks are almost pure dolomite rocks containing only 1—7 % calcite component and very low abundances of other minerals (Table 6). Determinations on the late veins of Stage V show an accidental occurrence of calcite component (Fig. 93). Actually, in places, the cavities of these veins contain more calcite as crystalline phase.

The general trend in calcite—dolomite proportions developed during the crystallization of the carbonatite massifs as a whole is from calcite to dolomite (Kukharenko *et al.*, 1965, Heinrich, 1966). The most common trend of the magmatic carbonatites at Sokli is:

Stage II		Stage IV		Stage IV		Stage V
Sövitic rocks		Sövitic rocks		Beforsites		Late veins
Calcite	⟶	Calcite + dolomite	⟶	Dolomite	⟶	Dolomite (and others)

These results are compatible with the experimental findings presented by Wyllie (1966 a, p. 323) from the system CaO—MgO—CO_2—H_2O, which show that »under isobaric conditions, the sequence of crystallization for the carbonates is calcite, followed by calcite plus dolomite.»

PETROCHEMISTRY

Experimental

The samples submitted to analyses were ground in a cone crusher, splitted and ground into the final analytical fineness of $d \leq 3$ μm in a tungsten carbite Tema mill. Most of the elements were analysed by a Philips PW 1212 X-ray spectrometer using the powder briquet sample preparation technique.

The ratio method was employed to minimize the effect of long term drift. The concentrations calculated and the overlaps and matrix effects corrected with the aid of a PDP 11/34 on-line computer with an RSX-11M operating system and a Fortran program developed by Rautaruukki Oy. The Fortran

Table 15

The accuracy for XRF analyses of Sokli samples. Numbers refer to the standard deviation δ.

Level of content in percentages	Al_2O_3 %	SiO_2 %	MgO %	CaO %	Fe %	V % [1]	Ti, Ba %	Mn %	P %	S %
0.001	—	—	—	—	—	—	—	—	—	—
0.01	0.02	0.02	—	0.2	—	0.01	0.01	0.01	0.02	0.01
0.1	0.02	0.02	0.1	0.2	0.2	0.02	0.02	0.02	0.02	0.02
1	0.15	0.1	0.2	0.1	0.2	0.03	0.03	0.06	0.08	0.05
10	0.5	0.3	0.6	0.3	0.3	—	0.2	0.2	0.2	0.4
50	1.5	1.2	1.8	0.8	0.5	—	—	—	—	—
100	1.0	1.0	1.5	—	—	—	—	—	—	—

Level of content in percentages	Cu, Co, Ni Zn, Cr %	K_2O %	U %	Th %	Ta %	Zr, Sr %	Nb %	Ce, La % [2]
0.001	0.002	—	0.003	0.003	0.003	0.003	0.003	—
0.01	0.002	0.02	0.003	0.003	0.003	0.01	0.004	0.02
0.1	0.005	0.05	0.008	0.008	0.006	0.01	0.008	0.04
1	0.02	0.2	0.04	0.04	0.02	0.02	0.02	0.06
10	—	0.2	—	—	—	—	0.2	—
50	—	—	—	—	—	—	—	—
100	—	—	—	—	—	—	—	—

[1] 0.004 × Ti % must be added to standard deviation
[2] 0.005 × Ba % must be added to standard deviation

program can be used for analysing samples with a wide concentration range. To correct the matrix effects due to carbonate, magnetic material and sodium (corrections for water of crystallization and fluorine can also be included), their contents in the samples were determined by other methods; the relevant data were then fed to the computer.

The accuracy of the analyses is given in Table 15.

The content of magnetic material in the samples was determined with a Satmagan (Saturation Magnetization Analyser).

The carbonate content was determined as CO_2, which was calculated from the total carbon content determined on a Leco IR 12.

Sodium was assayed by dissolving the samples in a mixture of $HClO_4$: HNO_3: HF: HCl. The solution was evaporated into dryness, and the residue was dissolved in hydrochloric acid (1: 4). The sodium content was determined from the solution with an IL 751 double beam absorption spectrometer.

FeO was analysed by dissolving the samples in inert atmosphere (CO_2-gas) in hydrochloric acid (1: 1) and in a few drops of conc. hydrofluoric acid. Five ml of conc. phosphoric acid were added and the Fe^{2+}-ions were determined from this solution by titrating potentiometrically with 0.1 M potassium dichromate.

In most cases only total iron was analysed. Because the bulk of iron is incorporated in magnetite the iron content was divided into Fe_2O_3 and FeO in the proportion indicated by magnetite (2/3 Fe^{3+} and 1/3 Fe^{2+}).

Composition of rocks

Major elements

A number of studies show the range in the composition of carbonatites in individual carbonatite complexes, e.g. Alnö (von Eckermann, 1948); Magnet Cove (Erikson and Blade, 1963); Kola province (Kukharenko *et al.*, 1965); South Africa and South West Africa (Verwoerd, 1967); Siberian carbonatites (Pozaritskaya and Samoilova, 1972); Iron Hill (Nash, 1972) and Sevattur in India (Krishnamurthy, 1977). The average composition of carbonatites has been reviewed by Pecora (1956), Heinrich (1966) and Gold (1966 b). The average composition of the magmatic phoscorites and sövitic rocks, and the bulk composition of the magmatic carbonatite core and the metacarbonatites of Sokli are compared to the average compositions of carbonatites in Table 18.

The averages of the Sokli rocks in Table 18 were computed from the data listed in Tables 16 and 17. The higher SiO_2 and MgO in the metaphoscorites and metasilicosövites than in magmatic carbonatites are due to the more abundant silicates in the former rocks. The difference is compensated by higher abundances of opaques and apatite in the magmatic phoscorites and by the higher carbonate content in magmatic sövitic rocks.

The bulk composition of the magmatic core was calculated by deducing the proportions of sövitic rocks and phoscorites with the aid of a detailed ground magnetic map. The phoscorites display magnetic highs and the background is regarded as an area of sövitic rocks. Owing to their small volume beforsite and late veins were not included. The planimetric measurement of the areas of magnetic highs and background showed the proportion of phoscorites to sövitic rocks to be 1: 25. The

Table 16

Average chemical compositions in weight percentages of ultramafites, metasomatites and metacarbonatites at Sokli

	Ultramafites		Metasomatites *			Metacarbonatites			
	Magnetite olivinites	Pyroxenites	Amphibole rock	Mica-amphibole rocks	Mica rocks in magmatic core	Metaphoscorites derived from magnetite-olivinites	pyroxenites	unknown rocks	Metasilicosövites
	**) 5	3	1	4	10	4	3	15	10
SiO_2	19.1	24.4	37.8	23.6	28.8	23.7	23.3	16.4	7.0
TiO_2	2.8	2.2	0.9	1.0	1.2	2.1	2.1	2.3	0.4
Al_2O_3	0.8	3.0	7.5	4.6	7.1	1.6	2.1	1.4	1.7
Fe_2O_3	26.9	16.9	7.0	9.4	11.6	18.6	18.0	21.2	5.7
FeO	12.1	7.6	3.1	4.2	5.1	8.4	8.1	9.5	2.6
MnO	0.7	0.3	0.3	0.3	0.2	0.6	0.4	0.5	0.3
MgO	24.5	9.1	7.9	9.7	18.3	22.3	15.7	16.6	7.5
CaO	5.4	17.4	15.8	21.7	8.5	10.4	16.4	15.8	40.4
K_2O	0.9	1.3	1.3	3.2	6.7	2.4	1.7	2.2	1.2
P_2O_5	2.2	4.0	4.8	7.1	2.5	4.6	2.6	6.0	4.1
CO_2	5.6	7.7	8.1	9.6	5.1	8.7	8.0	8.7	27.1
S	0.5	0.6	0.2	0.4	1.9	0.1	0.2	1.3	0.5
Total	101.5	94.5	94.2	94.8	97.0	103.5	98.6	101.9	98.5
Trace elements in p.p.m.									
Nb	200	100	100	100	1700	600	100	600	60
Ta	1 10	n.d.	n.d.	n.d.	230	n.d.	n.d.	30	n.d.
Zr	1400	9000	900	2100	3200	3800	2600	3300	70
V	700	500	300	300	200	500	500	400	—
La	100	100	200	300	100	100	200	300	300
Sr	600	800	1800	2600	1100	1400	1200	1900	5000
Ba	250	500	800	800	1200	1300	1200	500	1000
Th	1 30	n.d.	n.d.	n.d.	40	n.d.	n.d.	40	n.d.
U	1 —	n.d.	n.d.	n.d.	30	n.d.	n.d.	50	n.d.

1 3 analyses
* Deficiences are mainly due to H_2O and Na_2O, which were not analyzed
** Number of analyses
n.d. not determined

bulk composition of the magmatic core given in Table 18 was derived from the average compositions of the phoscorites and sövitic rocks by weighting them by the above proportion.

It is well known that the compositions of carbonatites vary conspicuously within and between complexes. This is due to not only the heterogeneity of the rocks, but also to the selection of samples. Thus the comparison of the average compositions is not very sound. According to Gold (1966 b), the »typical composition» values, as presented in Table 18 (op cit.), are more meaningful than those of the »average composition» reported by Heinrich (1966) and given in the same table. The bulk composition of Sokli is as a fairly representative of the magmatic carbonatites at Sokli. It has a distinctly closer affinity to the »typical composition» of Gold than has the average composition presented by Heinrich (Table 18). The lower SiO_2 (2.2 %) and Al_2O_3 (0.3 %) at Sokli refer to silicate contents in the Sokli carbonatites that are lower than in »typical» ones (5.67 % and 1.77 %, respectively). The CaO in the Sokli carbon-

Table 17

Average chemical compositions in weight percentages of magmatic carbonatites at Sokli

Stage	I	II		III		IV			V
Rocks	Phosco-rites	Silico-sövites	Sövites	Phosco-rites	Apatite-ferriphl. rocks	Silico-sövites	Sövites	Befor-sites	Late veins
Numb.	9	17	10	18	8	13	7	3	6
SiO_2	12.4	2.2	1.3	16.1	12.3	2.8	0.6	0.2	2.0
TiO_2	1.4	0.2	0.1	1.3	0.8	0.2	0.00	0.00	0.2
Al_2O_3	0.7	0.3	0.3	2.3	2.4	0.4	0.2	0.1	0.3
Fe_2O_3	25.9	5.7	3.0	19.9	17.4	6.0	1.1	1.3	10.2
FeO	11.7	2.6	1.2	9.0	7.8	2.7	0.5	0.6	4.6
MnO	0.7	0.3	0.3	0.3	0.2	0.4	0.3	0.3	0.8
MgO	15.6	4.5	3.2	15.2	11.4	6.3	3.4	21.6	13.4
CaO	16.5	45.6	50.4	16.2	22.3	42.3	50.4	47.0	23.1
K_2O	0.7	0.2	0.3	2.9	3.1	0.5	0.1	0.1	0.3
P_2O_5	9.1	3.8	2.5	7.4	13.3	3.3	2.4	2.2	1.5
CO_2	6.6	33.7	14.4	8.1	5.5	34.6	37.9	24.0	30.7
S	1.3	0.5	0.6	3.8	4.1	1.4	0.2	0.1	5.4
Total	102.6	99.6	97.5	102.5	100.6	100.9	97.1	98.0	92.5
Trace elements in p.p.m.									
Nb	1400	1100	1200	3300	6000	2500	1400	1300	600
Ta	[1] 180	[2] 30	20	10	[3] 110	[4] 10	[5] 10	n.d.	n.d.
Zr	2200	900	300	1500	1800	200	100	00	00
V	600	00	00	400	200	100	00	00	200
La	200	200	200	300	600	400	300	300	3400
Sr	2200	6200	7700	1700	2400	790	9400	8900	8300
Ba	400	600	600	600	900	800	800	300	29300
Th	[1] 310	[2] 200	150	340	857	100	70	n.d.	n.d.
U	[1] 170	[2] 20	50	90	60	20	10	n.d.	n.d.

[1] 6 analyses, [2] 10 analyses, [3] 4 analyses, [4] 9 analyses, [5] 4 analyses
n.d. = not determined

atites, which is almost ten percentage units higher than the »typical» value, is partly due to the higher apatite content at Sokli but mainly due to the more calcitic character of Sokli compared with »typical» carbonatites. This is also revealed by MgO that is lower and CO_2 that is higher than »typical».

The average composition of the metasilicosövites at Sokli is closer to the average composition given by Heinrich and the »typical composition» by Gold than is the bulk composition of the magmatic carbonatites at Sokli (Table 18). The P_2O_5 and CaO in the metasilicosövites are higher than the »average» and »typical» values in Table 18. This is due to the increased apatite content in the Sokli metasilicosövites.

Petrochemical calculation of major elements in magmatic carbonatites

There are no universally recognized or used methods for petrochemical calculations of carbonatites such as Niggli values or CIPW norms for magmatic silicate rocks. Von Eckermann (1948) has used the latter for the Alnö rocks including carbonatites. Verwoerd (1967) has plotted the analytical data of the carbonatite complexes of South Africa on a triangular diagram showing the variation in

Table 18

Average of major components in weight percentages of Sokli carbonatites and of carbonatites in general

	SOKLI					Averages in carbonatites	
	Magmatic carbonatites			Meta-		Heinrich, 1966, p. 222	Gold ** 1966b, p. 84
	Phosco-rites	Sövitic rocks	Bulk compo-sition *	phosco-rites	silico-sövites		
SiO_2	14.3	1.7	2.2	21.1	7.0	10.29	5.67
TiO_2	1.3	0.1	0.1	2.2	0.4	0.73	0.50
Al_2O_3	1.5	0.3	0.3	2.0	1.7	3.29	1.77
Fe_2O_3	22.9	4.0	4.7	19.3	5.7	3.46	3.88
FeO	10.4	1.8	2.1	8.7	2.6	3.60	3.71
MnO	0.5	0.3	0.3	0.5	0.3	0.68	0.78
MgO	15.4	4.4	4.8	18.2	7.5	5.79	6.10
CaO	16.3	47.2	46.6	14.2	40.4	36.10	37.06
K_2O	1.8	0.3	0.4	2.0	1.2	1.36	0.87
P_2O_5	8.3	3.1	3.3	4.4	4.1	2.09	1.73
CO_2	7.4	35.2	34.5	8.5	27.1	28.52	32.16
S	2.5	0.7	0.8	0.5	0.5	0.56	0.18
H_2O	n.d.	n.d.	n.d.	n.d.	n.d.	1.44	1.42
Total	102.6	99.1	100.1	101.6	98.5	97.91	95.83
Number of analyses	27	47	74	22	10	96—164	16—45***

* Weighted with area
** The average of the individual averages at different complexes, »typical composition».
*** The number of complexes sampled.
n.d. not determined

the molecular proportions of CaO, MgO and $FeO + 2Fe_2O_3$. On another triangular diagram he has given the composition of the carbonate phase in molecular percentages of $CaCO_3$, $MgCO_3$ and $FeCO_3$ calculated from the same data. Pozaritzkaya and Samoilova (1972) have shown the variation of elements as cation proportions according to the successive stages of metasomatic carbonatites. Maxey (1976) has used Fe_2O_3 (total iron)—$Na_2O + K_2O$—MgO and Na_2O—K_2O—CaO variation diagrams of oxides in weight percentages for the rocks of the Beemerville carbonatite–alkaline rock complex. Krishnamurthy (1977) has portraied schematically the variation in oxides plotted against successively younger phases of carbonatites. Bagdasarov (1979) has given a variation diagram in which the variation coefficients of the components are plotted against the average contents of the components. In his diagram, the magmatic alkaline silicate rocks form a hyperbole, but the metasomatic carbonatite plot outside it.

None of these methods are satisfactorily applicable to the petrochemical calculation of the analyses of the Sokli magmatic carbonatites. A new calculation procedure is suggested according to which the triangular variation diagram of dolomite — calcite — silicates + opaques has been constructed (Fig. 94). The procedure, based on the weight percentages of oxides, is as follows:

Dolomite. The basis of calculation is MgO in dolomite. First the MgO incorporated in silicates is subtracted from the total MgO.

Table 19

Major oxides (in weight percentages) in magmatic carbonatites of selected samples from Sokli, and dolomite, calcite and silicate + opaque components calculated as explained in the text.

Drill hole	Depth	SiO_2	Fe_2O_3 + FeO	MgO	CaO	CO_2	Dolomite	Calcite	Silicate + opaques	Total
					PHOSCORITE, STAGE I					
481	118.0	12.7	33.1	14.0	16.4	1.8	6.2	—	58.5	64.7
482	110.0	14.4	45.7	14.8	10.0	1.7	1.5	1.8	74.5	77.8
433	138.2	19.9	35.3	17.1	8.1	8.0	0	18.0	75.0	93.0
281	58.0	14.9	11.5	19.5	27.3	21.4	21.9	25.8	41.3	89.0
332	41.4	11.0	29.7	11.6	24.8	2.8	2.9	2.9	51.8	57.6
454	107.6	15.3	26.6	16.2	19.5	5.8	4.3	8.3	57.2	69.8
					SILICOSÖVITE AND SÖVITE, STAGE II					
428	127.5	6.1	24.8	9.9	32.5	18.3	16.7	23.2	37.0	76.7
464	25.4	1.7	21.5	5.1	40.3	27.5	16.2	44.3	24.9	85.4
428	44.2	2.1	11.7	4.2	43.3	32.0	10.0	61.2	15.9	87.1
250	128.8	2.4	9.2	5.0	44.6	33.3	12.4	61.4	14.0	87.8
477	152.7	1.1	7.1	3.2	48.8	33.3	10.0	64.1	8.8	82.9
425	42.5	2.1	6.6	3.5	48.5	31.0	6.7	61.8	10.8	79.3
358	200.1	2.0	6.9	3.4	47.6	35.4	6.7	72.5	10.9	90.1
488	105.7	2.9	8.8	3.0	45.3	32.3	0.4	72.3	14.6	87.3
428	102.9	2.4	11.0	6.0	42.3	33.6	17.1	57.2	15.8	90.1
464	74.7	1.4	4.4	4.3	54.3	29.5	13.8	51.5	7.2	72.5
477	192.0	1.0	2.0	2.3	52.2	37.9	4.3	80.1	4.0	88.4
338	108.3	0.8	1.2	0.9	51.6	42.7	1.9	94.1	2.8	98.8
428	70.8	0.6	1.6	1.9	52.1	36.5	4.3	81.5	2.8	88.6
					SILICOSÖVITES AND SÖVITES, STAGE IV					
340	131.9	1.2	4.1	9.8	48.5	32.2	41.0	28.1	6.5	75.6
456	98.0	3.9	16.1	5.8	39.6	25.1	9.1	46.6	23.9	79.6
428	49.1	1.0	5.6	3.2	49.2	32.2	10.5	61.2	7.6	79.3
342	110.2	1.3	7.7	4.1	46.6	33.3	13.3	60.5	10.3	84.1
477	143.2	0.6	8.9	4.0	43.3	29.1	16.2	47.9	10.1	74.2
477	263.0	0.5	1.8	2.6	51.5	39.9	10.0	79.0	2.8	91.8
428	50.7	0.8	3.2	2.5	50.8	31.5	8.1	62.1	4.8	75.0
428	61.5	0.5	1.5	1.8	53.0	37.2	6.2	77.0	2.5	85.7
343	198.5	0.8	1.3	8.7	44.7	39.2	37.7	47.5	2.9	88.1
343	243.0	0.7	0.7	2.8	51.0	41.4	10.0	82.4	2.1	94.5
333	34.2	0.3	0.7	3.4	51.3	41.0	14.8	76.3	1.7	92.8
					BEFORSITE, STAGE IV					
274	119.0	0.3	2.5	21.7	46.2	26.0	102.3	—	3.1	105.4
344	199.0	0.3	1.7	21.1	47.0	24.5	99.2	—	2.3	101.5
344	176.8	0.2	1.7	21.9	47.8	23.1	103.5	—	2.1	105.6
					LATE VEIN, STAGE V					
461	73.0	1.6	19.5	13.8	16.5	26.2	58.2	—	22.7	80.9
461	77.0	2.4	20.1	14.8	18.8	30.0	54.7	3.6	24.9	83.2
428	81.9	1.5	12.6	14.1	22.7	35.3	60.1	14.4	15.6	90.1
462	242.0	1.5	10.3	11.5	31.3	27.8	47.7	11.0	13.3	72.0
462	276.8	2.7	12.3	12.3	25.1	31.4	45.8	21.2	17.7	84.7
462	290.5	2.5	14.1	13.9	24.0	33.6	50.6	20.9	19.1	90.6

— = no calculated calcite

The principal silicates in the Sokli magmatic carbonatites are Mg silicates. Their abundances are essentially controlled by phoscorites (Tables 3 and 18) thus:

	Abundance	MgO %	SiO_2 %
Forsterite	42	51	42
Serpentine	14	42	42
Clinohumite	10	52	39
Richterite	10	22	57
Phlogopites	24	25	39
Averages	100	38	44

If the abundance of silicates is weighted by their MgO and SiO_2, one obtains 4070 (MgO) and 4248 (SiO_2). Note that the silicates contain roughly equal amounts of MgO and SiO_2. Hence, the MgO_{Dol} is calculated: $MgO_{Dol} = MgO—SiO_2$.

The principal components of dolomite recalculated as 100, are:

MgO	21 %
CaO	31 %
CO_2	48 %

The other components of dolomite can be computed from these proportions on the basis of known MgO_{Dol}:

$$CaO_{Dol} = 1.48 \times MgO_{Dol}$$
$$CO_{2,Dol} = 2.29 \times MgO_{Dol}$$

Calcite. The excess CO_2 over $CO_{2,Dol}$ is assigned to calcite. The calcite is obtained by multiplying $CO_{2,Tot}—CO_{2,Dol}$ by 1.25 (calcite assays 55.5 % CaO, 45.5 % CO_2).

Opaques and silicates. The oxides of iron equal opaques and $2 \times SiO_2$ silicates.

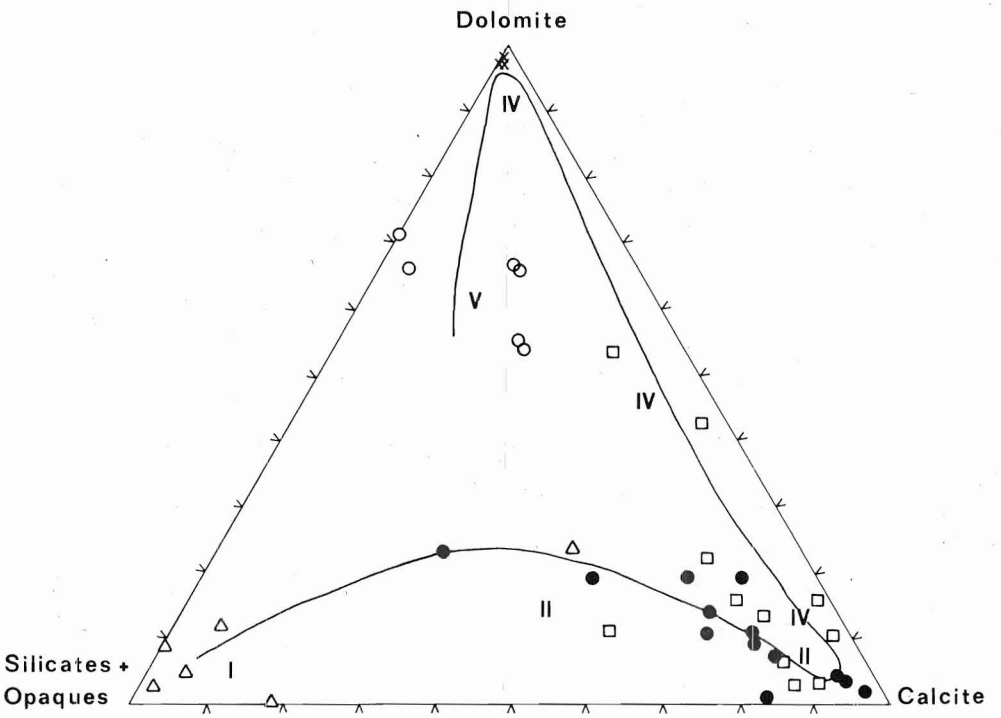

Fig. 94. Triangular diagram showing variation in weight percentages of the principal oxides in the magmatic carbonatites calculated as calcite, dolomite and silicates + opaques (see text). Numbers refer to magmatic stages; triangles, phoscorite (I); filled circles, sövite and silicosövite (II); squares, sövite and silicosövite (IV); x, beforsite (IV); open circles, late carbonate veins (V); curve, crystallization path of magmatic carbonatites.

Table 19 gives the major oxides of some selected type samples in weight percentages and the mineral components calculated from these analyses. The totals of the minerals calculated are reasonable. The deficiences from 100 are mainly due to apatite and subordinately to sulphur. The mineral components were recalculated to 100 before they were plotted on the diagram (Fig. 94). The diagram does not include the Stage III rocks, which represent hydrothermally altered or hydrothermally produced varieties and do not follow the cyrstallization sequence of carbonatite magma.

The general variation trend in the diagram (Fig. 94) demonstrates that the rock sequence accords with field evidence. The curve shows the path of crystallization. On the other hand, the diagram also shows the variation in the chemistry of the magmatic carbonatites due to changes in carbonate mineralogy and the variation in the abundance of silicate and opaque minerals.

The marked clustering of Stage I phoscorites towards the silicates + opaques corner shows their temporal position at the beginning of the crystallization sequence. The variation in carbonates is consistent with the calcite-dolomite proportions determined by X-ray techniques (Fig. 93). The one point of phoscorite that stands apart is closer to silicosövite than to phoscorite in composition. The diagram reveals the lack of the data for the rocks between the Stages I and II as well as for the rocks with compositions between sövite and beforsite in Stage IV. This is, at least partly, due to the selection of samples, which emphasized typical samples of different stages rather than those of intermediate compositions.

The silicosövites and sövites of Stages II and IV occupy the field adjacent to the calcite point (Fig. 94). The greatest disadvantage of the variation diagram presented here as a petrochemical model for illustrating the crystallization of the magmatic carbonatites is that it cannot reveal the temporal difference in the successive stages of these rocks.

The two intermediate plots between calcite and dolomite indicate the course of crystallization towards beforsites, which mark the end at crystallization in Stage IV. The marked change in composition between the beforsites and late veins causes a steep bend in the crystallization path. The late veins of Stage V contain appreciable sulphides, which is the only reason why the points approach the silicates + opaques corner. The calcite component is markedly higher than that suggested by the X-ray determinations of the calcite—dolomite proportions (Fig. 93). In fact, the calcite in the cavities of the veins is better represented in these samples. In accordance with petrography, the late veins display a distinctly separate group on the diagram.

As demonstrated from a number of carbonatite complexes and by experimental work (Wyllie and Biggar, 1966), the crystallization path presented on the triangular diagram (Fig. 94) follows the general trend from calcitic to dolomitic carbonatites. In this work the silicate-opaque rich portion (phoscorites) is added on the crystallization succession and considered to represent the first segregation or crystallization from the carbonatite magma.

Minor and trace elements

The values of minor and trace elements in Tables 16 and 17 are summarized in Fig. 95, thus enabling us to compare directly the variation in elements in each group. Fe_2O_3 is depicted with a dotted line in the upper part of Fig. 95 in correlation with siderophile elements. Typical abundances in carbonatites according to Gold (1966b) are indicated by

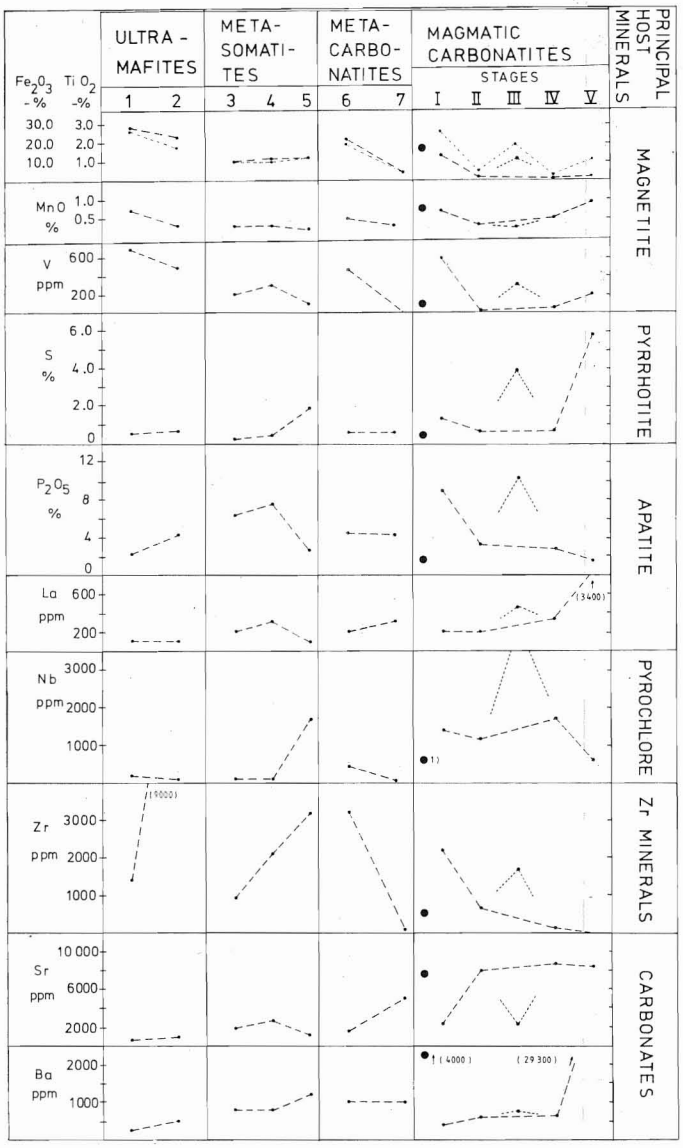

Fig. 95. Variation in minor and some trace elements of different rock groups in the Sokli massif. The dotted line in the upper part of the figure indicates the variation in Fe_2O_3. The filled circles in the magmatic carbonatite section refer to typical abundances in carbonatites (Gold, 1966b). The broken dotted lines in Stage III show the deviation from the magmatic sequence. 1. Magnetite olivinite; 2. Pyroxenite; 3. Amphibole rock; 4. Mice-amphibole rock; 5. Mica rock in magmatic core; 6. Metaphoscorite; 7. Metasilicosövite. I Magmatic phoscorite; II Magmatic sövite and silicosövite; III Magmatic phoscorite (hydrothermally altered) and apatite–ferriphlogopite rock; IV Magmatic sövite, silicosövite and beforsite; V Magmatic late vein.

filled circles (excluding La). The tie lines in the groups of ultramafites, metasomatic rocks and metacarbonatites show the proposed succession of rocks, and, in the magmatic carbonatites, the sequence of crystallization. The hydrothermal stage (Stage III), a deviation from the magmatic sequence, is indicated by a dotted line. The principal host mineral of each element is shown to the right in Fig. 95. The following features emerge:

TiO_2, MnO and V form a geochemically coherent group of elements showing distict correlation with the variation in Fe_2O_3. MnO in Stage III deviates slightly from the general trend as does V in the metasomatic mica–amphibole rock. Except in the late veins (Stage V), the abundance of mag-

netite largely controls the concentrations of these elements. Thus their concentrations (TiO_2 1.3—2.8 %; MnO 0.4—0.7 %; V 400—700 ppm) are highest in the ultramafites and in the phoscorites that are richest in magnetite. The amounts of other Ti-rich minerals, ilmenite, perovskite, zirkelite and pyrochlore, are negligible compared to that of magnetite. The geochemistry of TiO_2, MnO and V is more complicated in the late veins than in the other rocks. Fe is mainly incorporated in sulphide species, and high MnO concentrations (0.9 %) probably in carbonates; V has not yet been traced to any mineral The TiO_2, MnO and V in the metasilicosövites are below the »typical» values. The TiO_2 in the magmatic carbonatites is below the »typical» abundance but MnO and V are within the range of averages.

Sulphur content in the Sokli rocks is about half a per cent. The elevated concentration (1.9 %) in the mica rock of the magmatic core is probably due to hydrothermal activity, which shows up distinctly in the rocks of magmatic Stage III (S 3.7—4.1 %). Sulphur is enriched in the final stage of the magmatic carbonatites (S 5.8 %), where it occurs in pyrrhotite, pyrite, sphalerite and baryte.

Phosphorus. The averages of P_2O_5 in all rock groups are higher than the »typical» value (1.73 %). In the ultramafites P_2O_5 varies from 2.2 to 4.2 %; in the metasomatites variation is more pronounced 2.6 to 7.5 % and in the metacarbonatites P_2O_5 is about 4.0 %. In the magmatic carbonatites P_2O_5 decreases conspicuously from 8.9 % to 1.6 % as crystallization progresses. The highest value of 10.2 % for P_2O_5 concides with the hydrothermal Stage (III). Apatite is the principal or only phosphorus mineral, although in the late veins there may be also rare late phosphates that have not yet been identified.

Lanthanum (100—200 ppm) in the ultramafites, metasomatites and metacarbonatites roughly follows the fluctuation of phosphorus, indicating that La occurs mainly in apatite. The pair (La–P_2O_5) shows a reversal trend in the magmatic carbonatites. La becomes concentrated (3400 ppm) in the late veins as in carbonatite complexes in general (Heinrich, 1966). In the rocks of Stages I—IV La is chiefly enriched in pyrochlore, Zr minerals and apatite. The geochemistry of La in the late veins is under study.

Niobium is the element that most characteristically distinguishes geochemically the magmatic carbonatites from the other rocks in the massif. A striking feature is the low Nb in the metasilicosövites ($<$ 100 ppm) compared to that ($>$ 1 000 ppm) in the magmatic sövitic rocks. The enrichment of Nb (1700 ppm) in the mica rocks of the magmatic core is undoubtedly due to hydrothermal activity. The strong concentration of Nb is characteristic of the hydrothermal stage. Nb may exceed 2 % in individual samples of apatite–ferriphlogopite rocks. The late veins are depleted in Nb (600 ppm) relative to the usual contents in the magmatic carbonatites. As a whole, the abundance of Nb in the magmatic carbonatites is above the »typical» level of Nb in carbonatites (Nb + Ta 560 ppm). Pyrochlore, followed by zirkelite, is the predominant mineral of Nb. The distribution of Nb in other minerals has not yet been studied.

Zirconium. The highest concentrations of Zr occur in the rock groups of the ultramafites, metasomatites and metacarbonatites. In the pyroxenite Zr is about one per cent and in the other rock groups commonly over 100 ppm. The exception is metasilicosövite, in which the Zr content is below 100 ppm. Baddeleyite and zircon are the chief carriers of Zr in these rocks. Other minerals (silicates, opaques) may contain minor or trace amounts of Zr as in other complexes (Heinrich, 1966).

The marked decrease in the Zr trend in the magmatic carbonatites parallels the progress of crystallization. The hydrothermal stage

is geochemically different also in respect of Zr. The Zr content in the magmatic carbonatites is generally close to that of »typical» (461 ppm) in carbonatites. The main concentration of Zr in mineral species declines in the following order; zircon, baddeleyite, zirkelite and pyrochlore.

Strontium and barium. The averages in Fig. 95 show Sr to be concentrated in the carbonate rich rocks whereas Ba appears to remain stable in each rock groups. To study the correlation between these elements and the carbonate phase the Sr and Ba from Tables 16 and 17 were plotted against CO_2 (Fig. 96). Sr has a marked positive correlation with the CO_2 content, indicating that Sr became enriched in the carbonate phase independently of the host rock. Ba shows a different geochemical character and has no positive correlation with increasing CO_2 in the magmatic carbonatites. In the other rock groups Ba is obviously incorporated in other minerals than carbonates. Ba has become strongly enriched in the late veins (Ba 2.9 %). Barite and barytocalcite have been identified from the veins. In the sövitic magmatic carbonatites Sr is close to the »typical»

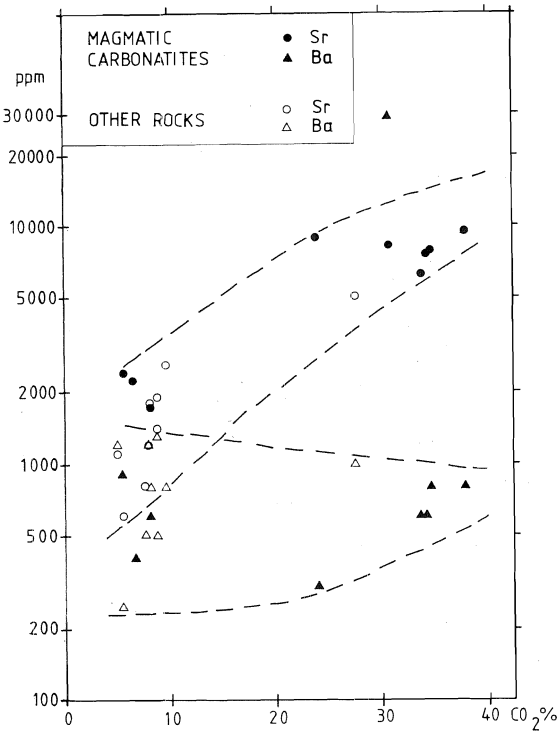

Fig. 96. Plot of Sr and Ba against CO_2; data taken from Tables 16 and 17.

Table 20

Nb/5, Ta, U, and Th contents in selected samples from different stages in the Sokli magmatic carbonatites

Drill hole	Depth, m	Nb/5 ppm	Ta ppm	U ppm	Th ppm
STAGE I, PHOSCORITE					
481	118.0	550	260	380	380
482	110.0	448	160	120	480
482	13.9	212	110	20	90
452	101.7	144	160	220	20
454	117.5	214	220	550	30
477	119.2	204	60	170	50
STAGE II, SILICOSÖVITE AND SÖVITE					
464	74.7	60	60	120	30
»	75.5	818	20	20	110
»	80.0	110	80	180	50
»	25.4	36	60	60	20
»	100.0	222	10	20	50
425	42.5	40	20	30	30
428	37.4	72	20	30	20
»	44.2	420	20	—	210
»	134.0	1078	40	10	570
»	134.7	456	10	—	240
»	127.5	1264	90	20	890
STAGE III, PHOSCORITE AND APATITE-FERRIPHLOGOPITE ROCK					
447	79.0	322	—	—	130
477	164.7	400	70	70	220
449	52.3	4236	80	10	2750
»	177.3	656	—	—	190
450	244.1	1394	20	—	360
452	54.0	3016	120	80	970
454	45.0	126	60	30	130
436	40.6	4796	260	110	2330
STAGE IV, SILICOSÖVITE AND SÖVITE					
456	109.4	582	20	—	90
477	270.4	574	—	20	220
450	244.1	1394	20	—	360
428	49.1	1328	—	—	270
»	50.7	702	20	—	170
»	61.5	376	—	—	80

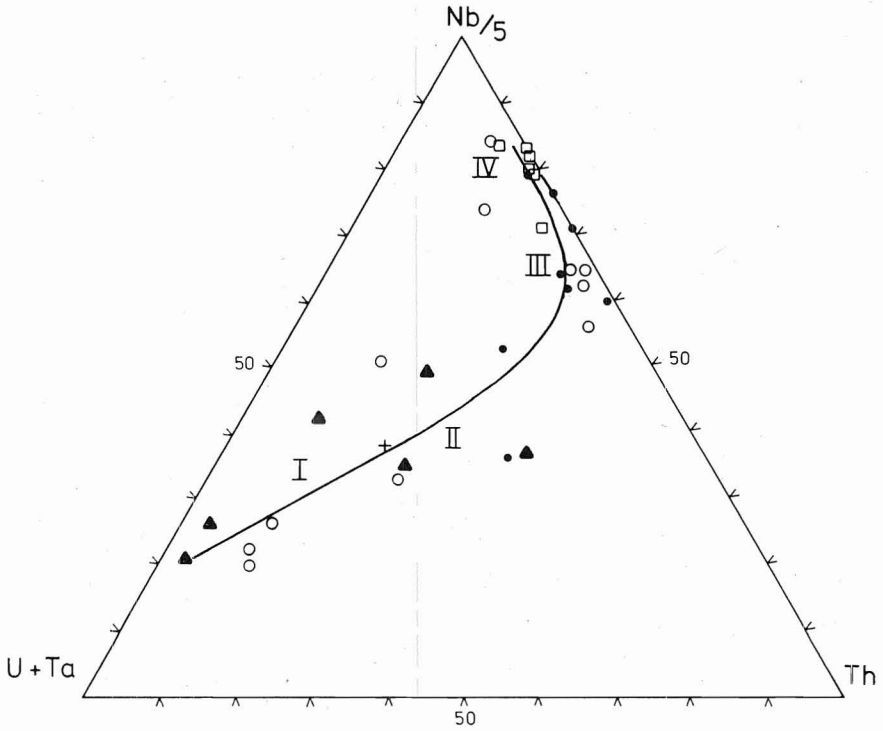

Fig. 97. Plot of the proportions of U + Ta – Th – Nb/5 in the magmatic carbonatites. Filled triangles, Stage I phoscorites; open circles, Stage II sövites and silicosövites; filled circles, Stage III phoscorites and apatite–ferriphlogopite rocks; open squares, Stage IV sövites and silicosövites. Curve defines the trend of crystallization of carbonatites, numbers refer to stages.

value whereas in the Sokli carbonatites Ba is markedly below it.

Verwoerd (1967) has shown that metacarbonatite and magmatic carbonatite cannot be distinguished by means of Sr and Ba content in South African and South West African carbonatites. The same is true at Sokli.

Uranium, thorium and tantalum. The contents of U, Th and Ta are too low to be detected by the x-ray method used in all other rocks except the magmatic carbonatites. The analytical data of the U, Th and Ta in the type samples from the magmatic carbonatites are given in Table 20. The variations in their proportions are given on a triangular diagram in terms of U + Ta—Th—Nb/5 (Fig. 97). There is a distinct decrease in the U + Ta trend with the succession of the magmatic carbonatites and a contemporaneous increase in the Nb/Ta ratio towards younger carbonatites. Pyrochlore is the principal mineral to control the U + Ta—Th—Nb proportions. The data from Fig. 97 show that two pyrochlore generations crystallized during Stage II: an older U + Ta-rich and a younger Th-rich pyrochlore. As pointed out by Heinrich (1966), the Th content generally increases with decreasing age in carbonatites. By plotting U/Th against Nb_2O_5/Ta_2O_5 in camaforites (phoscorites) Borodin *et al.* (1973) have shown that the U/Th proportion decreases with the increase in the Nb_2O_5/Ta_2O_5 proportion. The Sokli data are consistent with these findings.

Chemical characteristics of metasomatic and hydrothermal alterations

The petrographical study has revealed the mineralogical trends involved in the evolution of metaphoscorites and metasomatites from ultramafites, and of metasomatites from fenites. Alteration trends were also produced by hydrothermal activity that was mainly operative during magmatic Stage III. The data that characterize the chemical nature of the alterations include 32 analyses, which are given in Tables 21, 22, 24, 26 and 27. The

Table 21

Alteration trends of Sokli magnetite olivinite based mainly on XRF-analyses (percentage by weight). FeO determined chemically and Fe_2O_3 calculated from total iron.

	1	2	3	4	5	6	7	8	9	10
SiO_2	23.5	14.5	28.4	20.3	27.4	26.5	21.4	13.5	28.2	38.2
TiO_2	2.9	3.3	2.7	1.4	1.0	0.7	2.3	2.8	2.2	0.3
Al_2O_3	0.9	1.7	2.2	2.5	4.3	7.3	0.8	2.4	8.2	10.1
Fe_2O_3	15.0	31.5	24.6	17.0	17.2	6.4	22.2	24.3	13.4	4.2
FeO	13.8	16.3	13.2	10.9	9.7	6.7	12.6	15.4	9.6	3.0
MnO	0.8	0.5	0.4	0.4	0.3	0.1	0.6	0.6	0.3	0.1
MgO	27.5	12.1	16.6	13.7	16.8	18.0	16.1	11.7	15.4	26.2
CaO	6.4	7.3	2.2	11.8	7.9	13.3	7.9	11.5	7.7	2.4
Na_2O	0.1	0.2	0.4	1.4	1.4	0.7	0.2	0.4	0.4	0.6
K_2O	0.6	0.8	1.7	2.2	3.3	5.9	2.2	2.3	6.3	9.4
P_2O_5	1.9	6.1	0.1	1.9	0.8	9.3	2.7	2.2	5.4	0.4
H_2O	2.2	2.7	5.8	1.8	2.0	2.3	4.1	1.7	2.5	3.4
CO_2	4.3	2.2	2.1	13.3	9.2	3.3	6.6	10.9	1.8	2.0
F	0.2	0.3	0.2	0.2	0.2	0.7	0.5	0.2	0.4	0.1
S	0.2	0.1	0.0	0.7	0.2	0.3	0.1	0.5	0.3	0.1
	100.3	99.6	100.6	99.5	101.7	101.5	100.4	100.4	102.1	100.5
O = F, S	0.18	0.18	0.08	0.43	0.18	0.42	0.26	0.43	0.32	0.09
Total	100.1	99.4	100.5	99.1	101.5	101.1	100.1	100.0	101.8	100.4
Trace elements										
Nb	0.01	0.01	0.01	0.03	0.01	0.01	0.02	0.03	0.02	0.06
V	0.07	0.09	0.08	0.04	0.04	0.01	0.08	0.09	0.05	0.00
Zr	0.01	0.58	0.37	0.05	0.05	0.44	0.17	0.21	0.11	0.79
La	0.01	0.01	0.00	0.01	0.00	0.01	0.01	0.01	0.02	0.00
Sr	0.06	0.03	0.02	0.15	0.09	0.11	0.12	0.12	0.08	0.05
Ba	0.02	0.04	0.07	0.06	0.05	0.07	0.05	0.03	0.08	0.09

Alteration trend into richterite rock and further into phlogopite rock

1. Magnetite olivinite. Drill hole 331 at 169.0 metres.
2. Slightly altered magnetite olivinite. Drill hole 413 at 41.0 metres.
3. Intensely serpentinized magnetite olivinite. Drill hole 358 at 118.5 metres.
4. Richterite rock derived from magnetite olivinite. Drill hole 194 at 359 metres.
5. Phlogopitized richterite rock. Drill hole 194 at 360.4 metres.
6. Mica (phlogopite) rock derived from richterite rock. Drill hole at 360.8 metres.

Development of mica (phlogopite) rock from magnetite olivinite in drill hole 436

7. Slightly phlogopitized magnetite olivinite at 22.4 metres.
8. Moderately phlogopitized magnetite olivinite at 22.6 metres.
9. Intensely phlogopitized magnetite olivinite at 23.0 metres.
10. Mica (phlogopite) rock at 36.55 metres.

Table 22

Alteration trends of Sokli pyroxenite based mainly on XRF-analyses (percentage by weight). FeO determined chemically and Fe_2O_3 calculated from total iron.

	1	2	3	4	5	6	7
SiO_2	27.8	26.3	23.9	26.7	16.5	12.2	18.2
TiO_2	2.9	1.5	1.9	3.1	2.3	1.9	1.9
Al_2O_3	4.8	2.9	4.1	8.9	3.1	2.2	2.0
Fe_2O_3	19.7	0.3	8.3	7.4	19.0	14.3	13.6
FeO	12.3	7.4	8.0	12.3	12.4	10.7	8.6
MnO	0.3	0.3	0.2	0.2	0.3	0.4	0.2
MgO	11.0	8.6	10.2	12.4	6.4	8.4	6.1
CaO	9.5	20.2	21.1	11.2	18.8	21.1	24.9
Na_2O	1.5	3.0	2.2	0.8	1.6	1.7	3.5
K_2O	2.6	1.4	2.6	5.7	1.3	1.1	0.7
P_2O_5	1.7	8.1	10.8	6.5	8.9	11.1	7.6
H_2O	1.9	1.6	1.9	2.5	1.3	1.5	1.3
CO_2	4.1	7.1	4.9	2.5	7.6	11.5	11.9
F	0.1	0.3	0.5	0.4	0.4	0.8	0.3
S	0.3	0.3	0.6	1.4	0.3	0.8	0.3
	100.5	99.3	100.8	100.8	101.0	100.1	101.1
O = F, S	0.19	0.38	0.51	0.87	0.32	0.74	0.38
Total	100.3	98.9	100.3	99.9	100.7	99.4	100.7
Trace elements							
Nb	0.00	0.00	0.00	0.01	0.01	0.02	0.01
V	0.07	0.04	0.04	0.04	0.07	0.06	0.04
Zr	1.06	0.13	0.49	0.10	0.83	1.02	0.73
La	0.00	0.01	0.01	0.01	0.01	0.02	0.01
Sr	0.03	0.09	0.10	0.07	0.06	0.14	0.11
Ba	0.05	0.04	0.06	0.15	0.03	0.12	0.04

Drill hole 358

1. At 212.1 metres. Slightly phlogopitized pyroxenite.
2. At 259.4 metres. Alkali amphibole rock derived from pyroxenite.
3. At 267.7 metres. Phlogopitized alkali amphibole rock derived from pyroxenite.
4. At 267.9 metres. Mica (phlogopite) rock derived from former rock.

Drill hole 193

5. At 133.2 metres. Pyroxenite with moderately developed phlogopite and alkali amphibole.
6. At 125.0 metres. Phlogopite bearing alkali amphibole rock derived from pyroxenite with subordinate aegirine.
7. At 130.5 metres. Aegirine- and phlogopite-bearing alkali amphibole rock derived from pyroxenite.

problem of sampling such highly variable rock types was approached by studying petrographically a number of samples from each alteration trend and then selecting representative samples for analyses. The samples analysed for a particular alteration trend where usually taken from the same drill hole. Seven suites of alteration trends are characterized by the following changes:

Alterations from magnetite olivinite

— into richteritized rock and further into mica rock (in metacarbonatite area, Fig. 11, trend 1)

— into mica rock (in magmatic core, Fig. 11, trend 7).

Alterations from pyroxenite

— into alkali amphibole rock and further

into mica rock (in metacarbonatite area, Fig. 11, trend 5)
— into aegirine bearing rocks (in metacarbonatite area, Fig. 11, trend 6).

Alterations from fenite

— into pyroxene rock and further into mica-amphibole rocks and mica rock.

Hydrothermal alterations

— from magnetite olivinite into magmatic-like phoscorite (in magmatic core, Fig. 11, trend 8)
— from magmatic Stage I phoscorite to hydrothermal phoscorite of Stage III (in magmatic core).

The standard cell method of Barth (1962) was applied to describe the chemical changes in these alterations. The analyses were recalculated in terms of cations combined with 160 oxygen atoms (Tables 23, 25 and 27). Oxide percentages had to be used to evaluate of the alteration trend from magnetite olivinite into magmatic-like phoscorite because Fe was analysed as total iron. The application of the standard cell method was made feasible by the persistence of the original, massive texture through the alterations series, suggesting that metasomatic processes occurred in a roughly constant volume. The analytical techniques were described in the previous chapter.

Chemical changes due to metasomatism in magnetite olivinite and pyroxenite

Ten analyses of magnetite olivinite and seven of pyroxenite alteration trends were recalculated on the basis of 160 oxygen atoms (Table 23). In respect of the highly irregular fluctuation in the alteration of ultramafites, the number of analyses is too low to allow an index to be established for the degree of chemical changes in the major and minor

Table 23

Compositions of rocks in the alteration trends in Sokli ultramafites per 160 oxygen atoms

	From Table 21										From Table 22						
	1	2	3	4	5	6	7	8	9	10	1	2	3	4	5	6	7
Si	25.87	16.45	28.80	20.57	27.04	26.21	22.03	14.60	28.57	36.40	29.26	27.87	24.25	27.63	17.46	12.63	18.41
Ti	2.40	2.81	2.06	1.07	0.74	0.52	1.78	2.28	1.68	0.21	2.29	1.20	1.14	1.48	2.47	1.79	1.45
Al	1.17	2.27	2.63	2.99	5.00	8.51	0.97	3.06	9.79	11.34	5.95	3.62	4.90	10.85	3.87	2.68	2.38
Fe^{3+}	12.43	26.89	18.77	12.96	12.77	4.76	17.20	19.77	10.22	3.01	15.60	8.21	6.34	5.76	15.13	11.14	10.35
Fe^{2+}	12.71	15.46	11.20	9.24	8.01	5.54	10.85	13.93	8.13	2.39	10.82	6.56	6.79	10.64	10.97	9.26	7.27
Mn	0.75	0.48	0.34	0.34	0.25	0.08	0.52	0.55	0.26	0.08	0.27	0.27	0.17	0.18	0.27	0.35	0.34
Mg	36.10	20.46	25.09	20.69	24.71	26.54	24.86	18.86	23.26	37.22	17.25	13.58	15.42	19.13	10.09	12.96	9.20
Ca	7.57	8.87	2.39	12.81	8.35	14.10	8.71	13.32	8.36	2.45	10.71	22.93	22.94	12.42	21.31	23.40	26.98
Na	0.21	0.44	0.79	2.75	2.68	1.34	0.40	0.84	0.79	1.11	3.06	6.16	4.33	1.61	3.28	3.41	6.86
K	0.84	1.16	2.20	2.84	4.15	7.44	2.89	3.17	8.14	11.43	3.49	1.89	3.36	7.52	1.75	1.45	0.90
OH	16.16	20.43	39.24	12.16	13.16	15.18	28.16	12.26	16.90	21.61	13.34	13.43	12.86	17.26	9.18	10.36	8.77
P	1.77	5.86	0.09	1.63	0.67	7.79	2.35	2.01	4.63	0.32	1.51	7.27	9.28	5.69	7.97	9.73	6.51
C	6.46	3.41	2.91	18.40	12.39	4.46	9.28	16.09	2.49	2.60	5.89	5.93	6.79	3.53	10.98	16.25	16.43
O	143.84	139.57	120.76	147.84	146.84	144.82	131.84	147.74	143.10	138.39	146.66	146.57	147.14	142.74	150.82	149.64	151.23

For details of rock types and localities, see Tables 21 and 22

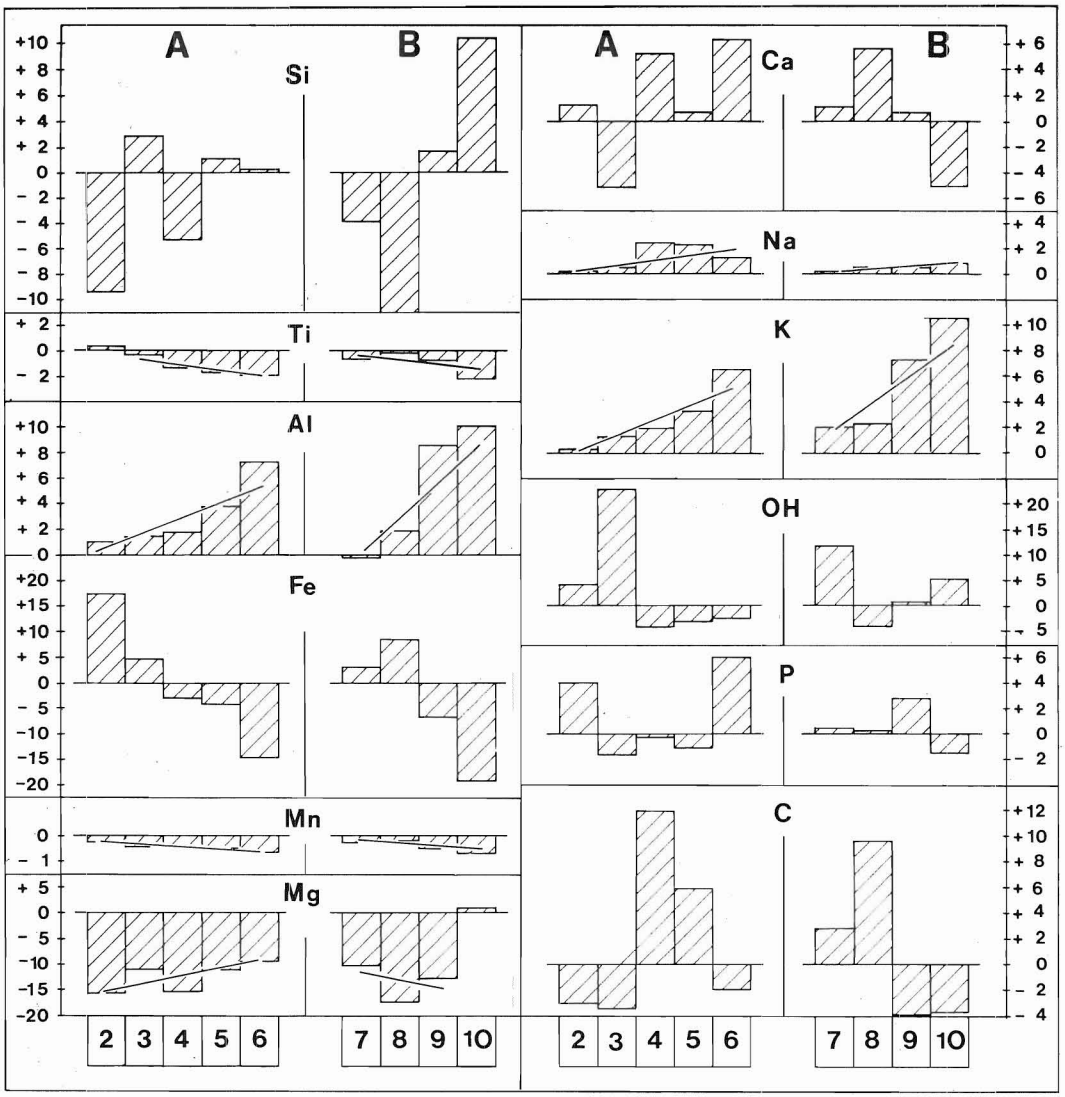

Fig. 98. Addition/subtraction diagram for major elements in alteration trends from magnetite olivinite based on the atoms per standard cell of 160 oxygen atoms.

A. Into richterite rock and further into mica rock (in metacarbonatite area).

B. Into mica rock (in magmatic core). Lines approximated by the least squares. Numbers as in Table 21.

elements. Thus an addition/subtraction method was applied to characterize the chemical changes. An unaltered magnetite olivinite and a slightly altered pyroxenite (the least altered sample of pyroxenite found so far) establish a foundation for chemical comparison that starts in these unaltered rocks and passes into different alteration trends.

Based on the data of Table 23, Figs. 98 and 99 illustrate the progressive quantitative changes in major and minor elements in 160 anion cells. The variation is notably irregular. Whenever the change is progressive a straight line approximated by least squares is drawn in the addition/subtraction diagrams (Figs. 98 and 99).

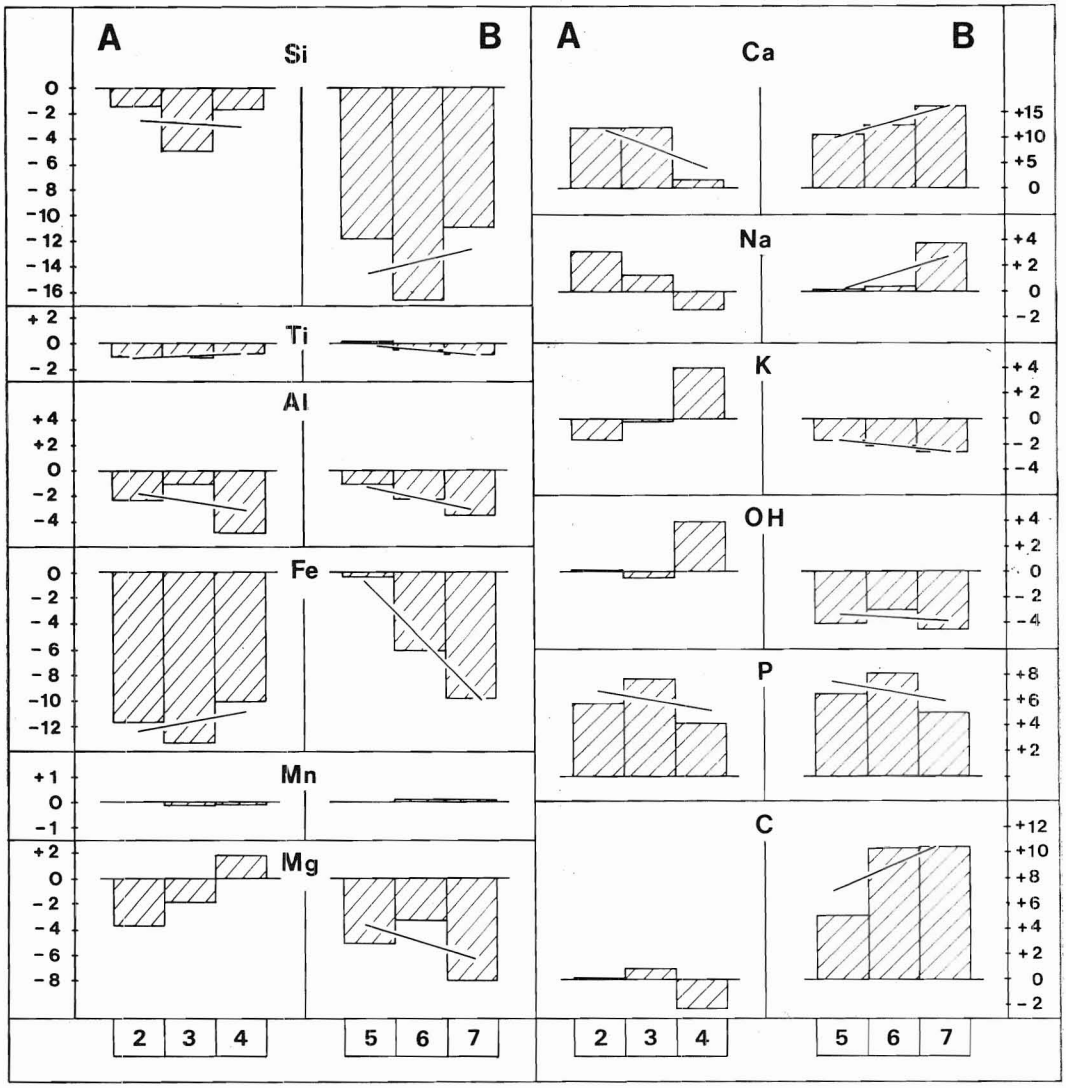

Fig. 99. Addition/subtraction diagram for major elements in alteration trends from slightly altered pyroxenite based on atoms per standard cell of 160 oxygen atoms.
A. Into alkali amphibole rock and further into mica rock (in metacarbonatite area).
B. Into aegirine bearing rocks (in metacarbonatite area). Lines are approximated by least squares. Numbers as in Table 22.

Alteration from magnetite olivinite into richterite rock and further into mica rock in the metacarbonatite area (Fig. 98, A), and into mica rock in the magmatic core (Fig. 98, B) shows more or less coherent chemical changes. The key features revealed by the data in Fig. 98 can be summarized as follows:

Gains: There is a considerable and progressively addition of Al and K, and a small addition of Na. The slopes of the lines for Al and K are distinctly steepest in the micatization of the magnetite olivinite (Fig. 98, B); in richteritization (Fig. 98, A) the addition of Na is more pronounced.

Losses: The most conspicuous feature is the abrupt and marked decrease in Mg displayed

by both trends. The loss of Mg reflects a rapid alteration in olivine abundance in these rocks. There are slight but distinct declining trends in Ti and in Mn with similar abundances in both alteration trends.

No definite trends: There is a wide fluctuation in the distributions of Si, Ca, OH, P and C in the alteration varieties but without any systematic trend. Fe is so regular that, in both series, its abundance first increases and then decreases. Note that neither regular apatitization nor carbonatization have occurred.

The alteration of pyroxenite into aegirine-bearing rocks (Fig. 99, B) shows distinct elementary gains and losses and is thus the most regular type of chemical variation in all the alteration series studied. The concentrations of Ca, C, P and Na increase in that order. The increase in the concentrations of Ca and C is closely related to the crystallization of calcite, the increase in P to apatitization and the increase in Na to development of alkali amphiboles and aegirine. There is a large decrease in the concentration of Si, a moderate decrease in Fe, Mg, OH, K and Al, and a slight decrease in Ti. Mn appears to be constant.

The chemical variation was more complicated during the metasomatism that produced alkali amphibole rock and mica rock from pyroxenite (Fig. 99, A). Ti and Al indicate similar decreases; Mn remained more or less constant. P and Ca increased at about the same concentrations. The loss of Si was not so pronounced. Correspondingly, Fe decreased more than in the aegirinic suite. The end product, the mica rock (Fig. 99, number 7), deviates conspicuously from the general trend of Na, which was depleted, and of K, OH and Mg, which were increased. These changes are closely related to the intense phlogopitization in the rock.

Chemical changes in major and minor elements during the metasomatic alteration of pyroxenite can be summarized as follows:

Gains: Ca, P, Na and C (Na and C were lost in the mica rock).

Losses: Fe, Si, Al, Ti, Mg, K and OH (Mg, K and OH were gained in the mica rock).

Trace elements in the alteration trends of magnetite olivinite and the pyroxenite

The trace element trends relevant to the alteration trends of magnetite olivinite and pyroxenite are given in Figs. 100 and 101. The tie lines indicate the variation in trace elements as the alteration proceeds from left (unaltered rocks) to right in the diagrams. The principal features in the trace element abundances during the alterations shown in Figs. 100 and 101 are as follows:

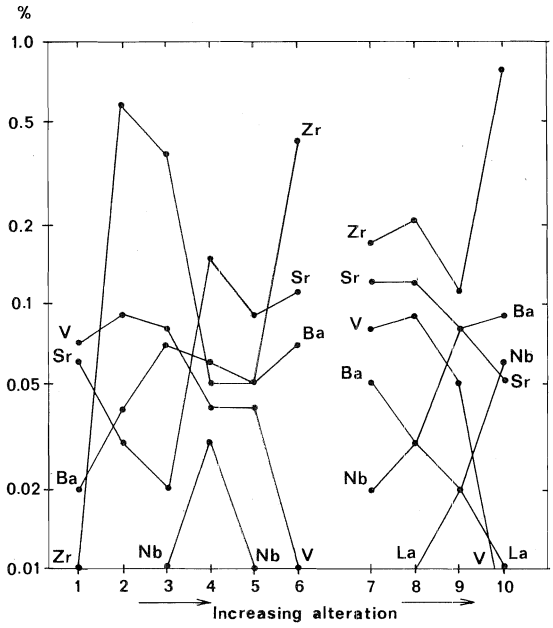

Fig. 100. Variation in the abundances of the trace elements analysed in the alteration trends of magnetite olivinite. Numbers as in Table 21.

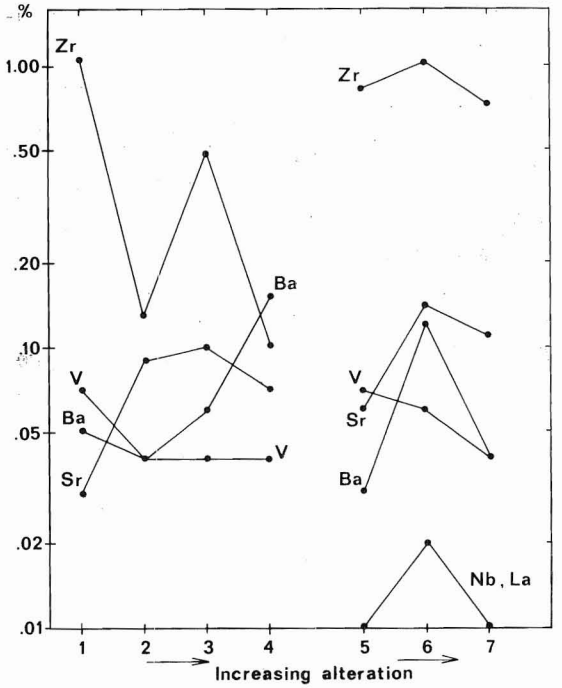

Fig. 101. Variation in the abundances of the trace elements analysed in the alteration trends of pyroxenite. Numbers as in Table 22.

Zirconium: An irregular variation in Zr indicates the original fluctuation in Zr in magnetite olivinite and pyroxenite rather than a trend during alterations. The low Zr (0.01 %) in the unaltered magnetite olivinite is exceptional (Fig. 100, sample 1) because the average for the magnetite olivinite is 0.14 % (Table 16).

Niobium: Nb remains low in all alteration trends but the formation of mica rock from the magnetite olivinite in the magmatic core (Fig. 100, samples 7—10), where it is concentrated into the mica rock.

Lanthanum: There is no significant variation in La.

Vanadium: The decreasing trend in V, which is the most marked of all the alteration trends in ultramafites is the most regular feature shown by any of the trace elements.

Barium and strontium: There is an irregular but distinct increase in Ba and Sr in all the alteration trends. The only exception is Sr in the transformation of magnetite olivinite into the mica rock in the magmatic core (Fig. 100, samples 7—10). This accords with the depletion in carbonates (Fig. 98, B).

The general variation in the trace element abundances can be summarized as follows:
Gains: Ba, Sr
Loss: V
No definite trend: Zr, La, Nb

Table 24

Alteration trend of fenite in the Sokli massif based mainly on XRF-analyses (percentage by weight). FeO determined chemically and Fe_2O_3 calculated from total iron.

	1	2	3	4	5	6
SiO_2	41.6	41.7	37.2	25.8	22.6	14.8
TiO_2	0.4	0.3	0.3	0.4	0.4	0.2
Al_2O_3	9.6	6.1	7.0	4.1	4.3	4.4
Fe_2O_3	4.3	9.0	7.0	6.1	3.3	4.1
FeO	3.3	2.8	3.1	3.7	3.8	12.9
MnO	0.0	0.4	0.4	0.5	0.3	0.4
MgO	7.8	7.1	7.9	9.4	11.5	10.8
CaO	11.1	15.2	15.3	22.6	24.5	19.9
Na_2O	6.1	6.1	5.9	3.7	2.2	0.8
K_2O	1.8	0.4	1.2	2.7	3.2	3.2
P_2O_5	1.5	1.5	1.4	5.3	1.8	0.5
H_2O	0.9	0.9	1.4	1.5	1.6	1.5
CO_2	8.2	6.6	9.1	12.4	17.8	19.7
F	0.2	0.1	0.1	0.5	0.2	0.1
S	0.2	0.1	0.0	0.0	0.0	6.1
	97.0	98.3	97.3	98.7	97.5	99.4
O = F, S	0.18	0.09	0.04	0.21	0.08	3.09
Total	96.8	98.2	97.3	98.5	97.4	96.3
Trace elements						
Nb	0.02	0.01	0.02	0.02	0.02	0.04
V	0.01	0.02	0.02	0.01	0.01	0.00
Zr	0.03	0.08	0.05	0.04	0.02	0.01
La	0.02	0.01	0.02	0.04	0.02	0.02
Sr	0.22	0.14	0.26	0.38	0.47	0.31
Ba	0.09	0.20	0.12	0.06	0.09	0.46

1. Fenite, DH 259 at 84.4 metres
2. Pyroxene rock, DH 441 at 285.8 metres
3. Calcic amphibole—alkali amphibole rock derived from pyroxene rock, DH 441 at 287.7 metres
4. Mica—alkali amphibole rock from the former rock, DH 441 at 287.8 metres
5. Mica—alkali amphibole rock derived from fenite, Drill hole 259 at 84.7 metres
6. Mica rock formed from the former rock, Drill hole 259 at 86.2 metres

Alteration from fenites

There are earlier reports of alkali amphibole rocks and mica rocks from the carbonatite—fenite contact zone, but their origin has not been established (Vartiainen and Woolley, 1976). In the area of metacarbonatites and metasomatites drillings have since shown that these rocks were transformed from fenites by metasomatism related to the carbonatite intrusion. Hence, these rock varieties are second-generation metasomatites. The chemical changes (Table 24) in the major and minor elements involved in the transformations of the fenites are given on the basis of the number of ions per standard cell (Table 25); the changes are visualized by an addition subtraction diagram (Fig. 102). As they pass from pyroxene rock (Fig. 102, number 2) into alkali amphibole-bearing variants (Fig. 102, numbers 3—5) and ultimately into mica rock (Fig. 102, number 6), the chemical changes

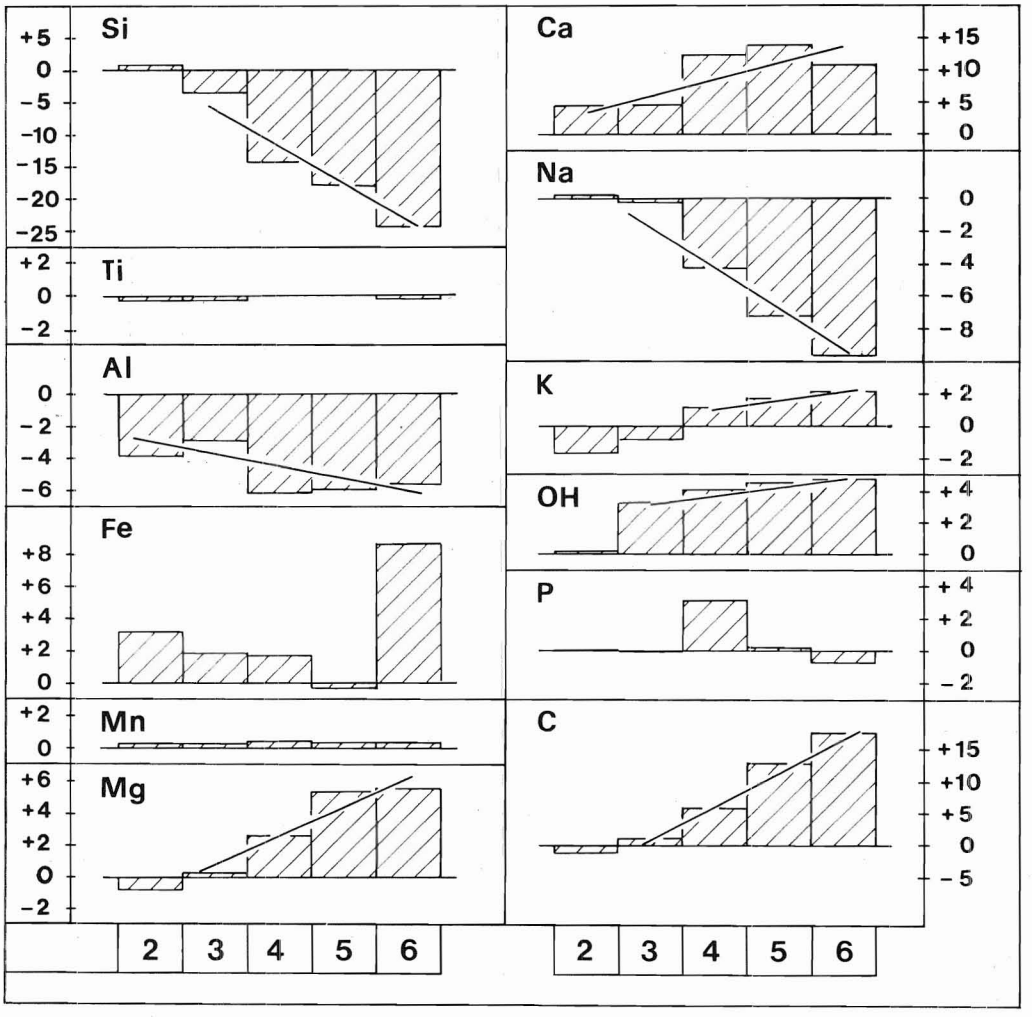

Fig. 102. Addition/subtraction diagram for major elements in alteration trends of fenite based on atoms per standard cell of 160 oxygen atoms. Lines approximated by the least squares. Numbers as in Table 24.

Table 25

Compositions of rocks in the alteration trend of fenite in the Sokli massif in cations per 160 oxygen atoms

	From Table 24					
	1	2	3	4	5	6
Si	39.73	40.51	36.03	25.25	21.80	15.42
Ti	0.29	0.22	0.22	0.29	0.29	0.16
Al	10.81	6.98	7.99	4.73	4.89	5.40
Fe^{3+}	3.09	6.58	5.10	4.49	2.40	3.22
Fe^{2+}	2.64	2.27	2.51	3.03	3.07	11.24
Mn	0.00	0.33	0.33	0.41	0.25	0.35
Mg	11.10	10.28	11.41	13.71	16.53	16.78
Ca	11.36	15.82	15.88	23.70	25.32	22.22
Na	11.30	11.49	11.08	7.02	4.11	1.62
K	2.19	0.50	1.48	3.37	3.94	4.25
OH	5.73	5.83	9.05	9.79	10.29	10.43
P	1.21	1.23	1.15	4.39	1.47	0.44
C	10.69	8.75	12.03	16.57	23.44	28.03
O	154.27	154.17	150.95	150.21	149.71	149.57

For details of rock types and localities, see Table 24

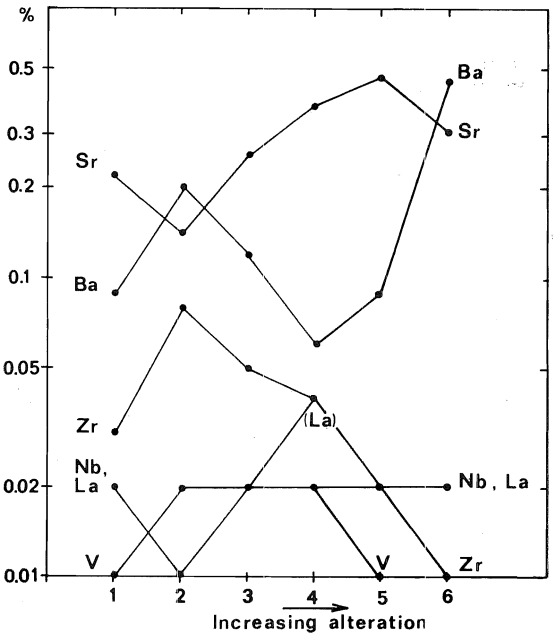

Fig. 103. Variation in the abundances of the trace elements analysed in the alteration of fenite. Numbers as in Table 24.

display conspicuous coherent trends, excluding Fe and P which fluctuate irregularly. Ti and Mn are almost constant. The pyroxene rock, which is mainly composed of pyroxene and recrystallized albite, is believed to have been formed at elevated temperature and only slightly affected by metasomatism. This is demonstrated by the changes in Si, Mg, Na, K and C (number 2 in Fig. 102) that are contrary to the common trend of elementary variation. Mg and K that were expelled during the first stage in the transformation of fenite presumably re-entered the rock as metasomatism advanced. After the formation of the pyroxene rock, the continuous chemical changes in the transformation of fenite into metasomatites took place in the following order of decreasing intensity:

Gains: Ca, C, Mg, OH, Fe, K.
Losses: Si, Na, Al.

The variations in trace element abundances are given in Fig. 103. The data reveal that:

— Nb, La and V exhibit no significant variation,
— Zr increases first and then decreases clearly,
— Sr and Ba are irregular but contrary to the mutual variation and show increasing tenors.

Hydrothermal alterations

Hydrothermal alteration of magnetite olivinite into a rock resembling magmatic phoscorite (Stage III)

Five samples were analysed (Table 26) to demonstrate the chemical variation in this alteration trend. Total Fe was calculated to Fe_2O_3 and hence the totals exceed one hundred for the first four samples. Weight

Table 26

Alteration trend of Sokli magnetite olivinite into magmatic-like phoscorite in DH 456 based mainly on XRF-analyses (percentage by weight)

	1	2	3	4	5
SiO_2	4.4	12.6	10.5	18.1	20.4
TiO_2	2.0	2.1	1.4	9.2	13.2
Al_2O_3	0.7	0.9	1.1	1.0	1.0
Fe_2O_3*	68.2	59.5	46.2	21.8	22.1
MnO	0.7	0.7	0.6	1.4	1.4
MgO	9.2	15.8	14.9	17.6	14.5
CaO	6.1	4.7	10.3	13.0	11.3
Na_2O	0.1	0.2	0.4	0.8	1.8
K_2O	0.7	1.4	1.6	1.8	1.7
P_2O_5	1.6	1.8	3.7	7.3	5.2
$CO_2 + H_2O+$	6.0	3.1	9.2	9.4	6.0
S	1.8	1.4	3.1	0.1	0.9
	101.5	104.2	103.0	101.5	99.5
O = S	0.90	0.70	1.55	0.05	0.45
Total	100.6	103.5	101.4	101.4	99.0
Trace elements					
Nb	0.02	0.07	0.09	0.45	0.53
V	0.07	0.07	0.05	0.06	0.06
Zr	0.01	0.06	0.26	0.95	1.55
La	0.03	0.01	0.02	0.03	0.03
Sr	0.07	0.06	0.14	0.21	0.15
Ba	0.07	0.08	0.07	0.12	0.10

* Total iron

1. Depth 122.9. Coarse-grained magnetite-rich olivinite with large-flaked phlogopite.
2. Depth 122.6. Coarse to medium-grained rock. Fine-flaked ferriphlogopite generation moderately developed. The first richterite needles have crystallized.
3. Depth 122.4. Medium-grained rock. Fine-flaked ferriphlogopite and richterite are the main silicates. Pyrochlore and zircon appears.
4. Depth 121.8; 5. Depth 122.2. Medium-grained rock with flowage texture. Richterite is a dominant silicate. Pyrochlore and zircon are considerably more abundant. The amount of ilmenite is marked.

oxide percentages together with the trace elements were plotted on the variation diagram (Fig. 104). Sodium was constantly added and hence Na_2O was used as an index of the degree of alteration. The principal chemical changes apparent from Fig. 104 and the relationship of the chemical changes to mineralogy are as follows:

1. There is a high decrease in iron due to the replacement of magnetite by silicate minerals and carbonates.
2. Addition of TiO_2 and P_2O_5 are the most prominent increases in major components. The increase in TiO_2 is due to the crystallization of ilmenite, and that of P_2O_5 to apatitization. Some titanium crystallized as ilmenite, may derive from the decomposition of magnetite.
3. MgO and SiO_2 show similar additative trends, which can be attributed to the increase in richterite. Nevertheless, most of its constituents derive from altered olivine. Although the samples analysed were collected from near each other, the original variation in the abundances of magnetite and olivine may reflect variation in MgO and SiO_2 and also in Fe_2O_3.
4. The increase in Na_2O is manifested by increase in richterite and pyrochlore abundances.
5. Carbonatization has brought from an external source all the CO_2 that is in magnetite olivinite.
6. Strontium and barium follow closely the variation in $CO_2 + H_2O^+$.
7. The increase in potassium and aluminium is indicated by the development of ferriphlogopite.
8. MnO follows a similar trend to TiO_2.
9. Sulphur displays strikingly irregular variation, which indicates sulphidization being independent of the usual alterations process.
10. There is a considerable increase in Nb and Zr. Some primary baddeleyite crystals showing no signs of alteration into zircon have been noted, suggesting that hydrothermally introduced zirconium crystallized as zircon. Niobium is incorporated in pyrochlore.
11. There are no significant changes in the abundances of V and La.

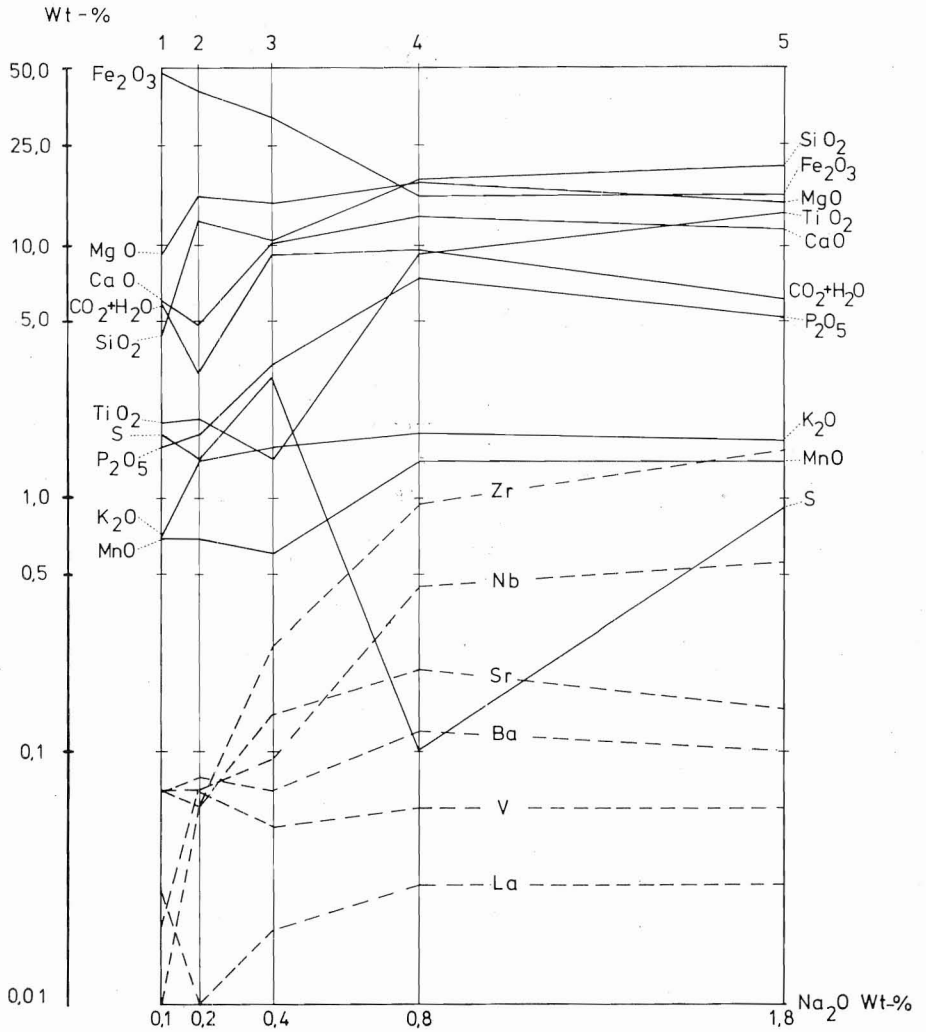

Fig. 104. Variation in the major, minor and trace elements against Na_2O in the hydrothermal alteration of magnetite olivinite into a rock resembling magmatic Stage III phoscorite. Numbers as in Table 26.

The new minerals were produced in the altered magnetite olivinite by the hydrothermal process as follows:

Element added	Mineral produced
Na	Richterite
Na + Nb	Pyrochlore
Zr	Zircon
Ti (Mn)	Ilmenite
P + Ca	Apatite
CO_2 + Ca (Sr + Ba)	Calcite
K + Al	Ferriphlogopite

Hydrothermal alteration of magmatic phoscorite I into phoscorite III

The chemical changes in this alteration trend were studied by three analyses (Table

Table 27

Mainly XRF-analyses in weight percentages showing the alteration trend from the Sokli magmatic phoscorite of Stage I into hydrothermal phoscorite of Stage III; compositions in cations per 160 oxygen atoms

	1	2	3
SiO_2	12.7	14.4	16.1
TiO_2	1.1	1.6	1.0
Al_2O_3	0.1	0.1	1.4
Fe_2O_3	9.7	28.9	15.4
FeO	22.1	16.6	10.6
MnO	0.5	0.7	0.4
MgO	14.0	14.8	12.8
CaO	16.4	10.0	16.8
Na_2O	0.1	0.1	1.2
K_2O	0.1	0.1	2.8
P_2O_5	13.2	7.6	11.2
CO_2	1.8	1.7	5.1
S	3.6	1.4	1.3
	95.4	98.0	96.1
O = S	1.80	0.70	0.65
Total	93.6	97.3	95.4
Trace elements			
Nb	0.16	0.22	0.58
V	0.03	0.05	0.03
Zr	0.21	0.18	0.20
La	0.02	0.01	0.02
Sr	0.10	0.06	0.16
Ba	—	0.04	0.28
U	0.038	0.012	0.017
Th	0.038	0.048	0.102
Ta	0.026	0.016	0.030
Composition in cations			
Si	15.81	17.44	18.34
Ti	1.03	1.46	0.86
Al	0.15	0.14	1.88
Fe^{3+}	9.09	26.33	13.20
Fe^{2+}	23.01	16.81	10.10
Mn	0.53	0.72	0.39
Mg	25.98	26.71	21.74
Ca	21.87	12.97	20.51
Na	0.24	0.23	2.65
K	0.16	0.15	4.07
P	13.91	7.79	10.80
C	3.06	2.81	7.93
O	160.00	160.00	160.00

1. Unaltered Stage I phoscorite. Drill hole 482 at 118.0 metres.
2. Serpentinized Stage I phoscorite. Drill hole 482 at 110.5 metres.
3. Stage III phoscorite derived from Stage I phoscorite. Drill hole 482 at 109.5 metres.

27). The results are visualized in Fig. 105, where major, minor and trace elements are given on variation diagrams. The major and minor elements were calculated to a standard cell of 160 anions. The internal relations of U + Ta, Th and Nb/5 are presented on a triangular diagram (Fig. 105, B). In the diagrams (Fig. 105) the alteration of the phoscorite I proceeds from left to right. Of the major elements, Si shows an increasing and the others (Fe, Mg, Ca and P) a decreasing trend due to the hydrothermal process. The increase in Fe can hardly be wholly attributed to the hydrothermal introduction; it more likely reflects the original difference in Fe between the samples analysed.

The alteration at the first stage (Fig. 105, break line) was mainly autometasomatic as is indicated by the serpentinization of olivine. The addition of Ba and the increased proportion of Th and Nb in U + Ta—Th—Nb/5 ratios were the only marked chemical changes at this stage compared with unaltered phoscorite I. The second stage (Fig. 105, number 3) represents a truly hydrothermally altered type that contains richterite, clinohumite, ferriphlogopite and carbonate as the main minerals of the alteration generation. The chemical changes involved in the hydrothermal alteration of the phoscorite I are:

1. Significant increase in C, K, Na, Al and Ba
2. Moderate increase in Si and Sr
3. Increase in Nb in U + Ta—Th—Nb/5 rations.

The additions of these elements are compensated by the decrease in Fe, Mg, P, Ti and Mn.

Conclusion on the chemistry of metasomatic alterations

The character of the metasomatism in the Sokli complex is indicated by the chemical

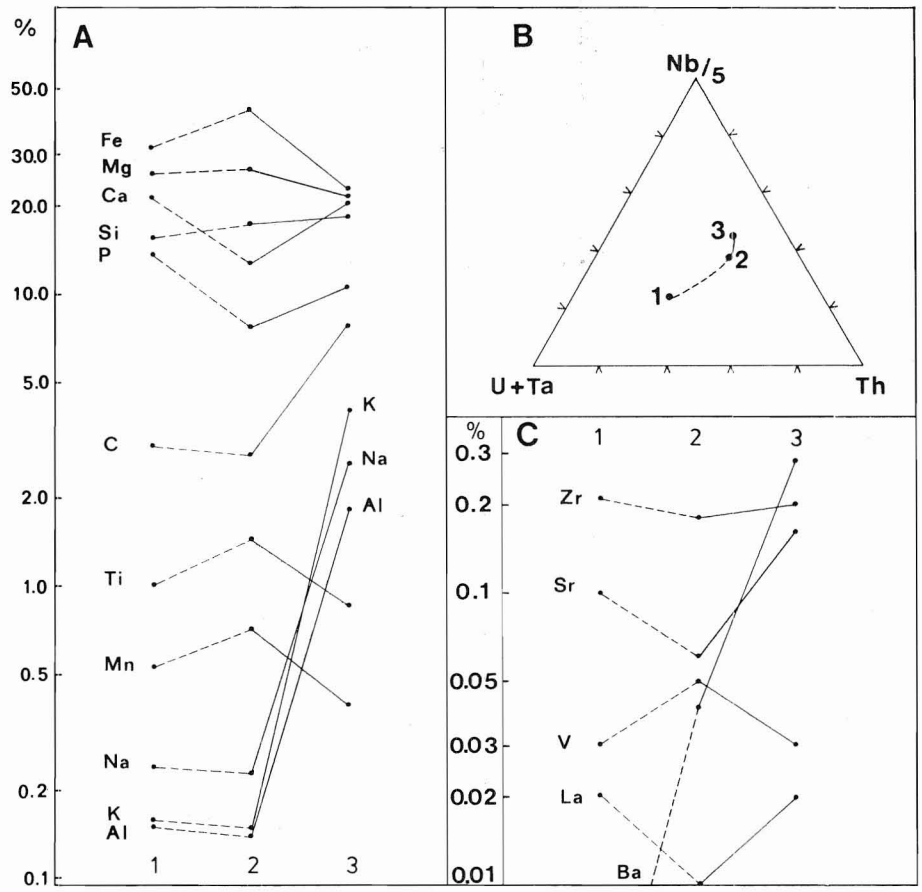

Fig. 105. Variation diagrams for the alteration of magmatic phoscorite I into magmatic phoscorite III. Numbers as in Table 27. Tie lines indicate the trend of alteration.

A. Variation in the major and minor elements on the basis of atoms per standard cell of 160 oxygen atoms.

B. Triangular diagram in terms of U + Ta—Th—Nb/5.

C. Variation in trace elements.

data on the different alteration trends. The analyses show elemental gains and losses compared to the unaltered rocks. The exact chemical balance of the overall complicated metasomatism, the amount of elements transfered from one alteration system to another and the amount of certain elements actually introduced into or expelled out from the complex during metasomatic alterations is difficult, if not impossible, to calculate because there is no way of determining the volumes of the alteration varieties. Vartiainen and Woolley (1976) attempted to elucidate the quantitative changes in the fenite aureole of Sokli for the major elements. An approach at evaluating the chemical balance in the whole Sokli complex on a qualitative basis is given in Table 28, which shows the changes involved in passing from country rocks into fenites, and from ultramafites and fenites into the main altered rock varieties in the area of metacarbonatites and in the transitional zone of metasomatites. The table also illustrates the changes involved in the

Table 28

Summary of gains and losses in the metasomatic alteration of the Sokli complex

Metasomatic trends	Gains/Losses											
Fenite aureole	Si	Ti	Al	Fe	Mn	Mg	Ca	Na	K	OH	P	C
From granite gneiss												
— into sodic fenite	−−	+	−	+	+	+	−	++	−	−	+	
— into potassic fenite	−−	+	+	+	+	+	−	−−	+	+	−	
From amphibolite/ hornblende schist												
— into sodic fenite	+	○	−	−	○	−	−−	++	+	+	○	
— into potassic fenite	+	+	−	−	+	−−	−−	−	++	+	○	
Metacarbonatite area and the transitional zone of metasomatites												
From magnetite olivinite												
— into richteritic rocks	○	−	+	○	−	−−	○	+	++	○	○	○
— into mica rock	○	−	++	○	−	−−	○	+	++	○	○	○
From pyroxenite												
— into amphibolic and mica rocks	−	−	−	−−	○	○	++	○	○	○	++	○
— into alkali amphibole and aegirine-bearing rocks	−−	−	−	−−	○	−−	++	+	−	−	++	++
From fenite												
— into amphibolic and mica rocks	−−	−	−−	+	+	+	++	−−	○	+	○	++
Development of metasilicosövites	−−	−	−	−−	○	−−	++	?	−	?	−	++

++ major gain
+ minor gain
○ no definite trend
−− major loss
− minor loss

development of metasilicosövites. The metasomatic trend in the development of metasilicosövites was not studied by analyses. The principal chemical changes involved in these transformations can be established by comparing the average composition of metasilicosövites with the compositions of the rocks from which they are derived. This is done in Table 29. The results show that large-scale elemental migrations were involved in the metasomatic alterations within the Sokli complex.

As discussed earlier (op. cit.) and indicated by Table 28 the elemental changes in the fenite aureole are in the order of decreasing abundance as follows:

Added: Na, K, OH, Fe, Ti, Mn
Removed: Si, Ca, Al

The overall elemental changes during the metasomatic alterations and development of metasilicosövites within the carbonatite massif can be deduced from the Table 28 as follows:

Added: Ca, C, P, K, Na
Removed: Si, Mg, Fe, Ti, Mn

With regard to the whole Sokli complex, it is evident that metasomatic processes introduced Na, K, P, OH and CO_2 (= C) and expelled Si, Mg, and Fe from the altered rocks.

Table 29

Comparison of the composition of the Sokli metasilicosövite and its precursory rocks (percentage by weight)

	1	2	3	4	5	Average 1—5	Metasilico-sövite *	Gains	Losses
SiO_2	37.8	23.6	21.1	26.5	23.9	26.2	7.1		—
TiO_2	0.9	1.0	2.2	0.7	1.9	1.4	0.4		—
Al_2O_3	7.5	4.6	2.0	7.3	4.1	4.8	1.7		—
Fe_2O_3	7.0	9.4	19.3	6.4	8.3	10.8	5.8		—
FeO	3.1	4.2	8.7	6.7	8.0	6.5	2.7		—
MnO	0.3	0.3	0.5	0.1	0.2	0.3	0.3		
MgO	7.9	9.7	18.2	18.0	10.2	12.8	7.6		—
CaO	15.8	21.7	14.2	13.3	21.1	18.2	41.0	+	
K_2O	1.3	3.2	2.0	5.9	2.6	3.1	1.2		—
P_2O_5	4.8	7.1	4.4	9.3	10.8	7.4	4.2		—
CO_2	8.1	9.6	8.5	3.3	4.9	7.1	27.5	+	

1. Amphibole rock (from Table 16); 2. Mica-amphibole rocks (from Table 16); 3. Metaphoscorites (from Table 18); 4. Mica rock derived from magnetite olivinite (Table 21/number 6); 5. Phlogopitized alkali amphibole rock derived from pyroxenite (Table 22/number 3).
* From Table 16.

Some of the Ca depleted from the fenite aureole may have migrated inwards and been a partial cause of carbonatization within the massif. The development of metasilicosövites, presumably required the introduction of Ca from an external source. The migrations of Ti, Al and Mn may be attributed to internal transfer within the complex.

DISCUSSION AND SUMMARY

Numerous researchers have discussed the origin of carbonatites, e.g. Heinrich (1966), Wyllie (1966 a), Verwoerd (1967), Borodin and Kapustin (1968), Hyndman (1972), Frolov (1975), Kapustin (1976) and (Le Bas, 1977). The various genetic hypotheses proposed in these discussions, and some others that apply to certain local conditions, are compiled in Table 30. The data are arranged chronologically. Metasomatic and magmatic groups were established to show the two main hypotheses for the origin of carbonatites. If the origin is magmatic the supposed parent magma for carbonatites and the chief development processes of carbonatite from the parent magma are given. A comparison between the results obtained by Western and Soviet scientists and given in Table 30 reveals that:

	Western	Soviet
Metasomatic origin	3	5
Magmatic origin	39	9
Metasomatic + magmatic origin	4	5

Although the review in Table 30 may be criticized in detail and representativeness, the results show plainly that Western scientists favour a magmatic origin for carbonatites whereas their Soviet colleaques show no definite preferance for any of the different hypotheses. The chronology indicates, however, that the magmatic origin is coming more popular in the Soviet school.

Table 30

Chronologically arranged simplified hypotheses for the origin of carbonatites

Author	Year	Locality	Origin		Parent magma	Development of carbonatite magma, fluid or residual melt
			Meta-somat.	Mag-matic		
Brögger, W. C.	1921	Fen, Norway		x	(Alkalic magma?)	Calcite magma by melting of limestone
Bowen, N. L.	1924	Fen, Norway	x			
Tomkeieff, S. I.	1938	Fen, Norway		x	Alkali pyroxenite	Crystallization differentiation
von Eckermann, H.	1948	Alnö, Sweden		x	Carbonatitic liquid	Limited crystal differentiation and gravitational settling
Holmes, A.	1950	General		x	Carbonatitic fluid	
Strauss, C. A. and Truter, F. C.	1951	Magnet Heights, Africa		x	Peridotite	Differentiation
Davies, K. A.	1952	Elgon and Uganda, Africa		x	Pyroxenite	Late derivative of igneous activity
Russell, H. D. *et al.*	1954	Palabora, S. Africa		x	Carbonatite magma	
Bassett, H.	1956	Africa		x	Nepheline syenite	Separation of carbonatite magma by slow cooling
Pecora, W. T.	1956	General		x		Crystallization yields carbonatic solutions
Smith, W. L.	1956	Africa, general		x	Pyroxenite ?	Concentration of carbon dioxide or of carbonatitic fluid
Bouwer, R. F.	1957	Palabora, Africa		x	Alkaline magma	Differentiation
Saether, E.	1958	Fen, Norway	(x)	x	Alkalic peridotite	Crystallization differentiation
King, B. C. and Sutherland, D. S.	1960	Africa		x	Carbonated alkali peridotite	Fractional crystallization
Wyllie, P. J. and Tuttle, O. F.	1960	General		x		
von Eckermann, H.	1961	Alnö, Sweden		x	Kimberlite or melilitebasalt	Immiscible liquidation
Tomkeieff, S. I.	1961	USSR	x	x	Alkali peridotite	Magmatic carbonate by metasomatic process
Pecora, W. T.	1962	Bearpaw Mountains, U.S.A.		x	?	
Erikson, R. L. and Blade, L. V.	1963	Magnet Cove, USA		x	Olivine basalt	Fractional crystallization and differentiation
Dawson, J. B.	1964	General		x	Carbonatite	
Rimskaya-Korsakova, O. M.	1964	Kovdor, USSR	x			
Hanekom, H. J. *et al.*	1965	Palabora, S. Africa	x	x		
King, B. C.	1965	Uganda, Africa		x	Ijolitic nephelinite	Differentiation
Kukharenko, A. A. *et al.*	1965	Kola and North Karelia, USSR	x			
Temple, A. K. and	1965	Powderhorn,	x			

Grogan, R. M.		USA				
Bailey, D. K.	1966	Zambia, Africa		x	Upper mantle material	Volatile-rich fugitive fraction
Dawson, J. B.	1966	General		x	Basalt	Differentiation or preferential gas streaming
Garson, M. S.	1966	Malawi, Africa	(x)	x	Mica peridotite	Differentiation
Johnson, R. L.	1966	Shawa and Dorova, Rhodesia		x	Ijolite	Residual fluid derivative
King, B. C. and Sutherland, D. S.	1966	Uganda, Africa		x	?	Enrichment of lime in late crystallization
Wimmenauer, W.	1966	Kaiserstuhl, W. Germany		x	Olivine nephelinite	
Wyllie, P. J.	1966 b	General		x	Carbonated alkali peridotite, nephelinite or primary alkali carbonate magma	Immiscible fractionation
Verwoerd, W. J.	1967	South Africa, general		x	Basalt	Diffusion-differentiation
Borodin, L. S. and Kapustin, Yu. L.	1968	General, USSR	x	x	Alkali basalt	Differentiation and interaction with alkaline carbonate emanations
Koster van Groos, A. F. and Wyllie, P. J.	1968	General		x	Alkali carbonatite	
Ternovoy, V. J. *et al.*	1969	Kovdor, USSR		x		Hydrothermal cavity filling
Currie, K. L.	1970	Oka, Canada		x	Upper mantle material	Desilication by flux of an aqueous phase
Egorov, L. S.	1970	Maimecha-Kotui, USSR		x	Ultrabasic alkaline	Formation of immiscible carbonate melt
Epstein, E. M.	1970	USSR	x			
Watkinson, D. H.	1970	Oka, Canada		x	Carbonated nephelinite	Fractional crystallization
Nash, W. P.	1972	Iron Hill, USA		x	Carbonated mafic nephelinite	Separation of carbonate fluid
Pozaritskaya, L. K. and Samoilova, V. S.	1972	Eastern Siberia, USSR	x			
Romanchev, B. P.	1972	East Africa		x	Alkali silicate	
Borodin, L. S. *et al.*	1973	USSR	x	x		
Rankin, A. H.	1975	Wasaki, East Africa		x	Ijolite, hyperalkaline silicate	Immiscibility differentiation
Cooper, A. F. *et al.*	1975	Oldoinyo Lengai, Africa, general		x	Nephelinite	Immiscible separation of alkaline carbonatite magma
Ernst, T.	1975	General		x	Peridotite	Immiscible carbonatite melt by differentiation
Fesq, H. W. *et al.*	1975	Premier mine, South Africa		x	»Kimberlite»	Fractionation
Frolov, A. A.	1975	General	x			
Gittins, J. *et al.*	1975	Arvida, Quebec, Canada		x	Kimberlite	Prolonged differentiation
Janse, A. J. A.	1975	Nama plateau, South West Africa	x	x	Alkaline ultrabasic	Differentiation, stoping, assimilation and metasomatism
Koster van Groos, A. F.	1975	General		x	Carbonatite	Concentration of carbonate droplets in mantle

Wyllie, P. J. and Huang, W. L.	1975	General		x	Mantle peridotite containing CO_2		Fractional crystallization
Kapustin, J. L.	1976 a	General	x	x	Alkali ultrabasic		Differentiation and introduction of CO_2
Lapin, A. V.	1976	General		x			Liquation and filter pressing
Rass, I. T. and Boronikhin, V. A.	1976	Kovdor, Guli, USSR	x	x			
Alkhazov, V. Yu, *et al.*	1977	Khanneshin, Afganistan		x			
Dontsova, Ye. I. *et al.*	1977	General		x	?		Differentiation
Orlova, G. P. and Rjabtšikov, J. D.	1977	General		x			Immiscibility of silicate and carbonate melts
Le Bas, M. J.	1977	East Africa		x	Volatile-rich alkaline ultramafic magma		Liquid immiscibility
Borodin, L. S. and Pjatenko, I. K.	1978	Kola, USSR		x	Mantle derived mela-nefelinite		
Lapin, A. V.	1978	USSR		x			Differentiation and liquation
Nielsen, T. F. D.	1980	Gardiner complex, East Greenland		x	Mela-nephelinite		Fractional crystallization
Secher, K.	1980	Safartôg, West Greenland		x			
Gittins, J. and McKie, D.	1980	Oldoinyo Lengai, Tanzania		x	Carbonatite		Differentiation and CO_2 concentration

The metasomatists maintain that the precursory rocks (usually ultramafites) were metasomatically converted into carbonatites. It is generally accepted that the metasomatizing material has its origin at great depth. Pozaritskaya and Samoilova (1972) are of the opinion that metasomatism produces, in sequential stages, fairly regular carbonatitic zones around the blocks of precursory rocks. Frolov (1975) emphasizes vertical regularity and lateral complexity in the development of metasomatic carbonatites. Western metasomatists consider that the formation of carbonatites is an irregular replacement process in precursory rocks.

One of the principal problems facing the magmatists is that of the parental magma from which the carbonatite magma, fluid or melt derives; even a primary carbonatite magma has been suggested. The answers to the parental magma question are summarized from Table 30 as follows:

Parent magma	Number of proposals
1. Upper mantle material	2
2. Peridotite, mica peridotite	5
3. Alkalic and/or carbonated peridotite	4
4. Alkaline ultrabasic magma	4
5. Basalt, olivine basalt, melilite basalt	4
6. Kimberlite	3
7. Pyroxenite, alkali pyroxenite	2
8. Nefeline syenite	1
9. Ijolite, nefelinite, melanefelinite, olivine nefelinite	12
10. Primary carbonatite magma (liquid, fluid, melt)	8

The processes by which carbonatite magmas are supposed to develop from the various parent magmas can be subdivided into the following ten groups:

1. Crystallization differentiation, fractional crystallization
2. Gravitational settling
3. Diffusion differentiation, preferential gas streaming
4. Desilication by flux of an aqueous phase
5. Immiscibility differentiation, immiscible liquidation
6. Liquidation and filterpressing
7. Differentiation and introduction of CO_2
8. Concentration of carbon dioxide or carbonatitic fluid
9. Concentration of lime in late crystallization
10. Residual fluid derivation

The number of hypotheses for the origin of carbonatites and the many proposals for the development processes of carbonatites from parent magmas suggest that there are several universally acceptable theories that elucidate the carbonatite problem. The location of the Sokli complex has been ascribed to deep tensional faulting in the foreland caused by down-buckling of crystal plates during the Caledonian orogeny (Vartiainen and Woolley, 1974). The zone in which Sokli occurs is called the Kandalaksha deep fracture (Paarma and Talvitie, 1976). Initially all the Sokli carbonatites were considered to be magmatic (Paarma, 1970; Vartiainen and Woolley, 1974); only later was the presence of metasomatic carbonatites demonstrated (Mäkelä and Vartiainen, 1978; Vartiainen and Paarma, 1979). The magmatic character of carbonatites is evidenced not only by petrological features but also by the isotopic composition of oxygen ($\delta^{18}0$ about + 7 ‰, Dontsova *et al.*, 1977), by the sulphur isotopes ($\delta^{34}S$ -0.6—5.6 ‰, Mäkelä and Vartiainen 1977) and by the fluid inclusion study in apatite (Haapala, 1978). Before the parent magma of the Sokli magmatic carbonatites can be established a simultaneous and critical examination of all the complexes in the Kola alkaline rock province must be carried out. This is, however, beyond the scope of this study, which is restricted to a reconstruction of the Sokli complex. A summarized reconstruction is given in Fig. 106.

Intrusion of ultramafites: Proterozoic and Paleozoic ultramafites occur in the region of the alkaline rock province of Kola (Kukharenko *et al.*, 1965). In the Sokli area ultramafites occur both within the carbonatite massif and beyond of it as the Tulppio olivinite massif (Fig. 1). The ultramafites are not dated, but the following arguments suggest that they are not comagmatic:

Tulppio olivinite	*Ultramafites in the carbonatite massif*
Olivinite is medium grained	Magnetite olivinite is from coarse-grained to pegmatoidal
Olivine is enriched in Ni (0.3 %) and depleted in MnO (0.11 %)	Olivine is depleted in Ni (< 0.05 %) and enriched in MnO (> 0.7 %)
Pyroxene is enstatite	Pyroxene is diopside
Magnetite content is generally 1—2 vol-%	Magnetite content is generally 10—30 vol-%
Baddeleyite is lacking	Baddeleyite is an accessory mineral

Differences in the average composition of magnetite (Heinänen and Vartiainen, 1980)

TiO_2	0.08 %	2.78 %
MnO	0.02 %	0.58 %
V_2O_5	0.04 %	0.21 %
Al_2O_3	0.08 %	0.32 %
Cr_2O_3	0.04 %	0.01 %

The mode of emplacement of the ultramafites in the Sokli massif is unknown because the structure of the original formation was disturbed by later alteration processes, carbonatite intrusions and tectonics. The ultramafites were presumably emplaced as composite arc-like bodies that were later broken into small blocks and pieces (Fig. 3).

The origin and mutual relations of the olivinites and pyroxenites in alkali rock complexes are disputable. Kukharenko *et al.*, (1965, 1971) regard olivinites and pyroxenites

RELATIVE TIME →

			STAGE OF ALKALI METASOMATISM			
	INTRUSION OF ULTRAMAFITES	METAMORPHISM OF ULTRAMAFITES	FENITIZATION	ALTERATION OF ULTRAMAFITES AND FENITES	CARBONATIZATION	INTRUSION OF MAGMATIC CARBONATITES
EVENTS	Crystallization of ultrabasic magma. Intense fracturing of granite gneiss, moderate fracturing of amphibolites and hornblende schists	Autometasomatism, slight addition of Na	Addition of Na, K, OH, Fe, Ti, Mn Removal of Si, Ca, Al Explosive brecciation	Addition of Ca, CO_2, P, K, Na Removal of Si, Mg, Fe, Ti, Mn Tectonization	Addition of Ca, CO_2, (Na?) Removal of Si, Fe, Mg, Ti, Al, K, P Mobilization	Stopping, brecciation and assimilation of earlier rocks. Crystallization of carbonatite magma in two phases. Pneumatolytic-hydrothermal alteration. Veining.
ROCKS	Magnetite olivinite Pyroxenite	Serpentinized magnetite olivinite Calcic amphibole rocks	Fenites	Metaphoscorites Mica-alkali amphibole rocks, etc.	Metasilico-sövites	Phoscorites Silicosövites Sövites Beforsites Late veins

Fig. 106. Correlation of events and resultant rocks in the evolution of the Sokli complex.

as separate intrusions in the complexes of Kola. Borodin and Kapustin (1968) distinguish primary olivinites and pyroxenites from which a new generation of olivinites and pyroxenites developed by metasomatic transformation within the same complexes in Kola, Maimech-Kotui and Aldan provinces. The olivinite—biotite pyroxenite series of Palabora are suggested by Russel *et al.* (1954) to be reactionary rocks between magmatic carbonatites and granites. According to Hanekom *et al.* (1965), the pyroxenite of Palabora is magmatic but the plug-like bodies of dunite are pneumatolytic—metasomatic alteration products of pyroxenite. Bouwer (1957) has described both of them as intrusive rocks, as has the present geological staff of Palabora (Palabora Mining etc. 1976). Johnson (1966) proposes a magmatic parentage for the Shawa dunite, and the pyroxenite of Powderhorn is definitely an intrusive rock (Temple and Grogan, 1965). Boettcher (1967) distinguishes two different pyroxenite intrusions derived from a common parent magma in the Rainy Creek complex. In the Sokli massif the sharp contacts between the magnetite olivinite and the pyroxenite suggest separate intrusion stages for these rocks. The magmatic origin for these rocks is further supported by the fact that olivine is not replaced by pyroxene, or vice versa, and by the lack of possible precursory rocks from which the magnetite olivinite and the pyroxenite could have been metasomatically transformed. Thus there are two different ultramafic groups in the Sokli area: the Tulppio olivinite massif which if not proterozoic, is a primary olivinite in the sense of Borodin and Kapustin (1968), and the ultramafites in the carbonatite massif.

Metamorphism of ultramafites: The emplacement of the ultramafites was obviously succeeded by a tranquil period in the evolution of the complex before the fenitization processes went into action. During that time the ultramafites underwent slight autometamorphic and Na-metasomatic changes. In the magnetite olivinite, olivine changed into serpentine; in pyroxenite, diopside altered into calcic amphibole (sodian edenite) accompanied by a slight increase in Na. As a result of amphibolization, amphibole rock with sodian edenite was formed (Fig. 106). Similar hornblende calcite rocks have been described from the Afrikanda massif (Borodin and Kapustin, 1968), where their formation was associated with general metasomatism.

Stage of alkali metasomatism: Multi-stage and basically alkaline metasomatism with far-reaching effects is an essential part of the evolution of the Sokli complex. Areally it can be subdivided into metasomatism in the fenite aureole and in the massif. It is generally accepted that fenitization precedes the emplacement of alkali rocks and carbonatites (Heinrich, 1966, McKie, 1966; Borodin and Kapustin, 1968; Le Bas, 1977). Chronologically fenitization at Sokli took place between the emplacement of the ultramafite and the carbonatite. The fenite aureole, which included fenitized granite gneisses, amphibolites and hornblende schists, and the fenitization process have been described previously in detail (Vartiainen and Woolley, 1976). The relationship of the metasomatic alteration processes in the ultramafites to the fenitization of granite gneisses, amphibolites and hornblende schists in terms of time and material is an interesting problem. All these rocks existed in the Sokli complex at the onset of the fenitization process. At Kovdor, which is the alkali rock complex nearest to Sokli (60 km SE of Sokli), persistent and intricate alteration processes acted upon the ultramafites of the complex. According to Kukharenko et al. (1965), they were active after alkali magmatism. In contrast, Borodin and Pavlenko (1974) maintain that these processes preceded the emplace-

ment of ijolite and other rocks. Borodin and Pjatenko (1978) later came to the conclusion that the alkaline and alkaline-carbonatic »through-magmatic» emanations from these magmas subjected the local rocks to intense metasomatic re-working. The metasomatism of the Palabora pyroxenites is considered to have taken place before the formation of the carbonatites (Hanekom *et al.*, 1965), whereas the Archean gneisses are presumed to have undergone fenitization at the same time as pyroxenite metasomatism (Palabora Mining etc., 1976). Hence the metasomatic alteration processes in the ultramafites are not generally considered to be associated with fenitization. The only reported example of fenitization of an ultramafite seems to be that from Rangwa, where autometasomatic fenitization has transformed peridotite into uncompahgrite (Le Bas, 1977, p. 273).

The intense gas and fluid emanations that produced fenitization probably also caused explosive brecciation in the fenite area and particularly in the adjacent ultramafites, just as when the explosive breccias developed in the Kovdor massif (Landa, 1971). Thus originally massive ultramafites broke up and channels were opened in them along which the metasomatizing gases and solutions circulated. Consequently, there is every reason to assume that the metasomatic alteration of ultramafites started at the latest during the closing stages of fenitization, and that the alteration processes in ultramafites may be compared to fenitization and that they are not separate events.

The fact that fenitization and metasomatic alteration of the ultramafites took place contemporaneously and in association with extensive alkali metasomatism is reflected in their geochemical character. The qualitative changes in the compositions were (Table 28):

	Gaines	Losses
Fenite area	Na, K, CO_2, Fe, Ti, Mn	Si, Ca, Al
Alteration of ultramafites	Na, K, CO_2, Ca, P	Si, Mg, Fe, Ti, Mn

The main features of both processes are the increase in alkalies and CO_2 and the depletion in Si. Both processes result partly in the formation of the same minerals: alkali amphiboles, aegirine and phlogopite. Alkali metasomatism as a change in the composition of the amphibole in the fenite area has been described by Vartiainen and Woolley (1976, p. 74—75); for the massif it is shown in Fig. 91. Na metasomatism in the alterations of olivine and pyroxene can be given as follows:

			Na_2O (%)		
Olivine	⟶	Richterite	0.4*	⟶	6—7
Diopside	⟶	Aegirine	0.2—0.4	⟶	13.5
Diopside	⟶	Alkali amphibole	0.2—0.4	⟶	9—11

* estimated on the basis of olivine from Alnö (von Eckermann, 1974) and Kovdor (Kukharenko *et al.*, 1965).

During the fenitization and metasomatic alteration of the ultramafites some elements were expelled, mainly because, in the fenite area, plagioclase altered into albite, and hornblende into alkali amphiboles. Thus Ca and Al were liberated. In the ultramafites the carbonatization and silicatization of magnetite liberated Fe, Ti and Mn, and the alteration of olivine produced Mg for expulsion. If the transfer of elements between the fenite area and the ultramafites had been possible, the Ti and Mn liberated from the ultramafites would have largely, and Fe to some extent, increased the abundances of these elements in the fenite area; correspondingly, the Ca liberated in the fenite area would have been consumed in the carbonatization of ultramafites. Consequently, during the alkali metasomatism at Sokli Na, K, CO_2, P and (OH) must have been introduced into the complex and Si, Mg, Fe and Al expelled from it.

It is not easy to imagine that the elements that entered the complex (Na, K, CO_2, P, OH) derived from anywhere else other than the same source as the carbonatite magma or the carbonatite magma itself. How and where the elements liberated during the alteration process (Si, Mg, Fe, Al) were transferred is the concern of experimental rather than descriptive petrology.

Carbonatization: The alkali metasomatic stage was presumably followed by intense CO_2 metasomatism, i.e. by carbonatization before and possibly partly during the emplacement of carbonatite. The carbonatization gave rise to the metasilicosövites (Fig. 11). It used to be assumed (Vartiainen and Woolley, 1976, p. 83) that the partial pressure of CO_2 dropped during fenitization, and that other gases became predominant (H_2O, F, S, SO_2) towards the end of carbonatization.

The fenites at Sokli are exceptionally rich in carbonate (op. cit. p. 53), and the fenite area is characterized by a network of carbonate veins accompanied by phlogopitization of fenites (op. cit. p. 35). The latter features in particular suggest that during or after the final fenitization stage the fenite area may have been affected by the CO_2 metasomatism that gave rise to the extensive formation of metasilicosövites in the massif. The calcite rocks that developed in association with fenites at Kaiserstuhl (Wimmenauer, 1966) suggest carbonatization after fenitization. Garson (1966) has described metasomatic carbonate-silicate rocks from the Tundulu magmatic carbonatite complex. Armbrustmacher (1979) has reported magmatic and metasomatic carbonatites from the Wet Mountain area in Colorado. Marked hydrothermal—metasomatic mass transfer at Fen has led to the formation of calcitic rocks from fenites and other rocks (Barth and Ramberg, 1966). According to Kapustin (1976 a), hydrothermal—metasomatic carbonatites develop in carbonatite complexes after the emplacement of magmatic carbonatites. Contact relations at Sokli demonstrate that the metasilicosövites acted like intrusive rocks, brecciating the older rocks in the same way as the metasomatic carbonatites at Powderhorn (Temple and Grogan, 1965). The banding and oriented structures so typical of the Sokli metasilicosövites show that these rocks underwent marked remobilization. The magmatic carbonatites intersect the metasilicosövites, although ill-defined contact relations between them also occur.

The carbonatization process that acted upon the carbonatite massif might have been almost entirely CO_2 metasomatism, provided that the large amounts of Ca that were liberated from the fenite area (Vartiainen and Woolley, 1976, p. 74) were available to form carbonates. Carbonatization acted mainly upon the rock variants that developed from ultramafites and fenite fragments through alkali metasomatism (Fig. 11). Hence, these

rocks became depleted in the following elements (Table 29):

Si, Ti, Al, Fe, Mg and K.

Intrusion of magmatic carbonatites: Contact relations indicate that the development of the Sokli complex came to an end with the formation of magmatic carbonatites. They crystallized in two main phases separated by a pneumatolytic-hydrothermal episode. The late carbonate veins crystallized at the very end. Alkaline lamprophyre dykes obviously formed throughout the development of the magmatic carbonatites. The petrochemical crystallization curve (Fig. 94) illustrates the succession of the rock-type formation as suggested by the contact relations.

The emplacement and crystallization of the first or early carbonate magma represent the plutonic intrusion model. The emplacement was intense (brecciation), but as demonstrated by the segregation of heavy minerals (magnetite, olivine, apatite) into phoscorites (Stage I) and by the massive and tabular structures in silicosövites and sövites (Stage II) crystallized from calcitic magma, the crystallization was tranquil. The magmatectonic brecciation of phoscorites by early sövites reveals that the calcitic magma had not completely crystallized after the segregation of phoscorites. The magnetite-banded structures indicate a tendency towards gravitative differentiation. The sharp contacts and the assimilation relations between the early sövitic rocks demonstrate that the magma crystallized irregularly. Presumably the very first magmatic intrusive was pipe-like in shape and thus largely contributed to the shape of the magmatic core exposed at the present erosion niveau (Fig. 3).

The other carbonatite complexes cut by a deep niveau also exhibit rock associations similar to the phoscorites and early sövites at Sokli. At Palabora carbonatite (sövite) intersects and brecciates phoscorite (Russel *et al.*, 1954). Phoscorite also grades in places into older banded carbonatite, suggesting that the latter may have formed from phoscorite through replacement (Lombaard *et al.*, 1964). According to Hanekom *et al.* (1965), the Palabora phoscorite and the older banded carbonatite are metasomatic alteration products of dunite. Current opinion (Palabora Mining etc., 1976) has it that rocks are intrusive and show the emplacement succession: phoscorite → banded carbonatite. According to Verwoerd (1967, p. 24), »the rapid alteration between phoscorite and carbonatite would be due to the simultaneous emplacement and upward movement (with local erasure of contacts through metasomatism) of two immiscible liquids.» Borodin *et al.* (1973) hold that camaforites (phoscorites) are partly magmatic, partly metasomatic rocks (probably corresponding to the metaphoscorites at Sokli) that have an accurately defined position in the evolution history of the alkali rock complexes before the appearance of carbonatites. According to Lapin (1978), the camaforites were formed through crystallization differentiation and liquation during the processes that gave rise to the carbonatites.

The second intrusive magmatic carbonatite phase was preceded by a period of intense pneumatolytic—hydrothermal activity (Stage III). The gases and solutions associated with it were under considerable pressure and gave rise to explosive brecciation (as had fenitization earlier). This produced cracking, jointing and above all a deep-seated fracture stockwork in the centre of the magmatic core (Fig. 3), where the hydrothermal activity was most intense. The position of the pneumatolytic—hydrothermal stage has been deduced from the contact relations between the rocks and mineral alterations. The apatite—ferriphlogopite rocks that deposited hydrothermally in the fractures and joints intersect the Stage I and II carbonatites, metasilicosövites and metaphoscorites but not the Stage IV and V carbonatites. The rocks of

the Stage I and II show more of the mineral alteration such as ferriphlogopitization, sulphidization of magnetite and zirkelitization of pyrochlore than the rocks of the Stage IV. Apatite inclusion studies (Haapala, 1978) demonstrate that pneumatolytic–hydrothermal activity has left its mark on a large area around the central fracture stockwork.

The first copper mineralization at Palabora developed in the fracture stockwork in the early carbonatites as a result of pneumatolytic–hydrothermal activity corresponding to that at Sokli before the emplacement of transgressive carbonatites (Lombaard *et al.*, 1964; Hanekom *et al.*, 1965). At Jacupiranga, apatite, magnetite and sulphide veinlets that cut the older carbonatites and were formed in a period between two carbonatite emplacements (Melcher, 1966) seem to represent the hydrothermal stage rather than the fractionation of the magma. At Oka, the hydrothermal activity that produced biotitization and introduced thorium pyrochlore took place after two carbonatite emplacements but before the formation of the late carbonate veins (Gold *et al.*, 1967).

The pneumatolytic–hydrothermal stage at Sokli was succeeded by the second intrusive magmatic carbonatite phase (Stage IV). It differs from the previous phase in being calcitic–dolomitic and having more fluidized magma, and also in that no phoscorites were developed. The fluidal feature is demonstrated by the flow structures and vertical banding in dolomite-bearing silicosövites and sövites. These structures also suggest that the rocks, which were previously consolidated in the conduit of the magmatic core plug, were not only brecciated and assimilated but also moved upwards at least in relation to the metacarbonatites and metasomatites. The cone dykes that intruded the metasomatic areas produced wedge-shaped blocks (Vartiainen and Paarma 1979, p. 1298) that possibly slid downwards along the surfaces of the cone dykes. The vein-like beforsites represent the last crystallization products of this stage.

The movement of carbonatites in their conduit is a typical mode of emplacement in the second magmatic phase at Sokli. It is best shown in volcanic and subvolcanic intrusives, such as those in Rufunsa province, where volcanic carbonatites have transferred intrusive carbonatites upwards. For more deep-seated complexes this mechanism has been described from Iron Hill (Temple and Grogan, 1965), where carbonatites have moved upwards, and from Oka, where »a late ijolite intrusive phase followed by movement in a somewhat mobile carbonatite. . .» (Gold *et al.*, 1967, p. 1134).

Almost any carbonatite complex that has been sufficiently well studied reveals that crystallization of the veins containing baryte, fluorite and rare earths (Stage V) is the final event in the formation of magmatic carbonatites. The same is true at Sokli. The late veins are concentrated within the central fracture system.

The predominant factor in the classification of carbonatites is often the depth facies. As already pointed out, the Sokli complex is plutonic and developed at temperatures ranging from 700° to 300°C (Vartiainen and Woolley, 1976; Mäkelä and Vartiainen, 1978). Sokli can be classified in the following groups (some characteristic features of groups mentioned):

The position of Sokli according to some classifications

Deep-seated plutonic stem. Garson, 1966
Carbonatites associated with
pyroxenite and olivine
vermiculite pegmatoid

Plutonic mesozone. Heinrich, 1966
Ring structure well defined,
typical fenitization

High-medium temperature stage 700°—300°C. Intrusive bodies, injection metasomatic zones, vein fillings	Borodin and Kapustin, 1968
Medium deep, formed at depth of 5 to 6 km. Intrusives with cores, circular horizontal section	Frolov, 1975

The carbonatite complex that most resembles Sokli in structure and lithological associations is Glenover in South Africa, which has a plug-like carbonatite core and forking cone dykes that extend from the core to pyroxenite (Verwoerd, 1967). Palabora is rather like Sokli in evolution history, formation depth and lithological association (syenite excluded). In the Kola alkali rock province the complex that most resembles Sokli is Vuorijärvi (Kukharenko *et al.*, 1965), which contains in addition to carbonatites and pyroxenites small amounts of ijolite. Carbonatite complexes exhibiting, like Sokli, the association carbonatite–ultramafites (and/or their alteration products)—fenite are rare. Worth mentioning are Firesand (Gittins, 1966) and Cargill in Canada (Sandvik and Erdosh, 1977), in which, however, the presence of fenite is not well-established, and Arbarastah in the USSR (Borodin, 1974), which contains minor intraformational syenite portions (that might be interpreted as fenite fragments).

ACKNOWLEDGEMENTS

I am indebted to the management of Rautaruukki Oy for giving me permission to use the geological material on Sokli and for putting the facilities of the company's Exploration Department at my disposal. The rock analyses were performed in the laboratory of Rautaruukki Oy, and I thank the staff for their cooperation. Dr. Seppo Sivonen and Mr. Tuomo Alapieti of the University of Oulu undertook the electron microprobe analyses of olivine, pyroxene and amphibole. Mr. Kyösti Heinänen carried out the x-ray determinations in the laboratory of Rautaruukki Oy. Miss Meeri Lantto drew the maps and diagrams and Miss Eeva Rinne-Kanto typed the manuscript. Prof. Kauko Laajoki, Prof. Atso Vorma, Dr. Juhani Nuutilainen and Dr. Thomas Deans (chapter on mineralogy) read the manuscript critically. Mrs. Gillian Häkli corrected the language of my English manuscript and translated some of the Finnish text. Prof. Herman Stigzelius, Director of the Geological Survey of Finland, arranged publication in the Survey's Bulletin series. To these persons and all the others who have cooperated with me at Sokli I express my sincere thanks.

Accepted for publication 8th May, 1980

REFERENCES

Alkhazov, V. Uu., Atakishiyev, Z. M. & Azimi, N. A., 1977. Geology and mineral resources of the early Quaternary Khanneshin carbonatite volcano (southern Afganistan). Int. Geol. Rev. 20, 281—285.

Armbrustmacher, T. J., 1979. Replacement and primary magmatic carbonatites from the Wet Mountains area, Fremont and Custer Counties, Colorado. Econ. Geol. 74, 888—901.

Bagdasarov, Yu. A., 1979. Variability of compositions of some rocks of ultrabasic alkalic carbonatite formations as criterion of their genesis. Dokl. Akad. Nauk. SSSR. 244, 1451—1455. (In Russian).

Bailey, D. K., 1966. Carbonatite volcanoes and shallow intrusions in Zambia. *In:* Carbonatites, 127—154. Eds. O.F. Tuttle and J. Gittins. John Wiley & Sons, New York. 591 p.

Barth, T. F. W., 1962. Theoretical petrology. John Wiley & Sons. New York. 416 p.

Barth, T. F. W. & Ramberg, J., 1966. The Fen circular complex. *In:* Carbonatites, 225—257. Eds. O. F. Tuttle and J. Gittins. John Wiley & Sons, New York. 591 p.

Basset, H., 1956. The carbonatite problem. Tang. Geol. Surv., Rec. 4, 81—92.

Boettcher, A. I., 1967. The Rainy Creek alkaline-ultramafic igneous complex near Libby, Montana I: Ultramafic rocks and fenite. J. Geol. 75, 530—553.

Borodin, L. S., 1974. The main provinces and formations of alkaline rocks. Nauka, Moscow. 376 p. (In Russian).

Borodin, L. S. & Kapustin, Yu. L., 1968. Carbonatite rare-element deposits. *In:* Geochemistry and mineralogy of rare elements and genetic types of their deposits, vol. 3, 197—246. Ed. K. A. Vlasov. Israel Prog. Sci. Trans., Jerusalem. 916 p.

Borodin, L. S., Lapin A. V. & Hartšenkov, A. G., 1973. Rare metals camaforites. Nauka, Moscow. 176 p. (In Russian).

Borodin, L. S. & Pavlenko, A. S., 1974. The role of metasomatic processes in the formation of alkaline rocks. *In:* The alkaline rocks, 515—534. Ed. H. Sørensen. John Wiley & Sons, London. 622 p.

Borodin, L. S. & Pjatenko, J. K., 1978. Rare-earth elements in dykes of alkali–ultramafic lamprophyres and general petrologic aspects of paleozoic alkaline magmatism, Kola Peninsula. Geohimija 1978, no. 6, 854—867. (In Russian).

Bouwer, R. F., 1957. The carbonate member of the Palabora igneous complex. Unpublished Ph. D. thesis, Univ. Cape Town. 152 p.

Bowen, N. L., 1924. The Fen area in Telemark, Norway. Am. J. Sci. 8, 1—11.

Brögger, V. C., 1921. Die Eruptivgesteine des Kristianiagebietes, IV, Das Fengebiet in Telemark. Kong. Norske Vid. Selsk. Skr. I, Mat. Nat. kl. no. 9, 1—408.

Bulakh, A. G., Yevdokimova, M. D. & Rudashevskiy, N. S., 1975. On the distribution of Ni and Co in the ultramafic alkalic rocks and carbonatites of the Turyi Peninsula (Murmansk region). Geochem. Int. 12, 77—83.

Cooper, A. F., Gittins, J. & Tuttle, O. F., 1975. The system Na_2CO_3–K_2CO_3–$CaCO_3$ at 1 kilobar and its significance in carbonatite petrogenesis. Am. J. Sci. 275, 534—560.

Currie, K. L., 1970. An hypothesis on the origin of alkaline rocks suggested by the tectonic setting of the Monteregian Hills. Can. Mineral. 10, 411—420.

Davies, K. A., 1952. The building of Mount Elgon (East Africa). Geol. Surv. Uganda, Mem. 7. 62 p.

Dawson, J. B., 1964. Reactivity of the cations in carbonate magma. Geol. Assoc. Canada Proc. 15, 103—113.

— » —, **1966.** Oldoinyo Lengai — an active Volcano with sodium carbonatite lava flows. *In:* Carbonatites, 155—168. Eds. O. F. Tuttle and J. Gittins. John Wiley & Sons, New York. 591 p.

Dontsova, Ye. J., Kononova, V. A. & Kuznetsova, L. D., 1977. The oxygen-isotope composition of carbonatites and similar rocks in relation to their sources and mineralization. Geochem. Int. 14, 1—11.

Eckermann von, H., 1948. The alkaline district of Alnö Island. Sveriges Geol. Unders., Ser. Ca. no. 36. 176 p.

— » —, **1961.** The petrogenesis of the Alnö alkaline rocks. Bull. Geol. Inst. Univ. Uppsala 40, 25—36.

— » —, **1974.** The chemistry and optical properties of some minerals of the Alnö alkaline rocks. Ark. Mineral. Geol. 5, 93—210.

Egorov L. S., 1970. Carbonatites and ultrabasic alkaline rocks of the Maimecha–Kotui region, N. Siberia. Lithos 3, 341—359.

— » —, **1975.** Camaforites or phoscorites and nelsonites? Geol. rudn. mestor. 17, 117—121. (In Russian).

Epstein, E. M. 1970. Genesis of apatite–magnetite ore of Kovdor. Short. comm. Works of All-Union Inst. Miner. Resour. (Vims), no. 1. (In Russian).

Epstein, E. M., Pančin, I. I., Moralev, V. M. & Volkodav, J. G., 1972. Vertical zonality of alkaline ultrabasic and carbonatitic massifs. Geol. mestor. redk. elem. 35, 49—68. (In Russian).

Erikson, R. L. & Blade, L. V., 1963. Geochemistry and petrology of the alkalic igneous complex at Magnet Cove, Arkansas. U. S. Geol. Surv., Prof. Pap. 425. 94 p.

Ernst, T., 1975. Erdmantelprobleme - Bericht und Theorie. Fortschr. Mineral. 52, 106—140.

Ferguson, A. K., 1978. Ca-enrichment in olivines from volcanic rocks. Lithos 11, 189—194.

Fesq, H. W., Kable, E. J. D. & Gurney, J. J., 1975. Aspects of the geochemistry of kimberlites from the Premier mine, and other selected South African occurences with particular reference to the rare earth elements. *In:* Physics and chemistry of the earth 9, 687—707. Eds. L. H. Ahrens, J. B. Dawson, A. R. Duncan & A. J. Erlank. Pergamon Press, New York. 940 p.

Fleet, M. E., MacRae, N. D. & Herzberg, C. T., 1977. Partition of nickel between olivine and sulfide: A test for immiscible sulfide liquids. Contrib. Mineral. Petrol. 65, 191—197.

Frolov, A. A., 1975. Structure and ore formation of carbonatite massifs. Nedra, Moscow. 159 p. (In Russian).

Carson, M. S., 1955. Flow phenomena in carbonatites in southern Nyasaland. Colonial Geol. Min. Res. 5, 311—318.

— » —, **1962.** The Tundulu carbonatite ring complex in southern Nyasaland. Nyasaland Geol. Surv., Mem. 2. 248 p.

— » —, **1966.** Carbonatites in Malawi. *In:* Carbonatites, 33—71. Eds. O. F. Tuttle and J. Gittings. John Wiley & Sons, New York. 591 p.

Gittins, J., 1966. Summaries and bibliographies of carbonatite complexes. *In:* Carbonatites 417—541. Eds. O. F. Tuttle and J. Gittins. John Wiley & Sons, New York. 591 p.

Gittins, J., Hewins, R. H. & Laurin, A. F., 1975. Kimberlitic-carbonatitic dikes of the Saguenay river valley, Quebec, Canada, *In:* Physics and chemistry of the earth, vol. 9, 137—148. Eds. L. H. Ahrens, J. B. Dawson, A. R. Duncan & A. J. Erlank. Pergamon Press, New York. 940 p.

Gittins, J. & McKie, D., 1980. Alkalic carbonatite magmas: Oldoinyo Lengai and its wider applicability. Lithos 13, 213—215.

Gold, D. P., 1966a. The minerals of the Oka carbonatite and alkaline complex, Oka, Quebec. Mineral. Soc. India, IMA Volume, 115—125.

— » —, **1966 b.** The average and typical chemical composition of carbonatites. Mineral. Soc. India, IMA Volume, 83—89.

Gold, D. P., Valleé, M. & Charette, J.-P., 1967. Economic geology and geophysics of the Oka alkaline complex, Quebec. Can. Min. Met. Bull. 60, 1131—1144.

Haapala, I., 1978. Fluid inclusion studies in apatite from the Sokli carbonatite, Northeastern Finland. IAGOD, Fifth Symp., Utah, Programs and Abstr., 94.

— » — , **1980.** Fluid inclusion in the apatite of the Sokli carbonatite, Finland — A preliminary report. Geologi 32, 83—87.

Hanekom, H. J., van Staden, C. M., Smit, P. J. & Pike, D. R., 1965. The geology of the Palabora igneous complex. S. Africa, Geol. Surv. Mem. 54. 179 p.

Hart, S. R. & Davis, K. E., 1977. Nickel partitioning between olivine and silicate melt. Earth Planet. Sci. Lett. 40, 203—219.

Heinänen, K. & Vartiainen, H., 1980. Magnetite of the Tulppio olivinite and the Sokli carbonatite massif. (In prep).

Heinrich, E. Wm., 1966. The geology of carbonatites. Rand McNally & Company, Chicago. 555 p.

Heinrich, E. Wm. & Anderson, R. J., 1965. Carbonatites and alkalic rocks of the Arkansas river area, Fremont County, Colorado 2. Fetid gas from carbonatite and related rocks. Am. Mineral. 50, 1914—1920.

Holmes, A., 1950. Petrogenesis of Katungite and its associates, Am. Mineral. 35, 772—792.

Hyndman, D. W., 1972. Petrology of igneous and metamorphic rocks. McGraw-Hill, New York. 533 p.

Janse, A. J. A., 1975. Kimberlite and related rocks from the Nama Plateau of South-West Africa. *In:* Physics and chemistry of the earth, vol. 9, 81—94. Eds. L. H. Ahrens, J. B. Dawson, A. R. Duncan & A. J. Erlank. Pergamon Press, New York. 940 p.

Johnson, R. L., 1966. The Shawa and Dorowa carbonatite complexes, Rhodesia. *In:* Carbonatites, 205—224. Eds. O. F. Tuttle and J. Gittins. John Wiley & Sons, New York. 591 p.

Kapustin, Yu. L., 1976 a. On the origin of carbonatites. Int. Geol. Rev. 19, 997—1009.

— » —, **1976 b.** Structure of the Vuoriyarvi carbonatite complex. Int. Geol. Rev. 19, 1296—1304.

King, B. C., 1965. Petrogenesis of alkaline igneous rock suites of the volcanic and intrusive centre of eastern Uganda. J. Petrol. 6, 67—100.

King, B. C. & Sutherland, D. S., 1960. Alkaline rocks of eastern and southern Africa, Part III, Petrogenesis. Sci. Prog. 48, 709—720.

King, B. C. & Sutherland, D. S., 1966. The carbonatite complexes of eastern Uganda. *In:* Carbonatites, 73—126. Eds. O. F. Tuttle and J. Gittins. John Wiley & Sons, New York. 591 p.

Kononova, V. A., Shanin, L. L. & Arakelyants, M. M., 1973. Times of formation of alkaline massifs and carbonatites. Int. Geol. Rev. 16, 1119—1130.

Koster van Groos, A. F., 1975. The effect of high CO_2 pressures on alkalic rocks and its bearing on the formation of alkalic ultrabasic rocks and the associated carbonatites. Am. J. Sci. 275, 163—185.

Koster van Groos, A. F. & Wyllie, P. J., 1968. Liquid immiscibility in the join $NaAlSi_3O_8$–Na_2CO_3–H_2O and its bearing on the genesis of carbonatites. Am. J. Sci. 266, 932—967.

Kresten, P., 1980. The Alnö complex. Lithos 13, 153—158.

Krishnamurthy, P., 1977. On some geochemical aspects of the Savattur carbonatite complex, North Arcot district, Tamil Nadu. J. Geol. Soc. India 18, 265—274.

Kukharenko, A. A., Bulakh, A. G., Ilinskii, G. A., Shinkarev, N. F. & Orlova M. P., 1971. Metallogenic special features of the alkaline formations in the eastern part of the Baltic shield. Trudy Leningradskogo obs. est. 72, Nedra. Leningrad. 280 p. (In Russian).

Kukharenko, A. A., Orlova, M. P., Bulakh, A. G., Bagdasarov, E. A., Rimskaya—Korsakova, O. M., Nevedov, E. J., Ilinskii, G. A., Sergejev, A. S. & Abakumova, N. B., 1965. Caledonian complex of ultrabasic, alkalic rocks and carbonatites of the Kola Peninsula and northern Karelia (Geology, petrology, mineralogy, geochemistry). Nedra, Moscow. 772 p. (In Russian).

Landa, E. A., 1971. Explosion breccia in the Kovdor iron deposit. Dokl. Akad. Nauk. SSSR. 199, 1386—1388.

Landa, E. A., Poršnev, G. J. & Šuvalova, V. Z., 1971. About apatite deposit of Essej carbonatite massif (in northern part of Siberian platform). Sov. Geol. no. 6, 89—96. (In Russian).

Lapin, A. V., 1976. Geologic examples of limited miscibility in ore–silicate–carbonate melts. Dokl. Akad. Nauk. SSSR. 231, 694—697.

— » —, **1978.** On some problems of the genesis of carbonatites. Geol. rudn. mestor. 20, 33—45. (In Russian).

Leake, B. E., 1978. Nomenclature of amphiboles. Am. Mineral. 63, 1023—1052.

Le Bas, M. J., 1977. Carbonatite–nephelinite volcanism. John Wiley & Sons, London. 347 p.

Le Bas, M. J. & Sörensen, H., 1978. Classification and nomenclature of carbonatites. *In:* IUGS Subcommission on the systematics of igneous rocks. Classification and nomenclature of volcanic rocks, lampro-

phyres, carbonatites and melilitic rocks, 1—14. Ed. A. Streckeisen. N. Jb. Miner. Abh. 134.

Lindqvist, K. & Rehtijärvi, P., 1979. Pyrochlore from the Sokli carbonatite complex, northern Finland. Bull. Geol. Soc. Finland 51, 81—93.

Lombaard, A. F., Ward-Able, N. M. & Bruce, R. W., 1964. The exploration and main geological features of the copper deposit in carbonatite at Loolekop, Palabora Complex. *In:* The geology of some ore deposits in southern Africa 2, 315—337. Ed. S. H. Haughton. Johannesburg, Geol. Soc. S. Africa. 739 p.

McKie, D., 1966. Fenitization. *In:* Carbonatites, 261—294. Eds. O. F. Tuttle and J. Gittins. John Wiley & Sons, New York. 591 p.

Mäkelä, M. & Vartiainen, H., 1978. A study of sulfur isotopes in the Sokli multi-stage carbonatite (Finland). Chem. Geol. 21, 257—265.

Mason, P. K., Frost, M. T. & Reed, S. J., 1969. B.M.-I.C.-N.P.L. computer programs for calculating corrections in quantitative X-ray microanalysis. Nat. Phys. Lab. IMS Report 2.

Maxey, L. R., 1976. Petrology and geochemistry of the Beemerville carbonatite-alkalic rock complex, New Jersey. Geol. Soc. Am. Bull. 87, 1551—1559.

Melcher, G. C., 1966. The carbonatites of Jacupiranga, Sâo Paulo, Brazil. *In:* Carbonatites, 169—181. Eds. O. F. Tuttle & J. Gittins. John Wiley & Sons, New York. 591 p.

Nash, W. P., 1972. Mineralogy and petrology of the Iron Hill carbonatite complex, Colorado. Geol. Soc. Am. Bull. 83, 1361—1382.

Nielsen, T. F. D., 1980. The petrology of a melilitolite, melteigite, carbonatite and syenite ring dike system, Gardiner complex, East Greenland. Lithos 13, 181—197.

Nuutilainen, J., 1973. Soklin karbonatiittimassiivin geokemiallisista tutkimuksista. English summary: Geochemical prospecting on the Sokli carbonatite massif. Geologi 25, 13—17.

Orlova, G. P. & Rjabtšikov, I. D., 1977. Solubility of carbon dioxide in alkaline rich alumosilicate melts and questions about the origin of carbonatic magmas. Izv. Akad. Nauk. SSSR, Ser. Geol. 1977, no. 12, 5—15. (In Russian).

Paarma, H., 1970. A new find of carbonatite in North Finland, the Sokli plug in Savukoski. Lithos 3, 129—133.

Paarma, H., Raevaara, H. & Talvitie, J., 1968. On the interpretation of Ektachrome infrared aerofilm type 8993 photographs used in mineral reconnaissance and geological surveys. Photogramm. J. Finland 2, 3—22.

Paarma, H. & Talvitie, J., 1976. Deep fractures — Sokli carbonatite. Univ. Oulu, Dept. Geophysics, Contrib. no. 65. 5 p.

Paarma, H., Vartiainen, H. & Penninkilampi, J., 1977. Aspects of photogeological interpretation of Sokli carbonatite massif. *In:* Prospecting in areas of glaciated terrain 1977, 25—29. Inst. Min. Met., London.

Palabora Mining Company Limited Mine Geological and Mineralogical Staff, 1976. The geology and the economic deposits of copper, iron and vermiculite in the Palabora igneous complex: A brief review. Econ. Geol. 71, 177—192.

Pecora, W. T., 1956. Carbonatites: A review. Geol. Soc. Am. Bull. 67, 1537—1556.

— » —, 1962. Carbonatite problem in the Bearpaw Mountains. Geol. Soc. Am. Petrol. Stud., Buddington Vol. 397—424.

Philpotts, A. R., 1970. Mechanism of emplacement of the Monteregian intrusions. Can. Mineral. 10, 395—410.

Pozaritskaya, L. K. & Samoilova, V. S., 1972. Petrology, mineralogy and geochemistry of carbonatites of eastern Siberia. Nauka, Moscow. 265 p. (In Russian).

Rankin, A. H., 1975. Fluid inclusion studies in apatite from carbonatites of the Wasaki area of western Kenya. Lithos 8, 123—136.

Rass, I. T. & Boronikhin, V. A., 1976. Indicator ratios of petrogenic elements in zones within coexisting silicate minerals in carbonatites. Geochem. Int. 13, 154—161.

Rimskaya-Korsakova, O. M., 1964. Genesis of the Kovdor iron-ore deposit. Int. Geol. Rev. 6, 1735—1746.

Romanchev, B. P., 1972. Inclusion thermometry and the formation conditions of some carbonatite complexes in East Africa. Geochem. Int. 9, 115—120.

Royse, C. F., Wadell, J. S. & Petersen, L. E., 1971. X-ray determination of calcite–dolomite. An evaluation. J. Sed. Petrol. 41, 483—488.

Russell, H. D., Hiemstra, S. A. & Groeneveld, D., 1954. The mineralogy and petrology of the carbonatite at Loolekop, eastern Transvaal. Geol. Soc. S. Africa, Trans. 57, 197—208.

Saether, E., 1958. The alkaline rock province of the Fen area in southern Norway. Kong. Norske Vid. Selsk., no. 1.

Sandvik, P. O. & Erdosh, G., 1977. Geology of the Cargill phosphate deposit in northern Ontario. CIM Bull. 70, 90—96.

Secher, K., & Larsen, L. M., 1980. Geology and mineralogy of the Safartôq carbonatite complex, southern West Greenland. Lithos 13, 199—212.

Simkin, T. & Smith, J. W., 1970. Minor-element distribution in olivine. J. Geol. 78, 304—325.

Smith, W. C., 1956. A review of some problems of African carbonatites. Geol. Soc. London, Quart. J. 112, 189—220.

Strauss, C. A. & Truter, F. C., 1951. Post-Bushveld ultrabasic, alkali, and carbonatitic eruptives at Magnet Heights, Sekukuniland, eastern Transvaal. Geol. Soc. S. Africa Trans. 53, 169—190.

Talvitie, J., 1979. Remote sensing and geobotanical prospecting in Finland. Bull. Geol. Soc. Finland 51, 63—73.

Temple, A. K. & Grogan, R. M., 1965. Carbonatite and related alkalic rocks at Powderhorn, Colorado. Econ. Geol. 60, 672—692.

Ternovoy, V. J., Afanasev, B. V. & Sulimov, B. J., 1969. Geology and research of vermiculite and phlogopite deposit of Kovdor. Nedra, Leningrad. 287 p. (In Russian).

Tomkeieff, S. J., 1938. The role of carbon dioxide in igneous magma. Rep. Brit. Assoc. 1938, Cambridge, 417—418.

— » —, **1961.** Alkalic ultrabasic rocks and carbonatites in the U.S.S.R. Int. Geol. Rev. 3, 739—758.

Tyler, R. C. & King, B. C., 1967. The pyroxenes of the alkaline igneous complexes of eastern Uganda. Mineral. Mag. 36, 5—21.

Vartiainen, H., 1975. Näytteenotto Soklin fosforimalmin inventoinnissa. English summary: Sampling in the inventation of the Sokli phosphate ore. Vuoriteollisuus — Bergshantering 33, 99—105.

— » —, **1976.** Sokli: Carbonatite prospecting by the heavy minerals in stream sediments. J. Geochem. Explor. 5, 335—337.

Vartiainen, H., Kresten, P. & Kafkas, Y., 1978. Alkaline lamprophyres from the Sokli complex, Northern Finland. Bull. Geol. Soc. Finland 50, 59—68.

Vartiainen, H. & Paarma, H., 1979. Geological characteristics of the Sokli carbonatite complex, Finland. Econ. Geol. 74, 1296—1306.

Vartiainen, H. & Woolley, A. R., 1974. The age of the Sokli carbonatite, Finland, and some relationships to the North Atlantic alkaline igneous province. Geol. Soc. Finland, Bull. 46, 81—91.

Vartiainen, H. & Woolley, A. R., 1976. The petrography, mineralogy and chemistry of the fenites of the Sokli carbonatite intrusion, Finland. Geol. Surv. Finland. Bull. 280. 87 p.

Vartiainen, H. & Vuotovesi, T., 1980. The Sokli carbonatite complex. Lithos 13, 224—225.

Verwoerd, W. J., 1967. The carbonatites of South Africa and South West Africa. S. Africa Geol. Surv., Handbook No. 6. 452 p.

Watkinson, D. H., 1970. Experimental studies bearing on the origin of the alkalic rock–carbonatite complex and niobium mineralization at Oka, Quebec. Can. Mineral. 10, 350—361.

Wimmenauer, V., 1966. Carbonatites of the Kaiserstuhl (W-Germany) and their magmatic environment. Mineral. Soc. India, IMA Vol., 54—57.

Wyllie, P. J., 1966 a. Experimental studies of carbonatite problems: The origin and differentiation of carbonatite magmas. *In:* Carbonatites, 311—352. Eds. O. F. Tuttle and J. Gittins. John Wiley & Sons, New York. 591 p.

— » —, **1966 b.** Experimental data bearing on the petrogenetic links between kimberlites and carbonatites. Mineral. Soc. India, IMA Vol., 67—82.

— » — **(Editor), 1967.** Ultramafic & related rocks. John Wiley & Sons, New York. 464 p.

Wyllie, P. J. & Biggar, G. M., 1966. Fractional crystallization in the »Carbonatite sys-

tems» $CaO-MgO-CO_2-H_2O$ and $CaO-CaF_2-P_2O_5-CO_2-H_2O$. Mineral. Soc. India, IMA Vol., 92—105.

Wyllie, P. J. & Huang, W-L., 1975. Influence of mantle CO_2 in the generation of carbonatites and kimberlites. Nature 257, 297—299.

Wyllie, P. J. & Tuttle, O. F., 1960. The system $CaO—CO_2—H_2O$ and the origin of carbonatites. J. Petrol. 1, 1—46.

Yoder, H. S. Jr. & Tilley, C. E., 1962. Origin of basalt magmas: an experimental study of natural and synthetic rock systems. J. Petrol. 3, 342—532.